Structured models of ecological communities in fluctuating environments

Sonya Dewi

7 December 1997

A thesis submitted for the degree of Doctor of Philosophy of the Australian National University

Ecosystem Dynamics Group
Research School of Biological Sciences
The Australian National University

Declaration

The contents of this thesis are the results of my original research. Assistance from others is fully described in the acknowledgements of the thesis. This thesis has not been submitted for a degree at any other university or institution.

Sonya Dewi
7 December 1997

Acknowledgements

I cannot thank Dr. Peter Chesson enough for supervising this project. Without his expertise, constant guidance, enthusiasm and encouragement, this work would never have been started and finished. His patience in teaching an old dog a bunch of new tricks is amazing. I am particularly grateful for his assistance in solving for the covariance between the environment and competition in Chapter 6, non-additivity in Chapter 6 and the order approximations in Chapters 3 and 4.

It must be a painful experience for Peter Chesson to read the drafts of this thesis, written in weird English. Many thanks for his great help in shaping this thesis. I am fortunate to have met Mamoru Matsuki who worked on a similar project. Our discussions, though not so many, have been fruitful for me. Mamoru has spent many of his precious evenings reading the whole draft of the thesis twice. I am very grateful for his very valuable comments on the contents and his efforts in making sense of my English. Dave King read part of the early draft and gave valuable comments and suggestions. Thanks to AusAID that funded the thesis editing. Nicola Fortune has done a wonderful job in editing a large part of this thesis. Raywadee has been very helpful with my final draft.

I also wish to thank Prof. Ian Noble, Prof. Chris Heyde and Prof. Hugh Possingham for being in my advisory committee. Thanks to Ian Davies for solving some printing problems. Special thanks to Michelle Cochrane who is always there when I am in my lowest in this foreign land.

This study is sponsored by AusAID through an ADCOS scholarship. I wish to thank Lynn Toohey for her effort in communicating with AusAID for me in my hard times. Without her competence, this work might never be finished. My mother helped us with some financial problems, especially toward the end of my study period.

My mother, my brother, my sister in law, my uncle, and my sister have provided with such wonderful moral support, particularly during tremendously

hard times. My two toddlers, Cil and Dina, have grown into helpful and understanding small adults during my study. Their beautiful smiles can always brighten my days. My husband and my best friend, Ahmady, cannot be more supportive than he has been. His love of mathematics and statistics enthuses me to know more about them. His optimism has been a source of never ending fuel for me. Last and tiniest, is the newest member of our family. Our Tin star was born in the busiest time in my study period. She makes sure that I always have enough rest, by constantly reminding me to have a break.

Abstract

The lottery model of competition between species in a variable environment has led to a general conception of a very important species coexistence mechanism, the storage effect. Although the storage effect depends on differences in the responses of different life-histories stages to fluctuating environmental factors and competition, the lottery model incorporates only a distinction between juveniles and adults.

The robustness of the storage effect under extensions of the lottery to include more general population structure is the main question of my study. The first extension is the addition of age-structure to the original lottery model by introducing age-dependent mortality and fecundity. Like the original lottery model, density dependence occurs only in the juvenile stage. I introduced functionals of mortality and fecundity schedules called the Δ-measures to summarize deviations from constant mortality and fecundity rates. These Δ-measures are important tools for comparing the dynamics of the lottery model with and without the age-structure. The study showed that the recovery rate of the invader from low density was changed with the addition of age-structure, however there was only a slight shift in the coexistence criterion, which was due to fluctuations in the age distribution. Chesson's quadratic measure of the magnitude of the storage effect was not changed with age-dependent mortality and fecundity.

The second extension of the lottery model included size-dependent mortality and fecundity with the density dependence in all size classes, except the largest. In this extension, the Δ-measure was shown to be a very useful tool for understanding the behaviour of the model. The expected lifetime and the net reproductive rate were greatly affected by density-dependent growth in size. Changes in the magnitude of the storage effect, the recovery rate of the invader, and the coexistence criterion could mainly be explained by changes in the density-dependent expected lifetime with size-dependent mortality and fecundity.

This study shows that the storage effect, a mechanism of species coexistence, was robust even in age- and size-structured populations. Moreover, incorporating stage-specific density-dependent mechanisms into the lottery model had stronger effects than merely incorporating age- and size-dependent mortality and fecundity.

Contents

List of Tables

List of Figures

Chapter 1

Introduction to ecological community and life-history models in temporally variable environments

1.1 Introduction

The past decade has favoured individual-based modelling in population and community ecology. Previously, models that considered only population averages of individual properties were predominant in the investigation of population and community dynamics. Reasons for this change in approach include the availability of powerful computers and software (Huston, DeAngelis, and Post 1988; Levin, Grenfell, Hastings, and Perelson 1997), and the recognition of the role of local interactions, and sizes or other characteristics of individuals in ecological systems (Bengtsson, Fagerstrom, and Rydin 1994; Caswell, Nisbet, de Roos, and Tuljapurkar 1997; Judson 1994). Arguments for and against individual-based models continue the long-running debate about reductionism versus holism, generality versus complexity, and strategic models versus tactical models. A major new element in the debate is mathematical analysis versus computer simulation. The term "individual-based models" refers to two groups of models: individual state distribution models, where there are classes of individuals within populations, and individual state configuration models, where each individual is a separate entity. With the individual state configuration models, we rely almost completely on computer simulations and draw conclusions which are specific to the particular population modelled.

The individual state distribution model is appropriate when we are satisfied with grouping individuals into classes defined by relatively homogeneous characteristics of interest. This model is intermediate between the unstructured population model and the state configuration model, and some mathematical analysis can be applied. In the individual state distribution model, populations are divided into classes based on one or more characteristics such as age, size, stage, or physiological characteristics, or based on spatial distribution. Adapting the term "state" from systems engineering, Caswell (1989) argues that the above characteristics could adequately define states. For single species individual state distribution models, advances in human demographic modelling techniques are applicable as long as theoretical ecologists are willing to ask questions similar to those asked by human demographers. However, whether those questions are relevant to ecological systems remains questionable.

Three main reasons why population structure should be included in a model are: (i) population structure affects population dynamics, (ii) model which incorporates vital rates of individual is closer to experimental or observational data, and (iii) individual differences lead to evolutionary dynamics in populations (Caswell, Nisbet, de Roos, and Tuljapurkar 1997).

One of the questions concerning the individual state distribution model is: How should we divide populations into classes; or How do we build a structured model? i.e., Which characteristics are important in which systems? Furthermore, How do we apply the individual state distribution concept to multispecies systems; and Why is this necessary?

In this thesis, I will approach the above questions using the lottery model, originally developed by Chesson and Warner (1981). Because of its capacity to demonstrate a very important concept in ecology, namely, the storage effect, this model has been influential. I believe that extending this model to age-structured and size-structured models will lead us toward a deeper understanding the storage effect as a mechanism of species coexistence associated with life-history characteristics.

1.2 Structured population models

Most techniques in structured population modelling are adapted from methods used in human demography. Such models attempt to answer questions such as: What is the stable age structure; What is the population projection in the near future; How long will it be before stable age structure is reached;

and How sensitive is this stable age structure to changes in vital rates? The primary tool to answer these questions analytically is the well-known non-negative Leslie matrix, which is a particular kind of population projection matrix. The elements of this matrix are the age-specific fecundity and survival rates (Bernadelli 1941; Leslie 1945; Leslie 1948).

In a deterministic model, where the Leslie matrix is constant over time and the dominant eigenvalue is the population growth rate, the above questions can easily be answered. Demographers then generalise further by varying the Leslie matrix over time. A stochastic model is biologically more realistic since vital rates always change with time. Cohen and Tuljapurkar developed the fundamental theorem of stochastic ergodicity in a stochastic demographic model where they allowed Leslie matrices to follow stochastic processes such as the independent process, the stationary Markov process, and even non-stationary processes (Cohen 1977; Tuljapurkar 1982; Tuljapurkar 1990; Tuljapurkar 1997). Properties of the product of non-negative matrices are the primary tools in their models. In the stochastic demographic models, the long-term population growth rate is estimated using the Lyapunov exponent, which is the generalised form of the eigenvalue. Unfortunately the computation of this exponent is more difficult than the eigenvalue computation. In fact, to show that this exponent exists for a particular system is not trivial (Metz, Nisbet, and Geritz 1992). However, with knowledge of stochastic ergodicity, some approximation techniques can be developed to estimate the long-term population growth rate (Tuljapurkar 1982; Tuljapurkar 1990; Tuljapurkar 1997).

While in human demography changes in vital rates with population densities might not be of a major concern, in ecological systems density dependence is believed to have a major role in population dynamics. Several works investigating structured population models with density dependence are listed in (Botsford 1997). The early works were dependent on simulations, such as Ricker's stock and recruitment model. Later works concentrate on the analysis of local stability in the linearised model. And some recent works try to unravel the non-linear aspects of such models. Most of these works do not involve stochasticity. Two well-known examples of deterministic age-structured models with density dependence are given by DeAngelis et al. and Levin and Goodyear (DeAngelis, Svoboda, Christensen, and Vaughan 1980; Levin and Goodyear 1980).

1.3 Non-structured community models

In ecology it is widely accepted that species interactions are important in shaping communities and that density dependence does play a significant role in community dynamics (Hutchinson 1961; MacArthur and Levins 1967). Therefore, in community ecology we are usually more interested in questions such as: How do we define coexistence; Under what circumstances will species coexist; What is the mechanism for coexistence; and What kind of interactions are important?

It is difficult to build a simple deterministic model with a single limiting resource that allows a large number of species to coexist (Chesson 1986). Such models fail to explain natural communities with a large number of coexisting species competing for very similar resources, for example many plant communities. However, simple models have led to the development of some important basic ecological concepts such as the niche, competitive exclusion, and limiting similarity. We can build on these to understand more complex concepts such as the storage effect, and to develop more realistic models.

Most analyses rely on the assumption of equilibrium population to make predictions about species coexistence. Population fluctuations are regarded as disturbances that tend to drive the ecological system into a non-equilibrium state leading to exclusion of species. Only recently have ecologists realised that fluctuations are not merely noise but can be central to mechanisms for coexistence.

Chesson and Warner successfully explained a fluctuation-dependent coexistence mechanism for a multispecies competition model, i.e., the lottery model (Chesson and Warner 1981), which is a simple model of competition between juveniles of different species for maturation to adulthood in the presence of density-independent fluctuations in birth rates or juvenile survival rates. The lottery model has made important contributions to ecological theory in introducing: (i) the phenomenon of diversity maintenance in a variable environment (i.e., the storage effect), (ii) a generalisation of the concept of resource partitioning/niche differentiation to differentiation in response to environment and competition, and (iii) the use of the stability concept stochastic boundedness and its relationship to the invasibility technique for predicting species coexistence. In the lottery model, the environment is defined as a density-independent parameter, and competition as a density-dependent parameter.

The storage effect, which is discussed in more detail below, refers to a phenomenon that gains in population growth when conditions are favourable

cannot be cancelled out by negative population growth when conditions are unfavourable. The storage effect is likely to play a very important role in maintaining species coexistence (Chesson and Huntly 1989). A number of authors have contributed important understanding of the storage effect including (Ellner 1984; Abrams 1984; Shmida and Ellner 1984; Iwasa, Sato, Kakita, and Kubo 1993). Recently, Ellner and Hairston have been emphasising that the storage effect idea applies also to the maintenance of genetic diversity within species (Ellner and Hairston 1994).

Invasibility analysis first introduced by MacArthur and Wilson (1967) to study invasion of a new species into an ecological system. Naturally, an invading species starts from low density and will successfully invade only if its population growth rate is positive. Invasibility analysis has been analytically proved to be generally applicable (Chesson and Ellner 1989; Chesson 1982; Ellner 1989) by relaxing the definition of coexistence. Formally, for species to coexist, their population densities must converge to a positive stationary distribution. This requirement is relaxed into stochastic boundedness, i.e., small populations have correspondingly small probabilities of occurrence. Invasibility analysis ~~is an implication of~~ implies stochastic boundedness. Proofs can be found in (Chesson 1982; Turelli and Gillespie 1980; Chesson and Ellner 1989). Ellner (1989) found general conditions under which the stronger requirement of convergence to a positive stationary distribution is applicable.

Using invasibility analysis, only a knowledge of the long-term population growth rate at low density is required to make predictions about the persistence of species. A low density population is defined as a population of sufficiently low abundance that it has no effect through competition on the growth rate of other populations and on its own growth rate.

There have been several applications of the lottery model in its original form, called here the nonstructured lottery model or NLM. Comins and Noble (1985) used a weighted lottery model to obtain the area of coexistence between fire adapted species and gap dominating species and found that the predicted area of coexistence was supported by data from Australian eucalypt forests. In investigating life-history evolution, Bulmer (1985) employed the NLM to demonstrate the process of selection for iteroparity in fluctuating environment (Bulmer 1985). Runkle (1989) formulated the hypothesis that the NLM and the storage effect can explain differences in species diversity between tropical forests and temperate forests. A wider temporal dimension for potential recruitment and growth in tropical forest can generate more asynchrony in regeneration between species, which creates a wider potential niche. In tem-

perate forests, regeneration is more synchronous, due to seasonality, and the temporal dimension is narrower. Therefore, fewer species can coexist. This hypothesis has been explored in theoretical studies of the NLM (Iwasa, Sato, Kakita, and Kubo 1993; Iwasa, Kubo, and Sato 1995; Kubo and Iwasa 1996) leading to the conclusion that, through its effect on niche width, the storage effect in the NLM is indeed an important mechanism for the maintenance of species richness in tropical forests.

In some modified forms, the NLM is used to explain coexistence in communities of shrubland in South Africa and Western Australia (Henri and Cowling 1994). It is also believed that lottery recruitment operates as a coexistence mechanism in temperate freshwater fish communities (Persson and Johansson 1992), coral reef fishes (Sale 1977), some Banksia species (Lamont and Witkowski 1995), and Hawaiian montane tropical tree species (Hatfield, Link, and Dawson 1996).

Chesson attempted to generalise the model (Chesson 1990), but it was not until recently that a comprehensive general framework and unified analysis were put together (Chesson 1994). To be general, a model must be simple and widely applicable. In Chesson's framework, simplicity is achieved by classifying any factors affecting population into two categories, and summarising their effects via two population parameters: the density-dependent parameter and the density-independent parameter. An example of the density-independent parameter is birth rate in the lottery model of Chesson and Warner. This choice of parameter can be justified biologically since density dependence commonly occurs primarily in the survival of immatures (e.g., Charnov 1993, pp. 8-9). Chesson obtains generality in the analysis of different specific examples of the general model through a standardisation procedure where the unit of measurement of the density-dependent parameter and the density-independent parameter is one unit of per capita population growth. Chesson also shows in (Chesson 1994) how several well known models, such as the Lotka-Volterra model, the lottery model, and models with a common limiting factor, can be fitted into the common framework and analysed to produce results that are consistent with those of model-specific analyses. The limitation of this general framework mainly stems from an assumption that competition can be written as a function of the environmentally dependent parameter and population densities for all species under study.

1.4 Multispecies-structured models in a variable environment

It is ironic that most models which consider communities composed of heterogeneous populations do not incorporate life-history characteristics. It is very common in such models that one parameter, such as population density, serves to represent the whole population. While patch community dynamics have started to enjoy some support, endogenous heterogeneity in populations, though recognised, is still largely neglected.

However, the importance of population heterogeneity in defining niche differentiation has been recognised by some. For example, Bengtsson et al. (1994) wrote:

> (two recent reviews of competition experiments) concluded that ... among plants, asymmetry in competition for nutrients and light is mainly a result of size differences, rather than of species differences, because aquisition of these resources usually depends more on plant size than on species identity. This means that classical resource partitioning, whereby species coexist through niche differentiation, may not be of major importance in plant communities.

Another example of recognition of the importance of heterogeneity on population dynamics comes from (Runkle 1989). In the context of a study of coexistence in a system of Australian eucalyptus, Comins and Noble suggest that demographic parameters are important (Comins and Noble 1985).

Meanwhile, models in evolutionary ecology, which examine how fitness varies as a function of life history, mostly define fitness as the population growth rate in a single-species system. The definition of fitness in multispecies systems with density dependence and species interactions is not yet settled.

Heterogeneity within a population in which individuals within a population are differentially sensitive to environment and competition can produce the storage effect promoting species coexistence (Chesson 1990; Chesson and Huntly 1988). This finding is suggestive of a bridge between the fields of evolutionary ecology and community ecology. Three major conditions required for the storage effect to operate are (i) sub-additivity, i.e., a weaker response to competition when environment is not favourable, (ii) positive covariance between environment and competition, i.e., increases in environmental favourability lead to stronger competition and (iii) species-specific response to environment, i.e., though living in the same environment, different species do not

have synchronous responses to environmental fluctuations. Sub-additivity is a condition in which the response of a population to competition, measured in terms of growth rate, is weaker when environment is unfavourable than when environment is favourable. In other words, the reduction in population growth rate due to competition occurs more slowly when environment is unfavourable. This means that increases in population size during favourable environmental conditions cannot be cancelled out by decreases in population size during unfavourable environmental conditions. To understand how sub-additivity arises, we need to recognise that a population can be subdivided into components such as age classes or life history stages. Different components of a population respond differently to fluctuations in the environment and competition. Sub-additivity arises when some components of a population are sensitive to both competition and the environment, while other components are less sensitive to both competition and the environment (Chesson 1990; Chesson and Huntly 1988). The lottery model is an important example of a model that shows sub-additivity. In the lottery model, juveniles compete with each other for space for the space needed to mature to adulthood ("recruitment"), and birth rates of adults fluctuate with environment in a density independent manner. Each population in the lottery model can be regarded as two subpopulations: juvenile and adult. The juvenile subpopulation is sensitive to competition, due to the need for space for recruitment, and sensitive to the environment, due to the fluctuations in birth rates feeding into the stage, or density-independent fluctuations in survival within the stage. Survival of adults, on the other hand, is not sensitive to either competition or the environment.

1.5 Research questions

The objective of this study is to look at how the incorporation of population age or size structure into the lottery model affects predictions of species coexistence. Age or size structures are incorporated through age- or size-dependent mortality and fecundity. Further, I will use the model to investigate the effects of density dependence occurring at different life-history stages, i.e., occurring only during recruitment, or occurring throughout the adult stages as well. I will focus on coexistence mechanisms in terms of the more general concept, the storage effect. I will look in detail at why changes in species coexistence and its mechanisms, if any, occur with the extension of the non-structured lottery model (NLM) into an age-structured lottery model with density depen-

dence during recruitment only (SLM), and further, into a size-structured lottery model with density dependence throughout adult stages as well (MSLM). Changes in the role of life-history characteristics in species coexistence, and changes in life-history characteristics with the density dependence, will be key in understanding the model. Finally, I will define the circumstances under which an explicit age or size structure will change the outcome of a model.

1.6 Chapter organisation

For simplicity, I will study the two-species model. We first need to understand the original lottery model without any age or size structure (NLM). Mathematical analysis of the lottery model has been carried out by Chesson and colleagues, and results have been published in several papers. Invasibility analysis has been used to obtain the formula for the long-term population growth rate (Chesson 1994), and the area of coexistence (Chesson and Warner 1981). The stationary distribution was found using diffusion approximation (Hatfield and Chesson 1989). I will use computer simulations to calculate the long-term population growth rate of the invader in the two-species NLM and compare of this with the quadratic approximation (Chesson 1994). Also, I will examine the storage effect and two of its ingredients, i.e., covariance between environment and competition, and sub-additivity, in the NLM. The correlation between the responses of the two species to the environment is held at zero during the whole study. This can be done without loss of generality because in the lottery model non-zero correlations have an effect identical to smaller variances with zero correlation.

The study of the NLM will provide readers some background understanding of how lottery competition during juvenile recruitment, together with environmental fluctuations, can promote species coexistence. This study will be presented in Chapter 2.

The computer simulations were performed on PC and DEC-Alpha 2000 machines using GAUSS (Aptech Systems 1992). We need to be sure that calculation of the long-term population growth rate does not involve transients in population dynamics resulting from failure of the resident species in the invasibility analysis to be at its stationary distribution. The time at which stationarity is achieved and standard errors of the long-term population growth rate from several runs are used to determine the adequate length of each run and the number of runs required to produce a particular level of accuracy.

In Chapter 4 I extend the NLM into an age-structured lottery model (SLM) by adding age-dependent mortality and fecundity to the adult stage, while density dependence occurs only during juvenile recruitment. Here I will rely more heavily on computer simulations because of the more complex nature of the model. Before progressing to the SLM, we need to know which life-history characteristics play on major role in the NLM. Chesson has derived a simple formula for the analysis of the NLM (e.g., Chesson 1994). The formula showing that the expected lifetime, the difference between the mean birth rate of the invader and the mean birth rate of the resident, and the fluctuations in the birth rates determine the long-term population growth rate of the invader. With this knowledge, comparison of the SLM with the NLM is done for fixed values of the expected lifetime, mean birth rate and fluctuations in the birth rate, then it is possible to see if the NLM and the SLM behave differently because of the inherent differences in the models, rather than quantitative differences in critical parameters. To do this, however, it is necessary to develop a technique to generate sets of different mortality and fecundity schedules with fixed expected lifetime and net reproductive rate.

Summarising the complex results of the SLM for various mortality and fecundity schedules becomes more difficult. There has been no general technique for summarising deviations from constant mortality and fecundity. The common way to present and summarise a life-history study that includes many different mortality and fecundity schedules is to assign an arbitrary code to each schedule and then present the results according to these codes (e.g., Orzack 1997; Benton and Grant 1996). A shape measure for schedules of births and deaths is proposed in Chapter 3. This measure summarises a mortality or fecundity schedule into a single parameter, which is also useful for estimating the growth rate of slowly growing population. This proposed shape measure, or Δ-measure, can be applied to any age- or size- dependent vital rates in a demographic or ecological model. This tool measures the difference between the shape of the distribution of deaths or births for a given mortality or fecundity schedule and that of the corresponding distribution for age-independent vital rates. This measure is used to summarise the results of the SLM (Chapter 4) and the MSLM (Chapter 6).

The SLM is studied in detail in Chapter 4, and the storage effect, focusing particularly on covariance between the environment and competition, and sub-additivity, is compared between the NLM and the SLM. The study of the SLM is presented in Chapter 4.

The Tuljapurkar approximation, an approximation technique to calculate the long-term population growth rate of a structured population in stochastic demographic models, is applicable to the 2-species SLM. The implementation of Tuljapurkar approximation to the SLM will be presented in Chapter 5 together with the results. Since this technique is computationally very cheap compared with stochastic simulation, I can work more extensively with larger parameter sets. The conclusion drawn about the general pattern will thus have a firmer base. Again, the shape measure (Δ-measure) is an important tool for understanding the results.

The next extension is to a size-structured lottery model with density dependence spread throughout adult stages (the MSLM). The MSLM is presented in Chapter 6. Since it is impossible to fix density-dependent life-history characteristics, I will only fix the density-independent life-history characteristics, i.e., the density-independent expected lifetime and net reproductive rate, as in the NLM and the SLM. The expected lifetime and net reproductive rate change substantially with mortality and fecundity schedules. I will study this change in life-history characteristics using the Δ-measure as a tool. The change in the storage effect together with its ingredients in various mortality and fecundity schedules is investigated.

With the concepts of the storage effect and life-history characteristics linking the models together, a summary of how the extensions change the behaviour of the models and species coexistence is presented in Chapter 7. Some implications of this study, particularly how it may lead to a broader, more general model, will be discussed.

Chapter 2

Introduction to competition models in temporally variable environments and Non-structured Lottery Model (the NLM)

2.1 Introduction

Questions concerning the dominance of competition in shaping communities, especially when the environment fluctuates, have motivated a large number of studies in community ecology. However, as Goldberg (1996) pointed out, the inconsistency of the definition of competitive ability between theories, and between theoretical and empirical studies, presents a major obstacle to the study of competition. Chesson and Huntly (1997) presented an attempt to clarify and standardise definitions across different competition models and studies. They analysed models and studies within a single general theoretical framework proposed by Chesson (1994).

Chesson and Huntly (1997) argue that fluctuation in environment does not change the role of competition, either to promote or not to promote species coexistence, unless competition affects niche dimensions. The ranking of dominance, the rate of extinction, and the timescale of the dynamics can be modified by environmental fluctuation, but the competitive exclusion principle remains. A fluctuating environment can promote coexistence only when it adds or modifies a niche dimension.

A multispecies competition model may be defined in terms of resource availability and the competitive response of each species in relation to each resource. If environmental fluctuations create a new niche dimension, competitive exclusion might not occur. For a new niche dimension to emerge, a model must either have relative non-linearity in the responses of species to competition, or the storage effect.

A model is non-linear in its competitive response when the responses of species to any particular competitive factor are non-linear functions, as in the model of Armstong and McGehee (1980). The new niche dimension is created by fluctuations in the competitive factor coupling with the non-linearity, because then the ranking of competitive superiority can change as the competitive factor fluctuates allowing each species to be dominant some of the time.

For the storage effect to operate, each species must respond to the environment differently, in terms of its population growth rate. Also, environment and competition must covary (usually positively). Descriptively, positive covariance occurs if more favourable environmental conditions for a species mean that it causes more competition. Finally, species must show non-additivity (usually sub-additivity). Sub-additivity occurs when, under conditions of poor environment and intense competition, the population growth rate of a species does not decrease as much as is predicted by the sum of the separate effects the poor environment and intense competition. Section 2.2.2 will be devoted to a more detailed discussion of the concept of the storage effect. Chesson and Huntly (1989) suggest that the storage effect might commonly be found in nature, and may be thought of as a form of niche differentiation with respect to varying environmental conditions.

A well-known example of a simple, non-additive model is the lottery model of Chesson and Warner (1981), which does not incorporate age or stage structure beyond a simple distinction between juveniles and adults. This model will be called the Non-structured Lottery Model (the NLM), to distinguish it from the extension to the model that will be introduced later. Non-additivity, which in the NLM is sub-additivity, is due to heterogeneity among the members of a population in their sensitivities to the environment and competition. Juveniles are affected by competition, and may be highly sensitive to the environment, suffering high mortality under poor environmental conditions. Adults, on the other hand, are not sensitive to competition, and may only be sensitive to the environment in terms of fecundity. The chief state variable in the model is

the number of adults at the end of the season during which recruitment to the adult population occurs. Two processes lead to this new adult population: survival of adults from the previous time, and recruitment of adults as the final outcome of reproduction, juvenile survival and maturation. Survival of adults is insensitive to environment and competition, while recruitment is sensitive to both. The joint variation of sensitivity to environment and competition over these two processes is called covariance of sensitivity. It can be measured by a formal statistical covariance, as discussion below, and in many cases can be shown to be equal to the negative of the quantity measuring non-additivity. It has been shown that the storage effect associated with sub-additivity is strong enough to change the outcome of competition in fluctuating environments, promoting species coexistence.

Below I will discuss a general model of species coexistence, comprising non-additivity and the storage effect, from Chesson (1994) and Chesson and Huntly (1997). Then I will introduce and discuss the NLM within the general framework. I will also compare some results produced using different methods. A short review of some studies examining the impacts and applications of the the NLM will be presented in the last section.

2.2 General model, non-additivity and storage effect

2.2.1 General model

For simplicity, we will consider only the two species model, but the model and analysis can be applied to any number of species, as discussed by Chesson (1994).

Let $P_i(t)$ denote the population density of species i at time t. Then the population growth rate of species i at time t ($r_i(t)$) can be defined as:

$$r_i(t) = \ln\{P_i(t+1)\} - \ln\{P_i(t)\}.$$

A general competition model, focusing on the population growth rate, can be written as:

$$r_i(t) = g_i\left(E_i(t), C_i(t)\right), \tag{2.1}$$

where

$E_i(t)$ is the environmentally dependent parameter of species i at time t. The

environmentally dependent parameter is a population parameter, and by definition, is density independent. $C_i(t)$ is the competition parameter, which is also a population parameter, and is defined as a density dependent parameter. g is a function which relates $E_i(t)$ and $C_i(t)$ to the population growth rate. E_i is usually defined such that g is an increasing function of E_i. Some examples of the environmentally dependent parameter are the birth rate, survival rate, and germination rate. An example of the competition parameter is the rate of recruitment of older juveniles to adults, when recruitment requires capturing resources (Chesson 1994).

Since models are likely to vary in their units of measurement of the environmentally dependent parameter and the competition parameter, some form of standardisation is necessary for general quantitative results. Chesson transforms the original environment parameter and the original competition parameter into the standard environment parameter and standard competition parameter in the following way:

$$\mathcal{E}_i(t) = g_i\left(E_i(t), C_i^*\right),$$

$$\mathcal{C}_i(t) = g_i\left(E_i^*, C_i(t)\right),$$

where E_i^* and C_i^* are chosen to satisfy:

$$r_i(t) = g_i\left(E_i^*, C_i^*\right) = 0,$$

with E_i^* chosen near the mean of $E_i(t)$: the mean of $E_i(t)$ must be no more that $O(\sigma^2)$ from E_i^*.

Using the second order Taylor approximation, the growth rate of species i, in terms of the standard parameters for the general model is:

$$g_i(\mathcal{E}_i(t), \mathcal{C}_i(t)) \approx \mathcal{E}_i(t) - \mathcal{C}_i(t) + \gamma_i \mathcal{E}_i(t)\mathcal{C}_i(t) \tag{2.2}$$

(Chesson 1994), where:

$$\gamma_i = \frac{\partial^2 g_i}{\partial \mathcal{E}_i \partial \mathcal{C}_i} \begin{cases} = 0 & \text{for an additive model} \\ < 0 & \text{for a sub-additive model} \\ > 0 & \text{for a super-additive model.} \end{cases}$$

Figure 2-1 illustrates additivity and non-additivity taken from (Chesson 1994). Growth rates in the figure are for the original environmentally-dependent and competition parameters $E_i(t)$ and $C_i(t)$ rather than the standard ones. The difference is simply that in the standard case the lines in these figures

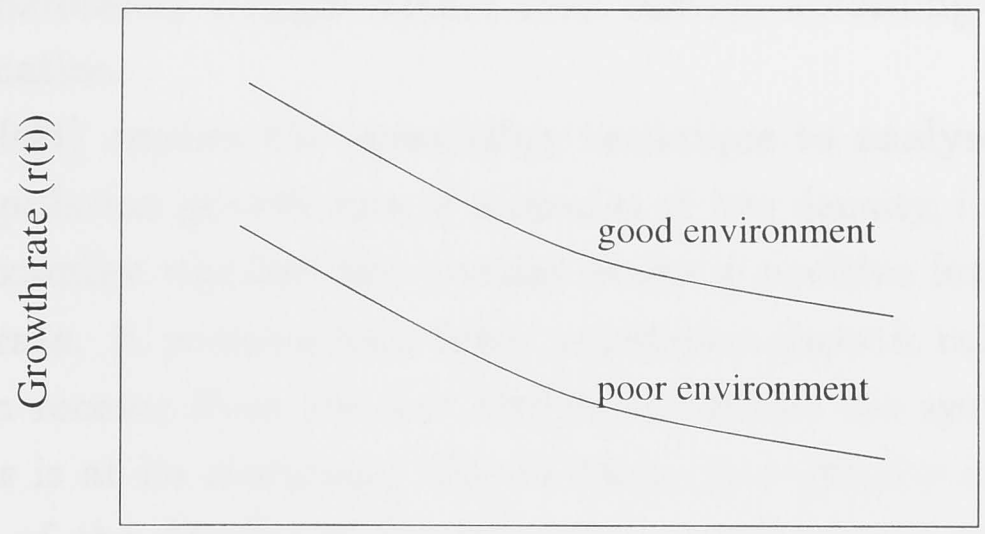

(a)

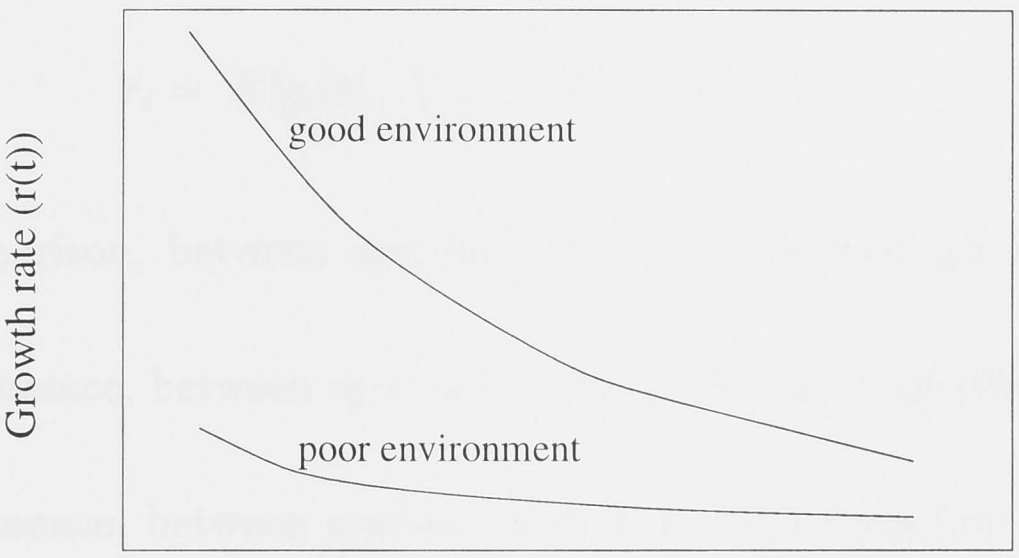

(b)

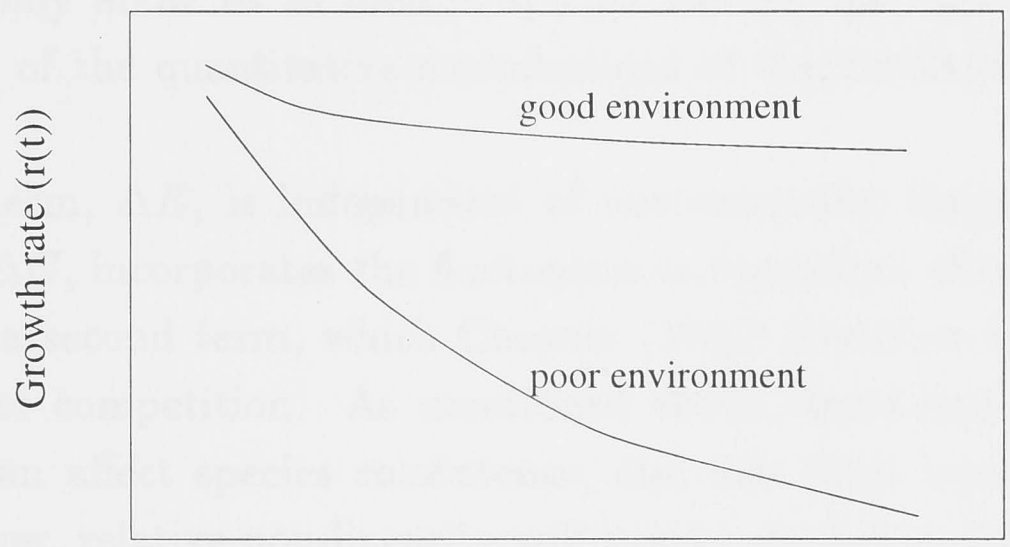

(c)

Figure 2-1: Additive growth rate (a), sub-additive growth rate (b) and super-additive growth rate (c). Good and poor environment mean respectively, high and low values of $E_i(t)$.

would be approximately straight rather than curved, according to the second order approximation.

Chesson (1994) applies the invasibility technique to analyse this general model. The population growth rate of a species at low density, i.e., an invader, is studied to examine whether the invader shows a positive long-term population growth rate. A positive long-term population growth rate means that the invader can recover from the low density, or invade the system while the resident species is at its stationary distribution. Low density is defined such that the effect of the density of the invader on the resident and on its own growth is negligible. If each species in the system has a positive long-term growth rate at low density then stable species coexistence is achieved.

Measuring the terms in relation to species j, the long-term growth rate of species i is:

$$\bar{r}_i = \mathrm{E}\left[g_i(\mathcal{E}_i, \mathcal{C}_i)\right] = \Delta E - \Delta C + \Delta I, \tag{2.3}$$

where

ΔE is a comparison, between species i and j, of the average effects of the environment,

ΔC is the difference, between species i and j, in the average effect of competition,

ΔI is the difference, between species i and j, in the interaction between the environment and competition.

Equation 2.3 is the key to invasibility analysis, since we concentrate on equation 2.3 to analyse the general model of species coexistence. Equation 2.3 does not only allow us to predict species coexistence, but also provides an assessment of the quantitative contributions of the mechanism to species coexistence.

The first term, ΔE, is independent of environmental fluctuations. The second term, ΔC, incorporates the fluctuation-independent effect of competition and also a second term, which Chesson (1994) describes as the relative non-linearity of competition. As mentioned above, non-linear responses to competition can affect species coexistence, and this term incorporates such effects. However, relative non-linearity will not be studied in this thesis, and does not appear in the cases of the models considered because all species have the same non-linearities.

The third term, ΔI (the storage effect), is more likely to play a key role in maintaining coexistence in general (Chesson and Huntly 1989), i.e., to produce positive long-term growth rates of species at low density. The storage effect

must be large enough to cancel the negative ΔE due to the inferiority of the invader.

Since I deal only with the two species system in this study, I will consistently use the notation i and j for invader and resident species, respectively. An inferior species, i.e., a species with negative ΔE, is chosen as the invader species. In the original lottery model (the NLM), particularly for a two-species system, the invader species is the species with the lowest mean birth rate. In this case, predictions of species coexistence can adequately be made by studying the long-term population growth rate of the invader, without studying the long-term population growth rate of the resident at low density.

2.2.2 Non-additivity and the storage effect

As an example of the storage effect operates, the Non-structured Lottery Model (NLM) shows how a species that is disadvantaged relative to other species in its ability to exploit a single common limiting resource can coexist indefinitely if the storage effect is strong enough to cancel that disadvantage.

As stated above, the storage effect will operate in a model in the presence of sub-additivity (as defined in the previous section), positive covariance between environment and competition (the competition parameter of a species increases as a function of the environmentally-dependent parameter of any resident species,while all other factors are held fixed), and species- specific responses to the environment (the correlations over time between the environmentally dependent parameters of any pair of species must be less than 1).

The storage effect in term of equation 2.3 (ΔI) is subdivided to give further insight into how the storage effect arises (Chesson 1994):

$$\begin{aligned} \Delta I &= \gamma_i \mathrm{E}[\mathcal{E}_i \mathcal{C}_i^{-i}] - \gamma_j \, \mathrm{E}[\mathcal{E}_j \mathcal{C}_j^{-i}] \\ &\approx -\gamma_j (1 - \theta b_e) \chi_{jj}^{-i}, \end{aligned}$$

where $\approx$ means that the error of the approximation is equal to $o(\sigma^2)$, with σ^2 the variance of $E_i(t)$, the superscript $-i$ simply emphasises that the calculations are done with species i the invader and the other species at their stationary distributions,
$\theta = \frac{\gamma_i}{\gamma_j}$, $\chi_{jj}^{-}i = \ \mathrm{cov}[\mathcal{E}_j, \mathcal{C}_j^{-i}]$,
b_e is the coefficient of linear regression of $\mathcal{E}_i$ on $\mathcal{E}_j$,

$$\mathrm{E}[\mathcal{E}_i | \mathcal{E}_j] = \ \mathrm{E}[\mathcal{E}_i] + b_e \, (\mathcal{E}_j - \ \mathrm{E}[\mathcal{E}_j]) + o(\mathcal{E}_j).$$

For simplicity I will deal only with complete asynchrony between species, i.e., $\text{cov}[E_i, E_j] = 0$, so that $\text{cov}[\mathcal{E}_i, \mathcal{E}_j] = 0$ and $b_e = 0$. There is no loss of generality for investigation of the lottery models in this thesis because making the covariance non-zero is found to have equivalent effects on population dynamics as changing the variance. With this simplifying assumption:

$$\Delta I \approx -\gamma_j \chi_{jj}^{-i}. \tag{2.4}$$

From equation 2.4 we can see that ΔI is positive when the resident is sub-additive (i.e., $\gamma_j < 0$) and shows positive covariance between environment and competition, $\chi_{jj}^{-i} > 0$. Alternatively, the resident could be super-additive (i.e., $\gamma_j > 0$) with negative covariance between environment and competition, $\chi_{jj}^{-i} < 0$. The first case seems more plausible in nature as many species have life-history traits likely to buffer a population against unfavourable conditions (Chesson and Huntly 1988), which implies sub-additivity. In addition, positive covariance between environment and competition seems likely because more favourable environmental conditions should lead to higher reproduction, survival or individual growth, any of which should place greater demands on resources.

2.2.3 The source of non-additivity

Using the NLM as an example, Chesson explains the intrinsic source of non-additivity (Chesson 1989; Chesson 1990). He shows how within-population variation in responses to the environment and competition will lead to non-additivity. Failing to recognise this within-population heterogeneity, by lumping subpopulations into one population, can result in the loss of important information, and may lead to invalid conclusions. This source of non-additivity can be studied from the perspective of life history, physiology, or any other heterogeneity within populations (Chesson 1990).

From equation 2.1 we define the finite rate of increase as:

$$G_i(E_i, C_i) = e^{g_i(E_i, C_i)}. \tag{2.5}$$

With population subdivision, the above finite rate of population increase can be written as a sum of contributions of each subpopulation:

$$G_i(E_i, C_i) = \sum_{l=1}^{m} G_{il}(E_i, C_i).$$

Sensitivity to the environment (α_{il}), competition (β_{il}), and their interaction (γ_{il}), for each subpopulation, are defined as follows:

$$\begin{aligned} \alpha_{il} &= \frac{\partial g_{il}}{\partial E_i}, \\ \beta_{il} &= -\frac{\partial g_{il}}{\partial C_i}, \text{and} \\ \gamma_{il} &= \frac{\partial^2 g_i}{\partial E_i \partial C_i}. \end{aligned}$$

Then non-additivity is:

$$\gamma_{io} = \bar{\gamma}_i - \sum_{l=1}^{m} (\alpha_{il} - \bar{\alpha}_i)(\beta_{il} - \bar{\beta}_i) G_i / \sum_{l=1}^{m} G_{il}, \tag{2.6}$$

where the subscript o stands for the original parameters of E and C, where γ is derived from, and $\bar{\alpha}_i$, $\bar{\beta}_i$ and $\bar{\gamma}_i$ are the weighted averages:

$$\bar{\alpha}_i = \sum_{l=1}^{m} \alpha_{il} G_{il} / \sum_{l=1}^{m} G_{il},$$

etc. Note that the sum term in formula 2.6 is a weighted covariance over subpopulations of the sensitivity to environment and the sensitivity to competition. In many cases, the subpopulations can be chosen so that $\gamma_{il} = 0$, and then non-additivity for the population is simply minus the covariance of sensitivities. Note also that the term "subpopulation" is used rather loosely here. Really what is needed is a way of dividing up the finite rate of increase into components, which may or may not correspond to actual subpopulations. For example, they may instead refer to processes. In the NLM, as discussed above and given in detail below, natural components are adult survival and recruitment.

Transformation to the standardised non-additivity, where the partial derivatives are taken with respect to the standard environment parameter ($\mathcal{E}$) and the standard competition parameter ($\mathcal{C}$), is:

$$\gamma_i = \gamma_{io} / \bar{\alpha}_i \bar{\beta}_i.$$

For a detailed description of non-additivity as a consequence of within-population heterogeneity of response to environment and competition, see (Chesson 1990; Chesson and Huntly 1988). An exposition of transformation from and into standardised parameters can be found in (Chesson 1989).

2.3 The Non-structured Lottery Model (the NLM)

2.3.1 The model

The NLM is a multispecies competition model in which juveniles compete with each other for space during recruitment, in a system which is always space limited (Chesson and Warner 1981). Once a juvenile successfully recruits to adulthood, the space is occupied and is only released when that particular adult individual dies. Then, the space becomes available for occupation by another juvenile.

The NLM, with two species, is defined by the following difference equation:

$$P_i(t+1) = (1-\delta_i)P_i(t) + (\delta_i P_i(t) + \delta_j P_j(t)) \left(\frac{b_i(t)P_i(t)}{b_i(t)P_i(t) + b_j(t)P_j(t)} \right), \quad (2.7)$$

where $P_i(t)$ is the proportion of space occupied by species i at time t, $b_i(t)$ is the birth rate of species i during $(t, t+1)$, and δ_i is the death rate of adults of species i. Environmental fluctuations enter the system through fluctuations in the birth rate of each species. The total amount of space occupied by both species is held equal to one at all times. Juveniles of both species are always more abundant than the available space, such that space is always limiting. Each juvenile of each species has exactly the same chance of occupying an available space. Therefore, competition is by lottery at the level of the individual juvenile, but competition is definitely not by lottery at the population level. The last assumption of the NLM is that failure of a juvenile to recruit during one unit time results in mortality.

The invader species will be denoted by i, and the resident species by j. For simplicity, the death rates of the invader and the resident species are held equal ($\delta_i = \delta_j = \tilde{\delta}$; $\tilde{\delta}$ denotes age-independent death rate). In this study, the birth rate of species i (b_i) and that of species j (b_j) are defined so that there is no correlation between b_i and b_j. Chesson (1994) has provided the analysis and formula for the most general case, i.e., for the n-species NLM with unequal death rates and birth rates correlated between species.

Equation 2.7 can be written as follows:

$$P_i(t+1) = P_i(t) \left[(1-\delta_i) + (\delta_i P_i(t) + \delta_j P_j(t)) \left(\frac{b_i(t)}{b_i(t)P_i(t) + b_j(t)P_j(t)} \right) \right].$$

The density of the invader, $P_i(t)$, is held at zero for all t, such that the density of the resident is always equal to one. The growth rate of the invader

can be written as:

$$\begin{aligned} r_i(t) &= \ln\left\{\frac{P_i(t+1)}{P_i(t)}\right\} \\ &= \ln\left\{1-\tilde{\delta}+\tilde{\delta}\frac{b_i(t)}{b_j(t)}\right\}, \end{aligned}$$

and the long-term population growth rate of the invader is:

$$\bar{r}_i = \mathrm{E}\left[\ln\left\{1-\tilde{\delta}+\tilde{\delta}\rho(t)\right\}\right], \tag{2.8}$$

where $\rho(t) = b_i(t)/b_j(t)$.

The invader species persists in the community whenever $\bar{r}_i > 0$. Small variance approximations (Chesson 1989; Chesson 1994) and diffusion approximation (Hatfield and Chesson 1989) of equation 2.8 give identical results. Both approximations agree closely with evaluation by numerical integration. To introduce and check my simulation methodology, I shall compare these results with the results of computer simulations. I shall also discuss the quadratic approximation to illustrate the general concepts associated with the storage effect.

2.3.2 Analysis within the general framework

Approximation to the second order is to be performed in the neighbourhood of $\bar{r}_i = 0$. The result is easy to interpret biologically. Different time scale effects are teased apart, and the behaviour of different models can be compared easily. Linearisation for near equilibrium analysis, proposed by May and MacArthur (1972), might be enough to capture the dynamics of a deterministic model. However, for some stochastic models, particularly non-additive models, quadratic approximation is necessary to unravel terms of higher order. Such terms often turn out to have very important roles. Chesson (1994) incorporates these terms into a single variable called the storage effect.

Since $\bar{r}_i$ is derived in terms of relative parameters to those of j, the environment and competition are initially defined for j. In the lottery model, competition is common for all species and thus needs no subscript. In the NLM, the environmentally dependent parameter and the competition parameter, specifically for the case of a single resident species j, are defined as follows:

$$E_j(t) = \ln\{b_j(t)\}, \tag{2.9}$$

$$C(t) = \ln\left\{\frac{b_j(t)}{\tilde{\delta}}\right\}, \tag{2.10}$$

and the mean of competition is:

$$\begin{aligned} \mathrm{E}[C(t)] &= \mathrm{E}\left[\ln\left\{\frac{b_j(t)}{\tilde{\delta}}\right\}\right] \\ &= \mathrm{E}[\ln R_0(t)]. \end{aligned} \tag{2.11}$$

The population growth rate of j is:

$$g_j(E_j, C) = \ln\left\{(1-\tilde{\delta}) + e^{E_j - C}\right\}.$$

First, let us obtain non-additivity of the resident using a population subdivision scheme. For this model, the most meaningful division would be a subpopulation of new recruits and a subpopulation of adults surviving from the previous time period:

$$\begin{aligned} G_{j1} &= 1-\tilde{\delta}, \\ G_{j2} &= e^{E_j - C}. \end{aligned}$$

Note that G_j sums to one, since the resident is always at equilibrium It is easy to see that by applying the technique from section 2.2.3 we get:

$$\begin{aligned} \alpha_{j1} &= \beta_{j1} = \gamma_{j1} = 0, \\ \alpha_{j2} &= \beta_{j2} = 1, \text{and} \\ \gamma_{j2} &= 0, \end{aligned}$$

such that:

$$\begin{aligned} \bar{\alpha}_j &= \bar{\beta}_j = \tilde{\delta}, \\ \bar{\gamma}_j &= 0, \end{aligned}$$

and:

$$\gamma_{jo} = -\tilde{\delta}(1-\tilde{\delta}).$$

When we transform this into standardised non-additivity we get:

$$\gamma_j = \frac{\gamma_{jo}}{\bar{\alpha}_j \bar{\beta}_j} = 1 - \frac{1}{\tilde{\delta}} < 0,$$

which means that the resident shows sub-additivity unless $\tilde{\delta} = 1$. The longer the expected lifetime, the less sensitive the population growth rate is to the environment, competition, and the interaction between the environment and competition.

From the definition of E_j and C, it is easy to see that $\mathrm{cov}[E_j, C] = \mathrm{var}[E_j] = \sigma^2$. The covariance between the standard environment parameter and the standard competition parameter (χ_{jj}^{-i}) can be calculated in terms of the original parameters (see (Chesson 1989)) as:

$$\begin{aligned} \chi_{jj}^{-i} &\approx \mathrm{cov}[E_j, C]\bar{\alpha}_j\bar{\beta}_j \\ &\approx \sigma^2\tilde{\delta}^2. \end{aligned}$$

The covariance in terms of standard parameters declines with longer expected lifetime.

A detailed description of this technique can be found in (Chesson 1989; Chesson 1994). The formula for $\bar{r}_i$ for the two-species NLM with symmetric death rates is found by substituting γ_j and χ_{jj}^{-i} into equation 2.4:

$$\frac{\bar{r}_i}{\tilde{\delta}} \approx \mathrm{E}[E_i] - \mathrm{E}[E_j] + \sigma^2(1-\tilde{\delta}), \tag{2.12}$$

with:

$$\begin{aligned} \Delta E &= (\mathrm{E}[E_i] - \mathrm{E}[E_j])\,\tilde{\delta}, \\ \Delta C &= 0, \text{and} \\ \Delta I &= \left(\sigma^2(1-\tilde{\delta})\right)\tilde{\delta}. \end{aligned}$$

The third term of equation 2.12 is the storage effect, whose value is non-zero only if the birth rate fluctuates, i.e., $\sigma^2 > 0$, and generations overlap, i.e., $\tilde{\delta} < 1$. Moreover, expected lifetime, which is equal to $1/\tilde{\delta}$, directly affects the strength of the storage effect through its effect on sub-additivity. The smaller the $\tilde{\delta}$, the stronger the sub-additivity. Also contributing the magnitude of the storage effect in the NLM is the magnitude of birth rate fluctuations, quantified by σ^2. Comparison of models in which organisms have different expected lifetimes is complicated by the fact that dynamics are naturally expected to be slower with longer expected lifetimes. This effect can be factored out by using the long-term population growth rate per generation as in the equation 2.12. Then comparisons can focus more effectively on other consequences of a longer expected lifetime. For example, in 2.12 we see that the expected lifetime has effects over and above those accounted for by speed of dynamics.

From equation 2.12, the condition for coexistence, to keep $\bar{r}_i > 0$, is:

$$\sigma^2 > \frac{-\left(\mathrm{E}\left[\ln b_i\right] - \mathrm{E}\left[\ln b_j\right]\right)}{(1-\tilde{\delta})}, \tag{2.13}$$

assuming $\mathrm{E}[\ln b_i] - \mathrm{E}[\ln b_j] < 0$, i.e., that the invader is the one with the smaller mean ln birth rate. Note that invasion automatically occurs if the resident has the smaller mean ln birth rate, and so this case is trivial and will not be mentioned further. The magnitude of birth rate fluctuation required for coexistence is larger with the larger death rate (i.e., small values of $1 - \tilde{\delta}$). Table 2.3.2 summarises the changes in some parameters with the increasing expected lifetime in the NLM.

	Notation	$\tilde{\delta}\downarrow$
Sensitivity to the environment	α_j	$\downarrow$
Sensitivity to competition	β_j	$\downarrow$
Sub-additivity (original)	$\lvert\gamma_{j0}\rvert$	$\downarrow$
Sub-additivity (standardised)	$\lvert\gamma_j\rvert$	$\uparrow$
Covariance between the environment and competition (original)	$\mathrm{cov}[E_j, C]$	$-$
Covariance between the environment and competition (standardised)	χ_{jj}^{-i}	$\downarrow$
Mean of competition	$\mathrm{E}[C]$	$\uparrow$
Population growth rate of the invader per unit time	$\bar{r}_i$	$\uparrow$
Coexistence criterion		$\downarrow$

Table 2.1: Summary of pattern of some parameters of the NLM with increasing expected lifetime ($\downarrow$=decrease or more easily satisfied, $\uparrow$=increase, $-$=not affected).

2.3.3 Simulation results

In this study, the birth rate $(b_i(t))$, is a lognormally distributed random variable with variance σ^2. There is no correlation between the birth rates of species i and species j, and temporal autocorrelation is also zero. We define the resident (j) and the invader (i) such that $\mathrm{E}[\ln b_i] < \mathrm{E}[\ln b_j]$. Throughout the study of the NLM, $\mathrm{E}[\ln b_j] = 0$ so $\mathrm{E}[\ln b_i] < 0$, and $\mathrm{E}[\ln b_i] - \mathrm{Eln}\, b_j]$ is denoted by μ. Note that μ alone is important–the separate values of the $\mathrm{E}[\ln b]$ are irrelevant to the dynamics of the model. The number of independent simulations and the length of each simulation are calculated such that the standard error of $\bar{r}$ between each simulation is less than 0.001. Twelve independent simulations,

each with a 2000 unit time length, are sufficient for all data sets.

Figure 2-2 shows the robustness of the approximation (equation 2.12) in terms of quantitative prediction. The magnitude of the long-term population growth rate of the invader ($\bar{r}_i$), from the quadratic approximation is close to that produced by simulations for variance up to 0.5. The maximum standard error of the simulation result of $\bar{r}_i$ is 0.002 for expected lifetime 9 and $\sigma^2 = 0.5$. The longer the expected lifetime, the higher the accuracy of quantitative prediction. The level of difference in μ and variance will be held as in the figure 2-2 throughout this chapter.

The coexistence criterion is expressed in terms of the magnitute of fluctuations in birth rate required for a zero long-term population growth rate of the invader. The coexistence criterion is expected to be more easily satisfied with longer expected lifetime (equation 2.13). This can also be seen from the figure 2-2, where the lines produced by several levels of σ^2 shift to the left with longer expected lifetime (from expected lifetime 9 (figure 2-2(a)) to 15 (figure 2-2(b))). With longer expected lifetime, the coexistence criterion is relaxed, meaning that the invader can tolerate more severe disadvantage relative to the resident, with a lower magnitude of fluctuation in the birth rate, without going extinct.

2.4 Conclusion

The Non-structured Lottery Model (NLM), which was originally developed to model coral reef fish communities (Chesson and Warner 1981), has been studied and used for various purposes in a number of modified forms.

For the purpose of understanding the more general theoretical concept, the storage effect (Chesson 1989; Chesson 1994; Chesson and Huntly 1997), the NLM has served well because of its simplicity. The NLM serves as a clear example of how the sensitivities to competition and environment may vary within a population. In the NLM, this variation in sensitivities arises simply from the division of the population into juveniles and adults, and the fact that juveniles need to compete for space to mature, while adults do not compete.

In this chapter I have discussed the NLM as a theoretical tool for understanding ecological concepts, rather than a practical tool for investigating real ecological systems. In the following chapters, I will ask whether further insights into the storage effect can be gained by adding age/size structure to the NLM, as recently suggested by Hatfield and Chesson (1997).

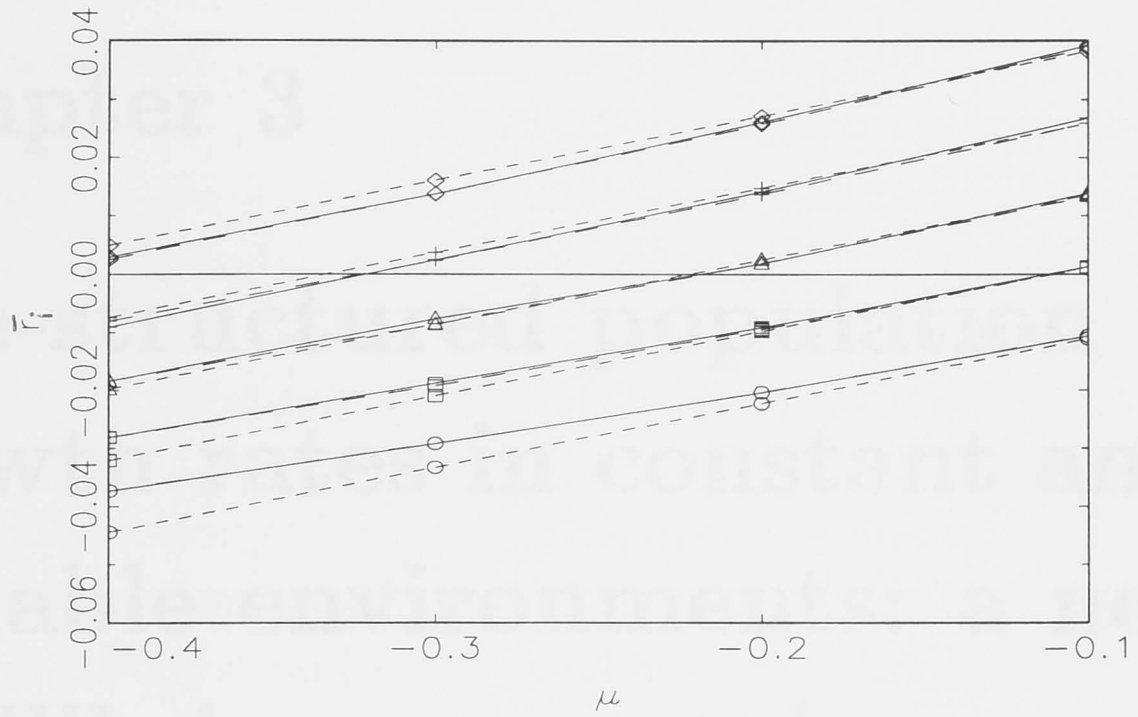

(a)

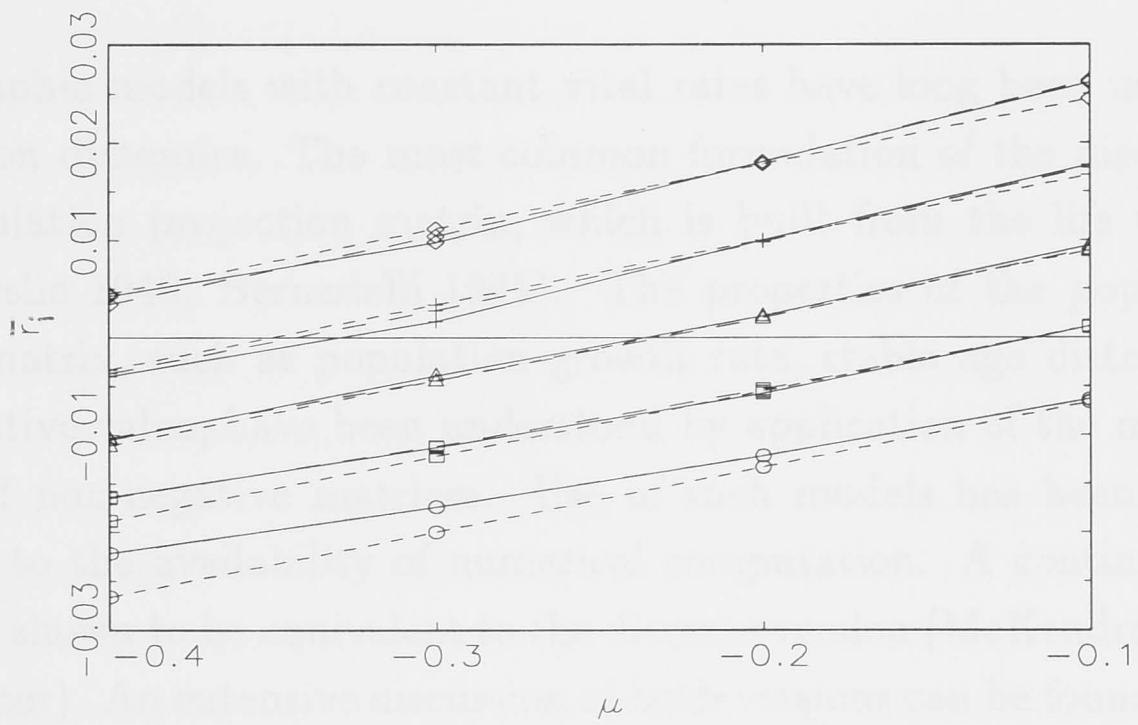

(b)

Figure 2-2: Long-term population growth rate of the invader ($\bar{r}_i$) from simulations (solid), equation 2.12 (short dashes), numerical integration of equation 2.8 (long dashes) with expected lifetime 9 (a) and 15 (b). σ^2 equals 0 ($\circ$), 0.125 ($\square$), 0.25 ($\triangle$), 0.375 ($+$) and 0.5 ($\diamond$).

Chapter 3

Age-structured population growth rates in constant and variable environments: a near equilibrium approach

3.1 Introduction

Demographic models with constant vital rates have long been used to study population dynamics. The most common formulation of the discrete form is the population projection matrix, which is built from the life table (Leslie 1945; Leslie 1948; Bernadelli 1941). The properties of the population projection matrix, such as population growth rate, stable age distribution, and reproductive value, have been understood by application of the mathematical theory of non-negative matrices. Use of such models has been very extensive due to the availability of numerical computation. A continuous version has been shown to be equivalent to the discrete version (McKendrick-von Foerster, Fisher). An extensive discussion of both versions can be found in (Caswell 1989; Charlesworth 1994).

Demographic models can be applied to the study of life-history evolution because the properties of their population projection matrices (Leslie matrices), especially population growth rates, can serve as a fitness measure. To put a model into the framework of life-history evolution, we must first choose a fitness measure. The question of whether there exists any general measure of fitness has been discussed elsewhere (e.g., de Jong 1994; Kozlowski 1993), with the conclusion that there is no such general fitness measure. In fact, a fitness

measure is simply a tool, and must be chosen carefully for each specific system under study (Stearns 1992). For a demographic model with birth and death processes only, the choice is generally not difficult. Commonly, the Malthusian parameter, also called the intrinsic rate of increase and the population growth rate (r), is adopted as the fitness measure in such models (Fisher 1930; Lande 1982; Charlesworth 1994; Cole 1954). Some authors use the expected lifetime reproduction as the fitness measure. However, this measure requires that the population under study is always at equilibrium (Kozlowski 1993). Cole (1954) pioneered the study of life-history evolution by developing evolutionary predictions from a demographic model using the population growth rate as the fitness measure.

Since Cole's study, the study of life-history evolution has become extensive. With the development of sensitivity and elasticity analysis techniques by Caswell (1978), it has become possible to study the changes in fitness with changes in each element of the vital rates. Evolution of senescence, optimum age of maturity, benefits of being annual, biennial, or perennial, and other similar questions have been explored (Stearns 1992; Roff 1992; Charlesworth 1994). Caswell (1982) also applied sensitivity analysis to macroparameter analysis where mortality and fecundity schedules are specified by parametric families.

Also several concepts have been tested by assuming that there is a trade-off in reproductive effort between different age classes. This reproductive effort approach has itself been explored extensively, with the general finding that maximising fitness is equivalent to maximising the reproductive value at each age class. Schaffer (1974) showed qualitatively for general cases of trade-offs whether the population growth rate will be maximised for iteroparous or semelparous reproductive strategies.

Ideally, life-history evolution theory should connect a life-history trait, which is more likely to be determined by genes and subject to natural selection than an individual class characteristic, to a fitness measure. However, because there is no quantitative measure to summarise the details of vital rates in different classes, the theory cannot proceed in this way directly. Nevertheless, in some cases a trait that is subject to strong selective pressure conveniently can be specified by a single parameter. Age at maturity is an example of such trait. To date more detailed and more general traits, such as mortality and fecundity schedules, which control death rate and birth rate for each age class, have not been quantified in such a way that the selective pressure on those traits can be assessed in a general way. Instead, sensitivity analysis is commonly applied

to a single element of the vital rates, e.g., the death rate of a particular age class. This does not lead to any general conclusions about the mortality schedule, because the death rate of a particular class cannot represent the whole mortality schedule.

In this chapter I propose a simple approach to this issue, by summarising the age-dependent vital rates into shape measures that can map the trait onto the population growth rate (r). The proposed technique is restricted to cases in which the population growth rate is low (a near equilibrium approach). One might question the benefits of a measure with such a restriction. With constant vital rates, the population reaches the stable age distribution and grows exponentially with constant r (strong ergodicity). This simply means that the population will become very large if the growth rate is positive, and will become extinct if the growth rate is negative. This phenomenon is certainly not common in nature, except in specific situations, such as after strong disturbance. I believe that density dependent mechanisms play the most important role in preventing r from being very large. Models with density dependence, together with fluctuating vital rates, are therefore more realistic.

The shape measure, or the Δ-measure, that I introduce here provides a simple functional relationship between the mortality/fecundity schedules, age-structureless population characteristics, and the population growth rate. The functional relationship is easy to interpret and produces an accurate qualitative pattern with moderate numerical accuracy. I anticipate that this shape measure of mortality and fecundity schedules can also give new insight into life-history evolution, at least qualitatively. Moreover, the shape measure can be used to explore the effects of population structure on competition in a variable environment as shown in later chapters.

In a variable environment, where the vital rates fluctuate, strong ergodicity cannot be retained, but stochastic ergodicity holds (Cohen 1977) whenever the projection matrices follow a Markov process. A quadratic approximation to the long-term population growth rate for small variance has been developed (Tuljapurkar 1982; Tuljapurkar 1990; Tuljapurkar 1997), and will be applied here to calculate the long-term population growth rate, using examples with fluctuations only in the birth rate.

We are able to apply the shape measure in such demographic models by assuming that the age distribution fluctuates around the stable age distribution. This assumption is valid when only fecundity is variable, because then the fluctuations in population density or age structure propagate from the first

age class. This means that the collection of adult stages of a long-lived organism is less vulnerable to environmental fluctuations than the juvenile stage, assuming there are fewer juvenile stages. In this study I will show that life-history traits can be linked to change in population growth rates in a variable environment, as they can be in a constant environment.

3.2 General demographic models

The standard, discrete-time demographic model in a constant environment is written in terms of a Leslie matrix as follows:

$$\mathbf{P}(t+1) = \mathbf{L}\mathbf{P}(t), \tag{3.1}$$

where

$\mathbf{P}$ is a column vector of population density of each class at time t, and:

$$\mathbf{L} = \begin{pmatrix} b_1 & b_2 & b_3 & \cdots & b_s \\ (1-\delta_1) & 0 & 0 & \cdots & 0 \\ 0 & (1-\delta_2) & 0 & \cdots & 0 \\ \vdots & \vdots & \ddots & \cdots & \vdots \\ 0 & 0 & \cdots & (1-\delta_{s-1}) & (1-\delta_s) \end{pmatrix},$$

where b_x is the birth rate of an individual in the age range x to $x+1$, and δ_x is the probability of an individual in that class dying in one unit of time.

Note that the above matrix formulation can accommodate an infinite number of age classes by defining $b_{s+j} = b_s$ and $\delta_{s+j} = \delta_s$ for $j \geq 0$. The non-zero value in the last element of the last row means that an individual can live and reproduce indefinitely, with a constant death rate and birth rate, after it has reached the age $s-1$. The behaviour of the model is well understood, (e.g., Caswell 1989). Asymptotically in time, each subpopulation (i.e., each age class) grows at exactly the same rate, r, which is the ln of the dominant eigenvalue of $\mathbf{L}$. The analysis relies on the stable age distribution theorem, first shown by Euler and Lotka. The population approaches a stable age distribution, and the proportion of the population in age class x is:

$$\frac{e^{-rx} l_x}{\sum_{x=1}^{\infty} e^{-rx} l_x}, \tag{3.2}$$

where

$l_x = \prod_{i=1}^{x-1}(1-\delta_i)$ is the probability of an individual surviving to age x.

When the population is stationary ($r = 0$), equation 3.2 is simply the stationary age distribution:

$$\frac{l_x}{\sum_{x=1}^{\infty} l_x}, \tag{3.3}$$

where
$\sum_{x=1}^{\infty} l_x$ is the expected lifetime, and $1/\sum_{x=1}^{\infty} l_x$ is the death rate corresponding to this expected lifetime in a non-structured model. I shall refer to it as the "non-structured" death rate and will denote it by $\tilde{\delta}$. With this notation, the stationary age distribution can be written as $\tilde{\delta} l_x$. I will also introduce a distribution of age at death for any given cohort of individuals ($\delta_x l_x$),which is closely related to the stationary age distribution. Note that both distributions sum to 1, i.e., both are probability distributions.

Defining $P.(t+1)$ to be the total population size, equation 3.1 implies:

$$P.(t+1) = \sum_{x=1}^{\infty} b_x P_x(t) + \sum_{x=1}^{\infty} (1 - \delta_x) P_x(t). \tag{3.4}$$

I will work more extensively with equation 3.4 later.

If the vital rates are not age-dependent, then $b_x = \tilde{b}$, and $\delta_x = \tilde{\delta}$ for all x, and equation 3.4 is reduced to the simplest birth and death processes:

$$P.(t+1) = (1 + \tilde{b} - \tilde{\delta}) P.(t).$$

3.3 Structured mortality

Let us consider a specific case of equation 3.4, with age-independent reproduction ($b_x = \tilde{b}$ for all x), and a mortality schedule following the classification of survivorship curves presented by Pearl and Minner (Roff 1992). Type I, II and III mortality schedules result respectively from increasing δ_x, constant δ_x, and decreasing δ_x with age. Type I, II, and III mortality schedules result respectively in concave, linear, and convex $\ln l_x$.

With age-independent reproduction, equation 3.4 can be written as:

$$P.(t+1) = \tilde{b} P.(t) + \sum_{x=1}^{\infty} (1 - \delta_x) P_x(t). \tag{3.5}$$

When the population attains a stable age distribution, equation 3.5 can be re-expressed as:

$$\begin{aligned} P.(t+1) &= \tilde{b} P.(t) + \left(\sum_{x=1}^{\infty} (1 - \delta_x) \frac{e^{-rx} l_x}{\sum_{y=1}^{\infty} e^{-ry} l_y} \right) P.(t) \\ &= \left(1 + \tilde{b} - \hat{\delta}\right) P.(t), \end{aligned} \tag{3.6}$$

where:

$$\begin{aligned}\hat{\delta} &= \frac{\sum_{x=1}^{\infty}\delta_x l_x e^{-rx}}{\sum_{x=1}^{\infty} l_x e^{-rx}} \\ &= \tilde{\delta}\frac{\sum_{x=1}^{\infty}\delta_x l_x e^{-rx}}{\sum_{x=1}^{\infty}\tilde{\delta} l_x e^{-rx}}. \end{aligned} \tag{3.7}$$

The expression 3.7 is the average death rate. Note that $\tilde{\delta}$ is the age-independent death rate as in the previous section.

Using equation 3.6, the population growth rate can be written as:

$$\begin{aligned} r &= \ln\left\{\frac{P_{\cdot}(t+1)}{P_{\cdot}(t)}\right\} \\ &= \ln\left\{1+\tilde{b}-\hat{\delta}\right\}. \end{aligned} \tag{3.8}$$

Note that $\hat{\delta}/\tilde{\delta}$ is a ratio of Laplace transforms of the two different age distributions, age at death and stationary age. Provided each transform exists in a neighbourhood of $r = 0$, we obtain:

$$\frac{\hat{\delta}}{\tilde{\delta}} = \frac{\sum_{n=0}^{\infty}\frac{(-r)^n}{n!}\mu_n(\delta_x l_x)}{\sum_{n=0}^{\infty}\frac{(-r)^n}{n!}\mu_n(\tilde{\delta} l_x)}, \tag{3.9}$$

where

$\mu_n(p_x) = \sum_{x=1}^{\infty} x^n p_x$ is the n^{th} moment of the probability distribution $\{p_x\}$.

Using the ratio theorem for power series (Gradshtein and Ryzhik 1980), I obtain:

$$\hat{\delta} = \tilde{\delta}\sum_{n=0}^{\infty}(-r)^n\Delta_m^{(n)}, \tag{3.10}$$

where:

$$\begin{aligned}\Delta_m^{(0)} &= 1, \\ \Delta_m^{(1)} &= \mu_1(\delta_x l_x) - \mu_1(\tilde{\delta} l_x), \\ \Delta_m^{(2)} &= \frac{1}{2}\left(\left(\mu_2(\delta_x l_x) - \mu_2(\tilde{\delta} l_x)\right) - \left(\mu_1(\delta_x l_x) - \mu_1(\tilde{\delta} l_x)\right)\mu_1(\tilde{\delta} l_x)\right), \\ \Delta_m^{(n)} &= \frac{\mu_n(\delta_x l_x)}{n!} - \sum_{k=1}^{n}\Delta_m^{(n-k)}\frac{\mu_k(\tilde{\delta} l_x)}{k!} \text{ for } n > 0. \end{aligned}$$

Independent of r, the Δ_ms are characteristics of a mortality schedule. There are two important uses of these characteristics. Firstly, the Δ_ms give shape measures for the sequence of mortality rates in terms of the difference between two distributions, namely the distribution of age at death for any given cohort of individuals $(\delta_x l_x)$, and the stationary age distribution $(\tilde{\delta} l_x)$. Examples of

type I, II, and III mortality schedules with their $\Delta_m^{(1)}$ are shown in figure 3-1. Secondly, by using the formula for the average death rate, $\hat{\delta}$, expressed by the Δ_ms, age-structured population dynamics can be reduced to simple, non-structured dynamics (equation 3.8). The average death rate is not independent of r but the power series equation for $\hat{\delta}$ enables a first order approximation to r i.e., to $o(r)$ by a linear approximation to equation 3.8 in r. Potentially more accurate higher order approximations to r are also available from polynomial approximations of equation 3.8, but their practical utility seems limited.

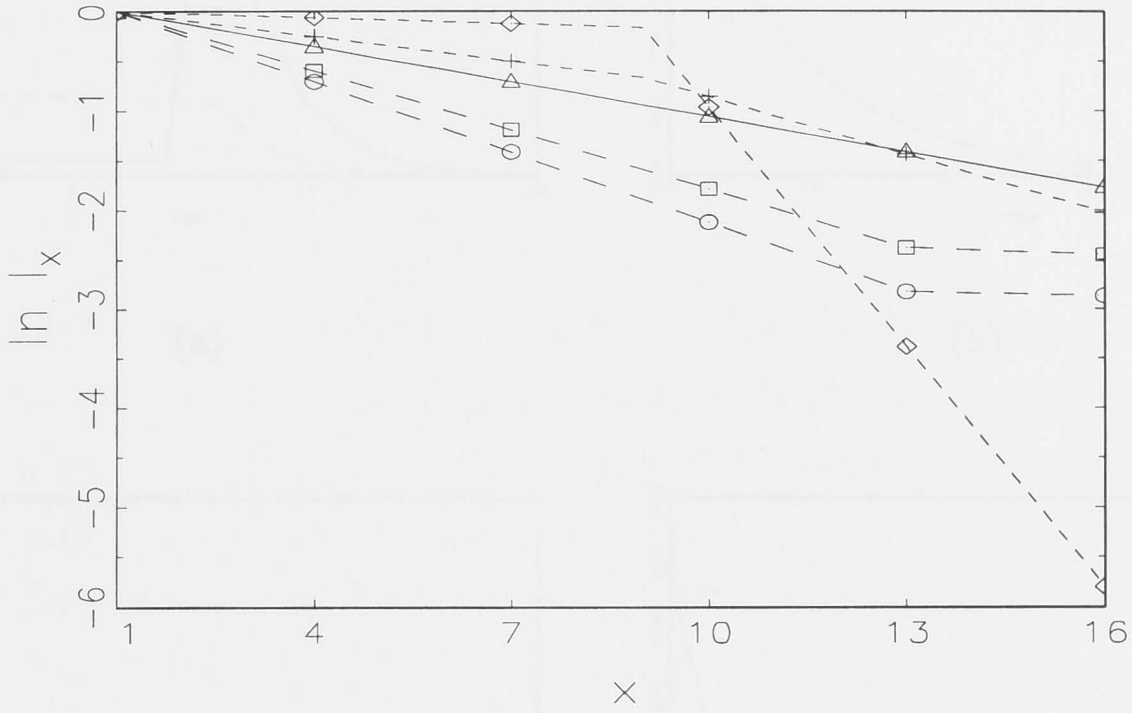

Figure 3-1: Mortality schedules of type I (short dashes) with $\Delta_m = 0.2025$ (+), $\Delta_m = 0.4086$ ($\diamond$), of type II ($\Delta_m = 0$) (solid, $\triangle$) and of type III (long dashes) with $\Delta_m = -4.1589$ ($\circ$), $\Delta_m = -1.9485$ ($\square$).

In general, the $\Delta_m^{(n)}$ depend on differences of moments, up to order n, of the two distributions. $\Delta_m^{(1)}$ measures the difference between the mean age at death for any given cohort of individuals and the mean age of a stationary population, and $\Delta_m^{(2)}$ measures half the difference between the variances of the two distributions plus half the square of $\Delta_m^{(1)}$:

$$\Delta_m^{(2)} = \frac{1}{2}\left[\mathrm{var}(\delta_x l_x) - \mathrm{var}(\tilde{\delta} l_x) + \left(\Delta_m^{(1)}\right)^2\right]. \tag{3.11}$$

These measures will be referred to as shape measures, or Δ-measures.

Figure 3-2 shows some examples of the two age distributions for different mortality schedules. For all distribution figures in this thesis, $y-$axis is relative frequency. For a type II mortality schedule (figure 3-2(b)), the two distributions coincide and so all the moments are equivalent. Therefore, the

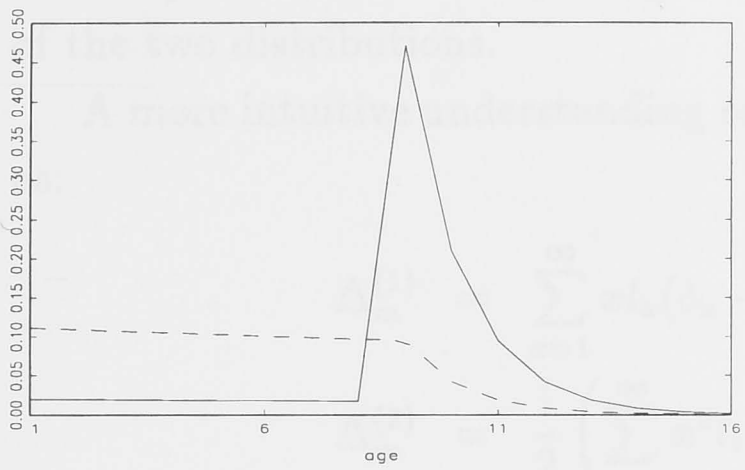

(a)

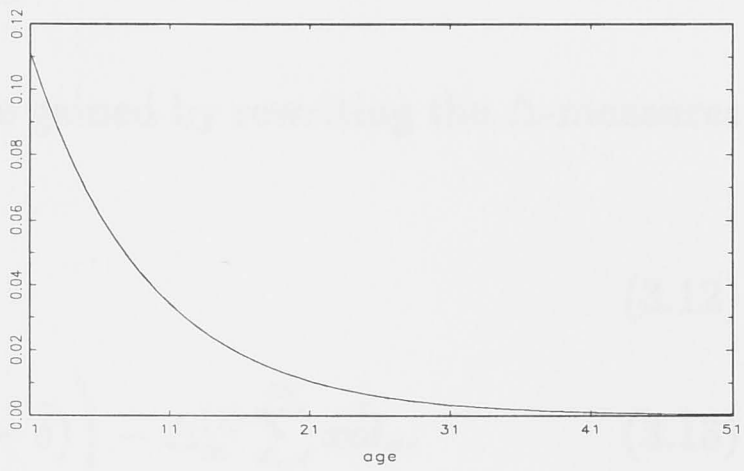

(b)

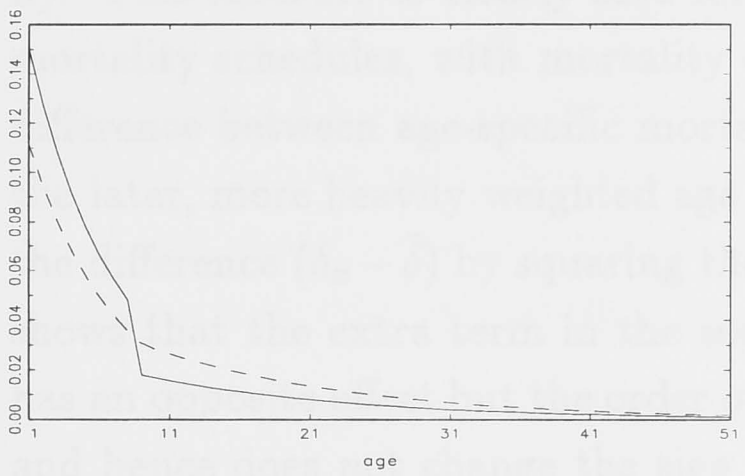

(c)

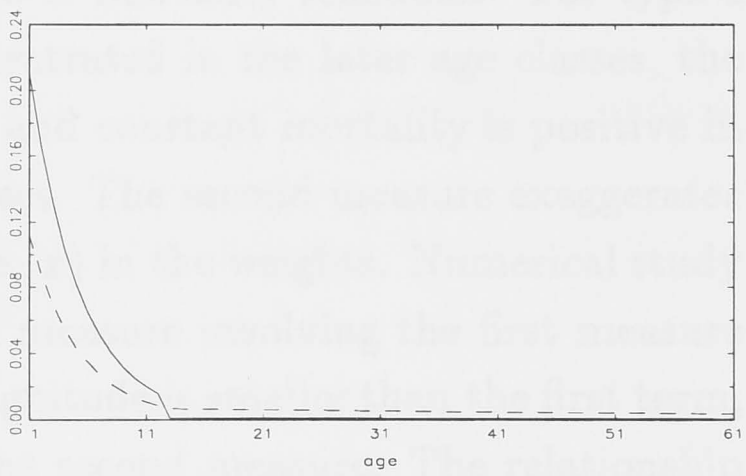

(d)

Figure 3-2: The distribution of cohort age at death, $\delta_x l_x$, (solid) and of stationary age, $\tilde{\delta} l_x$ (dashes) for a type I mortality schedule with $\Delta_m = 0.409$ (a), a type II mortality schedule (b), a type III mortality schedule with $\Delta_m = -0.410$, (c) and a type III mortality schedule with $\Delta_m = -4.1587$ (d), for expected lifetime = 9.

Δ_ms are all zero. For type III mortality schedules (figure 3-2(c) and 3-2(d)), the mean cohort age at death is smaller than mean age of a stationary population, which results in negative $\Delta_m^{(1)}$. Moreover, numerical investigation has consistently shown that the variance of cohort age at death is smaller than the variance of the stationary age distribution, plus the square of $\Delta_m^{(1)}$, which results in negative $\Delta_m^{(2)}$. Type I mortality schedules can be generated with a fixed expected lifetime only if $\Delta_m^{(1)}$ and $\Delta_m^{(2)}$ are small, because of the behaviour of the two distributions.

A more intuitive understanding can be gained by rewriting the Δ-measures as:

$$\Delta_m^{(1)} = \sum_{x=1}^{\infty} x l_x (\delta_x - \tilde{\delta}) \tag{3.12}$$

$$\Delta_m^{(2)} = \frac{1}{2}\left(\sum_{x=1}^{\infty} x^2 l_x (\delta_x - \tilde{\delta})\right) - \Delta_m^{(1)} \sum_{x=1}^{\infty} x\tilde{\delta} l_x. \tag{3.13}$$

The first measure sums the age-specific deviations from constant mortality, weighted by xl_x, which means that later age classes are weighted more heavily. This measure is clearly zero for type II mortality schedules. For type I mortality schedules, with mortality concentrated in the later age classes, the difference between age-specific mortality and constant mortality is positive in the later, more heavily weighted age classes. The second measure exaggerates the difference $(\delta_x - \tilde{\delta})$ by squaring the age (x) in the weights. Numerical study shows that the extra term in the second measure involving the first measure has an opposite effect but the order of magnitude is smaller than the first term, and hence does not change the sign of the second measure. The relationship between the Δ-measure and the three mortality schedules can be summarised as:

$$\Delta_m^{(n)} \begin{cases} > 0 & \text{for type I mortality schedule} \\ = 0 & \text{for type II mortality schedule} \\ < 0 & \text{for type III mortality schedule,} \end{cases} \tag{3.14}$$

for $n = 1, 2$. Expressions 3.12 and 3.13 give us a concise quantitative classification of mortality schedules.

I will now use the $\Delta_m^{(1)}$ measure to an approximation for r in the presence of structured mortality. By truncating the series 3.10 for the average death rate at the second term, we obtain:

$$\hat{\delta} = \tilde{\delta}(1 - r\Delta_m^{(1)}) + o(r). \tag{3.15}$$

Substituting for $\hat{\delta}$ in equation 3.8 we get:

$$r = \ln\left\{1 + \tilde{b} - \tilde{\delta} + \tilde{\delta}\Delta_m^{(1)} r\right\} + o(r), \tag{3.16}$$

which rearranges to

$$\begin{aligned} r &= \ln\left\{1 + \tilde{b} - \tilde{\delta}\right\} + \ln\left\{1 + \frac{\tilde{\delta}\Delta_m^{(1)} r}{1 + \tilde{b} - \tilde{\delta}}\right\} \\ &= \ln\left\{1 + \tilde{b} - \tilde{\delta}\right\} + \frac{\tilde{\delta}\Delta_m^{(1)}}{1 + \tilde{b} - \tilde{\delta}} r + o(r) \\ &= \tilde{r} + \frac{\tilde{\delta}\Delta_m^{(1)}}{1 + \tilde{b} - \tilde{\delta}} r + o(r), \end{aligned} \tag{3.17}$$

where:

$$\tilde{r} = \ln\{1 + \tilde{b} - \tilde{\delta}\}.$$

Solving equation 3.17 for r we get:

$$r = \frac{\tilde{r}}{1 - \tilde{\delta}\Delta_m^{(1)}/(1 + \tilde{b} - \tilde{\delta})} + o(r). \tag{3.18}$$

The quantity $\tilde{r}$ is the population growth rate for a type II mortality schedule, with the constant mortality rate equal to $\tilde{\delta}$.

In this study, to keep the algebra simple, I will use the following mortality functions with only two levels of death rate:

$$\delta_x = \begin{cases} \delta_1 & \text{for } x \leq s \\ \left[(1 - \delta_1)^{s-1}\delta_1\right] / \left[\delta_1/\tilde{\delta} - 1 + (1 - \delta_1)^s\right] & \text{for } x > s. \end{cases} \tag{3.19}$$

With fixed expected lifetime $(1/\tilde{\delta})$, formula 3.19 has two free parameters, the early death rate (δ_1), and the last age having the early death rate, (s). By varying these parameters, type I, II and III mortality schedules can be generated with a common expected lifetime. The procedure for the graphs below was to vary these two parameters over a rectangular grid of values. The measure $\Delta_m^{(1)}$ for each mortality schedule was calculated from equation 3.12. This procedure generates a range of $\Delta_m^{(1)}$ values, and it is possible to find different mortality schedules with similar $\Delta_m^{(1)}$ and different $\Delta_m^{(2)}$. However, here we will only consider $\Delta_m^{(1)}$ because it is all that appears in the approximation for r. In the graphs below of r against $\Delta_m^{(1)}$ there is a scatter of values attributable to the effects of varying values of $\Delta_m^{(2)}$ for fixed $\Delta_m^{(1)}$. In this study, the expected lifetime is held constant as a constraint, so that comparisons between mortality

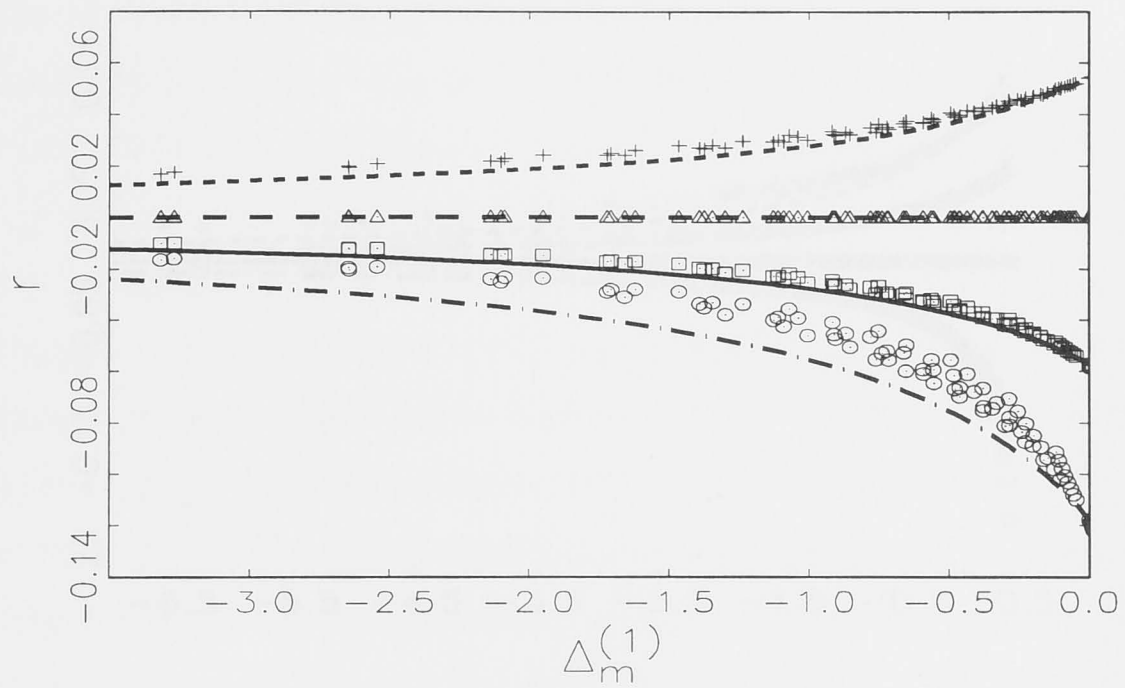

(a)

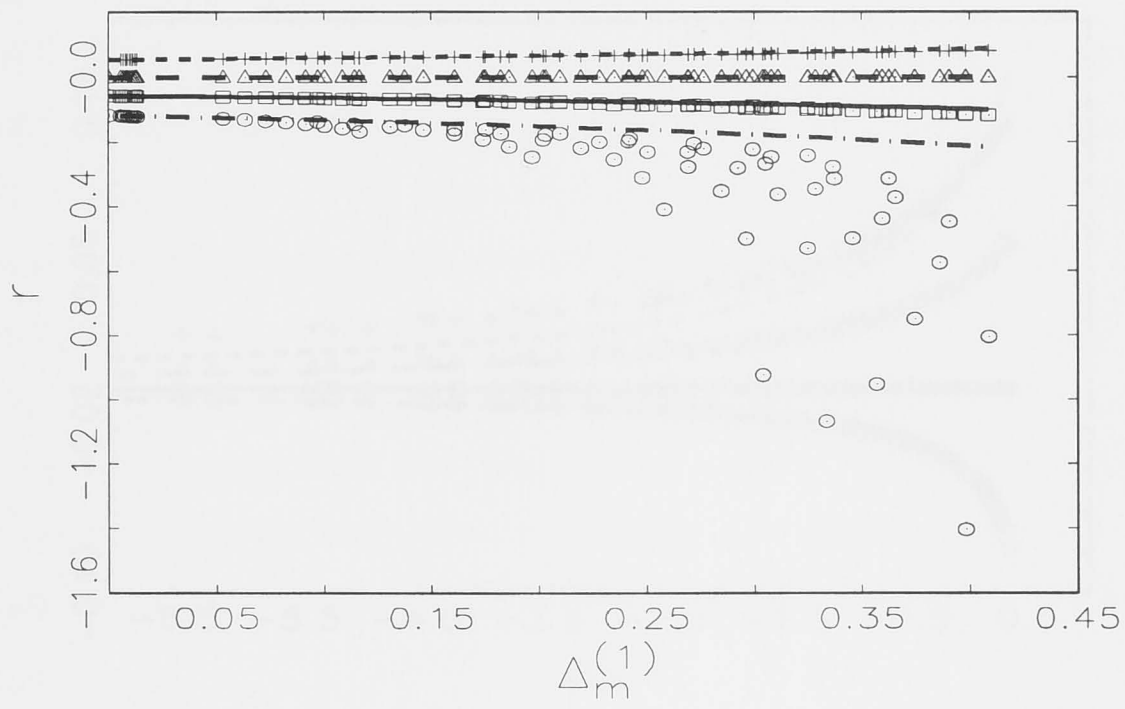

(b)

Figure 3-3: Population growth rate (r) with mortality schedules of type III (a) and type I (b) with expected lifetime = 9, calculated as ln of the dominant eigenvalue of the projection matrix (symbols), and calculated from the first order approximation, equation 3.18 (lines). $\tilde{b}$ equals 0 ($\circ$, dashes and dots), 0.0556 ($\square$, solid), 0.1111 ($\triangle$, dashes) and 0.1667 ($+$, short dashes)
.

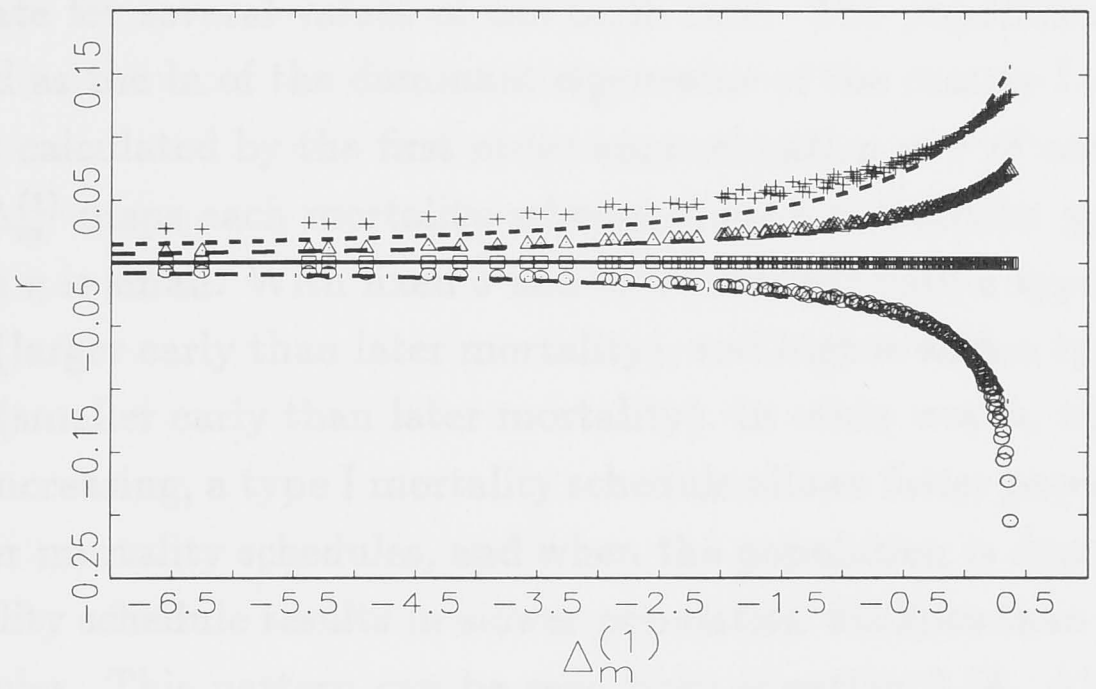

(a)

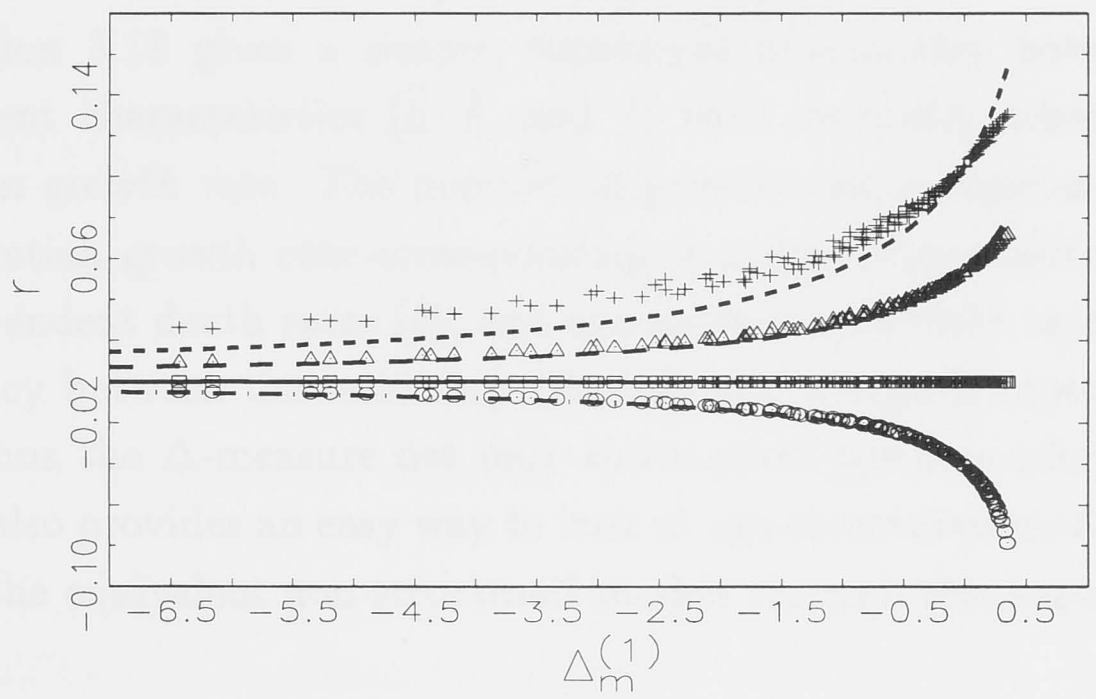

(b)

Figure 3-4: Population growth rate (r) with mortality schedules of expected lifetime = 15 (a) and expected lifetime = 25 (b), calculated as ln of the dominant eigenvalue of the projection matrix (symbols), and calculated from the first order approximation, equation 3.18 (lines). $\tilde{b}$ equals 0 ($\circ$, dashes and dots), 0.0667 ($\square$, solid), 0.1222 ($\triangle$, dashes) and 0.1778 ($+$, short dashes) .

schedules focus on the distribution of mortality over age classes rather than the magnitude of mortality, which is captured by the expected lifetime.

Figure 3-3 and 3-4 show the relationship between $\Delta_m^{(1)}$ and the population growth rate for several values of the birth rate. The population growth rate calculated as the ln of the dominant eigenvalue of the matrix $\mathbf{L}$ are compared with that calculated by the first order approximation of r of equation 3.18.

The $\Delta_m^{(1)}$ maps each mortality schedule into a population growth rate (r) well when r is small. With fixed $\tilde{\delta}$ and $\tilde{b}$, $|r|$ is lower with a type III mortality schedule (larger early than later mortality), and higher with a type I mortality schedule (smaller early than later mortality). In other words, when the population is increasing, a type I mortality schedule allows faster population growth than other mortality schedules, and when the population is decreasing, a type III mortality schedule results in slower population declines than other mortality schedules. This pattern can be seen from equation 3.18. Also, figures 3-3 and 3-4 show that the effect of age-dependent mortality on population growth rate is greater with greater $\tilde{\delta}$ (shorter lifespan). Therefore, for a population of long-lived organisms, the effect of structured mortality on population growth rate should only be evident when $\Delta_m^{(1)}$ is moderately large, i.e., when there is substantial deviation from a type II mortality schedule.

Equation 3.18 gives a simple, functional relationship between the age-independent characteristics ($\tilde{b}$, $\tilde{\delta}$, and $\tilde{r}$) with mortality schedules and the population growth rate. The population growth rate is expressed in terms of the population growth rate corresponding to a type II mortality schedule ($\tilde{r}$), age-independent death rates ($\tilde{\delta}$), and age-independent birth rates ($\tilde{b}$), and the discrepancy between the mortality schedule and a type II mortality schedule (Δ_m). Thus the Δ-measure not only summarises age-dependent characteristics, but also provides an easy way to look at age-structured models, by linking them to the equivalent non-structured models through the population growth rate.

Within the framework of life-history theory, by fixing the net reproductive rate, R_0, which is equal to $\tilde{b}/\tilde{\delta}$ here, varying the trade-offs within that constraint, we see varying effects on the population growth rate. By having an early high mortality rate and late low mortality rate (type III mortality schedule), some individuals that survive the early period will have a long lifespan. The effect of the type III mortality schedule on the population growth rate is, therefore, similar to that of expanding the reproductive lifespan. A type I mortality schedule affects the population growth rate similarly to reducing

the reproductive lifespan. It is widely recognised in the theory of life-history evolution that expanding the reproductive lifespan increases fitness when the population is decreasing, while reducing the reproductive lifespan decreases fitness when the population is increasing. Stearns (1992) stated that increases in the adult death rates and decreases in juvenile death rates (shortening of the reproductive lifespan, equivalent to type I mortality schedule in our setting) "increase the value of juveniles relative to adults" (p. 181-182). An interpretation of this statement is that juveniles contribute more to fitness than adults do. This will only be true in an increasing population, which is the case of most interest. That a type III mortality schedule is favoured in declining populations and a type I mortality schedule is favoured in increasing populations is also consistent with Caswell's findings (Caswell 1982).

One might question whether our constraint is biologically realistic. I have no simple answer, since there is no empirical evidence to support such a constraint. Similar difficulties occur in some well known studies which involve more complexity such as the reproductive effort (e.g., Schaffer 1974). However, by fixing the net reproductive rate we are assured that the comparison of models is performed within a very similar setting since, R_0 itself can be thought of as a useful fitness measure.

3.4 Structured fecundity

In this section, I will consider a standard demographic model with a structured fecundity. The fecundity schedule is expressed in terms of an overall fecundity level, $\tilde{b}$, which is an age-independent parameter, and age-dependent modulation of reproduction of age class x (k_x). The birth rate of age class x is $k_x\tilde{b}$.

I will first consider a model without structured mortality, i.e., $\delta_x = \tilde{\delta}$ for all x. I follow the idealisation of fecundity schedules given by Roff (1992). Consider four types of piecewise linear curve (figure 3-6) for the parameter k_x:

- Age-independent reproduction with $k_x = 1$ for all x
- Uniform fecundity, i.e., a juvenile period, with zero fecundity, followed by age-independent reproduction after maturity: $k_x = 0$ for $x < m$, and $k_x = k_m$ for $x \geq m$, where m is age of maturity
- Asymptotic fecundity schedule, i.e., an increasing k_x after the age of maturity and constant k_x after a maximum value is reached

- Triangular fecundity schedule, which is similar to the asymptotic schedule except that after the maximum value is attained, k_x declines until a certain age, after which it remains constant. Semelparity is a special case of the triangular schedule, in which the peak is reached at the age of maturity and k_x is zero in all subsequent age-classes. However, since our matrix approach for calculating the population growth rate as the real dominant eigenvalue requires primitivity for the Perron-Frobenius theorem to apply (see for example Caswell 1989), I will not discuss semelparity in relation to the population growth rate, but only in relation to the Δ_f.

The fecundity function can be restricted, such that $k_x\tilde{\delta}l_x$ is summed to one (probability distribution) by having $\sum_{x=1}^{\infty} k_x l_x = \sum_{x=1}^{\infty} l_x$. The effect of this constraint is to fix $R_0 = \tilde{b}/\tilde{\delta}$.

With this fecundity schedule, equation 3.4 can be written as:

$$P_{\cdot}(t+1) = \tilde{b}\sum_{x=1}^{\infty} k_x P_x(t) + (1-\tilde{\delta})P_{\cdot}(t). \tag{3.20}$$

Assuming a stable age distribution, equation 3.20 can be re-expressed as:

$$\begin{aligned} P_{\cdot}(t+1) &= \tilde{b}\left(\frac{\sum_{x=1}^{\infty} k_x e^{-rx} l_x}{\sum_{x=1}^{\infty} e^{-rx} l_x}\right) P_{\cdot}(t) + (1-\tilde{\delta})P_{\cdot}(t) \\ &= \left(1+\hat{b}-\tilde{\delta}\right) P_{\cdot}(t), \end{aligned} \tag{3.21}$$

where:

$$\hat{b} = \tilde{b}\frac{\sum_{x=1}^{\infty} \tilde{\delta} l_x k_x e^{-rx}}{\sum_{x=1}^{\infty} \tilde{\delta} l_x e^{-rx}}.$$

The term $\hat{b}$ is the average birth rate over age-classes.

From equation 3.21, the population growth rate is expressed as:

$$\begin{aligned} r &= \ln\left\{\frac{P_{\cdot}(t+1)}{P_{\cdot}(t)}\right\} \\ &= \ln\{1+\hat{b}-\tilde{\delta}\}. \end{aligned} \tag{3.22}$$

By applying the same techniques used in the previous section, the average birth rate ($\hat{b}$) can be expressed as:

$$\hat{b} = \tilde{b}\sum_{n=0}^{\infty}(-r)^n \Delta_f^{(n)}, \tag{3.23}$$

where:

$$\begin{aligned}
\Delta_f^{(0)} &= 1 \\
\Delta_f^{(1)} &= \mu_1(\tilde{\delta} l_x k_x) - \mu_1(\tilde{\delta} l_x) \\
\Delta_f^{(2)} &= \frac{1}{2}\left(\mu_2(\tilde{\delta} l_x k_x) - \mu_2(\tilde{\delta} l_x)\right) - \left[\mu_1(\tilde{\delta} l_x k_x) - \mu_1(\tilde{\delta} l_x)\right] \mu_1(\tilde{\delta} l_x), \\
\Delta_f^{(n)} &= \frac{\mu_n(\tilde{\delta} l_x k_x)}{n!} - \sum_{k=1}^{n} \Delta_f^{(n-k)} \frac{\mu_k(\tilde{\delta} l_x)}{k!} \text{ for } n > 0.
\end{aligned}$$

The two distributions compared using the Δ_f are the cohort age at reproduction ($\tilde{\delta} l_x k_x$), and the stationary age distribution ($\tilde{\delta} l_x$) (figure 3-5). Δ_f quantifies the deviation of a fecundity schedule from age-independent reproduction. The first measure ($\Delta_f^{(1)}$) describes the difference between mean age at reproduction and the mean age in a stationary population. The second measure ($\Delta_f^{(2)}$) describes the difference between the variances of the two distributions, plus an extra term which involves the first measure:

$$\Delta_f^{(2)} = \frac{1}{2}\left[\text{var}(\tilde{\delta} l_x k_x) - \text{var}(\tilde{\delta} l_x) + \left(\Delta_f^{(1)}\right)^2\right]. \tag{3.24}$$

I introduce some terms to describe fecundity schedules using Δ_f. Fecundity schedules are classified into three general classes based on the signs of the $\Delta_f^{(1)}$: (i) early peak reproduction when the majority of offspring are produced early in life (i.e., $\Delta_f^{(1)} < 0$), (ii) age-independent reproduction when reproduction is spread out evenly throughout the lifespan of an organism (i.e., $\Delta_f^{(1)} = 0$), and (iii) delayed peak reproduction when the majority of offspring are produced late in life (i.e., $\Delta_f^{(1)} > 0$). This classification does not exactly coincide with the four fecundity curves described above.

A more intuitive understanding of the measures is gained by rewriting Δ_f as:

$$\Delta_f^{(1)} = \sum_{x=1}^{\infty} x \tilde{\delta} l_x (k_x - 1) \tag{3.25}$$

$$\Delta_f^{(2)} = \frac{1}{2}\left(\sum_{x=1}^{\infty} x^2 \tilde{\delta} l_x (k_x - 1)\right) - \Delta_f^{(1)} \sum_{x=1}^{\infty} x \tilde{\delta} l_x. \tag{3.26}$$

The first measure ($\Delta_f^{(1)}$) expresses the difference between each age-dependent modulation of reproduction and constant reproduction (i.e., $k_x = 1$ for all age classes), weighted according to age class, such that more weight is applied to later age classes. Therefore, for constant fecundity, there is no difference in

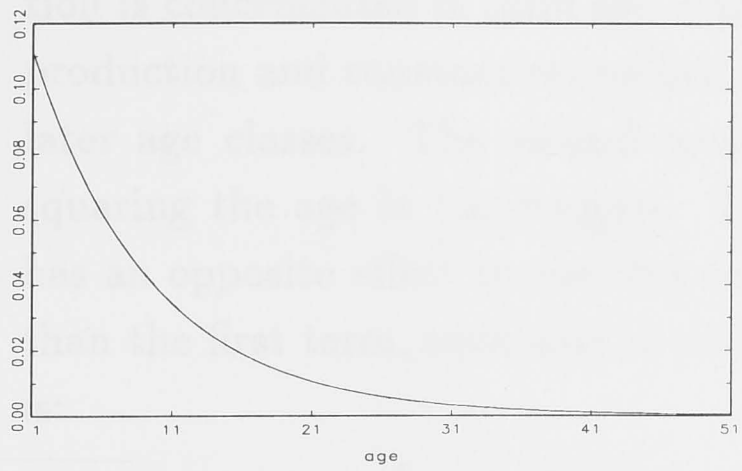

(a)

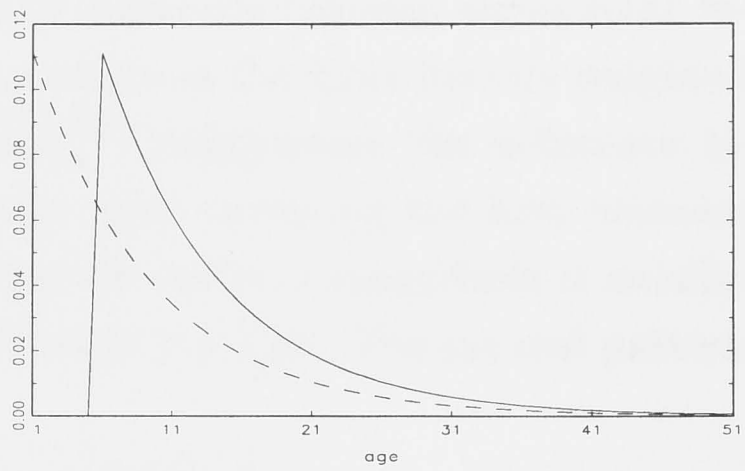

(b)

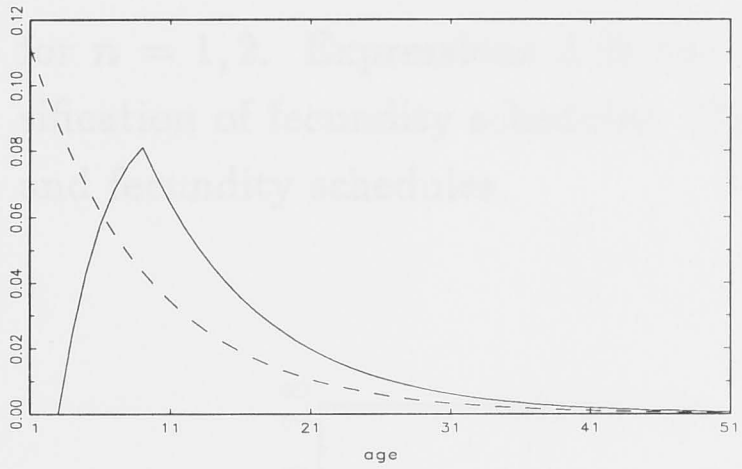

(c)

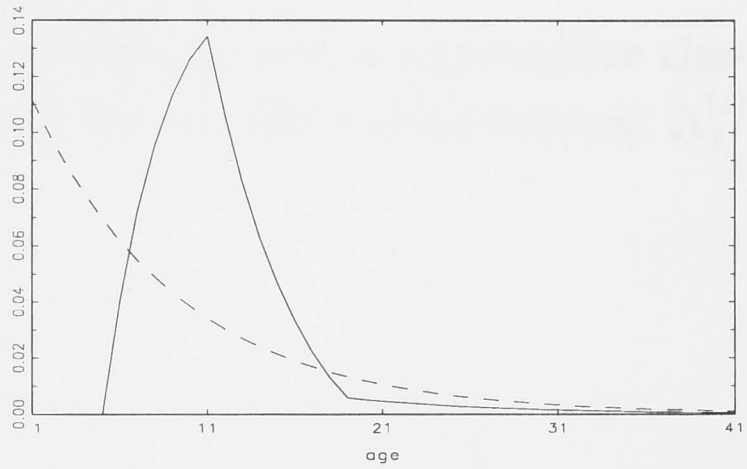

(d)

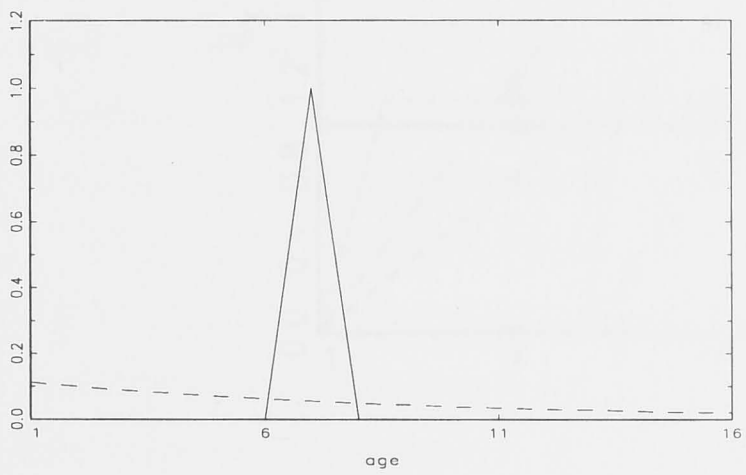

(e)

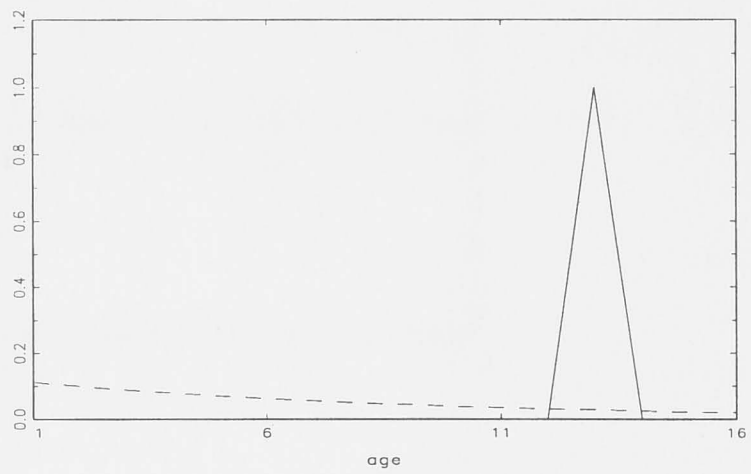

(f)

Figure 3-5: The distribution of cohort age at reproduction ($k_x\tilde{\delta}l_x$) (solid), and of stationary age ($\tilde{\delta}l_x$) (dashes) for age-independent reproduction (a), uniform curve with $\Delta_f = 5$ (b), asymptotic curve with $\Delta_f = 5.1594$ (c), triangular curve with $\Delta_f = 2.7455$ (d), semelparity with age at maturity of 7 with $\Delta_f = -2$ (e), and semelparity with age at maturity of 13 with $\Delta_f = 4$ (f), all with age-independent mortality and expected lifetime = 9.

reproduction between classes. For delayed peak reproduction, where reproduction is concentrated in later age classes, the difference between age-specific reproduction and constant reproduction is positive in the more heavily weighted later age classes. The second measure ($\Delta_f^{(2)}$) exaggerates the difference by squaring the age in the weights. The extra term involving the first measure has an opposite effect to the first term, but the order of magnitude is smaller than the first term, such that it will not change the sign. The general pattern is:

$$\Delta_f^{(n)} \begin{cases} > 0 & \text{for delayed peak reproduction} \\ = 0 & \text{for age-independent reproduction} \\ < 0 & \text{for early peak reproduction,} \end{cases} \tag{3.27}$$

for $n = 1, 2$. Expressions 3.25 and 3.26 provide us with a quantitative classification of fecundity schedules. Figure 3-6 shows relationships between $\Delta_f^{(1)}$ and fecundity schedules.

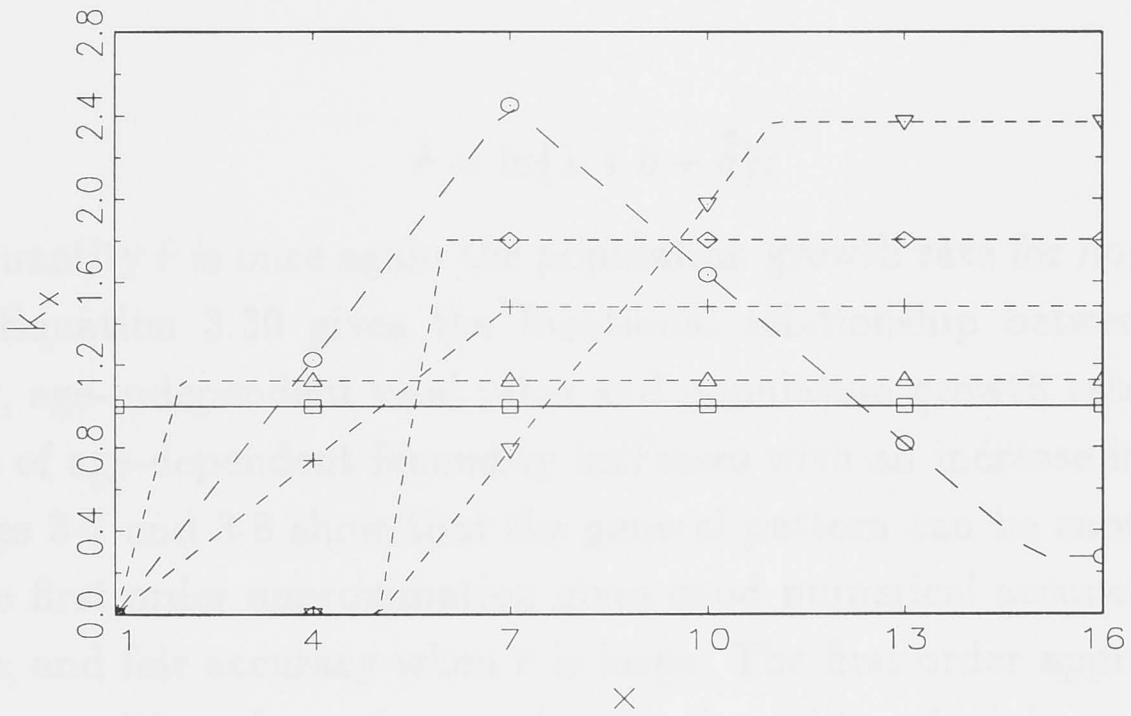

Figure 3-6: Age-dependent modulation of reproduction (k_x) for early peak reproduction (long dashes) with $\Delta_f = -1.2545$ ($\circ$), age- independent reproduction ($\square$), and delayed peak reproduction (dashes) with $\Delta_f = 1$ ($\triangle$), $\Delta_f = 3.1594$ ($+$), $\Delta_f = 5$ ($\diamond$), and $\Delta_f = 7.1594$ ($\triangledown$), when combined with a type II mortality schedule.

As in the previous section, only $\Delta_f^{(1)}$ will be considered as the measure of deviation of a fecundity schedule from age-independent reproduction, when exploring the relationship between fecundity schedules and the population growth

rates. The average birth rate, with fecundity schedule approximated by the first order of the Δ_f of equation 3.23, is:

$$\hat{b} = \tilde{b}\left(1 - r\Delta_f^{(1)}\right) + o(r). \tag{3.28}$$

By substituting equation 3.28 into equation 3.22 we get:

$$r = \ln\left\{1 + \tilde{b} - \tilde{b}\Delta_f^{(1)}r - \tilde{\delta}\right\} + o(r). \tag{3.29}$$

Solving equation 3.29, by taking the first order Taylor approximation of r in the neighborhood of $r = 0$, we get:

$$r = \ln\{1 + \tilde{b} - \tilde{\delta}\} - \frac{\tilde{b}\Delta_f^{(1)}}{1 + \tilde{b} - \tilde{\delta}}r + o(r),$$

which rearranges to

$$r = \frac{\tilde{r}}{1 + \left(\tilde{b}\Delta_f^{(1)}\right) / \left(1 + \tilde{b} - \tilde{\delta}\right)} + o(r), \tag{3.30}$$

where:

$$\tilde{r} = \ln\{1 + \tilde{b} - \tilde{\delta}\}.$$

The quantity $\tilde{r}$ is once again the population growth rate for non-structured model. Equation 3.30 gives the functional relationship between fecundity schedules, age-independent vital rates and population growth rate. Note that the effect of age-dependent fecundity increases with an increase in $\tilde{b}$.

Figures 3-7 and 3-8 show that the general pattern can be captured by the $\Delta_f^{(1)}$. The first order approximation gives good numerical accuracy when r is moderate, and fair accuracy when r is large. The first order approximation is less accurate with early peak reproduction fecundity schedule compared with delayed peak reproduction for similar magnitude of r. This indicates that early peak reproduction fecundity schedule, which are mostly produced by triangular shaped curves, cannot be measured adequately by the first order Δ-measure alone, while other fecundity schedules can be measured adequately using the first Δ-measure. This is not unexpected as the reproductive span for triangular curves is not as long as for other curves, and is thus more sensitive to the spread. Therefore, it is easy to produce different schedules with similar $\Delta_f^{(1)}$s and different $\Delta_f^{(2)}$s.

Delayed peak reproduction always gives smaller $|r|$ than early peak reproduction. When a population is increasing, delayed peak reproduction gives

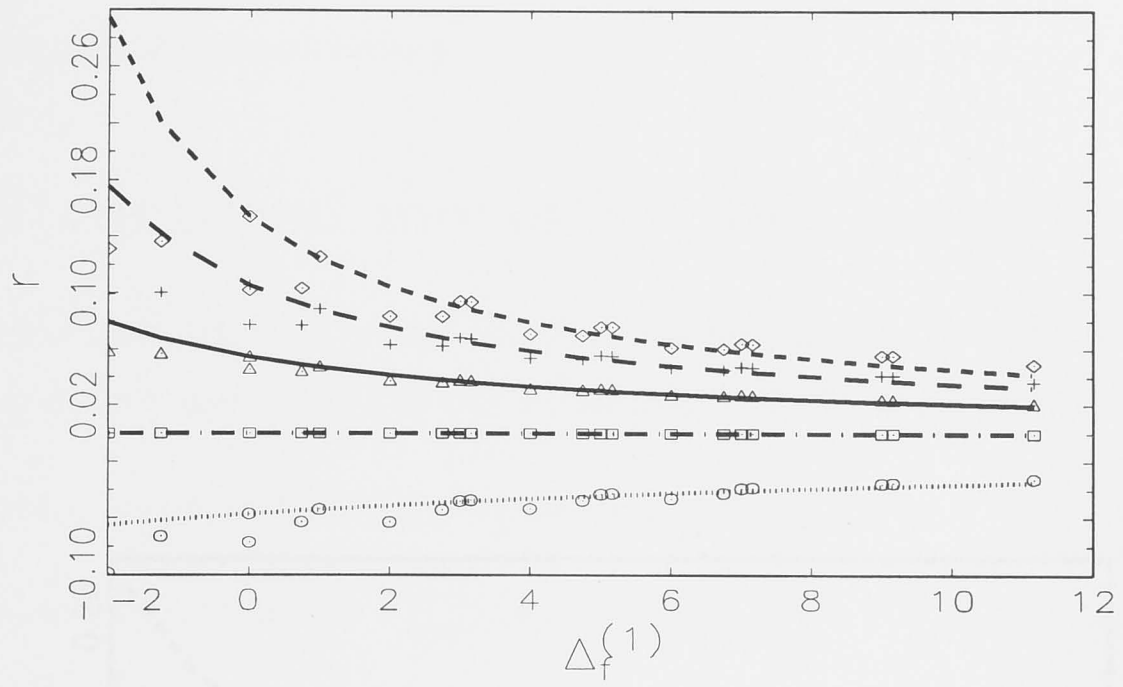

(a)

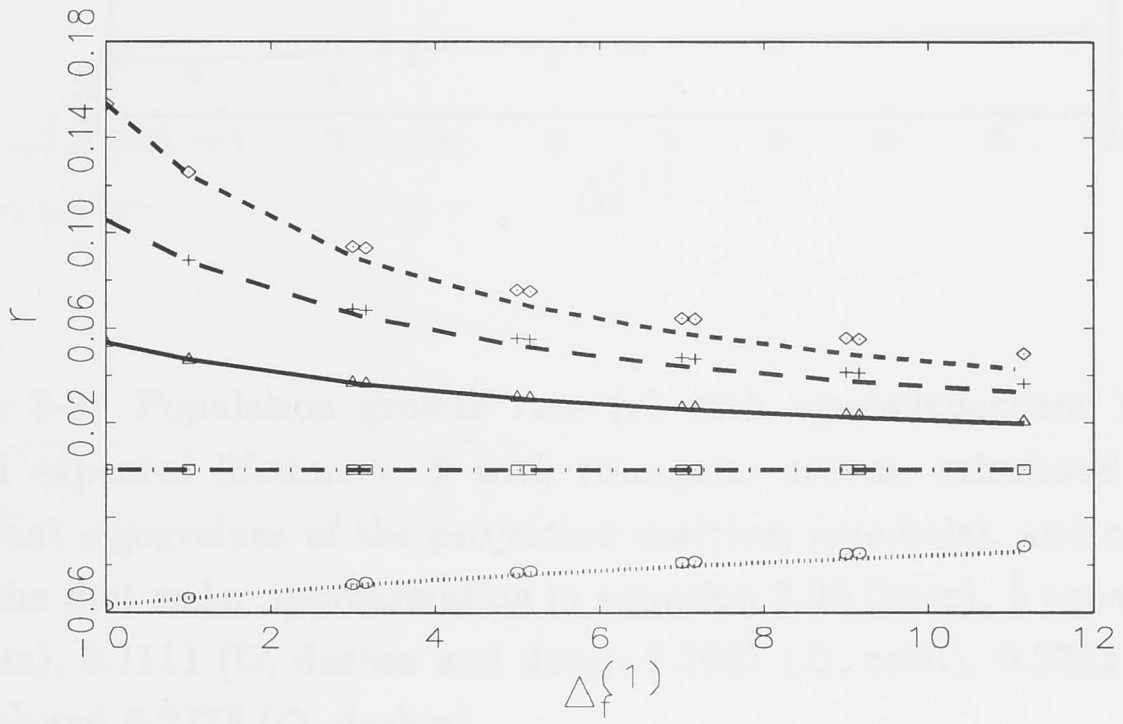

(b)

Figure 3-7: Population growth rate (r) with age-independent mortality of and expected lifetime = 9, for all fecundity schedules (a), and for fecundity schedules other than triangular curves (b), calculated as ln of dominant eigenvalues of the projection matrices (symbols), and calculated from the first order approximation in equation 3.30 (lines). $\tilde{b}$ equals 0.0556 ($\circ$, dots), 0.1111 ($\square$, dashes and dots), 0.1667 ($\triangle$, solid), 0.2222 ($+$, long dashes) and 0.2778 ($\diamond$, dashes).

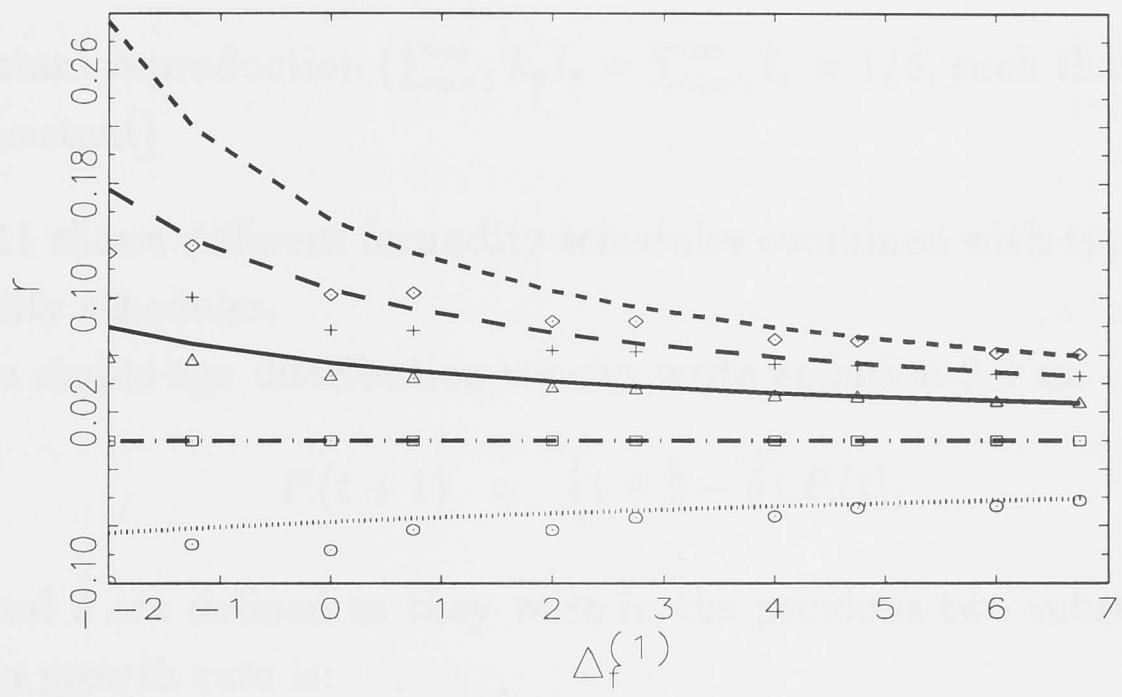

Figure 3-8: Population growth rate (r) with age-independent mortality of and expected lifetime = 9 with triangular curves, calculated as ln of dominant eigenvalues of the projection matrices (symbols), and calculated from the first order approximation in equation 3.30 (lines). $\tilde{b}$ equals 0.0556 ($\circ$, dots), 0.1111 ($\square$, dashes and dots), 0.1667 ($\triangle$, solid), 0.2222 ($+$, long dashes) and 0.2778 ($\diamond$, dashes).

lower r, and early peak reproduction gives higher r. The opposite pattern occurs in a decreasing population. This pattern is widely recognised and, shown to be robust in different settings. However, the overall quantitative pattern has not been determined before.

3.5 Structured mortality and fecundity

I now include both mortality and fecundity schedules in the demographic model by simultaneously applying the two constraints that have been used previously:

- constant expected lifetime at equilibrium ($\sum_{x=1}^{\infty} l_x = 1/\tilde{\delta}$)
- constant reproduction ($\sum_{x=1}^{\infty} k_x l_x = \sum_{x=1}^{\infty} l_x = 1/\tilde{\delta}$, such that $\tilde{b}\sum_{x=1}^{\infty} l_x k_x$ is constant)

Figure 3-11 shows different fecundity schedules combined with type I and type III mortality schedules.

With a stable age distribution we can write equation 3.4 as:

$$P_{\cdot}(t+1) \;=\; \left(1+\hat{b}-\hat{\delta}\right) P_{\cdot}(t), \tag{3.31}$$

where $\hat{b}$ and $\hat{\delta}$ are defined as they were in the previous two subsections. The population growth rate is:

$$r = \ln\left\{1+\hat{b}-\hat{\delta}\right\}. \tag{3.32}$$

Applying the first order Δ-measures, $\Delta_m^{(1)}$ and $\Delta_f^{(1)}$, as shape measures of the mortality and fecundity schedules, we get:

$$r = \ln\left\{1+\tilde{b}\left(1-r\Delta_f^{(1)}\right)-\tilde{\delta}\left(1-r\Delta_m^{(1)}\right)\right\}+o(r). \tag{3.33}$$

The first order Taylor approximation of equation 3.33 is:

$$r = \ln\left\{1+\tilde{b}-\tilde{\delta}\right\} - \frac{\tilde{b}\Delta_f^{(1)}-\tilde{\delta}\Delta_m^{(1)}}{1+\tilde{b}-\tilde{\delta}}r+o(r). \tag{3.34}$$

Solving equation 3.34 for r gives:

$$r \approx \frac{\tilde{r}}{1+(\tilde{b}\Delta_f^{(1)}-\tilde{\delta}\Delta_m^{(1)})/(1+\tilde{b}-\tilde{\delta})}, \tag{3.35}$$

where:

$$\tilde{r} = \ln\{1+\tilde{b}-\tilde{\delta}\}.$$

The term $\tilde{r}$ is the population growth rate for the non-structured model. Age-dependent fecundity and age-dependent mortality together will produce more subtle results since now we must consider the difference in magnitude between age-independent mortality ($\tilde{\delta}$), and age-independent fecundity ($\tilde{b}$). The effects of the mortality and fecundity schedules on the population growth rate are expressed using shape measures scaled by the magnitude of age-independent birth rate ($\tilde{b}$) and death rate ($\tilde{\delta}$). Figures 3-9 and 3-10 show the three distributions: (i) stationary age, (ii) cohort age at death, and (iii) cohort age at reproduction.

Equation 3.35 shows that the type III mortality schedule with delayed peak reproduction is favored in decreasing populations, and the the type I mortality schedule with the early peak reproduction is favoured in increasing populations. This is consistent with common belief. It is expected that the population growth rate with semelparous organisms and a type III mortality schedule will be sensitive to age at maturation. Early peak reproduction, when majority of offspring is produced at the age younger than the mean age at stationarity results in positive population growth rate, whereas delayed peak reproduction results in negative population growth rate for the same R_0, given that $\Delta_m^{(1)}$ is held constant.

3.6 Stochastic demographic models

I will now consider the same demographic model as 3.1, but with temporal fluctuations in birth rates as follows:

$$\mathbf{P}(t+1) = \mathbf{L}(t)\mathbf{P}(t), \tag{3.36}$$

where $\mathbf{P}(t)$ is the column vector of population density of each class at time t, and:

$$\mathbf{L}(t) = \begin{pmatrix} \tilde{b}(t)k_1 & \tilde{b}(t)k_2 & \tilde{b}(t)k_3 & \cdots & \tilde{b}(t)k_s \\ (1-\delta_1) & 0 & 0 & \cdots & 0 \\ 0 & (1-\delta_2) & 0 & \cdots & 0 \\ \vdots & \vdots & \ddots & \cdots & \vdots \\ 0 & 0 & \cdots & (1-\delta_{s-1}) & (1-\delta_s) \end{pmatrix}.$$

The term $\tilde{b}(t)$ varies with time, allowing fecundity to vary with both age and time. The term k_x is the modulation of reproduction at age x, and the term δ_x is the probability that an individual will die at age x to $x+1$.

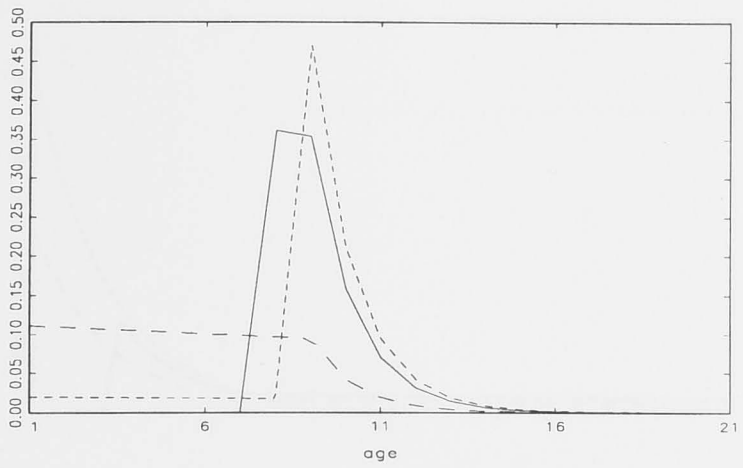

(a)

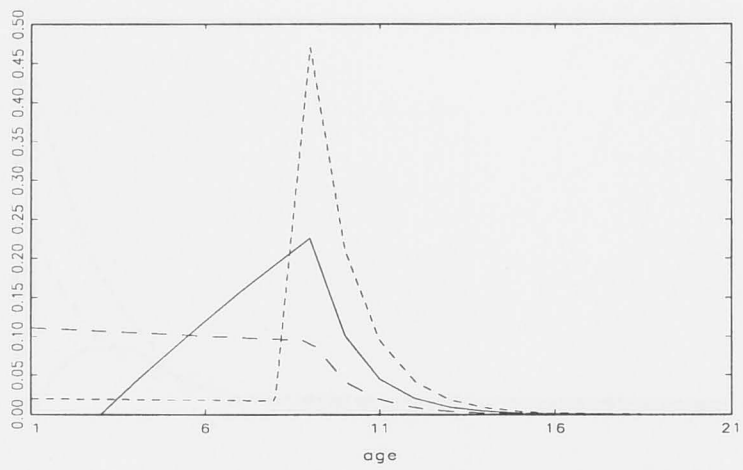

(b)

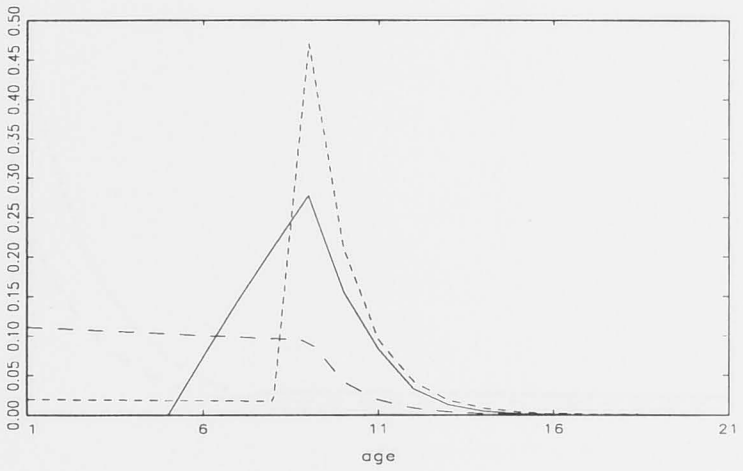

(c)

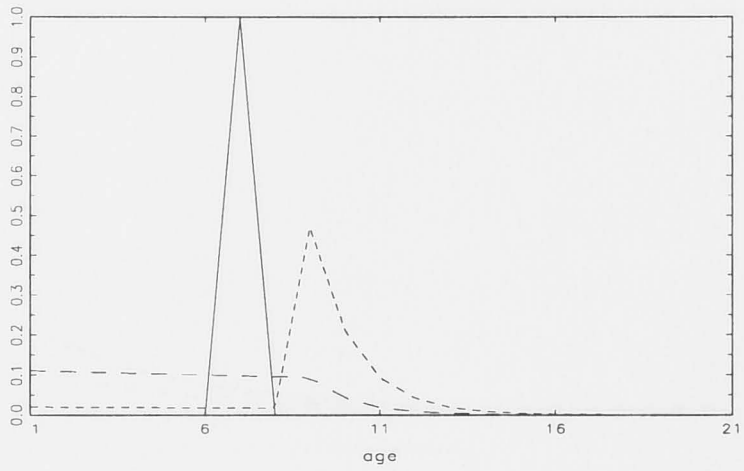

(d)

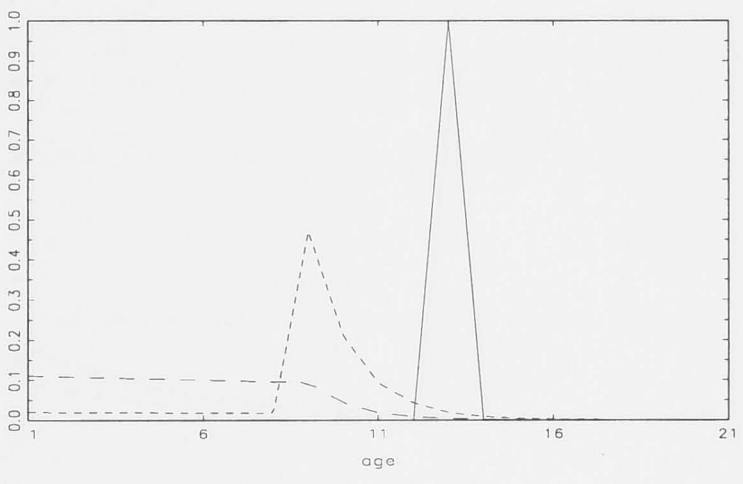

(e)

Figure 3-9: The distribution of cohort age at reproduction ($\tilde{\delta} l_x k_x$) (solid), cohort age at death ($\delta_x l_x$) (dashes), and stationary age ($\tilde{\delta} l_x$) (short dashes), for a uniform curve with $\Delta_f = 3.3836$ (a), an asymptotic curve with $\Delta_f = 2.6108$ (b), a triangular curve with $\Delta_f = 3.4733$ (c), semelparity with age at maturity of 7 and $\Delta_f = 1.6807$ (d), and semelparity with age at maturity of 13 and $\Delta_f = 7.6807$ (e), all with a type I mortality schedule with $\Delta_m = 0.4086$ and expected lifetime $= 9$.

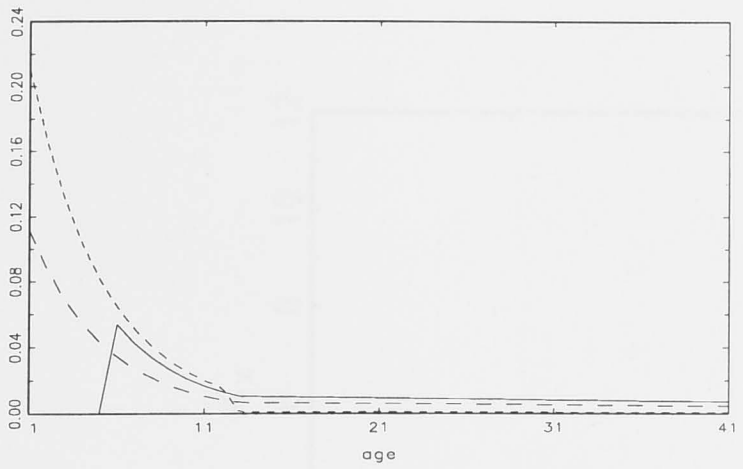

(a)

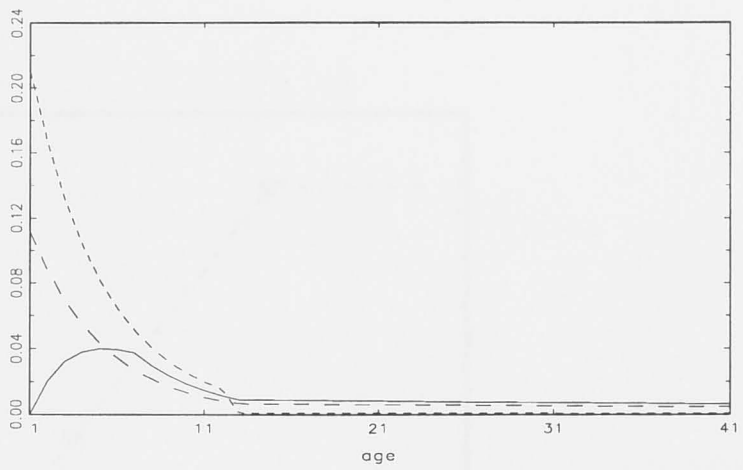

(b)

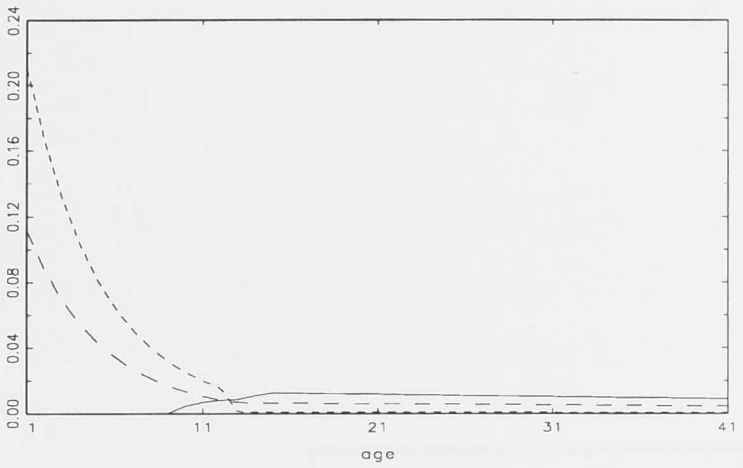

(c)

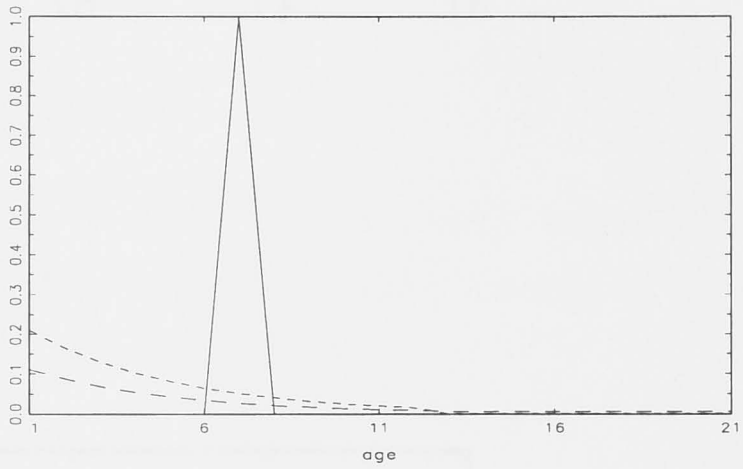

(d)

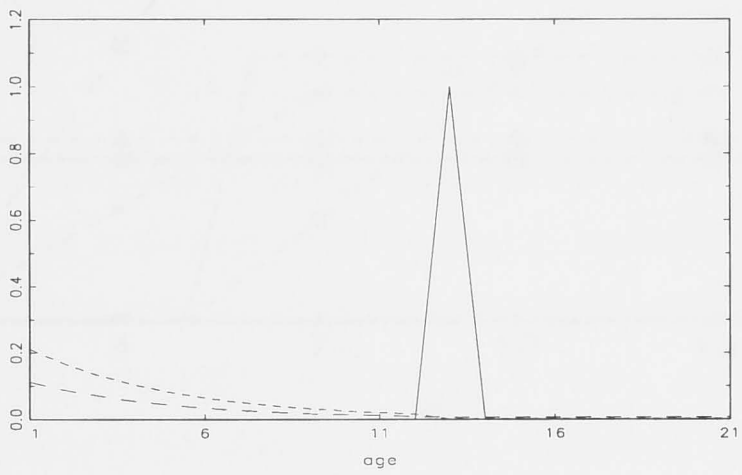

(e)

Figure 3-10: The distribution of cohort age at reproduction ($\tilde{\delta} l_x k_x$) (solid), cohort age at death ($\delta_x l_x$) (short dashes), and stationary age ($\tilde{\delta} l_x$) (dashes), for a uniform curve with $\Delta_f = 25.3683$ (a), an asymptotic curve with $\Delta_f = 17.0295$ (b), a triangular curve with $\Delta_f = 41.0359$ (c), semelparity with age at maturity of 7 and $\Delta_f = -39.4277$ (d), and semelparity with age at maturity of 13 and $\Delta_f = -33.4277$ (e), all with a type III mortality schedule with $\Delta_m = -4.1589$ and expected lifetime $= 9$.

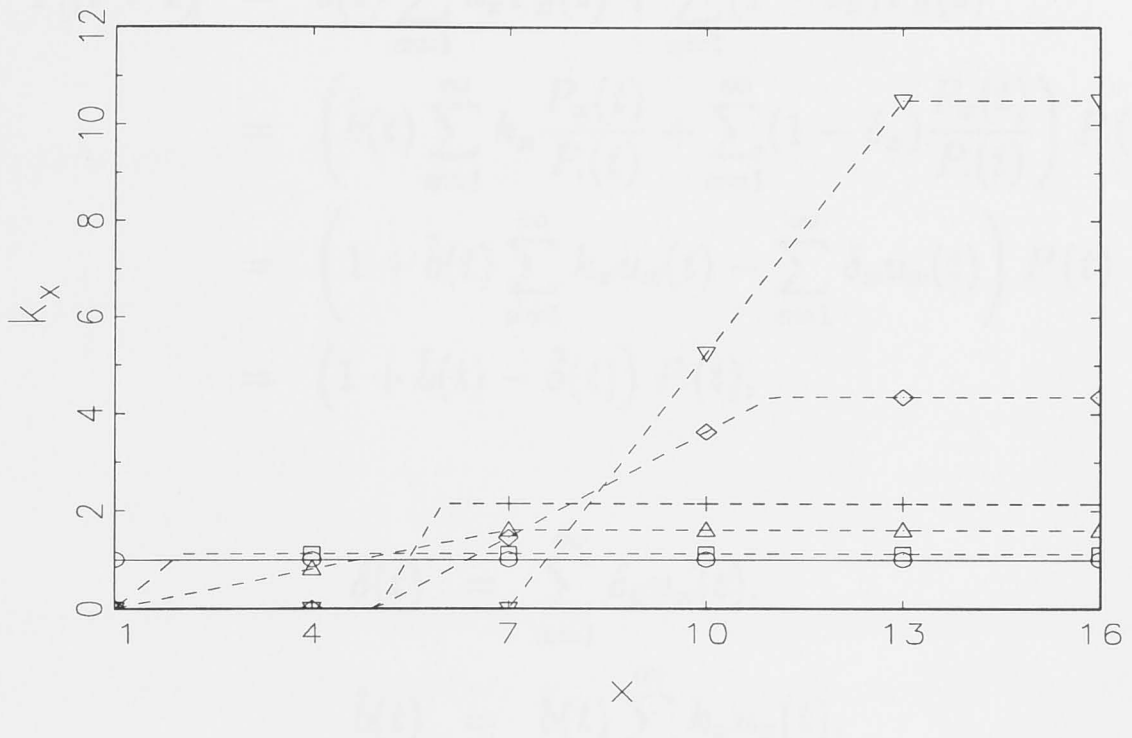

(a)

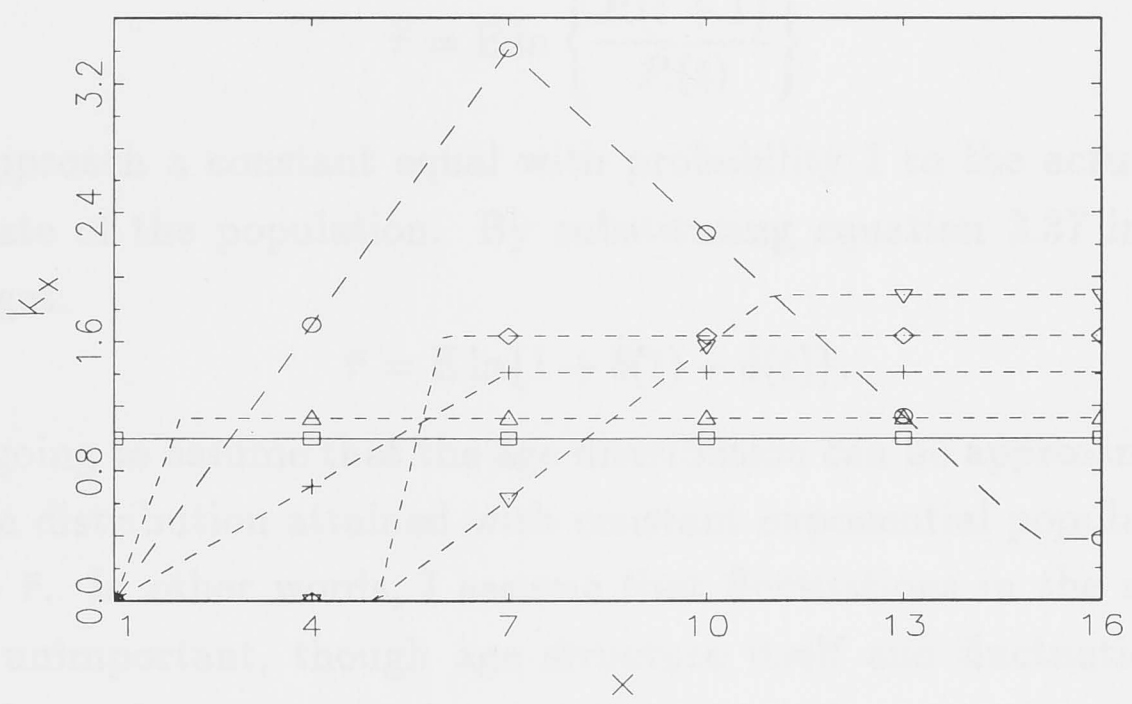

(b)

Figure 3-11: A type I mortality schedule with $\Delta_m = 0.4086$, with age-independent reproduction ($\circ$), and delayed peak reproduction, with $\Delta_f = 0.5399$ ($\square$), $\Delta_f = 1.6264$ ($\triangle$), $\Delta_f = 2.7015$ ($+$), $\Delta_f = 3.5373$ ($\diamond$), and $\Delta_f = 4.5645$ ($\triangledown$)(a). A type III mortality schedule with $\Delta_m = -1.9485$, early peak reproduction, with $\Delta_f = -12.2130$ ($\circ$), age- independent reproduction ($\square$), and delayed peak reproduction, with $\Delta_f = 3.1922$ ($\triangle$), $\Delta_f = 9.9659$ ($+$), $\Delta_f = 15.1978$ ($\diamond$), and $\Delta_f = 20.5213$ ($\triangledown$) (b).

With fluctuating reproduction, equation 3.4 is:

$$\begin{aligned} P_{\cdot}(t+1) &= \tilde{b}(t)\sum_{x=1}^{\infty} k_x P_x(t) + \sum_{x=1}^{\infty}(1-\delta_x)P_x(t) \\ &= \left(\tilde{b}(t)\sum_{x=1}^{\infty} k_x \frac{P_x(t)}{P_{\cdot}(t)} + \sum_{x=1}^{\infty}(1-\delta_x)\frac{P_x(t)}{P_{\cdot}(t)}\right) P_{\cdot}(t) \\ &= \left(1+\tilde{b}(t)\sum_{x=1}^{\infty} k_x u_x(t) - \sum_{x=1}^{\infty}\delta_x u_x(t)\right) P_{\cdot}(t) \\ &= \left(1+\hat{b}(t)-\hat{\delta}(t)\right) P_{\cdot}(t), \end{aligned} \tag{3.37}$$

where:

$$\begin{aligned} \hat{\delta}(t) &= \sum_{x=1}^{\infty}\delta_x u_x(t), \\ \hat{b}(t) &= \tilde{b}(t)\sum_{x=1}^{\infty} k_x u_x(t), \end{aligned}$$

and $\{u_x(t)\}$ is the actual age distribution at time t. Stochastic ergodicity theory (Lopez 1961; Cohen 1977) implies that $\{u_x(t)\}$ should converge in distribution and that, for large t, the quantity $(\bar{r})$ defined as:

$$\bar{r} = \mathrm{E}\ln\left\{\frac{P_{\cdot}(t+1)}{P_{\cdot}(t)}\right\} \tag{3.38}$$

should approach a constant equal with probability 1 to the actual long-term growth rate of the population. By substituting equation 3.37 into equation 3.38, we get:

$$\bar{r} = \mathrm{E}\ln\{1+\hat{b}(t)-\hat{\delta}(t)\}. \tag{3.39}$$

I am going to assume that the age distribution can be approximated by the stable age distribution attained with constant exponential population growth at a rate $\bar{r}$. In other words, I assume that fluctuations in the age distribution are unimportant, though age structure itself and fluctuations in birth rates both are important in determining population growth rates in fluctuating environments. There is no strong justification for such an assumption, but I would like to see if this assumption leads to an adequate technique for approximating $\bar{r}$.

With this assumption, I can use Δ_m and Δ_f from the previous sections to replace $\hat{\delta}$ and $\hat{k}$ in equation 3.39, to get the average population growth rate as follows:

$$\begin{aligned} \bar{r} &= \mathrm{E}\ln\left[\left\{1+\tilde{b}(t)(1-\bar{r}\Delta_f^{(1)}) - \tilde{\delta}(1-\bar{r}\Delta_m^{(1)}\right\}\right] + o(\bar{r}) \\ &= \mathrm{E}\ln\left[\left\{1+\tilde{b}(t)-\tilde{\delta}-\bar{r}\left(\tilde{b}(t)\Delta_f^{(1)} - \tilde{\delta}\Delta_m^{(1)}\right)\right\}\right] + o(\bar{r}). \end{aligned} \tag{3.40}$$

The first order Taylor expansion of expression 3.40 about $\bar{r} = 0$ is:

$$\bar{r} = \mathrm{E} \ln \left[\left\{ 1 + \tilde{b}(t) - \tilde{\delta} \right\} \right] - \mathrm{E} \left[\frac{\tilde{b}(t)\Delta_f^{(1)} - \tilde{\delta}\Delta_m^{(1)}}{1 + \tilde{b}(t) - \tilde{\delta}} \right] \bar{r} + o(\bar{r}). \tag{3.41}$$

Solving expression 3.41 for $\bar{r}$, we get:

$$\begin{aligned} \bar{r} &= \frac{\mathrm{E} \ln \left[\left\{ 1 + \tilde{b}(t) - \tilde{\delta} \right\} \right]}{1 + \mathrm{E} \left[(\tilde{b}(t)\Delta_f^{(1)} - \tilde{\delta}\Delta_m^{(1)})/(1 + \tilde{b}(t) - \tilde{\delta}) \right]} \\ &= \frac{\mathrm{E} \ln \left[\left\{ 1 + \tilde{b}(t) - \tilde{\delta} \right\} \right]}{1 + \mathrm{E} \left[\tilde{b}(t)/(1 + \tilde{b}(t) - \tilde{\delta}) \right] \Delta_f^{(1)} - \mathrm{E} \left[1/(1 + \tilde{b}(t) - \tilde{\delta}) \right] \tilde{\delta}\Delta_m^{(1)}}. \end{aligned}$$

Calculation of $\bar{r}$ will require some numerical integration. Instead, I will attempt to find a quadratic approximation of equation 3.40 by removing terms equal to $o(\bar{r})$.

Let b^* be the geometric mean of $\tilde{b}(t)$, i.e., $= e^{\mathrm{E} \ln \tilde{b}(t)}$ and $\sigma^2 = \mathrm{var}[\ln \tilde{b}(t)]$, and assume that $\mu = \mathrm{E}[\ln \tilde{b}(t) - \ln \tilde{\delta}] = O(\sigma^2)$. With this assumption, it follows from 3.41 that $\bar{r} = O(\sigma^2)$. Removing terms of smaller order from equation 3.40, we obtain:

$$\bar{r} = \mathrm{E} \ln \left[\left\{ 1 + \tilde{\delta} \left(\frac{b^*}{\tilde{\delta}} e^X - 1 \right) \right\} \right] - \frac{b^*\Delta_f^{(1)} - \tilde{\delta}\Delta_m^{(1)}}{1 + b^* - \tilde{\delta}} \bar{r}, \tag{3.42}$$

where:

$$X = \ln \left\{ \frac{\tilde{b}(t)}{b^*} \right\}.$$

The first term before taking the expected value can be re-written as:

$$\begin{aligned} \ln \left\{ 1 + \tilde{\delta} \left(\frac{b^*}{\tilde{\delta}} e^X - 1 \right) \right\} &= \ln \left\{ 1 + \tilde{\delta} \left(e^{\mu + X} - 1 \right) \right\} \\ &= \ln \left\{ 1 + \tilde{\delta} \left(\mu + X + \frac{1}{2}(\mu + X)^2 \right) \right\} + o\left((\mu + X)^2 \right) \\ &= \tilde{\delta} \left(\mu + X + \frac{1}{2}(\mu + X)^2 \right) - \frac{1}{2}(\tilde{\delta})^2 (\mu + X)^2 \\ &\quad + o\left((\mu + X)^2 \right). \end{aligned} \tag{3.43}$$

Taking expected values of equation 3.43 by noting that:

$$\begin{aligned} \mathrm{E}(\mu + X)^2 &= \mu^2 + \mathrm{E}X^2 \\ &= \mu^2 + \sigma^2 \\ &= \sigma^2 + o(\sigma^2), \end{aligned}$$

we get:

$$\tilde{\delta}\mu + \frac{1}{2}\tilde{\delta}(1-\tilde{\delta})\sigma^2.$$

Substituting this into equation 3.42, we find that:

$$\bar{r} = \tilde{\delta}\mu + \frac{1}{2}\tilde{\delta}(1-\tilde{\delta})\sigma^2 - \frac{b^*\Delta_f^{(1)} - \tilde{\delta}\Delta_m^{(1)}}{1+b^*-\tilde{\delta}}\bar{r} + o(\bar{r}). \tag{3.44}$$

Solving equation 3.44 for $\bar{r}$, we get:

$$\bar{r} = \frac{\tilde{\delta}\mu + \frac{1}{2}\tilde{\delta}(1-\tilde{\delta})\sigma^2}{1 + \left(b^*\Delta_f^{(1)} - \tilde{\delta}\Delta_m^{(1)}\right)/(1+b^*-\tilde{\delta})} + o(\bar{r}). \tag{3.45}$$

Since $b^* = \tilde{\delta}e^{\mu}$, we can express equation 3.45 in terms of $\tilde{\delta}$ and μ by noting that:

$$\begin{aligned}
\frac{b^*\Delta_f^{(1)} - \tilde{\delta}\Delta_m^{(1)}}{1+b^*-\tilde{\delta}} &= \frac{\tilde{\delta}\left(e^{\mu}\Delta_f^{(1)} - \Delta_m^{(1)}\right)}{1+\tilde{\delta}\left(e^{\mu}-1\right)} \\
&= \frac{\tilde{\delta}\left(\Delta_f^{(1)} - \Delta_m^{(1)} + \mu\Delta_f^{(1)}\right)}{1+\tilde{\delta}\mu} + o(\sigma^2) \\
&= \tilde{\delta}\left(\Delta_f^{(1)} - \Delta_m^{(1)} + \mu\Delta_f^{(1)}\right)(1-\tilde{\delta}\mu) + o(\sigma^2). \qquad (3.46)
\end{aligned}$$

Substituting equation 3.46 back to equation 3.45 we get:

$$\begin{aligned}
\bar{r} &= \frac{\tilde{\delta}\mu + \frac{1}{2}\tilde{\delta}(1-\tilde{\delta})\sigma^2}{1+\tilde{\delta}\left(\Delta_f^{(1)} - \Delta_m^{(1)} + \mu\Delta_f^{(1)}\right)(1-\tilde{\delta}\mu)} + o(\sigma^2) \\
&= \frac{\tilde{\delta}\mu + \frac{1}{2}\tilde{\delta}(1-\tilde{\delta})\sigma^2}{1+\tilde{\delta}\left(\Delta_f^{(1)} - \Delta_m^{(1)}\right)} + o(\sigma^2). \qquad (3.47)
\end{aligned}$$

In equation 3.47, we can see how age-structured mortality and fecundity affect population growth rate. Without age structure, the population growth rate is simply the numerator of equation 3.47. A negative $\Delta_f^{(1)}$ (early peak reproduction), and a positive $\Delta_m^{(1)}$ (type I mortality), increase the absolute value of the population growth rate. For long-lived organisms (small $\tilde{\delta}$), age structure becomes less important, unless mortality and fecundity schedules are of extreme type (i.e., very large $\Delta_m^{(1)}$ and $\Delta_f^{(1)}$), since denominator of equation 3.47 is close to one. Therefore, in studies of very long-lived organisms, negligence of age-structure, or lumping age classes with similar k_x and δ_x, may be justified.

It is interesting to note the similarity between equation 3.47 and equation 2.12 of the NLM from the previous chapter. However, equation 3.47 was

derived assuming that $\mu = O(\sigma^2)$, and μ is defined as $\mathrm{E}[\ln \tilde{b}(t) - \ln \tilde{\delta}]$, while in equation 2.12 of the NLM μ is defined as $\mathrm{E}[\ln b_i]$ - $\mathrm{E}[\ln b_j]$. In equation 3.47, σ^2 is defined as the variance of ln birth rate of the single species in this stochastic demographic model, while in the NLM σ^2 is defined as the variance of the difference between ln birth rate of the invader and the resident.

Only the case with structured mortality will be considered here, because structured fecundity is not expected to produce a different pattern. Figure 3-12 shows the plot of $\Delta_m^{(1)}$ against the long term population growth rate, with σ^2 equals 0.25. Equation 3.47 can approximate the population growth rate when $\mathrm{E}|[\ln \tilde{b}]| < 2.9$. Otherwise, the equation can only capture qualitatively the effect of different mortality schedules on the population growth rate.

To see whether the order approximation of the stochastic demographic model (equation 3.47) is as useful as that of the NLM (equation 2.12), we must look at a similar domain, i.e., similar values of μ and σ^2. The quadratic order approximation of the NLM works well on the domain of μ between -0.4 to -0.1. For expected lifetime of 9, and the range of the mean ln birth rate ($\mathrm{E}[\ln \tilde{b}]$), from -3.2 to -2, as I used in figure 3-12, the range of μ is from -1.0028 to 0.1972. $\mathrm{E}[\ln \tilde{b}]$=$-2.6$ in the stochastic demographic model is equivalent to $\mu = -0.4028$ in the NLM. This shows that with a similar domain of μ, the quadratic order approximation of stochastic demographic model 3.47 works equally well as the quadratic order approximation of the NLM 2.12 in predicting the population growth rate of the stochastic demographic model, and the NLM, respectively.

3.7 Discussion

The proposed shape measure, or Δ-measure, can characterise and provide functional relationships between life-history traits, age-independent characteristics and population growth rate. This measure applies to the general mortality schedule and fecundity schedule in the demographic model, and to any age-structured model involving mortality and fecundity schedules, as long as the requirements of stable age distribution and near equilibrium population are met.

Within the range of my simulation experiment, in which I use fixed net reproductive rate as a constraint, the results generalise to a previous work of the NLM. An increasing population favours a type I mortality schedule and early peak reproduction, while a decreasing population favours a type III

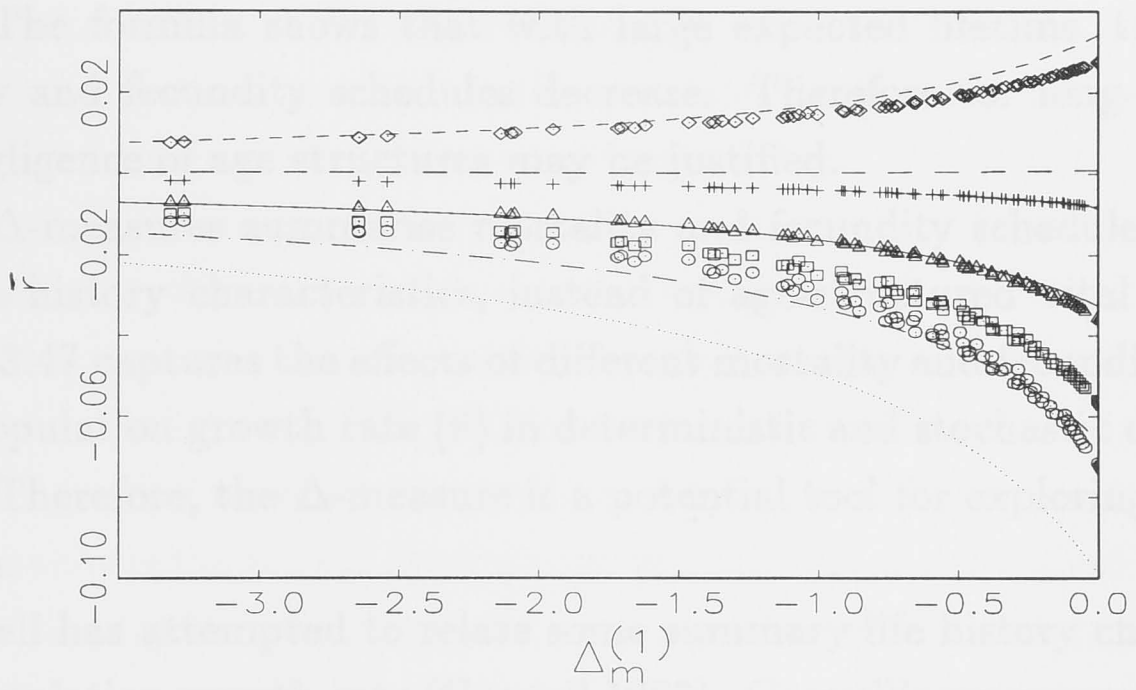

(a)

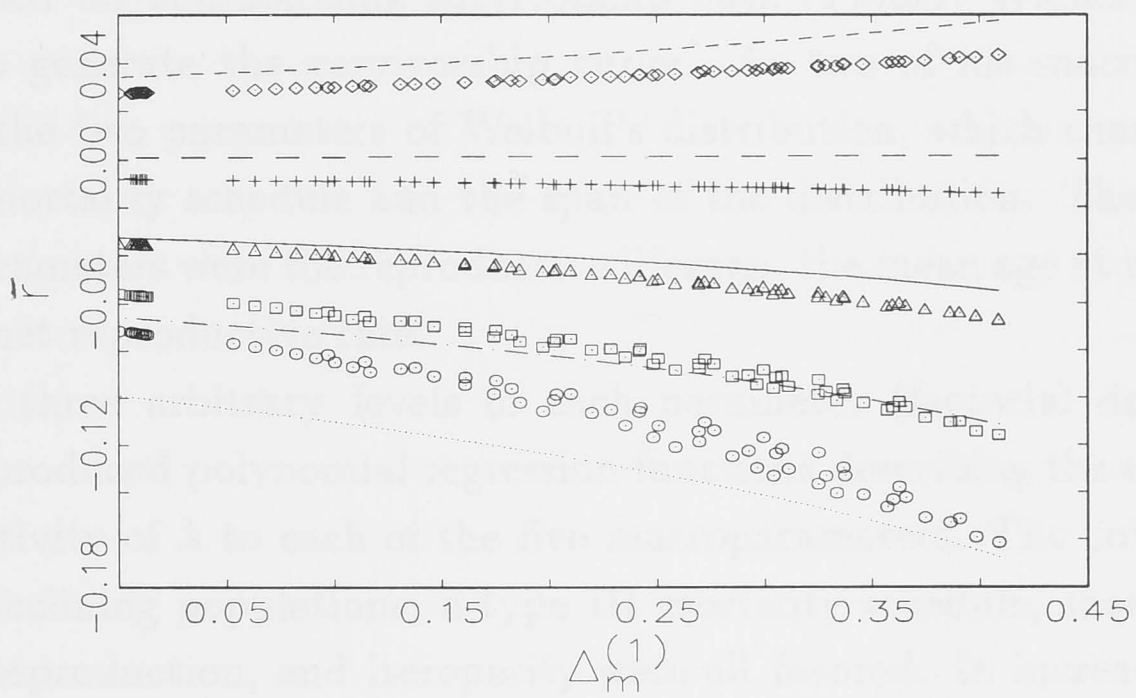

(b)

Figure 3-12: Population growth rate ($\bar{r}$) with mortality schedules of type I (a), and type III (b), with expected lifetime = 9, age-independent reproduction, and $\sigma^2 = 0.25$, calculated from simulation (symbols), and order approximation of equation 3.47 (lines). $E[\ln(\tilde{b})]$ equals -3.2 ($\circ$, dots), -2.9 ($\square$, dots and dashes), -2.6 ($\triangle$, solid), -2.3 ($+$, dashes), and -2 ($\diamond$, short dashes).

mortality schedule and delayed peak reproduction.

With the Δ-measure, the population growth rate in deterministic and stochastic demographic models can be approximated by a simple formula (3.47). The formula shows that with large expected lifetime, the effects of mortality and fecundity schedules decrease. Therefore for long-lived organisms, negligence of age structures may be justified.

The Δ-measures summarise mortality and fecundity schedules and relate those life history characteristics, instead of age-structured vital rates, to $\bar{r}$. Formula 3.47 captures the effects of different mortality and fecundity schedules on the population growth rate ($\bar{r}$) in deterministic and stochastic demographic models. Therefore, the Δ-measure is a potential tool for exploring life-history evolution.

Caswell has attempted to relate some summary life history characteristics to the population growth rate (Caswell 1982). Caswell's macroparameter analysis is important in generalising life-history evolution theories. To see the relationship between the macroparameter properties of life-histories with $\lambda = e^r$, Caswell used numerical sensitivity analysis of λ with respect to five important life history parameters. Caswell used the Weibull's distribution, which is commonly used for summarising survivorship data (Pinder, Wiener, and Smith 1978), to generate the survivorship curve. As two of his macroparameters he used the two parameters of Weibull's distribution, which characterise the type of mortality schedule and the span of the distribution. The other three macroparameters were the reproductive lifespan, the mean age at reproduction and the net reproductive rate.

With three arbitrary levels of each parameter (factorial design of 3^5), Caswell produced polynomial regression functions describing the effect of λ on the sensitivity of λ to each of the five macroparameters. The conclusion was that in declining populations, a type III mortality schedule, shorter lifespan, delayed reproduction, and iteroparity were all favored. In increasing populations, a type I mortality schedule, early reproduction, and semelparity were favored, while no firm conclusions about length of lifespan and reproductive lifespan were drawn. Larger net reproductive rate was favored in all cases, but with poor correlation.

In this study, with fixed net reproductive rate, the above conclusions were supported with a more detailed and general pattern. The fact that varying mortality and fecundity schedules within one level of net reproductive rate (R_0) can have a profound effect on population growth rates, might explain

of the poor correlation between λ and the sensitivity of λ with respect to expected lifetime reproduction in Caswell's study. The work described here generalises and quantifies macroparameter analysis. It achieves this by formulating general measures for mortality and fecundity schedules, and by taking direct measurements, i.e., the death rate and birth rate in each age class, instead of indirect measures, i.e., macroparameters.

I will briefly outline Schaffer's work on reproductive effort (Schaffer 1974). Schaffer showed that concave trade-offs between birth rate, as expression of the reproductive effort, and probability of survival, would lead to iteroparity, whereas convex trade-offs would lead to semelparity in order to maximise population growth rate (r). An analytical solution was not provided, but the general conclusion was that maximising growth rate is equivalent to maximising the future reproductive value of each age class relative to each age class.

The above conclusion about iteroparity and semelparity can also be seen given that, with any trade-off curves, the order of magnitude of the birth rate is held constant. It is relevant to note the difference between the constraint applied by Schaffer and the constraint applied in this study. Here, I have used a fixed net reproductive rate, while Schaffer constrains the trade-off between probability of survival and reproduction in each class. In Schaffer's setting, r varies because the net reproductive rate varies due to the variation in trade-off curves, while in my setting the net reproductive rate remains fixed while the reproductive value at age 1 varies because of the variation in r, due to variation in the mortality and fecundity schedules. The reproductive value at age 1 is the net reproductive rate discounted by r. Therefore, the two constraints coincide if a population is stationary.

Both constraints can be criticised in view of evolution theory. Schaffer makes the assumption that there is unlimited genetic variation to determine reproductive effort in each class, but no genetic variation to determine the trade-off curve itself. Why should there be a concave trade-off curve, given that only a population with positive r can survive? My assumption of fixed net reproductive rate is based on an unjustified physiological constraint and limited genetic variation which tends to increase the expected lifetime reproduction. However, this specific constraint is not central to my study. The main objective of this study is to summarise life-history traits using Δ-measure, which provides a tool for exploring life-history evolution.

In his influential paper, which gave rise to life-history evolution theory, Cole (1954) compared semelparity with iteroparity in relation to population

growth rate as the fitness measure without applying any trade-offs or constraint between the life-history traits. Lewontin (1965) implicitly applied a constraint, by maintaining a fixed net reproductive rate, R_0, at $r = 0$, as I have done in this study. Lewontin explored changes in r as the $l_x b_x$ curve was shifted to the left or right. The most interesting result is that population growth rate (r) is sensitive to age at maturity. However, no general pattern was found, as the study only covered a small range of parameters. MacArthur (1969) generalised this result by introducing the mean age at reproduction. The mean age at reproduction is a way of measuring a fecundity schedule, which is similar to the Δ-measures that I have proposed here, but with the opposite "offset". While MacArthur used semelparity as a standard of comparison to measure a particular fecundity schedule, I have used evenly spread fecundity (age-independent reproduction). The latter approach results in more flexibility and generality. Age at maturity, or mean age at reproduction, might provide a good measure of a fecundity schedule if the reproductive lifespan is narrow, as it was in the parameter space used by Lewontin. If not, the span itself must be taken into account.

Chapter 4

Age-structured Lottery Model (the SLM) in variable environments

4.1 Introduction

The Non-structured Lottery Model (NLM) has been studied and discussed in Chapter 2, along with the general model and the general concept of the storage effect. The storage effect is an important species coexistence mechanism in variable environments. Because the storage effect is an important mechanism for species coexistence, it is necessary to gain a deeper understanding of it in more complex models, such as stage-structured models (Hatfield and Chesson 1997). In this chapter, the NLM is extended by incorporating age structure in the adult population, through age-dependent adult mortality and fecundity. Density dependence only occurs in the juvenile stage, i.e., before reaching the first age class, as in the NLM.

In Chapter 3, I introduced the Δ-measure as a tool for summarising mortality and fecundity schedules in populations with low growth rates. In this chapter, I will use the Δ-measure as a tool to study the age-structured lottery model (SLM), and to approximate the long-term population growth rate of the invader.

In order to compare the NLM and SLM, several constraints must be imposed to ensure that any differences in the behaviour of the two models are due to inherent characteristics of the models. It is useful to remember that the SLM is the general case, and the NLM is a special case of the SLM where mortality and fecundity are independent of age.

We know from Chapter 2 that two life-history characteristics determine the behaviour of the NLM: (i) the expected lifetime ($= 1/\tilde{\delta}$, where $\tilde{\delta}$ is the age-independent death rate), and (ii) the mean birth rate, which is also age-independent. The values of parameters in the SLM will be constrained to achieve an expected lifetime and mean net reproductive rate, equivalent to that in the NLM, but in and age-dependent format.

I will focus on the long-term population growth rate of the invader in an invasibility analysis, criterion for coexistence, and the storage effect. In addition to providing a conceptual understanding of species coexistence in the SLM, the findings might be able to show when age structures can be ignored in the study of a biological system. The negligence of age structure, if justified, will simplify theoretical studies substantially, since an age-structured model is more complicated to analyse than a non-structured model and collecting field data on age-independent characteristics is less labour intensive than on age-dependent characteristics.

4.2 The model

The analysis will cover the general case of a two-species system, where the two species may have different mortality and fecundity schedules (i.e., asymmetric mortality and fecundity schedules). However, simulation studies will only be performed for symmetric cases where the two species have the same mortality and fecundity schedules, i.e., identical age-specific mortality rates, and identical age-specific modulation of reproduction, i.e., equal k_x values in the notation of Chapter 3, but do not necessarily have the same values for overall reproduction, $\tilde{b}$ in the notation of Chapter 3.

In the invasibility analyses, the invader species is chosen to be the species with lower mean birth rate, and is denoted by the subscript i. The resident species, denoted by the subscript j, is always at its stationary distribution. A species with higher mean birth rate than the resident will always be able to invade, given that all other parameters are equal. Therefore, the conditions necessary for coexistence, according to the invasibility criterion, are the same as the conditions necessary for invasion of a single-species system by an inferior competitor. Reproduction is varied independently at each time step using the multiplicative model that the fecundity of species i age-class x is $b_i(t)k_{ix}$.

The difference equation for the invader in the two-species age-structured

lottery model (SLM) is written as follows:

$$\begin{aligned} P_{i.}(t+1) &= \left(\sum_{x=1}^{\infty}(1-\delta_{ix}P_{ix}(t)\right) + \\ &\left(\sum_{x=1}^{\infty}\delta_{ix}P_{ix}(t)+\delta_{jx}P_{jx}(t)\right) \\ &\left(\frac{b_i(t)\sum_{x=1}^{\infty}k_{ix}P_{ix}(t)}{(b_i(t)\sum_{x=1}^{\infty}k_{ix}P_{ix}(t))+(b_j(t)\sum_{x=1}^{\infty}k_{jx}P_{jx}(t))}\right), \end{aligned} \quad (4.1)$$

where $P_{i.}(t)$ is the population density of the invader at time t, and $P_{ix}(t)$ is population density of the invader of age x at time t,
δ_{ix} is the age-specific adult death rate of the invader of age x to $x+1$,
$b_i(t)$ is the overall reproduction of the invader at time $(t, t+1)$,
k_{ix} is the age-dependent modulation of reproduction of the invader, which is a time-independent parameter satisfying the constraint $\sum_{x=1}^{\infty}k_{ix}l_x = \sum_{x=1}^{\infty}l_x = 1/\tilde{\delta}$, $\tilde{\delta}$ is the corresponding age-independent death rate.

It is assumed that the amount of space is constant and always limiting, and that vacancies created by death of adults are filled by new recruits during the same interval of time. In the two-species SLM, juveniles of both species must compete with each other for available space in order to enter the first age class. Competition is purely by lottery, in the sense that the species to which an individual juvenile belongs does not advantage or disadvantage that individual in obtaining space for recruitment. If a juvenile succeeds in gaining a space (i.e., is "recruited"), it will then be counted as an individual of age class one. The individual will move to the next class, given that it survives during one unit of time, according to its age-dependent survival probability, and it will produce offspring according to its age-dependent birth rate. If it dies during one unit of time, the individual leaves the system and releases one unit of space. Figure 4-1 shows this cycle for the invader species. The specific rates on the arrows are justified in the next section.

4.3 Analysis

I will first write out equation 4.1 for each species. For the resident, equation 4.1 is:

$$\begin{aligned} P_{j.}(t+1) &= P_{j.}(t)\sum_{x=1}^{\infty}(1-\delta_{jx})u_{jx}(t) + \\ &\left(P_{i.}(t)\sum_{x=1}^{\infty}\delta_{ix}u_{ix}(t) + P_{j.}(t)\sum_{x=1}^{\infty}\delta_{jx}u_{jx}(t)\right) \end{aligned}$$

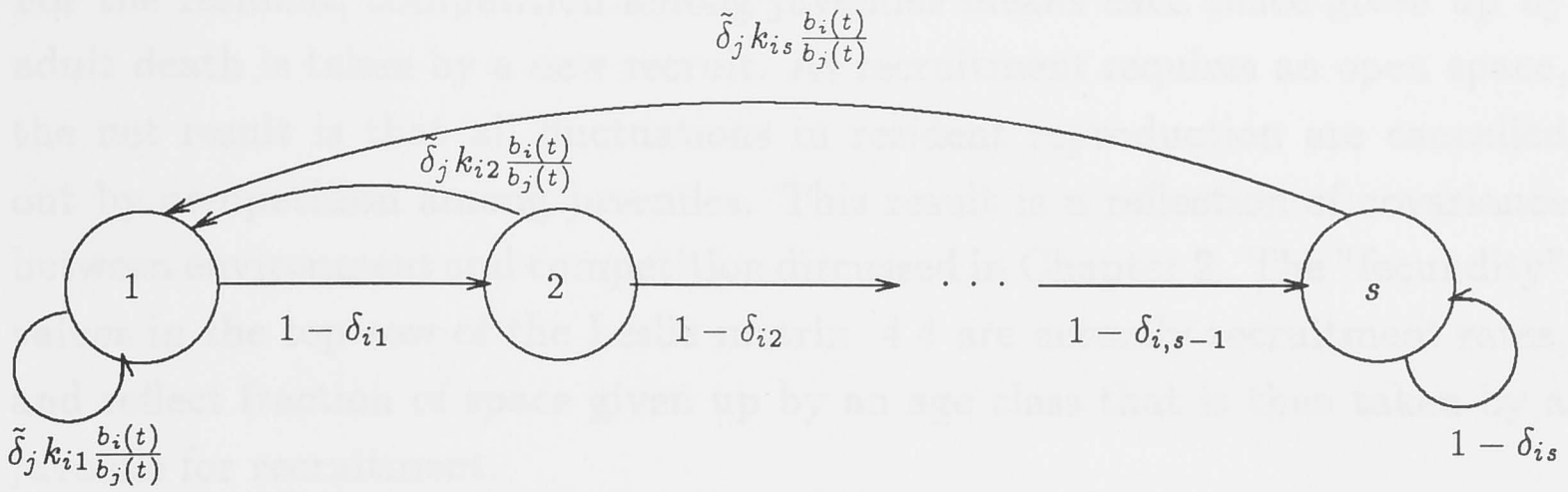

Figure 4-1: The life cycle of the invader species in SLM.

$$\begin{aligned} & \frac{P_{j.} b_j(t) \sum_{x=1}^{\infty} k_{jx} u_{jx}(t)}{P_{i.}(t) b_i(t) \sum_{x=1}^{\infty} k_{ix} u_{ix}(t) + P_{j.}(t) b_j(t) \sum_{x=1}^{\infty} k_{jx} u_{jx}(t)} \\ = \; & P_{j.}(t) \left\{ \sum_{x=1}^{\infty} (1-\delta_{jx}) u_{jx}(t) + \right. \\ & \left(P_{i.}(t) \sum_{x=1}^{\infty} \delta_{ix} u_{ix}(t) + P_{j.}(t) \sum_{x=1}^{\infty} \delta_{jx} u_{jx}(t) \right) \\ & \left. \frac{b_j(t) \sum_{x=1}^{\infty} k_{jx} u_{jx}(t)}{P_{i.}(t) b_i(t) \sum_{x=1}^{\infty} k_{ix} u_{ix}(t) + P_{j.}(t) b_j(t) \sum_{x=1}^{\infty} k_{jx} u_{jx}(t)} \right\}, \end{aligned} \tag{4.2}$$

where $u_{jx}(t) = P_{jx}(t)/P_{j.}(t)$ is the age distribution of the resident.

Assuming that $P_{i.}(t) = 0$ and $P_{j.}(t) = 1$ for all t, equation 4.2 is reduced to:

$$\begin{aligned} P_{j.}(t+1) &= P_{j.}(t) \left\{ \sum_{x=1}^{\infty} \left((1-\delta_{jx}) u_{jx}(t) + \delta_{jx} u_{jx}(t) \right) \right\} \\ &= P_{j.}(t). \end{aligned} \tag{4.3}$$

Equation 4.3 shows that the density of the resident is always constant, and therefore, the population growth rate of the resident is always zero. It is obvious from equation 4.3 that the dynamics of the resident are linear. Therefore, we can express equation 4.3 as a Leslie matrix as follows:

$$\begin{pmatrix} P_{j1} \\ P_{j2} \\ P_{j3} \\ \vdots \\ P_{js} \end{pmatrix} (t+1) = \begin{pmatrix} \delta_{j1} & \delta_{j2} & \delta_{j3} & \cdots & \delta_{js} \\ (1-\delta_{j1}) & 0 & 0 & \cdots & 0 \\ 0 & (1-\delta_{j2}) & 0 & \cdots & 0 \\ \vdots & \vdots & \ddots & \cdots & \vdots \\ 0 & 0 & \cdots & (1-\delta_{j,s-1}) & (1-\delta_{js}) \end{pmatrix} \begin{pmatrix} P_{j1} \\ P_{j2} \\ P_{j3} \\ \vdots \\ P_{js} \end{pmatrix} (t). \tag{4.4}$$

For the resident, competition among juveniles means each place given up by adult death is taken by a new recruit. As recruitment requires an open space, the net result is that all fluctuations in resident reproduction are cancelled out by competition among juveniles. This result is a reflection of covariance between environment and competition discussed in Chapter 2. The "fecundity" values in the top row of the Leslie matrix 4.4 are actually recruitment rates, and reflect fraction of space given up by an age class that is then taken by a juvenile for recruitment.

The above Leslie matrix model satisfies the condition for convergence to stable age distribution of Perron-Frobenius theorem (see, e.g., Caswell 1989), because the Leslie matrix is positive and primitive. Therefore, the resident is always at its stable age distribution, i.e., u_{jx} does not fluctuate over time. Moreover, as the resident's growth rate it zero, the stable age distribution is the stationary age distribution given by the equation:

$$u_{jx} = \frac{l_{jx}}{\sum_{x=1}^{\infty} l_{jx}}.$$

As a consequence of convergence on the stationary age distribution, the average death rate of the resident over all age classes, $\hat{\delta}_j(t)$, does not fluctuate over time and converges to the age-independent death rate corresponding to its mortality schedule given by the equation

$$\begin{aligned} \hat{\delta}_j = \sum_{x=1}^{\infty} \delta_{jx} u_{jx} &= \frac{\sum_{x=1}^{\infty} \delta_{jx} l_{jx}}{\sum_{x=1}^{\infty} l_{jx}} \\ &= \frac{1}{\sum_{x=1}^{\infty} l_{jx}} \\ &= \tilde{\delta}_j. \end{aligned} \tag{4.5}$$

As a consequence also of the stationary age distribution, the average modulation of reproduction of the resident (not to be confused with recruitment of the resident which comes after competition among juveniles does not fluctuate over time) is given by the equation:

$$\begin{aligned} \hat{k}_j &= \sum_{x=1}^{\infty} k_{jx} u_{jx} \\ &= \frac{\sum_{x=1}^{\infty} k_{jx} l_{jx}}{\sum_{x=1}^{\infty} l_{jx}} \\ &= \tilde{k}_j. \end{aligned} \tag{4.6}$$

The constraint we apply is:

$$\sum_{x=1}^{\infty} k_{jx} l_{jx} = \sum_{x=1}^{\infty} l_{jx} = \frac{1}{\tilde{\delta}_j}. \tag{4.7}$$

Therefore, the modulation of reproduction of the resident reduces to:

$$\tilde{k}_j = 1.$$

This constraint fixes the net reproductive rate, R_0, in a constant environment.

For the invader, equation 4.1 can be written as:

$$P_{i.}(t+1) = P_{i.}(t)\left\{\sum_{x=1}^{\infty}(1-\delta_{ix}u_{ix}(t)) + \sum_{x=1}^{\infty}\delta_{jx}u_{jx}\frac{b_i(t)\sum_{x=1}^{\infty}k_{ix}u_{ix}(t)}{b_j(t)\sum_{x=1}^{\infty}k_{jx}u_{jx}(t)}\right\}. \quad (4.8)$$

By substituting equations 4.5 and 4.6 into equation 4.8, we get:

$$P_{i.}(t+1) = P_{i.}(t)\left\{\sum_{x=1}^{\infty}(1-\delta_{ix}u_{ix}(t)) + \tilde{\delta}_j\frac{b_i(t)\sum_{x=1}^{\infty}k_{ix}u_{ix}(t)}{b_j(t)}\right\}. \quad (4.9)$$

From equation 4.9, the mortality schedule of the resident does not affect population dynamics of the invader at all. It is only the age-independent death rate of the resident ($\tilde{\delta}_j$) that matters. Since equation 4.9 does not involve density of the resident in any form, we can express equation 4.9 in a matrix form:

$$\begin{pmatrix} P_{i1} \\ P_{i2} \\ P_{i3} \\ \vdots \\ P_{is} \end{pmatrix}(t+1) = \begin{pmatrix} \tilde{\delta}_j k_{i1}\rho(t) & \tilde{\delta}_j k_{i2}\rho(t) & \tilde{\delta}_j k_{i3}\rho(t) & \cdots & \tilde{\delta}_j k_{is}\rho(t) \\ (1-\delta_{i1}) & 0 & 0 & \cdots & 0 \\ 0 & (1-\delta_{i2}) & 0 & \cdots & 0 \\ \vdots & \vdots & \ddots & \cdots & \vdots \\ 0 & 0 & \cdots & (1-\delta_{i,s-1}) & (1-\delta_{is}) \end{pmatrix}\begin{pmatrix} P_{i1} \\ P_{i2} \\ P_{i3} \\ \vdots \\ P_{is} \end{pmatrix}(t), \quad (4.10)$$

where $\rho(t) = b_i(t)/b_j(t)$. The above Leslie matrix is a special case of the Leslie matrix of equation 3.36 discussed in section 3.6.

In this chapter, instead of applying standard methods matrix model analysis, I will follow Chesson's proposed framework and apply approximations allowing solution a difference equation. This will allow us to investigate some meaningful biological mechanisms, rather than merely to calculate the long-term population growth rate of the invader. Chapter 5 will deal with the model as a matrix model, enabling us to work with a larger parameter set.

4.3.1 The SLM with structured mortality only

First, let us consider only the addition of structured mortality to the model. Equation 4.1 is reduced to:

$$P_{i.}(t+1) = \left(\sum_{x=1}^{\infty}(1-\delta_{ix}P_{ix}(t)\right) + \left(\sum_{x=1}^{\infty}\delta_{ix}P_{ix}(t) + \delta_{jx}P_{jx}(t)\right) \frac{b_i(t)\sum_{x=1}^{\infty}P_{ix}(t)}{(b_i(t)\sum_{x=1}^{\infty}P_{ix}(t)) + (b_j(t)\sum_{x=1}^{\infty}P_{jx}(t))}, \quad (4.11)$$

where $b_i(t)$ is the age-independent birth rate of species i during the time period $(t, t+1)$, and δ_x is the adult death rate for age x to $x+1$.

The resident species is always at a stable age distribution, since it does not fluctuate because the resident occupies the entire space. Therefore, the population growth rate of the resident is always zero, $\bar{r}_j(t) = 0$, with zero variance over time. The population density of the invader fluctuates, the the variance of $r_i \neq 0$, and the population does not approach or remain at a stable age distribution. However, the population is known to fluctuate about the "stable" age distribution, which does not depend on the initial distribution, according to stochastic ergodicity theory (Cohen 1979). Therefore, provided that the variance of r_i is not too large, the invader is always close to its stable age distribution.

Without structured fecundity, $k_{ix} = k_{jx} = 1$ for all x. The average death rate of the resident over age classes converges to the age-independent death rate $(\tilde{\delta}_j)$, as shown above. Equation 4.9 becomes:

$$P_{i\cdot}(t+1) = P_{i\cdot}(t)\left\{1 - \sum_{x=1}^{\infty} \delta_{ix} u_{ix}(t) + \tilde{\delta}_j \frac{b_i(t)}{b_j(t)}\right\}. \tag{4.12}$$

It is worth remembering that the distribution of age at death, $\{\delta_x l_x\}$, is a probability distribution, since it sums to one.

The long-term population growth rate of the invader is:

$$\begin{aligned} \bar{r}_i &= \mathrm{E}\left[\ln\left\{\frac{P_{i\cdot}(t+1)}{P_{i\cdot}(t)}\right\}\right] \\ &= \mathrm{E}\left[\ln\left\{1 - \sum_{x=1}^{\infty} \delta_{ix} u_{ix}(t) + \tilde{\delta}_j \frac{b_i(t)}{b_j(t)}\right\}\right] \\ &\approx \mathrm{E}\left[\ln\left\{1 - \hat{\delta}_i(t) + \tilde{\delta}_j \frac{b_i(t)}{b_j(t)}\right\}\right], \end{aligned} \tag{4.13}$$

where the average death rate of the invader over age classes, which now is time-dependent, due to fluctuation in the age distribution over time, is as follows:

$$\hat{\delta}_i(t) = \sum_{x=1}^{\infty} \delta_{ix} u_{ix}(t). \tag{4.14}$$

Now I will apply the Δ-measure into the SLM, as I did in the the general stochastic demographic model in section 3.6. Since I will only consider $\Delta_m^{(1)}$, I will reduce the notation to Δ_m hereafter. Also, because it is only the mortality schedule of the invader that matters to the population dynamics of the invader, I will refer to the measure of the mortality schedule of the invader as Δ_m. By assuming that fluctuation in the age distribution is not important and by

approximating the stable age distribution using $\bar{r}_i$, the average death rate of the invader over age classes can be expressed as:

$$\hat{\delta}_i(t) \approx \tilde{\delta}_i(1 - \bar{r}_i \Delta_m), \tag{4.15}$$

where:

$$\Delta_m = \sum_{x=1}^{\infty} x l_{ix}(\delta_{ix} - \tilde{\delta}_i). \tag{4.16}$$

Three types of mortality schedules are represented by Δ_m as follows (cf. expression 3.14):

$$\Delta_m = \begin{cases} > 0 & \text{for type I mortality schedule} \\ = 0 & \text{for type II mortality schedule} \\ < 0 & \text{for type III mortality schedule,} \end{cases}$$

All three types of mortality schedule will be investigated, each with two levels of death rates through age classes. This simplification to the two-level death rate is helpful as it keeps algebra simple without loosing generality. In the type II mortality schedule, death rate (δ_x) is constant throughout all age classes, which is equivalent to the setting in which there is no mortality schedule. In the type I mortality schedule:

$$\delta_x = \begin{cases} \delta_1 < \tilde{\delta} & \text{if } x \leq s \\ \delta_2 > \tilde{\delta} & \text{otherwise,} \end{cases}$$

where s is the age at which death rate changes from the early mortality rate (δ_1) to the late mortality rate (δ_2). The type III mortality schedule is opposite to the type I mortality schedule in that mortality is higher among youngsters than older individuals.

In comparing the performance of the NLM and SLM, I will fix the age-independent death rate ($\tilde{\delta}$). By fixing the age-independent death rate, or fixing the expected lifetime ($1/\tilde{\delta}$), we focus on the shape of the mortality schedule. First we must decide on the early mortality rate (δ_1), and the age at which the death rate is to change from the early mortality rate to the late mortality rate (s). Then the late mortality rate (δ_2) can be obtained using the following function:

$$\delta_x = \begin{cases} \delta_1 & \text{if } x < s \\ \frac{(1-\delta_1)^{s-1}\delta_1}{(\delta_1/\tilde{\delta})-1+(1-\delta_1)^{s-1}} & \text{otherwise,} \end{cases}$$

Then Δ_m for each mortality schedule can be calculated using 4.16. By using this Δ_m, we can study how the deviation of a mortality schedule from a type II mortality schedule affects the behaviour of the SLM.

4.3.2 The SLM with structured mortality and fecundity

Now, I will include structured fecundity in my examination of the SLM as presented in equation 4.1. Modulation of reproduction (k function) will take the most common shapes: uniform, asymptotic, and triangular (see figure 3-11) (Roff 1992). The triangular shape is not reduced to zero for old individuals but is given a small positive value for the purpose of imposing primitivity on the projection matrices. This feature is important in the next chapter relying on matrix methods.

Given the stable age distribution of the resident, and low density of the invader, equation 4.1 can be written as:

$$\begin{aligned} P_{i.}(t+1) &= P_{i.}(t)\left\{1-\sum_{x=1}^{\infty}\delta_{ix}u_{ix}(t)+\sum_{x=1}^{\infty}\delta_{jx}u_{jx}\frac{b_i(t)}{b_j(t)}\frac{\sum_{x=1}^{\infty}k_{ix}u_{ix}(t)}{\sum_{x=1}^{\infty}k_{jx}u_{jx}}\right\} \\ &= P_{i.}(t)\left\{1-\sum_{x=1}^{\infty}\delta_{ix}u_{ix}(t)+\tilde{\delta}_j\frac{b_i(t)}{b_j(t)}\sum_{x=1}^{\infty}k_{ix}u_{ix}(t)\right\}. \end{aligned} \tag{4.17}$$

The long-term population growth rate of the invader is:

$$\begin{aligned} \bar{r}_i &= \mathrm{E}\left[\ln\left\{\frac{P_{i.}(t+1)}{P_{i.}(t)}\right\}\right] \\ &= \mathrm{E}\left[\ln\left\{1-\sum_{x=1}^{\infty}\delta_{ix}u_{ix}(t)+\tilde{\delta}_j\frac{b_i(t)}{b_j(t)}\sum_{x=1}^{\infty}k_{ix}u_{ix}(t)\right\}\right] \\ &= \mathrm{E}\left[\ln\left\{1-\hat{\delta}_i(t)+\tilde{\delta}_j\frac{b_i(t)\hat{k}_i(t)}{b_j(t)}\right\}\right], \end{aligned} \tag{4.18}$$

where $\hat{\delta}_i(t)$ is as in equation 4.14, and the average modulation of reproduction of the invader over age classes is:

$$\hat{k}_i(t)=\sum_{x=1}^{\infty}k_{ix}u_{ix}(t). \tag{4.19}$$

By applying Δ_f, assuming that fluctuations in age structure are not important, and approximating the stable age distribution using $\bar{r}_i$, we can express the average modulation of reproduction over age classes as:

$$\begin{aligned} \hat{k}_i(t) &\approx \tilde{k}_i(t)(1+\bar{r}_i\Delta_f) \\ &= 1+\bar{r}_i\Delta_f, \end{aligned} \tag{4.20}$$

where:

$$\Delta_f=\tilde{\delta}\sum_{x=1}^{\infty}xl_{ix}(k_{ix}-1). \tag{4.21}$$

The general pattern of fecundity schedule is (cf. expression 3.27):

$$\Delta_f = \begin{cases} > 0 & \text{for delayed peak reproduction} \\ = 0 & \text{for age-independent reproduction} \\ < 0 & \text{for early peak reproduction.} \end{cases}$$

Fecundity schedules are classified in terms of the age at which the majority of offspring is produced, rather than the age at which reproduction begins.

The long-term population growth rate of the invader and the storage effect

I will now examine the long-term population growth rate of invader with structured mortality and fecundity, given in equation 4.18. By considering the equation for the long-term population growth rate of the invader in the SLM as a special case of the population growth rate of the stochastic demographic model from the previous chapter, i.e.,

$$r = \mathrm{E}\left[\ln\{1 - \hat{\delta}(t) + \hat{b}(t)\}\right], \tag{4.22}$$

we can see that, in the SLM:

$$\hat{b}(t) = \tilde{\delta}_j \hat{k}_i(t) \frac{b_i(t)}{b_j(t)}.$$

According to the definition of μ used in the previous chapter, we have:

$$\begin{aligned} \mu &= \mathrm{E} \ln \frac{\hat{b}(t)}{\tilde{\delta}_i \hat{k}_i(t)} \\ &= \mathrm{E} \ln \frac{b_i(t)}{b_j(t)} - \ln \frac{\tilde{\delta}_i}{\tilde{\delta}_j}. \end{aligned}$$

Note that here σ^2 is equivalent to $\frac{1}{2}\sigma^2$ in the previous chapter, as $\sigma^2 = \mathrm{var}[b_i(t)] = \mathrm{var}[b_j(t)]$, and no covariance between $b_i(t)$ and $b_j(t)$ is assumed. Substituting all these into equation 3.47 from the previous chapter, we get:

$$\bar{r}_i = \frac{\tilde{\delta}_i \left[\mu + (1 - \tilde{\delta}_i)\sigma^2\right]}{1 + \tilde{\delta}_i(\Delta_f - \Delta_m)} + o(\sigma^2). \tag{4.23}$$

Criterion for coexistence are calculated by equating the above equation to 0. We get:

$$\sigma^2 > \frac{|\mu|}{(1 - \tilde{\delta}_i)},$$

which agrees with the coexistence criterion of the NLM (cf. expression 2.13). According to this formula, mortality and fecundity schedules do not affect criterion for coexistence.

The fluctuation-dependent term in equation 4.23 is:

$$\frac{\tilde{\delta}_i(1-\tilde{\delta}_i)\sigma^2}{1+\tilde{\delta}_i(\Delta_f-\Delta_m)},$$

which agrees with the storage effect in the NLM (cf. expression 2.12) when $\Delta_m = 0$ and $\Delta_f = 0$ as it should. When the mortality schedule is of type I, and the fecundity schedule is early peak reproduction, the strength of the storage effect is increased.

Covariance between the environment and competition, and sub-additivity

In the SLM, the environment and competition are defined as:

$$\begin{aligned} E_j(t) &= \ln b_j(t), \\ C(t) &= \ln\left\{\frac{b_j(t)\sum_{x=1}^{\infty} P_{jx}(t)}{\sum_{x=1}^{\infty}\delta_{jx}P_{jx}(t)}\right\}, \\ &= \ln\left\{\frac{b_j(t)}{\tilde{\delta}_j}\right\} \end{aligned} \tag{4.24}$$

and:

$$\begin{aligned} \mathrm{E}[C] &= \mathrm{E}\ln\left\{\frac{b_j(t)}{\tilde{\delta}_j}\right\} \\ &\approx \ln \mathrm{E}\left[\frac{b_j(t)}{\tilde{\delta}_j}\right] - \frac{1}{2}\mathrm{var}[C] \\ &= \ln R_0 - \frac{1}{2}\mathrm{var}[C], \end{aligned} \tag{4.25}$$

where the approximation above can be replaced by equality in the case that $b_j(t)$ is lognormal, as it is in the simulations. by standard results.

The E_j and C_j are exactly the same as those in the NLM. Hence in the SLM, $\mathrm{cov}[E_j, C] = \mathrm{var}[E_j] = \sigma^2$. By defining the environment and competition as in 4.24, the growth rate of the resident is

$$r_j(t) = \ln\{1 - \tilde{\delta}_j + e^{E_j - C}\}.$$

As in the NLM, to calculate the non-additivity the resident population is subdivided into new recruits and survivors. We learn from equation 4.5 that

the age-structured mortality and fecundity of resident in the SLM do not affect the dynamics of the resident and the invader. Therefore, I subdivide the resident population into new recruits and survivors as in the NLM. Contributions of new recruits (G_{i1}) and those of survivors (G_{i2}) to the population growth rate can be expressed as:

$$\begin{aligned} G_{j1} &= 1 - \tilde{\delta}_j, \\ G_{j2} &= e^{E_j - C}. \end{aligned}$$

As in the NLM, G_j^* sums to one, because the resident is always at its stationary distribution. We can drop the subscript j from $\tilde{\delta}$, since we are dealing with the symmetrical case only. Then, by applying the technique used in section 2.2.3, αs, βs and γs from the SLM are:

$$\begin{aligned} \alpha_{j1} &= \beta_{j1} = \gamma_{j1} = 0, \\ \alpha_{j2} &= \beta_{j2} = 1, \text{and} \\ \gamma_{j2} &= 0, \end{aligned}$$

which lead to

$$\begin{aligned} \bar{\alpha}_j &= \bar{\beta}_j = \tilde{\delta}, \\ \bar{\gamma}_j &= 0, \end{aligned}$$

and

$$\gamma_{jo} = -\tilde{\delta}(1 - \tilde{\delta}).$$

Transforming this into standardised non-additivity we get:

$$\gamma_j = \frac{\gamma_{jo}}{\bar{\alpha}_j \bar{\beta}_j} = 1 - \frac{1}{\tilde{\delta}},$$

which means that the sub-additivity of the resident is equivalent with that of the NLM as long as the expected lifetime $(1/\tilde{\delta})$ between the SLM and NLM are equal. The non-additivity of the invader can be expressed in term of the non-additivity of resident and the asymmetrical age-independent death rates between the resident $(\tilde{\delta})$ and the invader $(\hat{\delta}_i)$.

The equivalence in the covariance between the environment and competition and in the magnitude of sub-additivity suggests that there is no difference between the NLM and SLM in the magnitude of the storage effect of the resident given that the expected lifetime and the variance of ln birth rates between the two models are equal.

4.4 Results

Below I will present results from simulations: the long term population growth rate of the invader, mean values of $\hat{\delta}_i$ and $\hat{k}_i$ from equations 4.14 and 4.19, respectively. Disadvantaged invaders are our main focus, since if these species can invade, coexistence can occur. Some of the mortality and fecundity schedules to be used in the simulations are of the same set used in the previous chapter. Examples are presented in the figures 3-1 and 3-6. For the simulations, I consider only the symmetric case described in the introduction, of equal mortality schedules for the two species and equal modulation of fecundity by age. I assume throughout that the expected lifetime is equal to 9, and impose the usual constraint (equation 4.7) that the population average of k_x for a stationary population is equal to 1. I use the simulation methodology described in Chapter 2.

Before I present the results, let us first refresh our memory about the mortality and fecundity schedules I used in the study. It can be seen from figure 3-1 that the larger the magnitude of $|\Delta_m|$, the more a mortality schedule departs from a type II schedule. The larger the magnitude of $|\Delta_f|$, the more a fecundity schedule deviates from age-independent reproduction, even though the classification of fecundity schedules is less distinct than that of mortality schedules. Age-independent reproduction means that the age of mean reproduction is equal to the expected lifetime (i.e., equal to 9 in our case). Figure 3-6 shows that, with early peak reproduction, more than half of the area under the curve lies before $x = 9$, meaning that the majority of offspring are produced early in life. With the delayed peak reproductions, less than half of the area lies before $x = 9$, meaning that the majority of offspring are produced later in life. Figure 3-6 also shows that a delayed peak reproduction with $\Delta_f = 7.1594$ produces a curve which has small area under the curve before $x = 9$, compared with delayed peak reproduction with smaller Δ_f, e.g., $\Delta_f = 1$.

When structured mortality and fecundity are combined, the mean age of reproduction is shifted according to the mortality schedule (figure 3-11). A type I mortality schedule will shift the age of mean reproduction for age-independent reproduction to the right (later age), such that, for my parameter set, it is difficult to find an early peak reproduction fecundity schedule that will fulfill the requirement of fixed net reproductive rate. The opposite shift occurs with the type III mortality schedule.

Differences between the mean of ln birth rates for the invader and the resident (μ) in simulations ranged from -0.4 to -0.1. Variances of ln birth

rates for the invader and the resident are kept equal, and the common variances (σ^2) ranged from 0 to 0.5.

4.4.1 The long-term population growth rate of the invader

First, let us compare the simulation results for the long-term population growth rate of the invader when mortality and/or fecundity are structured (the SLM), with these when mortality is of type II and reproduction is independent of age (the NLM) (figures 4-2, 4-4, and 4-5).

I will first consider the SLM with structured mortality only (figure 4-2). When the invader population is decreasing, the long-term population growth rate of the invader is lower with a type I mortality schedule than with type II mortality schedule. When the population is increasing, long-term population growth rate is higher with a type I than a type II mortality schedule (figure 4-2(a)). In other words, when an invader is recovering from low density, an invader with a type I mortality schedule will recover faster than an invader with type II mortality schedule. However, when the population is declining, a type I invader will decline faster than a type II invader. The comparison is not direct, as the invaders live in two different systems, and the resident has the same mortality schedule as the invader in each system. In fact, I compare two different two-species system: (i) a system with both species are of type I mortality schedules, and (ii) a system with both species are of type II mortality schedule. If the invaders in both system persist, then the invader in the first system will recover faster than the invader in the later system.

However, since the resident is always at its stationary distribution, the average death rate of the resident over age classes ($\hat{\delta}_j$) is always equal to the age-independent death rate ($\tilde{\delta}_j$), regardless of its mortality schedule. Therefore, it is meaningful to compare the long-term population growth rates of invaders across different systems, even though mortality schedules of residents are different in different systems.

With type III mortality schedule (figure 4-2(b)), the recovery rate of a type III invader is lower than that of type II invader (and therefore, a type I invader), and the extinction rate is also lower than that of type II and type I invaders.

The fecundity schedules behave similarly to the mortality schedules (figure 4-4) in their effects on the recovery rate of the invader. Early peak reproduction behaves like a type I mortality schedule, i.e., increases $|\bar{r}_i|$, and delayed

peak reproduction behaves like a type III mortality schedule, i.e., decreases $|\bar{r}_i|$.

Now let us look at how mortality and fecundity schedules affect the coexistence criterion, i.e., the magnitude of σ^2 required for the invader to have zero long-term population growth rate. Looking closely at the horizontal line ($\bar{r}_i = 0$) in figures 4-2(a) and (b), the lines of type I is in the right of that of type II which is in the right of that of type III. This pattern is less obvious with smaller σ^2. The pattern shows that, in order to persist, the type I invader requires larger σ^2 than the type II invader, which requires larger σ^2 than the type III invader with the same level of inferiority (μ), even though little quantitative difference between the three can be seen in the figures.

The small quantitative effect of structured mortality on coexistence is consistent with the assumption used in deriving approximation 4.15, that stochastic fluctuations in age distribution have negligible effect on the overall adult mortality rate of the invading population. According to equation 4.15, the average death rate of the invader over age classes ($\hat{\delta}_i(t)$) should be approximately equal to $\tilde{\delta}_i$ when $\bar{r}_i = 0$. However, figure 4-3 shows that there are some small discrepancies between the mean values of $\hat{\delta}_i$ from equation 4.14, calculated using simulation, and $\tilde{\delta}$. With a type I mortality schedule (figure 4-3(a)), the mean value of the average death rate of the invader over age classes ($\hat{\delta}_i$) calculated using simulation is slightly larger than the age-independent death rate ($\tilde{\delta}$) when the long-term population growth rate of the invader ($\bar{r}_i$) is equal to zero. The opposite pattern occurs with a type III mortality schedule, i.e., mean of $\hat{\delta}_i$ calculated using simulation is slightly smaller than $\tilde{\delta}$ when $\bar{r}_i = 0$. This non-zero $\ln\{\tilde{\delta}_i(t)/\hat{\delta}_i\}$ when $\bar{r}_i = 0$ appears to be responsible for the small quantitative effect of structured mortality on coexistence.

In figures 4-4 and 4-5 there are no apparent differences in the location of the intercept $\bar{r}_i = 0$ between age-dependent and age-independent reproduction fecundity schedules. Thus, it appears that coexistence is not affected by fecundity schedules. The mean value of the average modulation of reproduction of the invader over age classes ($\hat{k}_i(t)$) from equation 4.19 calculated using simulation is very close to one (figure 4-6), when the long-term population growth rate of the invader ($\bar{r}_i$) is zero. This explains why there is no appreciable effect of structured fecundity on coexistence.

The invader with early peak reproduction has the mean value of $\hat{k}_i$ than 1 when the population is decreasing, and greater than 1 when the population is increasing. The opposite pattern occurs for delayed peak reproduction. This qualitative pattern of the mean values of $\hat{k}_i$ is found to be consistent

throughout all combinations of fecundity schedules and mortality schedules in the parameter set.

Approximation of the long-term population growth rate of the invader, given in equation 4.23, works well, both qualitatively and quantitatively in all cases: (i) with structured mortality (figures 4-7(a)), (ii) with structured fecundity (figures 4-7(b) and 4-8(a)), and (iii) with structured mortality and structured fecundity (figure 4-8(b)).

4.5 Discussion

I have extended the non-structured lottery model (NLM) to an age-structured lottery model (SLM) with age-dependent mortality and fecundity in the adult stage. Competition for space occurs only in the juvenile stage in both models. The behaviour of the NLM has been investigated (Chesson and Warner 1981; Hatfield and Chesson 1989; Chesson 1990; Chesson 1994). The life-history characteristics that determine the outcome of the NLM are the expected lifetime and the mean birth rate of each species, and combining the two gives the net reproductive rate.

To compare the NLM and SLM intrinsically, I imposed some constraints based on our knowledge of the NLM. I chose to compare the NLM and SLM using fixed expected lifetime and fixed net reproductive rate.

In the NLM, the average mortality rate and the average birth rate in the invader and the resident are equivalent to the individual mortality rate and the individual birth rate, respectively, because mortality and fecundity are unstructured. In the SLM, when the population is stationary, or mortality and/or fecundity are unstructured, the above relationship continues to hold, i.e., the average mortality rate in the population ($\hat{\delta}$) and the average birth rate in the population ($b\hat{k}$) are equal, respectively, to the reciprocal of the expected lifetime ($\tilde{\delta}$) and the net reproductive rate divided by the expected lifetime (b). These relationships are true for the the resident because it is stationary. In non-stationary populations with structured mortality or fecundity, the above relationships do not hold, due to the shifts in age distributions with changes in the population growth rates. As the invader is in general non-stationary, the population average mortality rate of the invader and the population average birth rate of the invader differ from the reciprocal of the expected lifetime, and the ratio of net reproductive rate to expected lifetime. These effects on the invader, but not on the resident, in the SLM, explain the effects of mortality

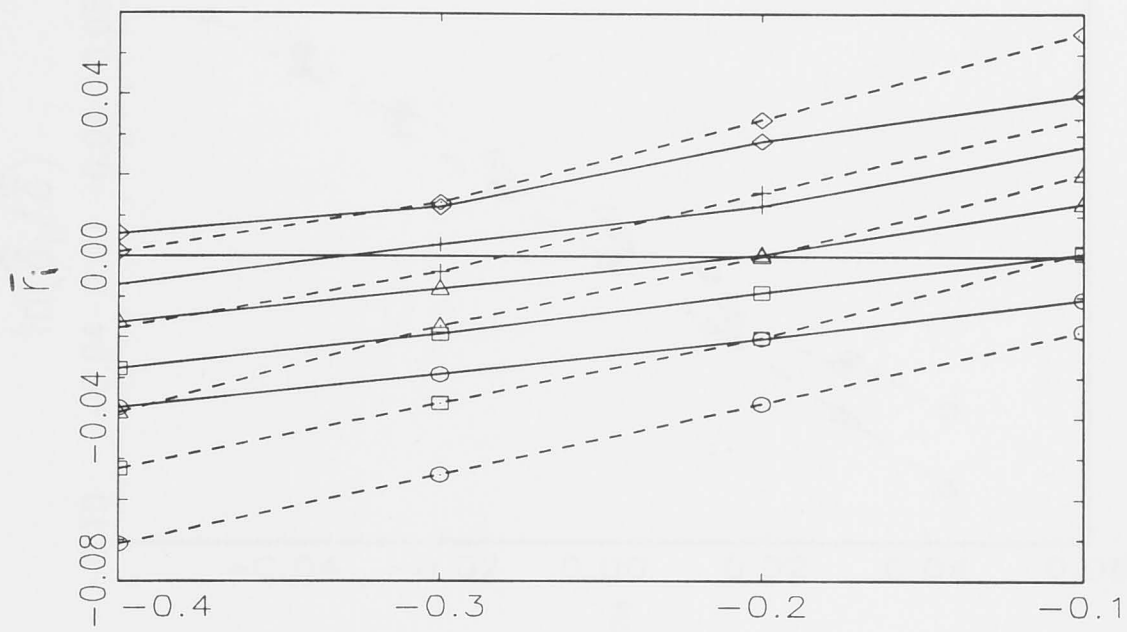

(a)

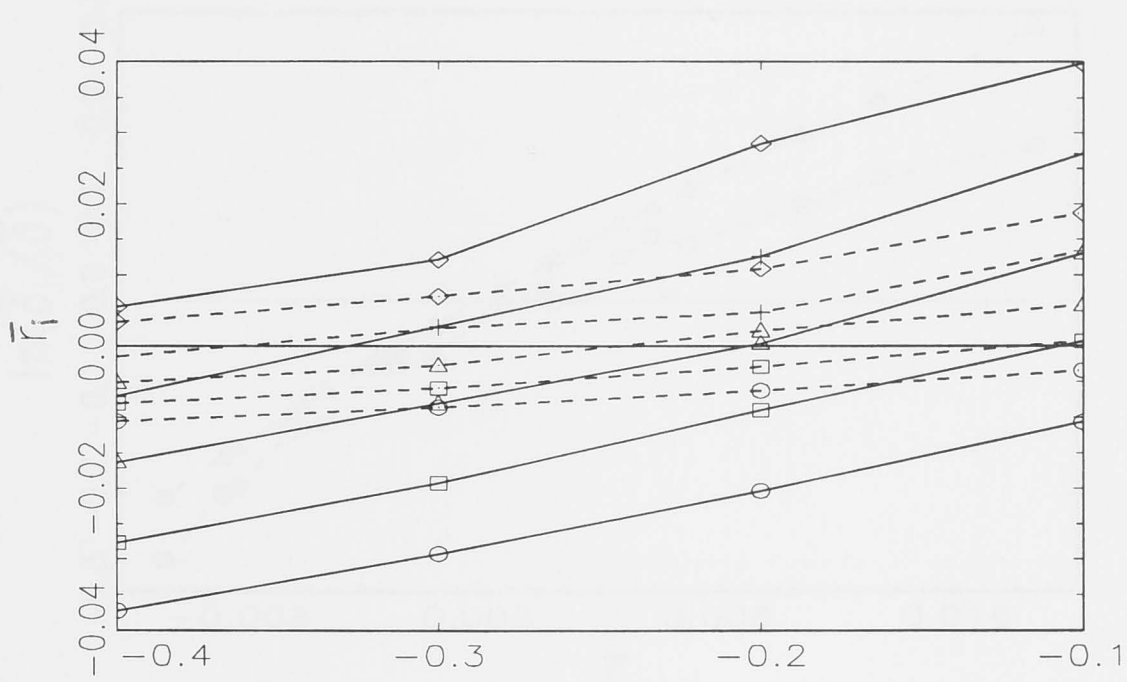

(b)

Figure 4-2: Long-term population growth rate of the invader ($\bar{r}_i$) calculated using simulations with mortality schedules of type II (solid lines) and type I with $\Delta_m = 0.4086$ (dashes) (a), and type III with $\Delta_m = -1.9485$ (dashes) (b). σ^2 equals 0 ($\circ$), 0.125 ($\square$), 0.25 ($\triangle$), 0.375 ($+$), and 0.5 ($\diamond$).

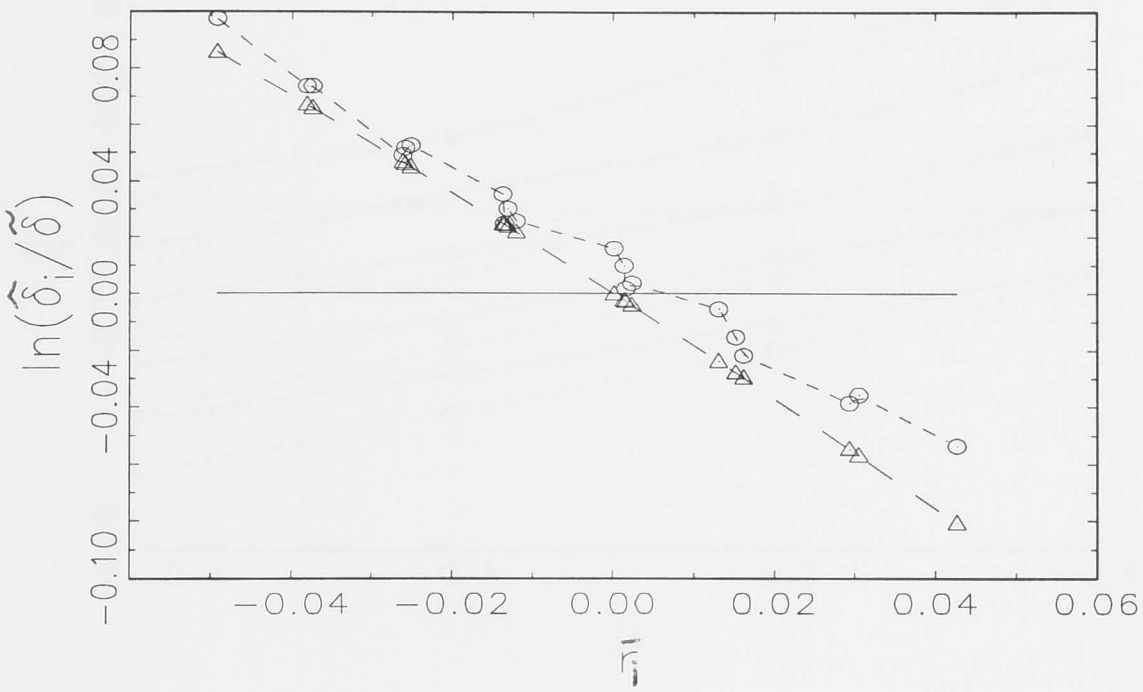

(a)

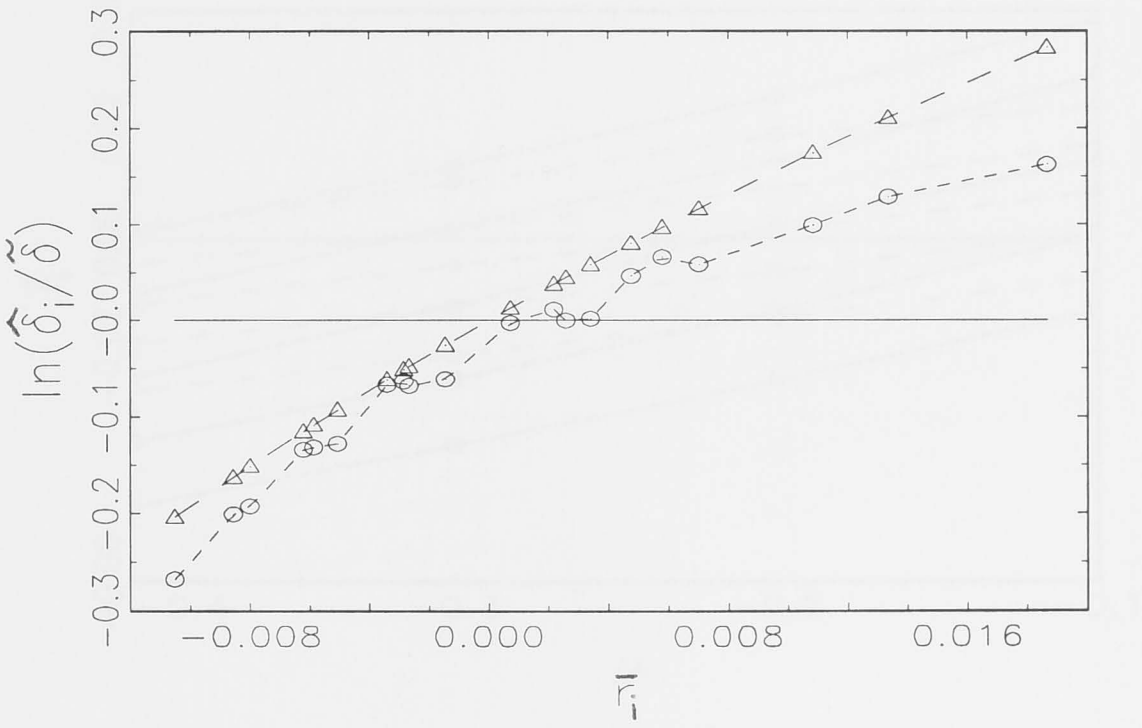

(b)

Figure 4-3: The ln of ratio of mean value of $\hat{\delta}_i(t)$ from equation 4.14, calculated using simulation, and age-independent death rate ($\tilde{\delta}$) ($\circ$), and the ln of ratio of $\hat{\delta}_i$, from equation 4.15, and age-independent death rate ($\tilde{\delta}$) ($\triangle$), with a type I mortality schedule with $\Delta_m = 0.2025$ (a) and a type III mortality schedule with $\Delta_m = -1.9485$ (b).

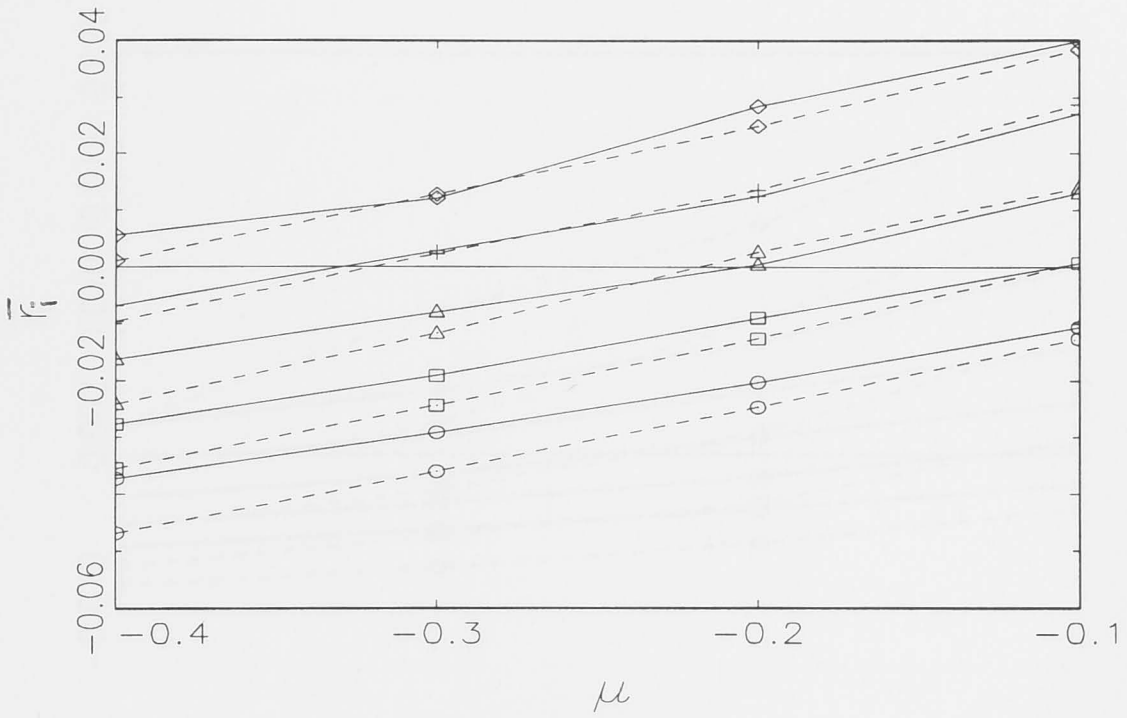

(a)

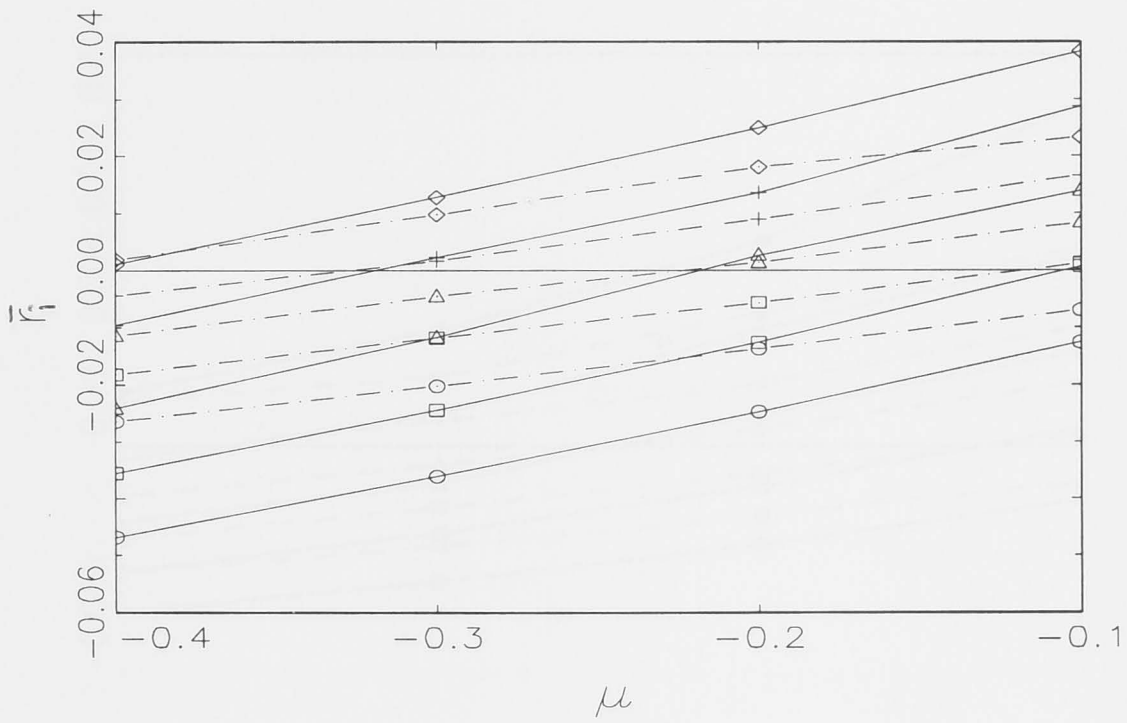

(b)

Figure 4-4: Long-term population growth rate of the invader ($\bar{r}_i$), calculated using simulations, with mortality schedule of type II and age-independent reproduction (solid lines), and with an early peak reproduction with $\Delta_f = -1.2545$ (shor dashes) (a), and with a delayed peak reproduction with $\Delta_f = 5$ (long dashes) (b). σ^2 equals 0 ($\circ$), 0.125 ($\square$), 0.25 ($\triangle$), 0.375 ($+$), and 0.5 ($\diamond$).

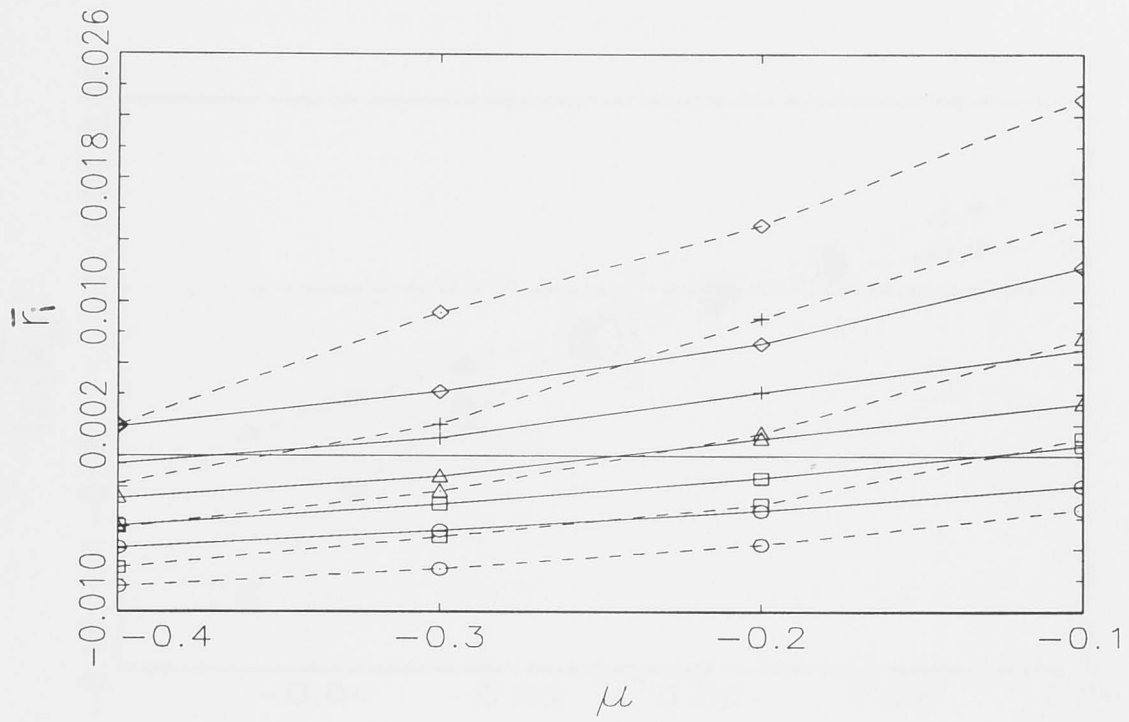

(a)

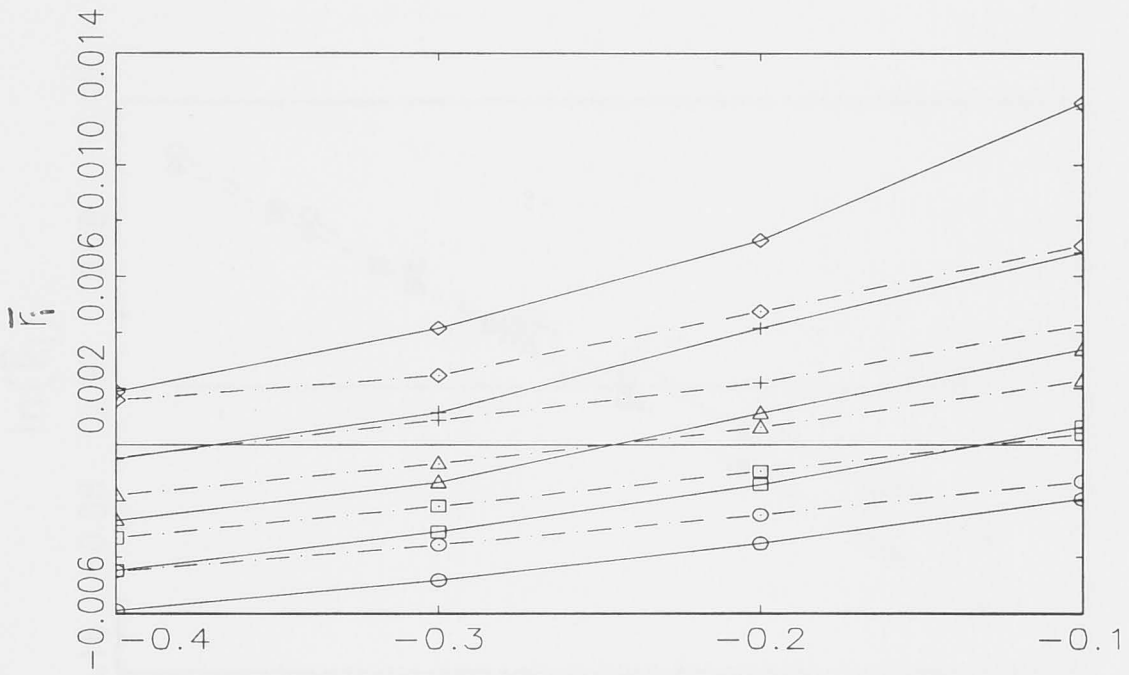

(b)

Figure 4-5: Long-term population growth rate of the invader ($\bar{r}_i$), calculated using simulations, with mortality schedule of type III with $\Delta_m = -4.1589$ and age-independent reproduction (solid lines), and with an early peak reproduction with $\Delta_f = -22.6039$ (short dashes) (a), and with a delayed peak reproduction with $\Delta_f = 25.3683$ (long dashes) (b). σ^2 equals 0 ($\circ$), 0.125 ($\square$), 0.25 ($\triangle$), 0.375 ($+$), and 0.5 ($\diamond$).

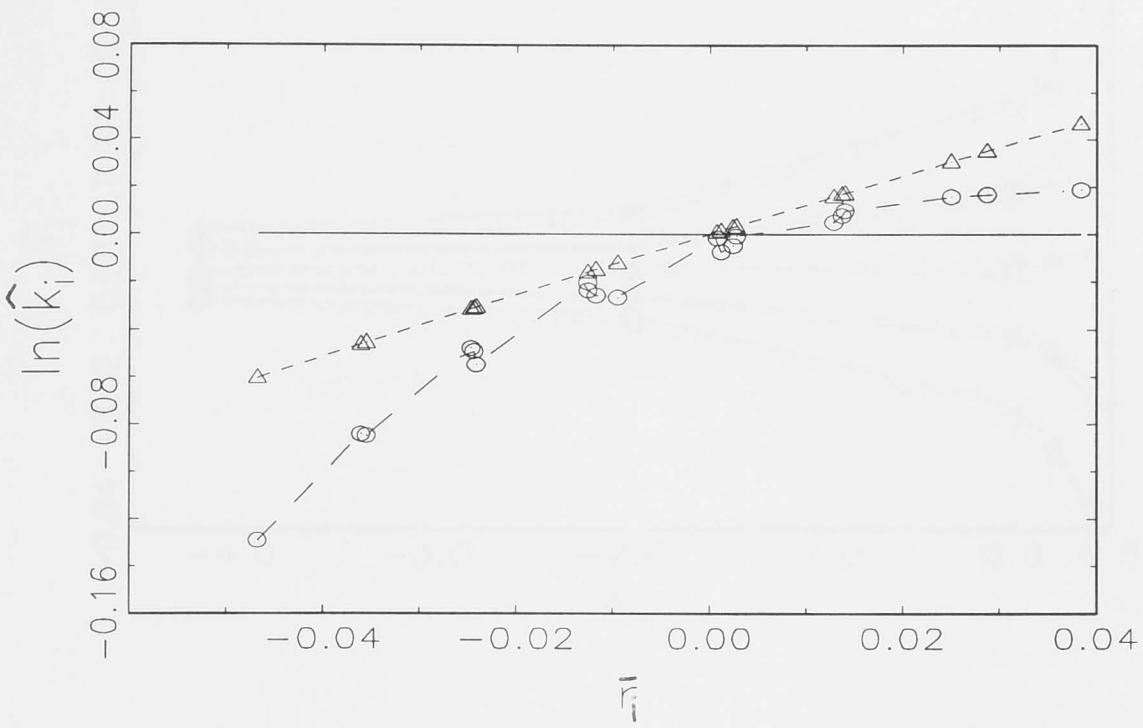

(a)

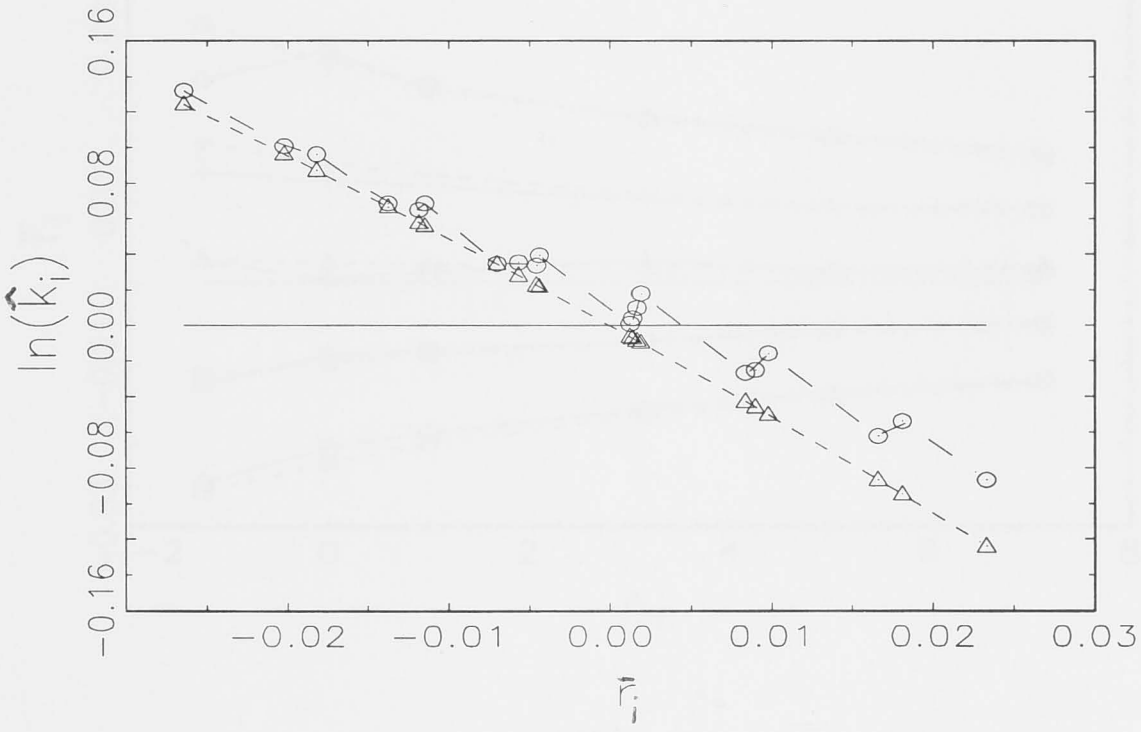

(b)

Figure 4-6: The ln of mean value of $\hat{k}_i(t)$ from equation 4.19, calculated using simulation ($\circ$), and $\ln \hat{k}_i$ from equation 4.20 ($\triangle$), with an early peak reproduction with $\Delta_f = -1.2545$ (a), and a delayed peak reproduction with $\Delta_f = 5$ (b).

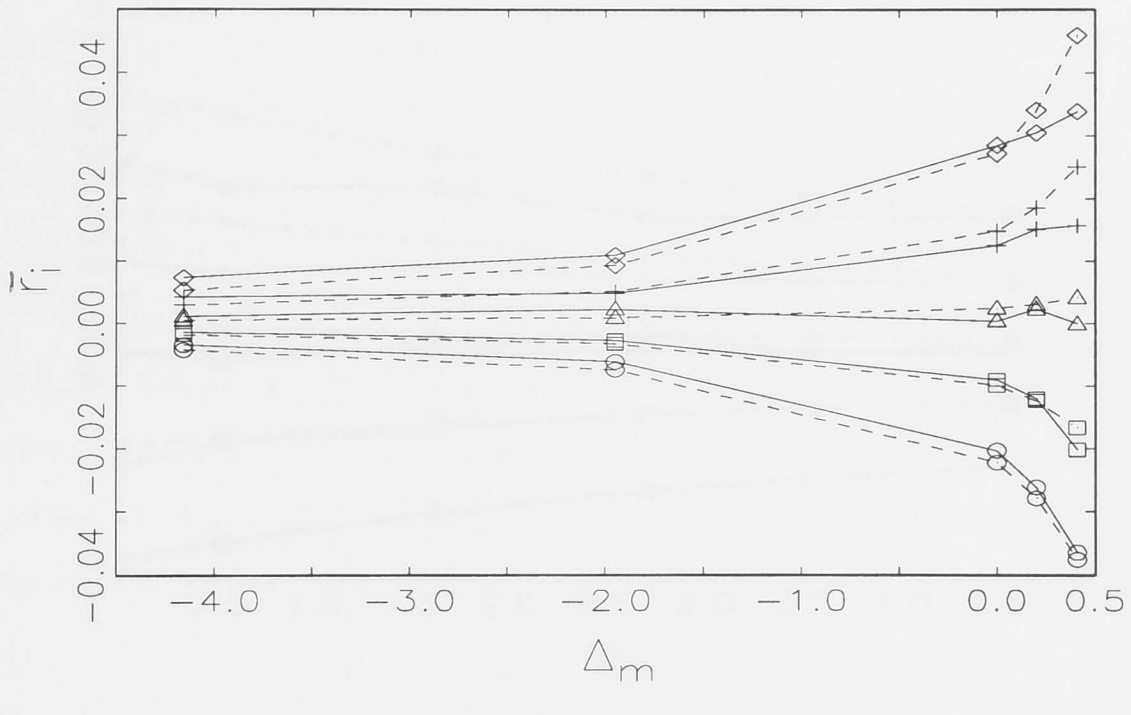

(a)

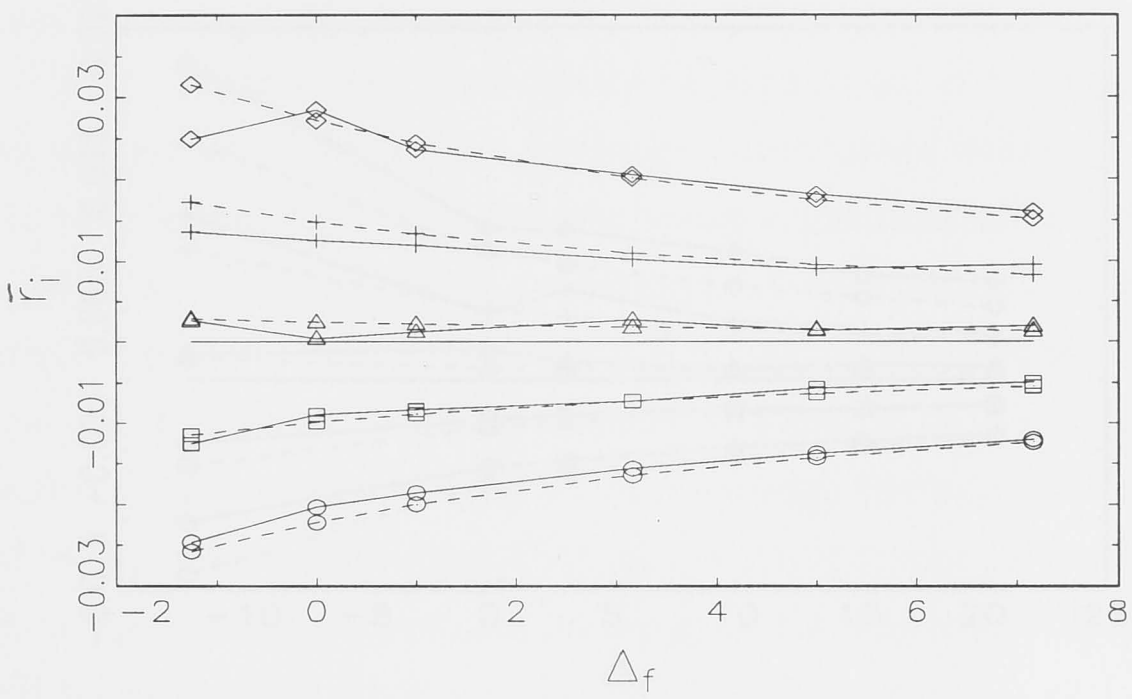

(b)

Figure 4-7: Long-term population growth rate of the invader ($\bar{r}_i$) with various mortality schedules and age-independent reproduction, calculated using simulation (solid), and equation 4.23 (dashes) (a). Long-term population growth rate of the invader ($\bar{r}_i$) with various fecundity schedules and a type II mortality schedule, calculated using simulations (solid), and equation 4.23 (dashes) (b). σ^2 equals 0 ($\circ$), 0.125 ($\square$), 0.25 ($\triangle$), 0.375 ($+$), and 0.5 ($\diamond$). $\mu = -0.2$.

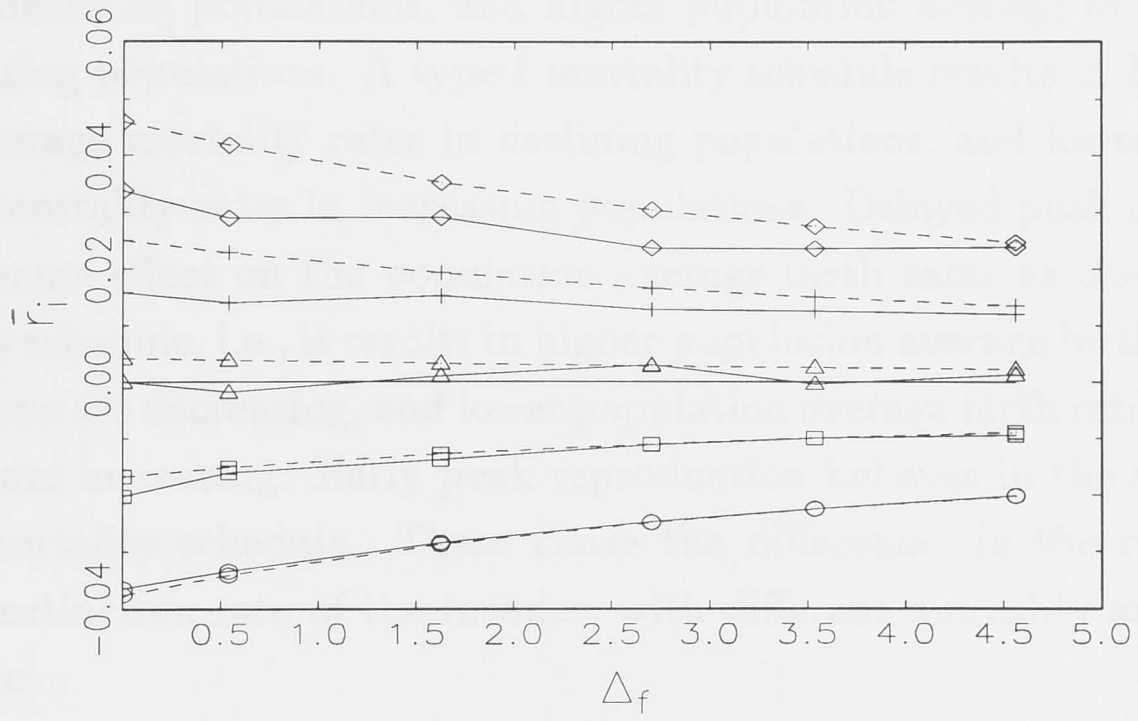

(a)

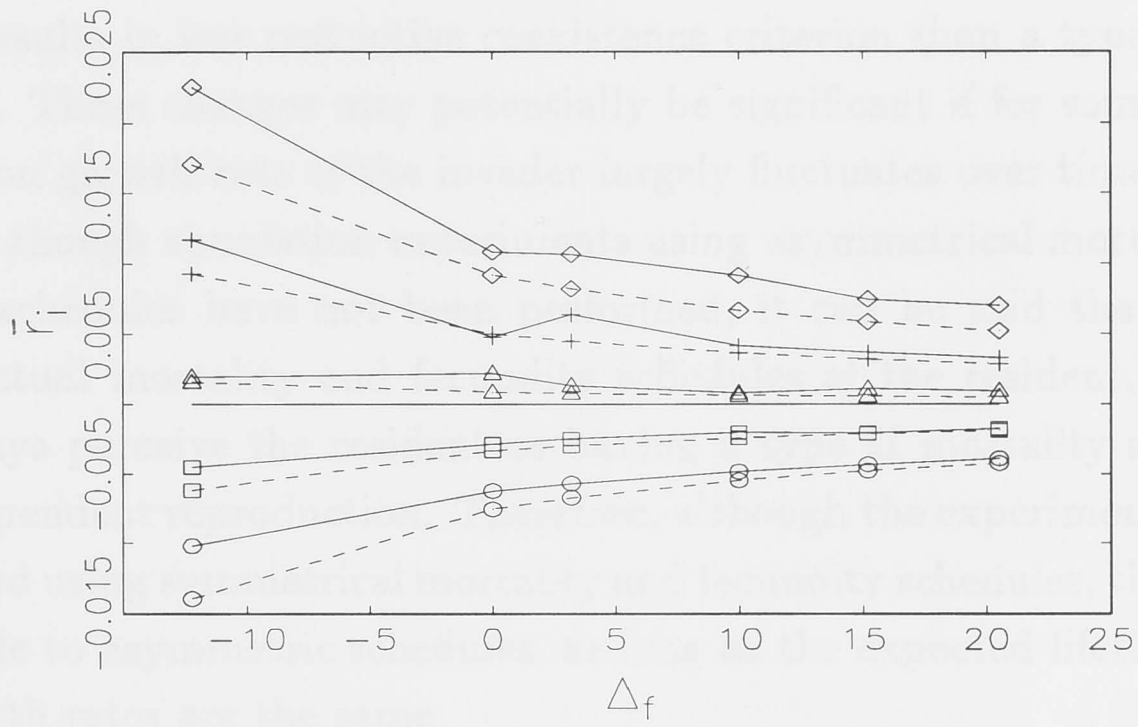

(b)

Figure 4-8: Long-term population growth rate of the invader ($\bar{r}_i$) with various fecundity schedules and a type I mortality schedule with $\Delta_m = 0.4086$, calculated using simulations (solid), and equation 4.23 (dashes) (a). Long-term population growth rate of the invader ($\bar{r}_i$) with various fecundity schedules and a type III mortality schedule with $\Delta_m = -1.9485$ calculated using simulations (solid), and equation 4.23 (dashes) (b). σ^2 equals 0($\circ$), 0.125($\square$), 0.25 ($\triangle$), 0.375 (+), and 0.5 ($\diamond$). $\mu = -0.2$.

and fecundity schedules on the long-term population growth rate of the invader.

A type III mortality schedule results in lower population average mortality rates in declining populations, and higher population average mortality rates in increasing populations. A type I mortality schedule results in higher population average mortality rates in declining populations, and lower population average mortality rates in increasing populations. Delayed peak reproduction has the same effect on the population average birth rates as does a type III mortality schedule, i.e., it results in higher population average birth rates when populations are decreasing, and lower population average birth rates when populations are increasing. Early peak reproduction behaves in the same way as type I mortality schedule. These cause the differences in the recovery rate and the extinction rate of the invader, with different mortality and fecundity schedules.

The criterion for coexistence, i.e., the magnitude of fluctuations in birth rates required for the invader to have at least zero long-term population growth rates, does change with changes in mortality schedules, but quantitatively the changes may not be significant. This changes are due to the fluctuations in the population growth rate of the invader over time. A type III mortality schedule always results in less restrictive coexistence criterion than a type I mortality schedule. These changes may potentially be significant if for some reason the population growth rate of the invader largely fluctuates over time.

Even though simulation experiments using asymmetrical mortality and fecundity schedules have not been performed, it can be said that, regardless of the actual mortality and fecundity schedules of the resident, the invader will always perceive the resident as having a type II mortality schedule and age-independent reproduction. Therefore, although the experiments have been performed using symmetrical mortality and fecundity schedules, the results are applicable to asymmetric schedules, as long as the expected lifetimes and the mean birth rates are the same.

In terms of the long-term population growth rate of the invader and the storage effect, the SLM incorporates extra terms involving the Δ-measure of mortality and fecundity schedules. Except for the small change in coexistence criterion due to fluctuation in the population growth rate of the invader over time, the behaviour of the SLM is similar to that of the NLM. Competition, covariance between the environment and competition, sub-additivity and the magnitude of the storage effect of the resident in the SLM are equivalent to those in the NLM.

Chapter 5

Tuljapurkar's approximation to the Age-structured Lottery Model (the SLM) in variable environments

5.1 Introduction

In Chapter 4, I followed Chesson's framework in analysing the SLM, making use of the order approximation to calculate long-term population growth rate of the invader. The age-structured model was reduced to a non-structured model, which was possible due to the stationary age distribution in the resident population. The effects of age-structure in the invader could be approximated using the Δ-measure. In this chapter, I will again examine the long-term population growth rate of the invader in the SLM, by applying the quadratic approximation proposed by Tuljapurkar (1982) to the full matrix formulation of the model. As shown in Chapter 4, since the resident is always at the stationary distribution, the SLM was reduced to a special case of the general demographic model presented in Chapter 3.

The matrix formulation and analysis for the general demographic model was first proposed by Leslie (1945, 1948), and is now commonly used by ecologists (e.g., Caswell 1989). Matrix population models are especially common in studies with time-independent projection matrices, i.e., when vital rates are constant over time, and there is no stochasticity. Applications of matrix population models very broad, as can be seen from the large volume of publications to date.

Stochastic demographic models were developed starting with the work of Cohen (1976, 1977) on the stochastic ergodic theorem. Tuljapurkar proposed quadratic approximation as a method to calculate the long-term population growth rate in stochastic demographic models (Tuljapurkar 1982). Tuljapurkar and Orzack used this technique to analyse life-history evolution following the evolutionary stable strategy (ESS) approach (Orzack and Tuljapurkar 1989; Orzack 1993; Orzack 1997). However, there have been few applications of Tuljapurkar's quadratic approximation compared with applications of deterministic demographic models, although the approximation technique is straight forward and is very efficient computationally. An example of recent application of Tuljpurkar's quadratic approximation can be found in (Benton and Grant 1996), as a tool for analysing life-history evolution of red deer.

I will show that the Tuljapurkar's approximation is applicable to the two-species SLM, despite the density-dependent recruitment. I must say that the restriction to the two-species system is quite strong. However, considering the importance of the lottery competition model it is useful to explore the the matrix approach as an alternative computation method. Moreover, if most communities are at equilibrium in the long-term (i.e., population growth rate fluctuates around zero), then this simple approach to the two-species SLM will potentially have broader implications, as does Tuljapurkar's approximation.

5.2 Matrix population model

The general demograhic model without stochasticity is commonly written as:

$$\mathbf{P}(t+1) = \mathbf{L}\mathbf{P}(t), \tag{5.1}$$

or

$$\begin{pmatrix} P_1 \\ P_2 \\ P_3 \\ \vdots \\ P_s \end{pmatrix}(t+1) = \underbrace{\begin{pmatrix} b_1 & b_2 & b_3 & \cdots & b_s \\ (1-\delta_1) & 0 & 0 & \cdots & 0 \\ 0 & (1-\delta_2) & 0 & \cdots & 0 \\ \vdots & \vdots & \ddots & \cdots & \vdots \\ 0 & 0 & \cdots & (1-\delta_{s-1}) & (1-\delta_s) \end{pmatrix}}_{\mathbf{L}} \begin{pmatrix} P_1 \\ P_2 \\ P_3 \\ \vdots \\ P_s \end{pmatrix}(t), \tag{5.2}$$

where $P_x(t)$ is population size of age x at time t, $\mathbf{L}$ is a projection matrix, with elements b_x is the birth rate of an individual in the age range x to $x+1$, and $(1-\delta_x)$ is probability of survival of age x. By defining $b_{s+j} = b_s$, and $\delta_{s+j} = \delta_s$, for $j \geq 0$, we allow an infinite number of age classes.

The population growth rate (r) is ln of the dominant eigenvalue of $\mathbf{L}$. The dominant eigenvalue is guaranteed to be a positive, real number since $\mathbf{L}$ is a non-negative, primitive matrix (Perron-Frobenius theorem; see for example Caswell 1989; Caswell 1997). The corresponding left eigenvector is the vector of reproductive values, and the corresponding right eigenvector is the vector specifying the stable age distribution (Leslie 1945). This matrix formulation and analysis are exactly equivalent to the Lotka's model. For detailed exposition see (Caswell 1989; Caswell 1997).

5.3 Tuljapurkar's approximation

When there is some stochasticity involved in the model, i.e., either birth rate, death rate, or both, randomly fluctuate over time, a sequence of randomly varying projection matrices are used to incorporate the fluctuations in the birth rates and death rates. Thus, equation 5.1 becomes:

$$\mathbf{P}(t+1) = \mathbf{L}(t)\mathbf{P}(t), \tag{5.3}$$

where $\mathbf{L}(t)$ is the projection matrix at time t, whose elements are random variables replacing the constant elements of the projection matrix $\mathbf{L}$ in equation 5.1.

At the present time, analytical tools do not allow the complete solution for the population growth rate (r). However, some approximation techniques are available. Tuljapurkar's approximation (Tuljapurkar 1982; Tuljapurkar 1990; Tuljapurkar 1997) is the most general technique and is shown to be robust (Orzack and Tuljapurkar 1989; Orzack 1993; Orzack 1997). The technique will be described briefly here.

Given a sequence of projection matrices $\mathbf{L}(t), \ldots, \mathbf{L}(1)$, equation 5.3 can be re-expressed as:

$$\mathbf{P}(t+1) = \mathbf{L}(t)\mathbf{L}(t-1)\ldots\mathbf{L}(1)\mathbf{P}(1).$$

Question of interest is how to assign a logarithmic population growth rate function to $\mathbf{L}(t)\mathbf{L}(t-1)\ldots\mathbf{L}(1)$. Tuljapurkar used the property of weak ergodicity. Weak ergodicity implies that:

$$r = \lim_{t\to\infty} \mathrm{E}\left[\frac{1}{t}\ln\left\{\mathbf{V}_t' \prod_{i=1}^{t} \mathbf{L}(i)\mathbf{U}_1\right\}\right], \tag{5.4}$$

where r is the logarithmic population growth rate, $\mathbf{V}_t$ is the left eigenvector corresponding to the dominant eigenvalue of $\mathbf{L}(t)$, and $\mathbf{U}_1$ is the right eigenvector corresponding to the dominant eigenvalue of $\mathbf{L}(1)$ (Ruelle 1979).

Next, the matrix $\mathbf{L}(t)$ is decomposed into:

$$\mathbf{L}(t) = \mathbf{A} + \mathbf{B}(t), \tag{5.5}$$

such that
$\mathbf{A}$ is the average of the projection matrices over time, and
$\mathbf{B}(t)$ is fluctuation about $\mathbf{A}$ over time, with $\mathrm{E}[\mathbf{B}(t)] = 0$. By substituting equation 5.5 into the equation 5.4, we get:

$$r = \lim_{t\to\infty} \mathrm{E}\left[\frac{1}{t}\ln\left\{\mathbf{V}_t' \prod_{i=1}^{t}(\mathbf{A} + \mathbf{B}(t))\mathbf{U}_1\right\}\right]. \tag{5.6}$$

Applying the second order Taylor expansion to the term inside the curly brackets of equation 5.6, the logarithmic growth rate is approximated as:

$$r \approx \underbrace{\ln\lambda_0}_{1} - \underbrace{\frac{\tau^2}{2\lambda_0^2}}_{2} + \underbrace{\frac{\theta}{\lambda_0^2}}_{3}, \tag{5.7}$$

where:

$$\begin{aligned}
\tau^2 &= \frac{(\mathbf{V}_0 \otimes \mathbf{V}_0)'\mathbf{C}_0(\mathbf{U}_0 \otimes \mathbf{U}_0)}{T_0^2}, \\
\theta &= \sum_{\alpha=1}^{k-1} \frac{1}{T_0 T_\alpha}(\mathbf{V}_0 \otimes \mathbf{V}_\alpha)' \left\{\sum_{l=1}^{\infty}\left(\frac{\lambda_\alpha}{\lambda_0}\right)^{l-1} \mathbf{C}_l\right\}(\mathbf{U}_\alpha \otimes \mathbf{U}_0), \\
T_\alpha &= (\mathbf{V}_\alpha'\mathbf{U}_\alpha), \\
\mathbf{C}_m &= \mathrm{E}[\mathbf{B}_{t+m} \otimes \mathbf{B}_t], \\
m &= 0, 1, 2, \ldots
\end{aligned}$$

The operator $\otimes$ is the Kronecker product. Terms λ_0, $\mathbf{V}_0$ and $\mathbf{U}_0$ are the dominant eigenvalue of matrix $\mathbf{A}$, the corresponding left eigenvector, and the right eigenvector, respectively. Note that $\mathbf{V}$ and $\mathbf{U}$ are now properties of matrix $\mathbf{A}$, and not those of matrix $\mathbf{L}$.

The first term of r in equation 5.7 reflects only the deterministic part of the model. The second term takes account the variances of the vital rates over time, and the covariances between them. This term does not include temporal correlations, however. Unless vital rates of different classes are negatively correlated, the effect of the second term is always discounting to the first term. The strength of the discounting effect depends also on how large T_0^2 is. Some demographic literature refers to T_0^2 as the mean generation length. The third term of the equation deals with temporal correlations in vital rates.

5.4 The SLM as a matrix model

In section 4.3 I showed how the equation for the dynamics of the invader in the two-species SLM converges to a matrix equation. I will use Tuljapurkar's approximation technique to calculate the long-term population growth rate of the invader. Species coexistence in the two-species SLM can then be inferred by the arguments of invasibility analysis.

Now let us consider a special case of equation 4.10, where mortality, but not fecundity, is age-dependent. Applying Tuljapurkar's framework, the projection matrices of the SLM are decomposed into:

$$\mathbf{L}(t) = \mathbf{A} + \mathbf{B}(t),$$

where the average projection matrix is

$$\mathbf{A} = \begin{bmatrix} \tilde{\delta}\mathrm{E}\left[\rho(t)\right] & \tilde{\delta}\mathrm{E}\left[\rho(t)\right] & \tilde{\delta}\mathrm{E}\left[\rho(t)\right] & \cdots & \tilde{\delta}\mathrm{E}\left[\rho(t)\right] \\ (1-\delta_1) & 0 & 0 & \cdots & 0 \\ 0 & (1-\delta_2) & 0 & \cdots & 0 \\ \vdots & \vdots & \ddots & \cdots & \vdots \\ 0 & 0 & \cdots & (1-\delta_{s-1}) & (1-\delta_s) \end{bmatrix},$$

with $\tilde{\delta}\mathrm{E}\left[\rho(t)\right] = \tilde{\delta}e^{\mu_i - \mu_j + \sigma^2}$, $\rho(t) = b_i(t)/b_j(t)$. The terms μ_i and μ_j are the expected value of $\ln b_i(t)$ and $\ln b_j(t)$, respectively. The term σ^2 is variance of $\ln b_i(t)$ and $\ln b_j(t)$, since $b(t)$ is lognormally distributed (see section 2.3). In this study, $\ln b_i$ and $\ln b_j$ are assumed to be independent. This assumption is important, as only the variance for $\ln \rho$ is at issue. For other cases, the correct variance has to be substituted for $2\sigma^2$ in the formula of $\mathrm{E}[\rho(t)]$. This also allows the variance of ln birth rates to be unequal. In my setting, the correlations between each element of the first row of $\mathbf{A}$ are one, and there is no autocorrelation of birth rates over time. Also, there are no cross correlations between birth rates of the species.

Fluctuations of $\mathbf{L}(t)$ over time are incorporated in:

$$\mathbf{B}(t) = \begin{bmatrix} \alpha(t) & \alpha(t) & \alpha(t) & \cdots & \alpha(t) \\ 0 & 0 & 0 & \cdots & 0 \\ 0 & 0 & 0 & \cdots & 0 \\ \vdots & \vdots & \ddots & \cdots & \vdots \\ 0 & 0 & \cdots & 0 & 0 \end{bmatrix},$$

where $\alpha(t) = \tilde{\delta}\rho(t) - \tilde{\delta}\mathrm{E}\left[\rho(t)\right]$.

The general formula of the Tuljapurkars's approximation of equation 5.7 is reduced, for the above setting, to:

$$\bar{r}_i \approx \ln \lambda_0 - \frac{(\mathbf{V}_0[1])^2(\mathbf{1}'\mathbf{U}_0)^2 \mathrm{Var}[\alpha(t)]}{2\lambda_0^2 T_0^2}, \tag{5.8}$$

where
$\mathrm{Var}[\alpha(t)] = \tilde{\delta}^2 e^{2(\mu_i - \mu_j + \sigma^2)}(e^{2\sigma^2} - 1)$,
λ_0,$\mathbf{V}_0$, and $\mathbf{U}_0$ are the dominant eigenvalue, its corresponding left eigenvector, and right eigenvector of $\mathbf{A}$, respectively, and
$T_0 = \mathbf{V}_0'\mathbf{U}_0$.

For the SLM with both structured mortality and fecundity, we have the average projection matrix over time as:

$$\mathbf{A} = \begin{bmatrix} \tilde{\delta}k_1 \mathrm{E}\left[\rho(t)\right] & \tilde{\delta}k_2 \mathrm{E}\left[\rho(t)\right] & \tilde{\delta}k_3 \mathrm{E}\left[\rho(t)\right] & \cdots & \tilde{\delta}k_s \mathrm{E}\left[\rho(t)\right] \\ (1-\delta_1) & 0 & 0 & \cdots & 0 \\ 0 & (1-\delta_2) & 0 & \cdots & 0 \\ \vdots & \vdots & \ddots & \cdots & \vdots \\ 0 & 0 & \cdots & (1-\delta_{(s-1)}) & (1-\delta_s) \end{bmatrix},$$

where $\tilde{\delta}k_x \mathrm{E}\left[\rho(t)\right] = \tilde{\delta}k_x e^{\mu_i - \mu_j + \sigma^2}$.

Fluctuations of $\mathbf{A}$ over time are incorporated in:

$$\mathbf{B}(t) = \begin{bmatrix} \alpha_1(t) & \alpha_2(t) & \alpha_3(t) & \cdots & \alpha_{s'}(t) \\ 0 & 0 & 0 & \cdots & 0 \\ 0 & 0 & 0 & \cdots & 0 \\ \vdots & \vdots & \ddots & \cdots & \vdots \\ 0 & 0 & \cdots & 0 & 0 \end{bmatrix},$$

where $\alpha_x(t) = \tilde{\delta}k_x\rho(t) - \tilde{\delta}k_x \mathrm{E}\left[\rho(t)\right]$.

Compared with the model without the fecundity schedule, $\mathbf{B}(t)$ is slightly different, since now $\alpha_x(t)$ is age dependent. Therefore, $\mathrm{cov}[\alpha_x(t), \alpha_y(t)] \neq \mathrm{var}[\alpha_x(t)] \neq \mathrm{var}[\alpha_y(t)]$, whenever $k_x \neq k_y$.

The approximation of the long-term growth rate of the invader is:

$$\bar{r}_i \approx \ln \lambda_0 - \frac{(\mathbf{V}_0[1])^2(\mathrm{E}\left[\mathbf{B}_{1.}(t) \otimes \mathbf{B}_{1.}(t)\right])'(\mathbf{U}_0 \otimes \mathbf{U}_0)}{2\lambda_0^2}, \tag{5.9}$$

where
$\mathrm{E}\left[B_{1x}(t)B_{1y}(t)\right] = \sqrt{\mathrm{var}[B_{1x}(t)]\mathrm{var}[B_{1y}(t)]}$, relying on our special conditions that $\mathrm{E}[B_{1x}] = 0$, and B_{1x} and B_{1y} are proportioned to each other,
$\mathrm{var}[B_{1x}(t)] = \tilde{\delta}^2 k_x^2 e^{2(\mu_i - \mu_j + \sigma^2)}(e^{2\sigma^2} - 1)$, and
$\mathbf{U}_0$,$\mathbf{V}_0$ are scaled such that $T_0 = \mathbf{V}_0'\mathbf{U}_0 = 1$.

5.5 Results and discussion

I am going to compare the long-term population growth rate of the invader, calculated from computer simulations, with that calculated from Tuljapurkar's approximation, given in equations 5.8 and 5.9. Then, I will exhibit similar results to Chapter 4 using a larger data set, since the computation of Tuljapurkar's approximation is computationally cheaper than simulations. A more extensive set of results on the long-term population growth rate of the invader, using a larger set of mortality and fecundity schedules than in Chapter 4, are given in figures 5-3 and 5-4.

The difference between the mean ln birth rate of the invader and resident $(\mu_i - \mu_j)$ is denoted by μ. Figures 5-1 and 5-2 show that the Tuljapurkar's approximation works well in general, with high numerical accuracy up to $\sigma^2 = 0.125$ both with structured mortality and fecundity.

Consistent patterns are found between the long-term population growth rate of the invader and mortality and fecundity schedules, quantified by the Δ-measures. Because the growth rate of the resident is always zero, the average death rate and birth rate of the resident converge to its age-independent death rate and birth rate (see Chapter 4 for derivation). Therefore, matrices $\mathbf{A}$ and $\mathbf{B}(t)$ incorporate only the age-independent death rate and birth rate of the resident, instead of its mortality and fecundity schedules. The long-term population growth rate of the invader is not affected by the mortality and fecundity schedules of the resident. We can disregard the mortality and fecundity schedules of the resident, and conclude that in a growing population, an invader has a higher rate of recovery from low density when it shows the type I mortality schedule, compared with invaders that show other types of mortality schedule. Moreover, an invader with early peak reproduction shows higher rates of recovery than that with other fecundity schedules. In declining populations, the rate of extinction of the invader is lower when it shows a type III mortality and delayed peak reproduction, compared with invaders that show other types of mortality schedules and fecundity schedules.

Coexistence of the two species in the SLM is more likely to occur when the invader shows a type III mortality schedule than either a type I or type II mortality schedule. This is because the average death rate in the population for an invader with a type III mortality schedule is smaller than that for an invader with type I and type II mortality schedules (shown in Chapter 4).

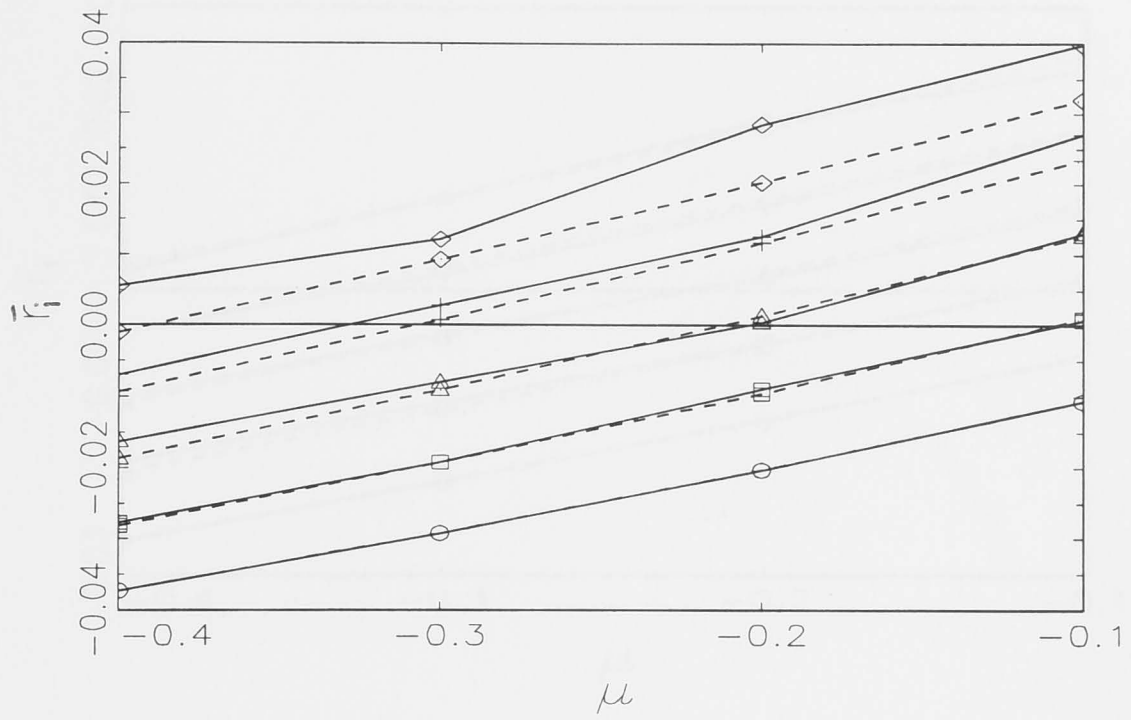

(a)

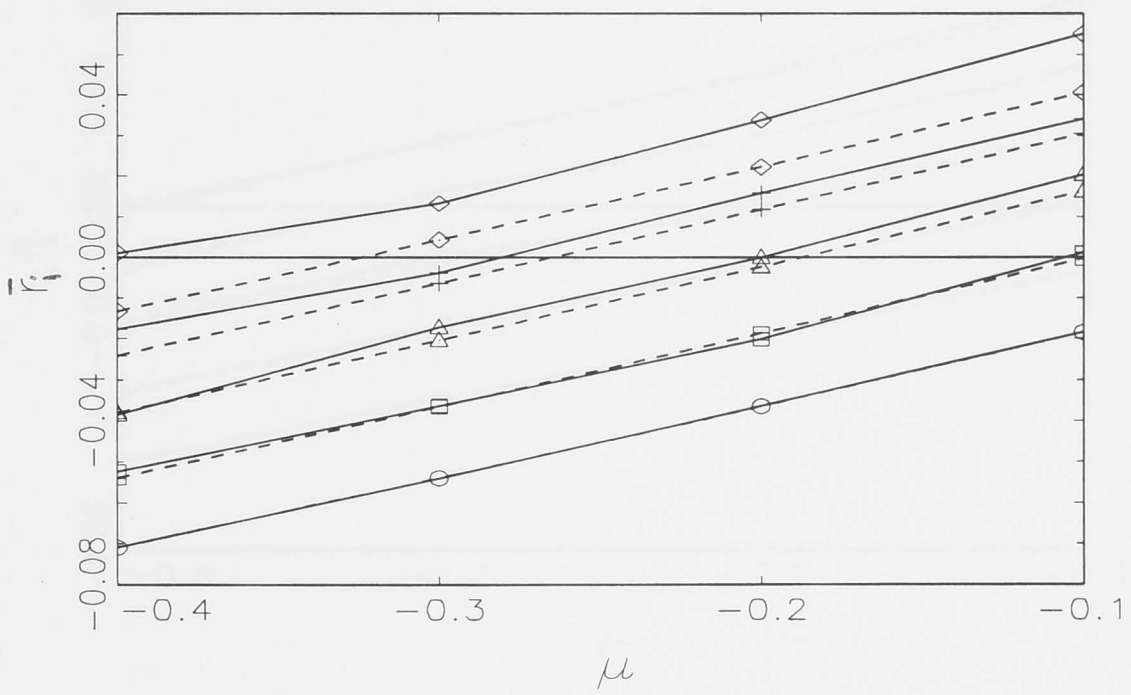

(b)

Figure 5-1: Long-term population growth rate of the invader ($\bar{r}_i$) from simulation (solid), and from Tuljapurkar's approximation (short dashes), with type II mortality schedule (a), and type I mortality schedule with $\Delta_m = 0.4086$ (b). σ^2 equals 0 ($\circ$), 0.125 ($\square$), 0.25 ($\triangle$), 0.375 ($+$) and 0.5 ($\diamond$).

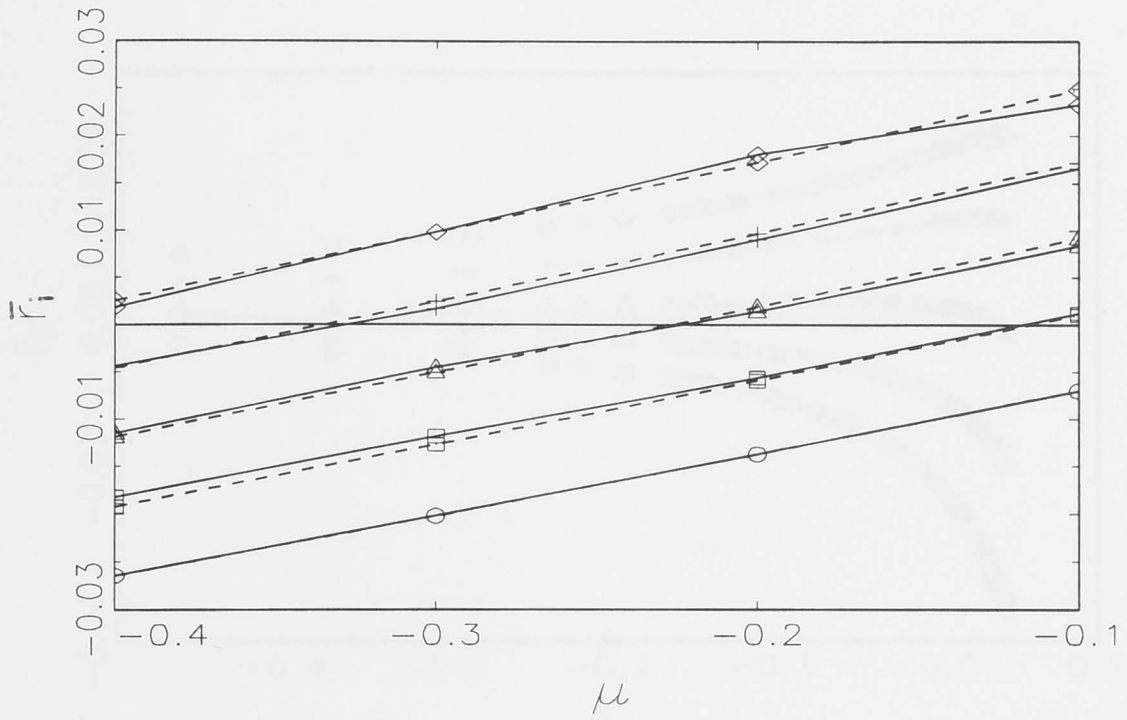

(a)

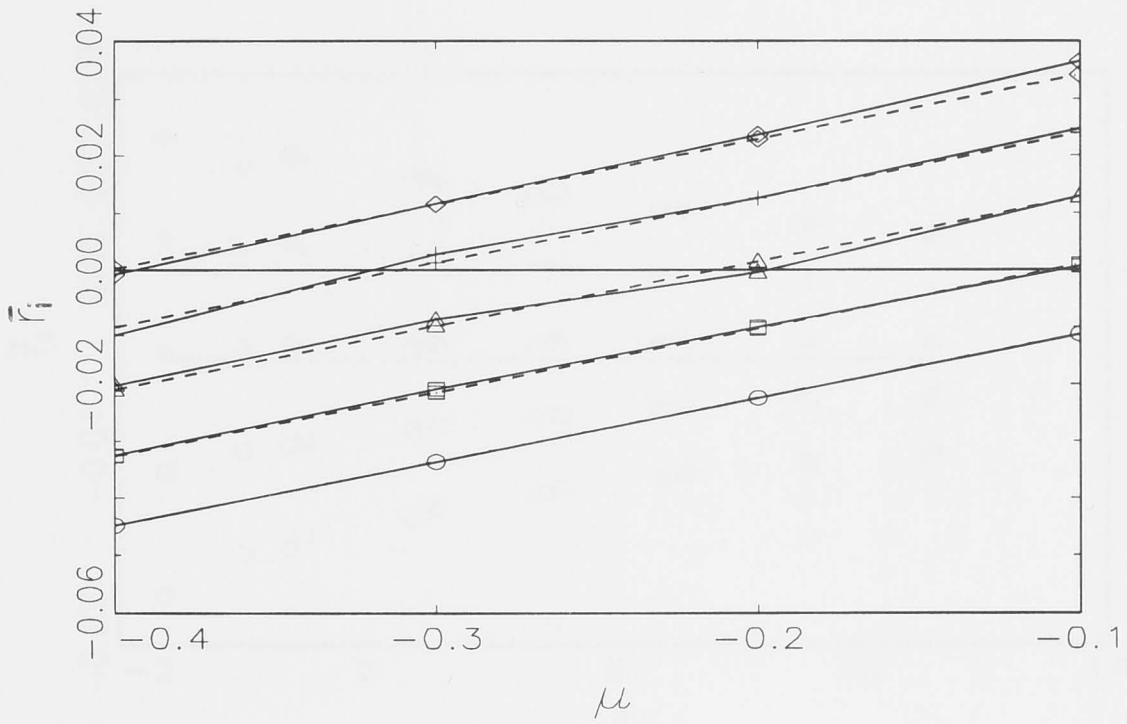

(b)

Figure 5-2: Long-term population growth rate of the invader ($\bar{r}_i$) from simulation (solid), and from Tuljapurkar's approximation (short dashes), with type II mortality schedule and delayed peak reproduction with $\Delta_f = 5$ (a), and type I mortality schedule with $\Delta_m = 0.4086$ and delayed peak reproduction with $\Delta_f = 3.5373$ (b). σ^2 equals 0 ($\circ$), 0.125 ($\square$), 0.25 ($\triangle$), 0.375 ($+$) and 0.5 ($\diamond$).

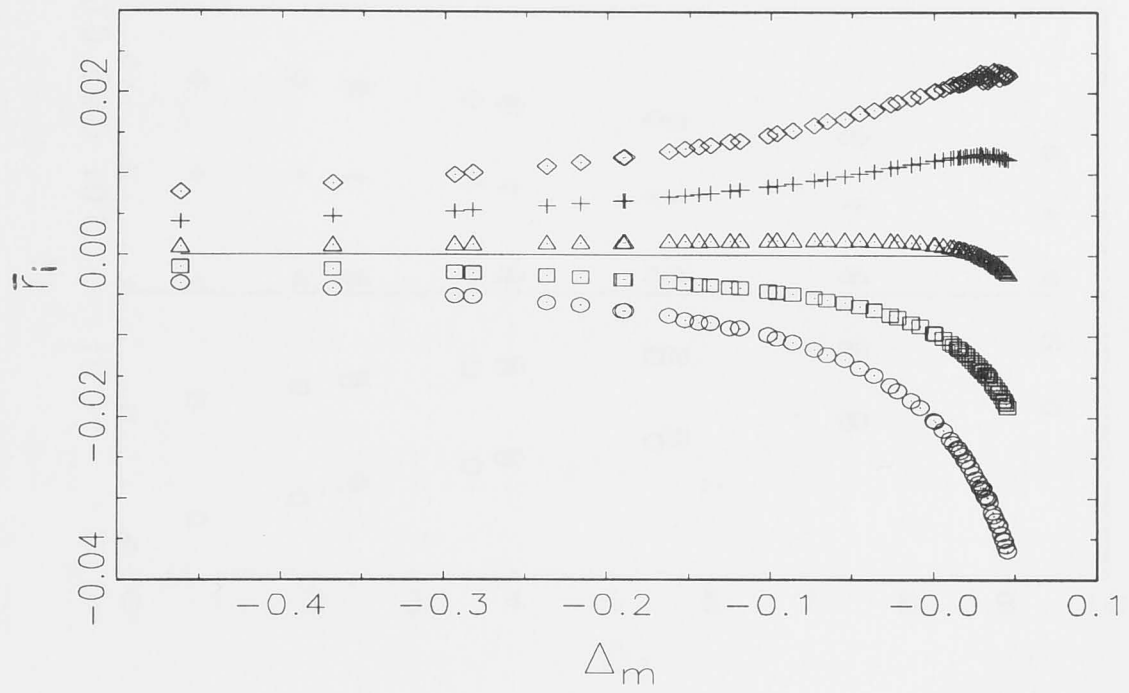

(a)

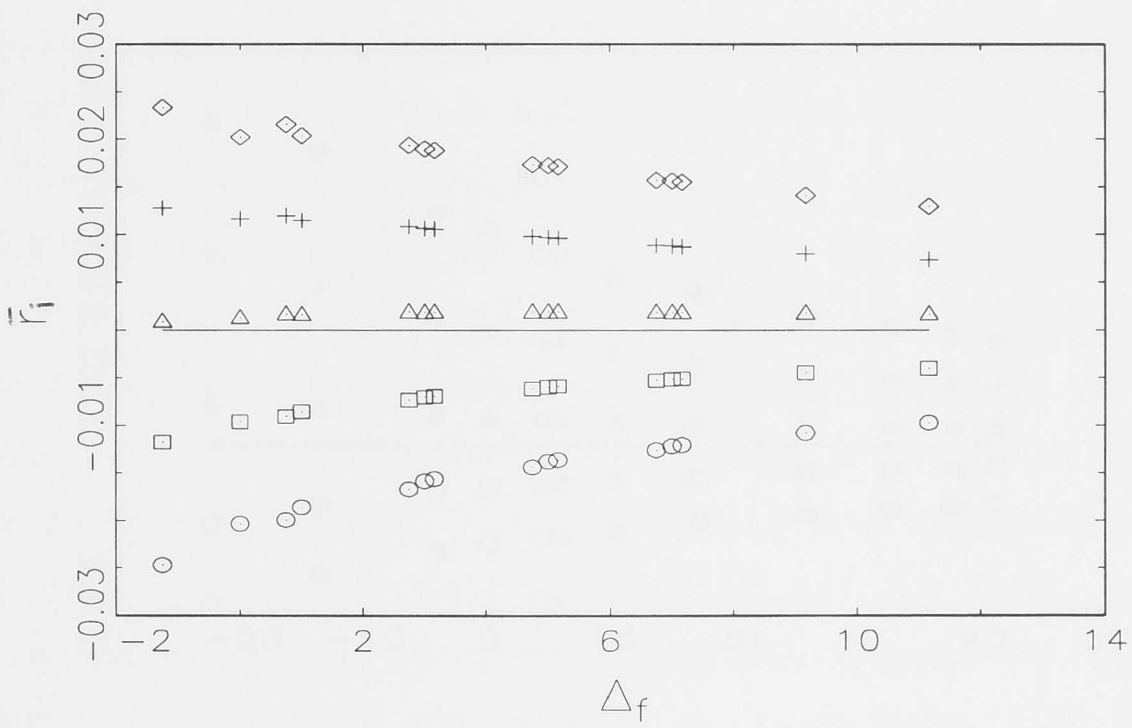

(b)

Figure 5-3: Long-term population growth rate of the invader ($\bar{r}_i$) from Tuljapurkar's approximation, with various mortality schedules and age-independent reproduction (a), and with type II mortality schedule and various fecundity schedules (b), all with $\mu = -0.2$. σ^2 equals 0 ($\circ$), 0.125 ($\square$), 0.25 ($\triangle$), 0.375 ($+$) and 0.5 ($\diamond$).

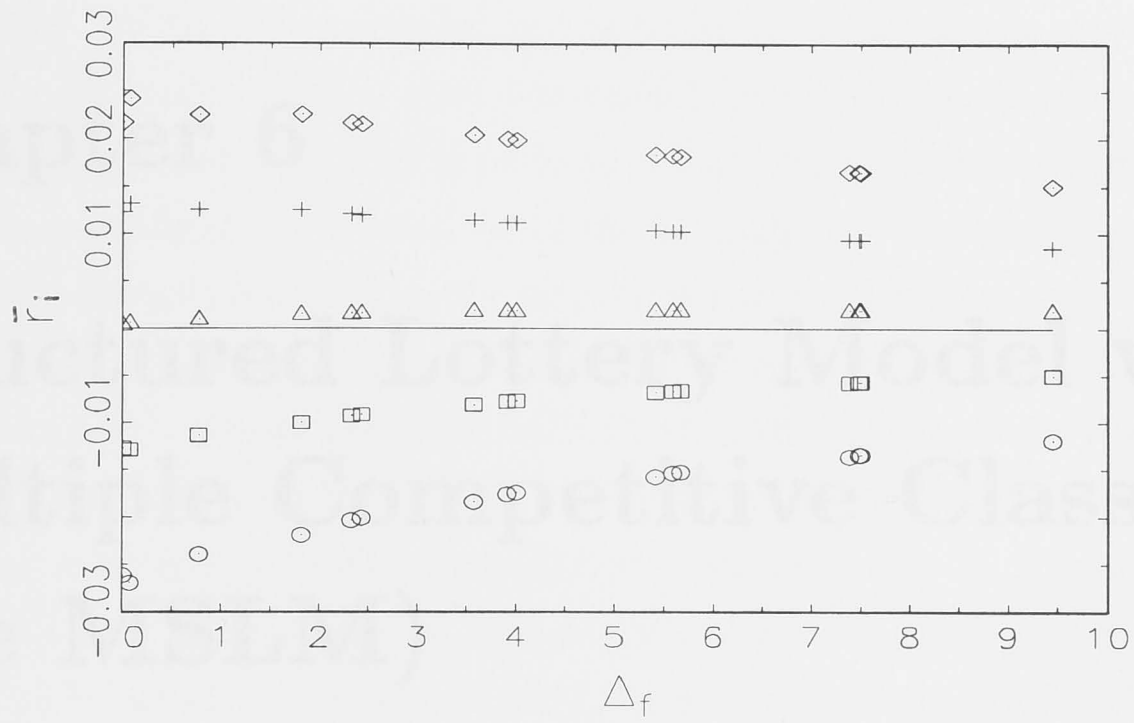

(a)

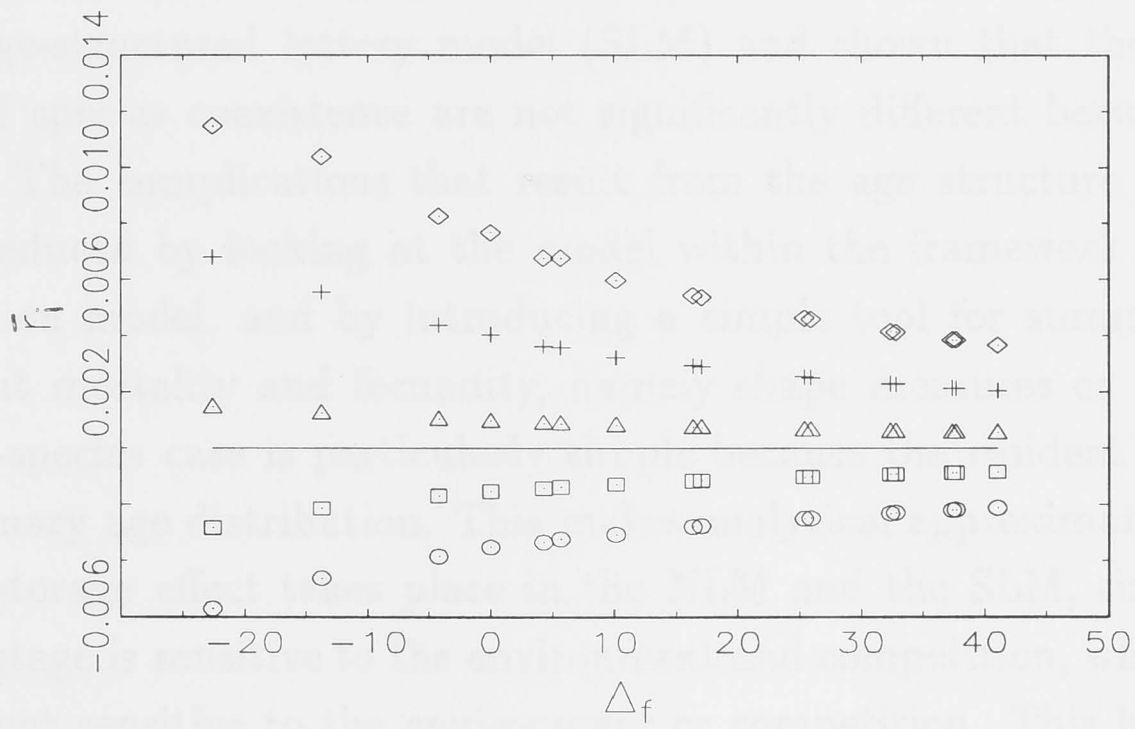

(b)

Figure 5-4: Long-term population growth rate of the invader ($\bar{r}_i$) from Tuljapurkar's approximation, with type I mortality schedule with $\Delta_m = 0.2025$ and various fecundity schedules (a), and with type III mortality schedule with $\Delta_m = -4.1589$ and various fecundity schedules (b), all with $\mu = -0.2$. σ^2 equals 0 ($\circ$), 0.125 ($\square$), 0.25 ($\triangle$), 0.375 ($+$) and 0.5 ($\diamond$).

Chapter 6

Structured Lottery Model with Multiple Competitive Classes (the MSLM)

6.1 Introduction

I have examined the extension of the non-structured lottery model (NLM) to the age-structured lottery model (SLM) and shown that the qualitative results of species coexistence are not significantly different between the two models. The complications that result from the age structure in the SLM can be reduced by looking at the model within the framework of a general competition model, and by introducing a simple tool for summarising age-dependent mortality and fecundity, namely shape measures or Δ-measures. The two-species case is particularly simple because the resident is always at its stationary age distribution. This makes analytical approximation possible.

The storage effect takes place in the NLM and the SLM, since only the juvenile stage is sensitive to the environment and competition, while the adult stage is not sensitive to the environment or competition. This heterogeneity within the population results in sub-additivity (Chesson 1990; Chesson and Huntly 1989). Competition and the environment show positive covariation, through common dependence on the birth rate of the resident. As long as the correlation between the birth rate of the invader and that of the resident is not near 1, there is asynchrony between the two species in their response to the environment. In my study, I have assumed that the correlation between the birth rate of the invader and that of the resident is zero.

In Chapters 2 and 5 I have shown that the storage effect does not differ

between the NLM and the SLM. The SLM is fully full age-structured, while the NLM has no age-structure. However, in terms of within-population heterogeneity of responses to the environment and competition, the two models do not differ. With only juveniles in the SLM are sensitive to competition, age classes can be lumped, such that the model becomes the NLM.

In this chapter, the model is extended further, by introducing competition into adult reproductive, as well as juvenile stages. This multiple competition class lottery model (MSLM) is one step closer to reality, since it is unlikely that only juveniles compete with each other in nature. The incorporation of competition in the adult stages gives the MSLM an intrinsic structure that is different to that of the NLM and the SLM. The differences in the structure are mostly due to the addition of within-population heterogeneity in terms of responses to competition. Depending on the degree of heterogeneity, sub-additivity is expected to be weakened in the MSLM, since the adult subpopulations are also sensitive to competition. Consequently, the storage effect will be weakened.

The main objective of this study of the MSLM is to examine (i) how and when changes in the storage effect and species coexistence occur with the extension of competition into the adult stages, and (ii) how these changes are affected by mortality and fecundity schedules.

The MSLM is a size-structured model, rather than an age-structured model. Competition is expressed through growth in size, rather than through recruitment alone. Competition for space is assumed without any explicit spatial structure. This assumption is a necessary first step approximation, and is commonly used (e.g., Kohyama 1993; Roughgarden, Iwasa, and Baxter 1985). However, in some situations, such as when seed dispersal is sufficiently large, ignoring spatial structure may be justified (Pacala and Silander Jr. 1985). Kohyama employed a differential equation for a size-structured model also without explicit spatial structure (Kohyama 1993). Roughgarden et al. analysed a demographic model of sesile marine organisms with competition for space (Roughgarden, Iwasa, and Baxter 1985). Although neither model had explicit spatial structure, both contribute to our understanding of competition.

Kohyama developed a forest model which combined age/size-structures, variable environments, and multispecies competition to produce a general pattern of forest structure (Kohyama 1993). However, his model does not provide an insight into the underlying mechanism of the community dynamics. To my knowledge, Kohyama's is the most complex piece of theoretical work in the area of community dynamics, except for individual-based models such as the

forest simulator. Individual-based models depend heavily on computer simulation, and mainly focus on making detailed predictions for a specific model setting. Usually, general patterns and mechanisms are difficult to obtain using these sorts of models.

The study presented here is based on a combination of computer simulations and mathematical analyses. The main contribution of this study will be to examine when and how structured population models are necessary in order to draw valid conclusions.

6.2 The model

The MSLM is a size-structured model, in which every individual must compete in order to progress to the next size class. An individual that reaches the maximum size stays in the system until it dies. There is still competition for space for establishment in the first size class, which corresponds to recruitment in the NLM and SLM. Mortality and fecundity are size-dependent, but independent of density. Thus, competition only affects establishment and the probability of progressing from one size class to the next, or of staying in the same size class, during one unit of time.

This study is restricted to the two-species case. The invasibility technique is used to examine coexistence of the resident and the invader. As in the NLM and the SLM, life histories are symmetric throughout the study, i.e., the mortality and fecundity schedules of both species are the same. Only mean birth rates differ between the invader and the resident. The species with the higher mean birth rate is identified as the resident, since it is clear in this model also that it cannot be eliminated by the other species. A study of invasion by the inferior species is sufficient to draw conclusions about long-term coexistence of the two species. As in previous chapters, the invader and the resident will be denoted using subscripts i and j, respectively.

6.2.1 Formulation of MSLM

The dynamics of species i are expressed as:

$$\mathbf{P}_i(t+1) = \mathbf{L}_i(t)\mathbf{P}_i(t), \tag{6.1}$$

where

$\mathbf{P}_i$ is a column vector which gives the population density of each size class within species i at time t. The size-class index is assumed to be proportional

to the area that an individual of that size class occupies. $\mathbf{L}_i(t)$ is:

$$\left(\mathbf{L}_{i1}(t) \,\middle|\, \mathbf{L}_{i2}(t) \right)$$

where $\mathbf{L}_{i1}(t)$ is:

$$\begin{pmatrix} (1-p_{i2}(t))\,s_{i1} + k_{i1}b_i(t)p_{i1}(t) & k_{i2}b_i(t)p_{i1}(t) & \dots & k_{in}b_i(t)p_{i1}(t) \\ p_{i2}(t)s_{i1} & (1-p_{i3}(t))\,s_{i2} & \dots & 0 \\ 0 & p_{i3}(t)s_{i2} & \dots & 0 \\ \vdots & \vdots & \ddots & \vdots \\ 0 & 0 & \dots & (1-p_{i,n+1}(t))\,s_{in} \\ 0 & 0 & \dots & p_{i,n+1}(t)s_{in} \end{pmatrix}$$

and $\mathbf{L}_{i2}(t)$ is:

$$\begin{pmatrix} k_{i,n+1}b_i(t)p_{i1}(t) \\ 0 \\ 0 \\ \vdots \\ 0 \\ s_{i,n+1} \end{pmatrix}.$$

The number $n+1$ is the maximum size class, in which the individual no longer has any opportunity to leave through growth and ceases to compete,
$s_{ix} = (1 - \delta_{ix})$,
δ_{ix} is the probability of death of an individual of species i in size class x, and the whole function δ_{ix} is referred to as the mortality schedule,
$b_i(t)$ is the reproductive rate of species i at time t,
k_{ix} is the size-dependent modulation of reproduction of species i, and the whole function k_{ix} is referred to as the fecundity schedule,
$p_{ix}(t)$ is the probability that a given individual of species i in size-class $x-1$ progresses to size-class x during $(t, t+1)$, given that it survives. It is defined as:

$$p_{ix}(t) = c_{ix}\frac{A(t)}{R(t)}, \tag{6.2}$$

where
$A(t)$ is the available space, released by the death of individuals,
c_{ix} is the competitiveness of species i in size-class x,
and $R(t)$ is the total amount of space required for all juveniles to recruit into the first size class, and for survivors to progress to their next size class.

Since the invader is at low density, its contributions to the space released and space required in the system can be neglected. Therefore:

$$\begin{aligned} A(t) &= \sum_x x\delta_{jx}P_{jx}(t), \\ R(t) &= \sum_{x=1}^{n} c_{jx}(1-\delta_{jx})P_{jx}(t) + c_{j1}b_j(t)\sum_{x=1}^{n+1} k_{jx}P_{jx}(t). \end{aligned} \tag{6.3}$$

For p in equation 6.2 to be a probability, $A(t)/R(t)$ must be less than 1 for all t, i.e., space must always be limiting. The total area is kept fixed in the system, and all space vacated by death must be filled by recruitment or growth within the same unit of time.

It is important to note that the matrix $\mathbf{L}_i(t)$ is not a linear operator because of the density dependence term in $p_{ix}(t)$ through $A(t)$ and $R(t)$. This matrix formulation is used to describe the MSLM compactly without intention to analyse the MSLM as a matrix model. The above model is quite general. For example, the competitiveness function (c_{ix}) can be linearly decreasing, increasing, flat, convex, concave, etc. In this study I assume that the resident and the invader exhibit identical mortality and fecundity schedules ($\delta_{ix} = \delta_x = \delta_x$ and $k_{ix} = k_{jx} =$ for all x). Also, the resident and the invader have identical competitiveness functions, and competitiveness does not change with size ($c_{ix} = c_{jx} = c$). Thus, $p_{ix}(t) = p_{jx}(t) = p(t)$. For simplicity, c will be kept equal to one throughout the study. I apply the same constraints on δ_x and k_x as in previous chapters, except now they are based on size structures instead of age structures. This means that the constraints are applied by treating the system as if $p(t) = 1$ for all t, such that:

$$l_x = \Pi_{y=1}^{x-1}(1-\delta_y), \tag{6.4}$$

for $y < x$.

A juvenile, assumed to have size 0, enters the system and must compete with other individuals to obtain one unit area of space. The degree of competition a juvenile experiences depends on the ratio of the amount of available space to the amount of required space at that time. The amount of available space is the sum of all units of area released by deaths; the amount of required space is the sum of all births, plus the number of individuals smaller than the maximum size, as these need one unit of space to progress to the next size class. Proportionately with its competitiveness, the degree of competition experienced will determine the probability of a juvenile obtaining one unit area

of space (equation 6.2). If the juvenile succeeds in obtaining one unit area, either it stays in the first size class, or dies and leaves the system. If it dies it releases one unit area of space. since it was in the first size-class. If it survives for one unit time it must compete again to progress to the second size-class, with the probability of obtaining one unit area is (equation 6.2). If it competes unsuccessfully it remains in the first size-class. This cycle continues until an individual, having survived, reaches the maximum size (i.e., class $n+1$), and stays there, not competing, until it dies and releases $n+1$ units of area. Throughout this process, each individual reproduces according to its size-dependent modulation of reproduction (k_x), and its species-specific, time-dependent modulation of reproduction, $b_i(t)$. Figure 6-1 shows this cycle for the invader.

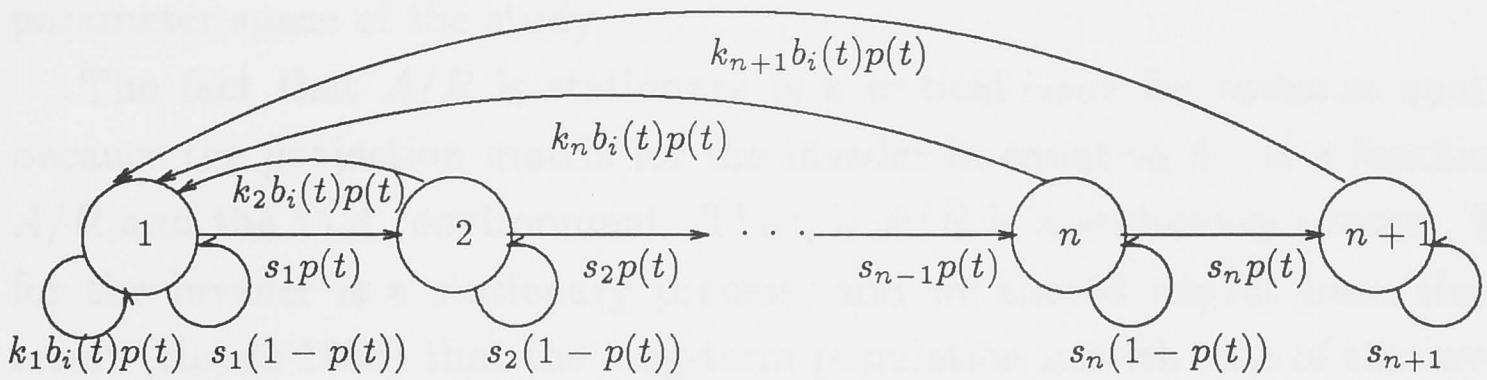

Figure 6-1: The life cycle of invader.

6.3 Analysis

In the SLM, ergodicity and a stationary age distribution play key roles in simplifying our analysis and facilitating our understanding. Thus, the obvious question arises: Does the initial structure matter; or equivalently, Does the MSLM follow weak stochastic ergodicity?

Computer simulations will be used to answer this question. In the simplest case, i.e., fecundity and mortality are size independent, after some the average size distribution of the resident is independent of initial size. This ergodicity is found consistently for all levels of variance and for all values of mean birth rate. This finding holds for cases in which fecundity and mortality are size dependent. The expected values of the size distributions are very similar for

several independent simulations, with maximum coefficients of variation less than 0.007.

This ergodicity is not surprising, since in a two-species system, though the population growth rate of the resident fluctuates over time, the average population growth rate of the resident must be 0, due to my constraint of a fixed total area with no vacant space. Compared with that of the SLM, the matrix $\mathbf{L}(t)$ in the MSLM has one extra random variable, namely $p(t)$.

The A/R is constant over time when there are no temporal fluctuations in the birth rate. When there are fluctuations, A/R fluctuates over time and $\mathrm{E}[A/R]$ increases with (i) increasing variance and mean of the difference in the ln of the birth rates of the invader and the resident, and (ii) decreasing Δ_m, i.e., with a more extreme type III mortality schedule. From figure 6-2, a time series plot of $\ln\{R/A\}$, it appears that A/R is a stationary process that follows a lognormal distribution closely except in the lower tail which is truncated (figure 6-3). This stationarity and lognormality is consistent throughout the parameter space of the study.

The fact that A/R is stationary is a critical issue for invasion analysis, because the projection matrix for the invader in equation 6.1 is a function of A/R and the i.i.d. environment. Thus, if A/R is a stationary process, $\mathbf{L}_i(t)$ for the invader is a stationary process, and we should expect from Heyde's result (Heyde 1985) that the long-term population growth rate of the invader will converge.

Kohyama also suggested, from field observation, that primary rainforest maintains its stationary tree size distribution with a regular pattern (Kohyama and Hara 1989; Kohyama, Hara, and Tadaki 1990). Also, from the simulation studies using his size-structured, one-sided, multispecies competition model, a stationary tree size distribution is always reached (Kohyama 1991; Kohyama 1992; Kohyama 1993).

I define the competition parameter, C, as $\ln\{R/A\}$, instead of A/R, for two reasons. Firstly, the quantiles plot suggests that $\ln\{R/A\}$ is approximately normally distributed, although with a lower tail that is a little thinner than normal, which makes analysis easier. Secondly, defining C as $\ln\{R/A\}$ maintains consistency with the NLM and the SLM, in which the competition parameter is defined as the natural logarithm of the ratio of the number of competing juveniles (number of required spaces) to the number of deaths (number of available spaces).

For the purpose of understanding the simulation result, I need to examine

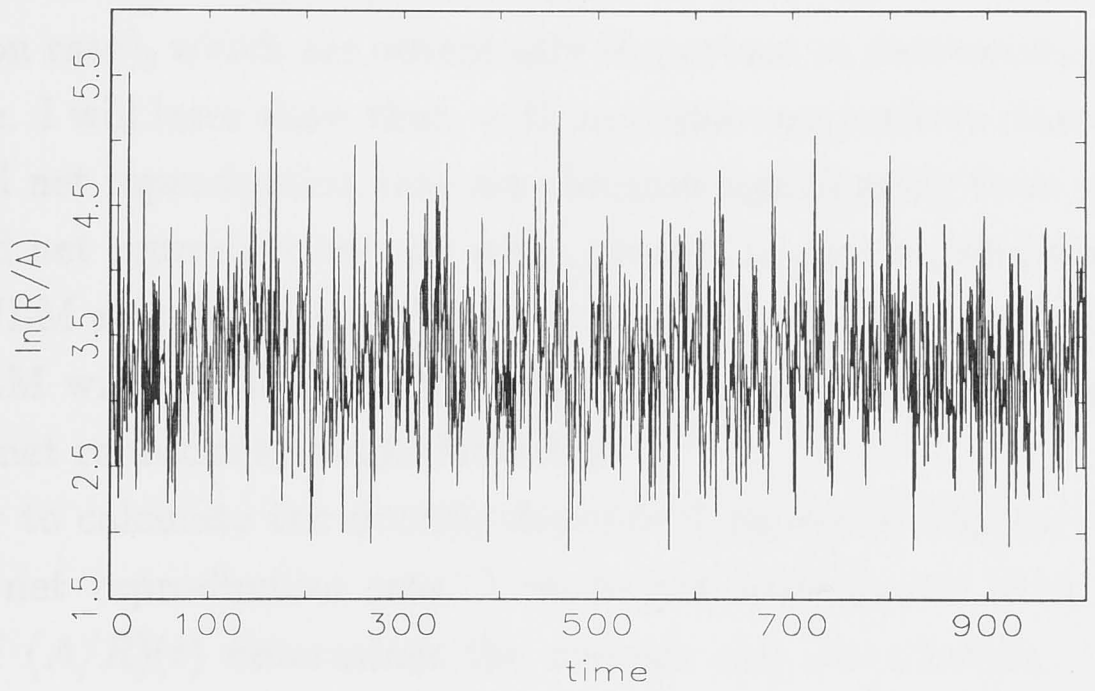

Figure 6-2: Time series of $\ln(R/A)$ from a simulation of the MSLM with a type III mortality schedule with $\Delta_m = -1.9485$ and an early peak reproduction with $\Delta_f = -12.2130$. $\mu = -0.4$ and $\sigma^2 = 0.5$.

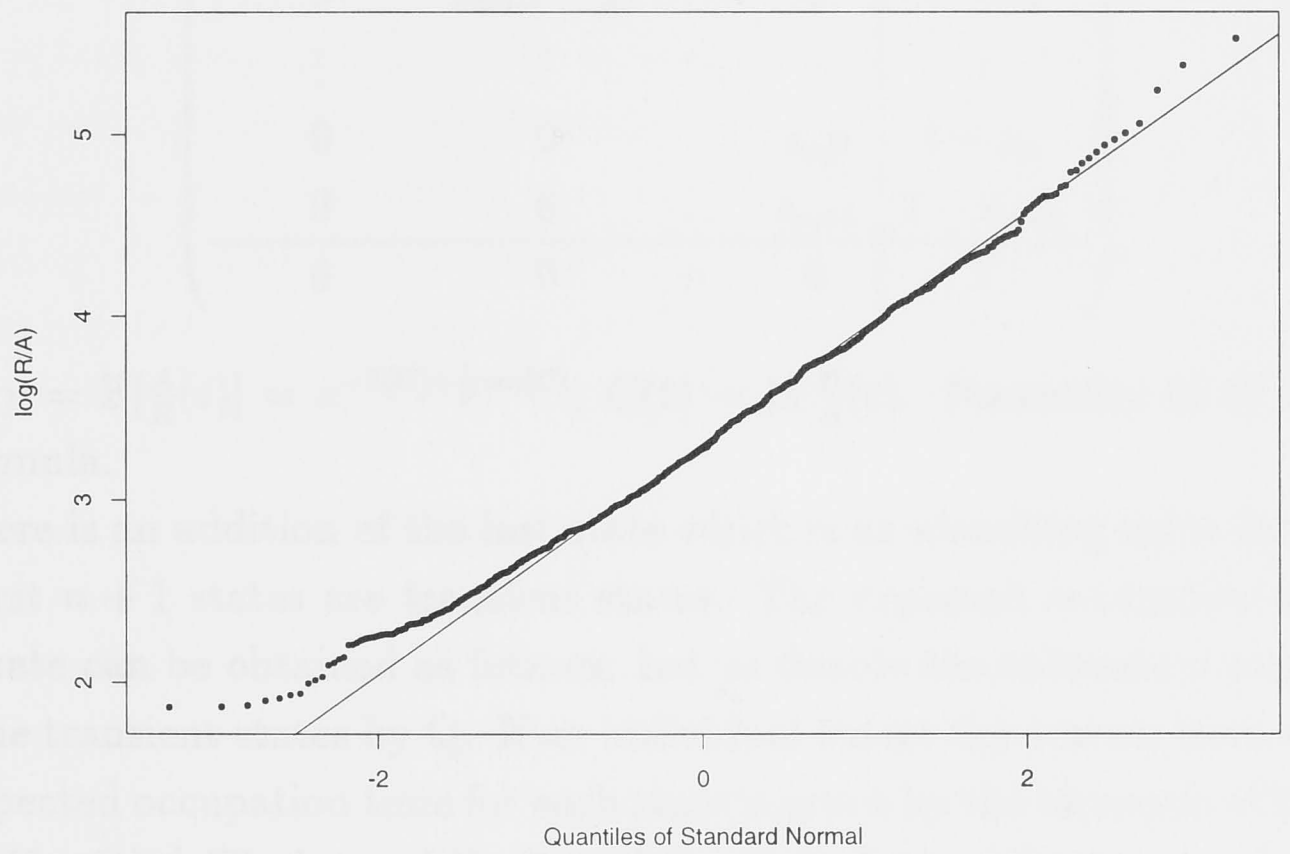

Figure 6-3: Quantiles of standard normal plot of $\ln(R/A)(t)$ from a simulation of the MSLM with a type III mortality schedule with $\Delta_m = -1.9485$ and an early peak reproduction with $\Delta_f = -12.2130$. $\mu = -0.4$ and $\sigma^2 = 0.5$.

how each mortality schedule and fecundity schedule behaves differently in the MSLM in affecting life-history characteristics (i.e., expected lifetime and net reproduction rate), which are potentially important in determining population growth rate. I will later show that, with multiple competitive classes, expected lifetime and net reproduction rate are changed significantly from the expected lifetime and net reproductive rate when growth in size is density independent (as in the NLM and the SLM). The expected lifetime and net reproductive rate in the MSLM will be called density-dependent expected lifetime and density-dependent net reproductive rate hereafter.

In order to calculate the density-dependent expected lifetime and density-dependent net reproductive rate, I make the assumption that the average behavior of $(A/R)(t)$ determines the average size distribution. There is no theoretical justification for this assumption, but it will be shown later from simulation results that the assumption is not unreasonable. The Markov chain properties will be used to calculate the density-dependent expected lifetime (L) and the density-dependent net reproduction (R_0). The transition matrix of the graph in figure 6-1 is as follows:

$$\left(\begin{array}{cccc|c} s_1(1-p) & s_1 p & \dots & 0 & 1-s_1 \\ 0 & s_2(1-p) & \dots & 0 & 1-s_2 \\ \vdots & \vdots & \ddots & \vdots & \vdots \\ 0 & 0 & \dots & s_n p & 1-s_n \\ 0 & 0 & \dots & s_{n+1} & 1-s_{n+1} \\ \hline 0 & 0 & \dots & 0 & 1 \end{array}\right)$$

where $p = \mathrm{E}[\frac{A}{R}(t)] = e^{-\mathrm{E}[C]+\frac{1}{2}\mathrm{var}[C]}$, $C(t) = \ln \frac{R}{A}(t)$. Normality of C justifies the formula.

There is an addition of the last state which is an absorbing state for death. The first $n+1$ states are transient states. The expected occupation time in each state can be obtained as follows. Let us denote the submatrix containing only the transient states by $\mathbf{Q}$. If an individual enters the system from state 1, the expected occupation time for each state is given by the elements of the first row of $(\mathbf{I}-\mathbf{Q})^{-1}$ (Taylor and Karlin 1994), where $\mathbf{I}$ is an identity matrix of size $n+1$. These elements correspond to the l_x in the standard demographic models (equation 6.4. I will use notation l'_x for density-dependent l_x. The density-dependent expected lifetime (L), the density-dependent net reproduction (R_0), and the density-dependent expected size distribution (u_x) can be calculated as

follows:

$$L = \sum_{x=1}^{n+1} l'x, \tag{6.5}$$

$$R_0 = \mathrm{E}[b] \sum_{x=1}^{n+1} l'x k_x, \tag{6.6}$$

$$u_x = \frac{l'x}{\sum_{x=1}^{n+1} l'x}. \tag{6.7}$$

Note that the l'_xs obtained here are not used to constrain the δ_xs and k_xs because l'_xs are output from the model, not given input.

Using Mathematica (Wolfram 1988), an analytical formula can be obtained for $l'x$ if p is known. The formula is:

$$l'x = \frac{p^{x-1} s_{x-1}}{\prod_{i=1}^{x} (1 - s_i(1-p))}. \tag{6.8}$$

Using formula 6.8, I can perform a much simpler calculation directly for L and R_0, rather than using a Markov chain.

The density-dependent expected size distribution, calculated using formula 6.7 and taking the value p in formula 6.8 from computer simulation, is very similar to that computed directly by taking the average of the size distribution over time from simulation (see figures 6-21, 6-22, and 6-23). This suggests that our assumption that the average of $(A/R)(t)$ determines the average size distribution is quite reasonable, and therefore that the calculation of L and R_0 is fairly accurate. Note that, even though I still have to depend on computer simulations to calculate p, the formulae 6.8 enable us to see roughly the relationships among the life-history characteristics (equations 6.5, 6.6, and 6.7).

By assuming that a 'stationary' density-dependent size distribution given by 6.7 is a sufficient approximation, the relationships between mortality schedules, fecundity schedules, and the mean of C can be studied. The ratio of available space to required space at time t is:

$$\frac{A}{R}(t) = \frac{\sum_{x=1}^{x=n} x\delta_x P_{jx}(t)}{b_j(t) \sum_{x=1}^{x=n+1} c_x k_x P_{jx}(t) + \sum_{x=1}^{x=n} c_x(1-\delta_x) P_{jx}(t)}. \tag{6.9}$$

Equation 6.9 only contains densities of the resident subpopulations. The mean of the competition parameter can be approximated by:

$$\mathrm{E}[C] = \mathrm{E}\left[\ln \frac{b_j \sum_{x=1}^{n+1} k_x u_x + \sum_{x=1}^{n} (1-\delta_x) u_x}{\sum_{x=1}^{n} x\delta_x u_x}\right]$$

$$
\begin{aligned}
&= \ln \frac{\mathrm{E}[b_j] \sum_{x=1}^{n+1} k_x u_x + \sum_{x=1}^{n} (1-\delta_x) u_x}{\sum_{x=1}^{n+1} x \delta_x u_x} - \frac{1}{2}\mathrm{var}[C] \\
&= \ln \frac{\mathrm{E}[b_j] \sum_{x=1}^{n+1} k_x l'x + \sum_{x=1}^{n} (1-\delta_x) l'x}{\sum_{x=1}^{n+1} x \delta_x l'x} - \frac{1}{2}\mathrm{var}[C] \\
&= \ln \left(R_0 + \sum_{x=1}^{n} (1-\delta_x) l'x \right) - \ln \left(\sum_{x=1}^{n+1} x \delta_x l'x \right) \qquad (6.10) \\
&\quad -\frac{1}{2}\mathrm{var}[C].
\end{aligned}
$$

The assumptions which underlie this formulation are the normality of $C = \ln(R/A)$, and the 'stationary' density-dependent size distribution of the resident.

In the NLM, the mean of competition parameter is simply $\ln\{\mathrm{E}[b_j]/\tilde{\delta}\} - 0.5\mathrm{var}[C]$, which is equal to $\ln R_0$ when mortality and fecundity are age/size-independent. In the SLM, the mean of competition parameter agrees exactly with that of the NLM. The mean of the competition parameter in the MSLM, as given in equation 6.10, also has $\ln R_0$ as the main component, which indicates that how competition in the lottery model is robust to major extensions, such as the incorporation of size-dependent mortality, size-dependent fecundity, and multiple competitive classes.

Although an analytical solution cannot be found, we can see that the magnitude of competition is approximately similar to that of $\ln R_0$ of the resident. This improves our understanding of the model substantially, and provides us with a tool for comparing the NLM, the SLM, and the MSLM. The role of C in species coexistence will be investigated in section 6.5.

6.4 Simulation studies

In this section I will study the long-term population growth rate of the invader both qualitatively and quantitatively. To investigate coexistence, i.e., the magnitude of σ^2 required for the invader to have non-negative long-term population growth rate, only qualitative information about the long-term population growth rate of the invader is needed. As long as the long-term population growth rate of the invader is positive, the invader will coexist with a superior resident. This application of invasibility technique has been described briefly in Chapter 2, and has been used in previous chapters.

The magnitude of the long-term population growth rate of the invader determines the rate of recovery of a species. The higher the long-term growth rate of the invader, the faster the invader will recover from low density. There

is a conceptual difference between the interpretation of the population growth rate here, and fitness in life-history theory. In life-history theory, growth rate as a fitness measure is only characteristic of the dynamics of a single species. Thus, to compare fitness between species, several parallel single species dynamics are studied and the outcomes compared. Fitness is solely determined by the particular model of population dynamics under study and by the difference between species. This is not the case in our study. In our investigation of two-species dynamics, the long-term growth rate is determined not only by the model (i.e., the limiting resource(s), the nature of density dependence, and the difference between the invader), but also by the resident. By comparing the population growth rates of invaders from different systems, we do not only look at differences in the life histories of different invaders, but we compare their relative ability to recover from low density in the presence of the particular resident with whom they compete. Our study is restricted to the case of symmetric life histories. I make no attempt to apply the concept of optimality, or to find an ESS. The conceptual difficulty caused by density dependence has been pointed out, e.g., (Kisdi and Meszena 1993). This study is focused on the rate of invasion, not of life-history evolution. However, the model does provide a density-dependent means of studying life-history evolution.

I use GAUSS to conduct the computer simulations on a Dec ALPHA 2000 machine and a PC. Throughout the simulations, the density-independent, size-dependent mortality (mortality schedule) is generated such that the expected lifetime without density-dependent growth in size is fixed at nine. Note that formula 3.19 in Chapter 3 generates mortality schedules, while maintaining a constant expected lifetime, as the parameters δ_1 and s are varied. In demographic models and in the SLM, an individual advances from class to the next in one unit time. In the MSLM, the classes are size classes, not age classes, and success in competition is necessary for growth in size. As a consequence, whenever mortality rates vary with size, the expected lifetime varies with the degree of competition. The quantification of mortality schedules follows the techniques described in Chapter 3, with negative Δ_m for a type III mortality schedule, zero Δ_m for a type II mortality schedule, and positive Δ_m for a type I mortality schedule. The magnitude of Δ_m determines the size of the deviation of a mortality schedule from a type II mortality schedule (size-independent mortality). Please note that in calculating Δ-measures, they no longer involve the l'_xs but are calculated with l_xs from formula 6.4.

Since there is some density-dependent probability that an individual stays

in the same size class for more than one unit time, the expected lifetime in the MSLM will not be equal to a constant as in the SLM and demographic models. The deviation of the expected lifetime and other life-history characteristics, such as net reproductive rate, from those in the age-structured model without density-dependent growth in size (the SLM and general demographic models), is due to density-dependent growth in size. This can be seen through equation 6.8, in which $l'x$ depends on the density-dependent probability (p) of capturing a unit of space. The expected lifetime (equation 6.5), net reproductive rate (equation 6.6), and size distribution (equation 6.7), all depend on $l'x$. I will refer to these three emergent parameters as density-dependent expected lifetime, density-dependent net reproductive rate, and density-dependent size distribution.

For each model setting I run several independent simulations, each running for a long period of time, to reduce the standard error. I average over these independent simulations to obtain the results for each model setting. The standard error of the long-term population growth rate of the invader combining all independent simulations is controlled such that it is always less than 0.001.

The fecundity schedule is fixed in the same way as in the SLM, but this does not guarantee uniform R_0 across settings, as density-dependent growth rate in size changes survivorship. The varying fecundity schedules will give us early peak reproduction and delayed peak reproduction. The quantification of fecundity schedules in Chapter 3 gives zero Δ_f for uniform fecundity (size-independent reproduction), and large positive Δ_f for delayed peak reproduction. As used here, early and delayed peak reproduction do not indicate which is the first size class to reproduce, but the size classes in which the majority of offspring are produced. Delayed peak reproduction means that the majority of offspring are produced in large size classes.

The constraint applied in this study is not as stringent as that applied in the SLM and the NLM, because we cannot fix the density-dependent expected lifetime and the density-dependent net reproductive rate. However, we can fix the density-dependent expected lifetime and the density-dependent net reproductive rate when mortality and fecundity are independent of size.

Together with the expected lifetime and the net reproductive rate, I investigate two other parameters in this study, namely: (i) the difference between the mean birth rates of the invader and the resident ($\mu = \mathrm{E}[\ln b_i] - \mathrm{E}[\ln b_j]$), which ranges from -0.4 to -0.1, and (ii) the variance of the birth rates, which is the same for the invader and the resident, (σ^2), ranges from 0 to 0.5. I will

concentrate on the effects of the mortality schedule (measured by Δ_m), the fecundity schedule (measured by Δ_f), μ, and σ^2 on the long-term population growth rate of the invader. I will also investigate the effects of $\Delta_m, \Delta_f, \mu, \sigma^2$ on intermediate variables which potentially have more direct effects on the long-term population growth rate of the invader, such as density-dependent expected lifetime (L), density-dependent net reproductive rate (R_0), density-dependent size distribution (u_x), the mean of competition (E[C]), and the covariance between the environment and competition.

6.4.1 Long term population growth rate of the invader

An interesting relationship is found between the long-term population growth rate of the invader ($\bar{r}_i$) and the mortality schedule of both the invader and the resident, when fecundity is uniform (size-independent reproduction, $\Delta_f = 0$) (figure 6-4). The effects of μ and σ^2 are similar qualitatively. Increase in the variance of birth rate of the invader and the resident (σ^2) increases $\bar{r}_i$. Similarly, increase in the difference between the mean birth rate of the invader and that of the resident increases $\bar{r}_i$. With fixed $\mu = -0.2$, $\bar{r}_i$ changes from negative to positive when σ^2 increases beyond 0.375 (figures 6-4(a)). A type III mortality schedule ($\Delta_m < 0$, high early mortality rate) gives higher $\bar{r}_i$, when $\bar{r}_i > 0$ (figure 6-4). With a type I mortality schedule ($\Delta_m > 0$), $\bar{r}_i$ changes slightly with σ^2 (figure 6-4(a)) and with μ (figure 6-4(b)). Even though the magnitude of $\bar{r}_i$ changes considerably with different mortality schedules, the sign of $\bar{r}_i$ does not change with mortality schedule. The same degree of inferiority of the invader (μ), with the same magnitude of environmental fluctuations (σ^2), will result in the same sign of $\bar{r}_i$, regardless of the type of mortality schedule of the invader and the resident. In general, $|\bar{r}_i|$ decreases with increasing Δ_m, except in a few cases with strong type III mortality schedules (large $|\Delta_m|$, i.e., very high early mortality rate and very low late early mortality rate), and $\bar{r}_i < 0$.

Let us now look at the long-term population growth rate of the invader in relation to its density-dependent expected lifetime (L). Here, we look at the per generation long-term population growth rate of the invader ($\bar{r}_i L$), rather than the per unit time long-term population growth rate of the invader ($\bar{r}_i$). The behaviour of $\bar{r}_i L$ with increasing Δ_m (figure 6-5) is opposite to that of the long-term population growth rate per unit time ($\bar{r}_i$) (figure 6-4). Generally, $|\bar{r}_i|L$ increases with increasing Δ_m, except in cases with a strong type III mortality schedule (large $|\Delta_m|$) and $\bar{r}_i L < 0$.

When fecundity is size dependent, the pattern of $\bar{r}_i$ and $\bar{r}_i L$ over Δ_f, μ, and

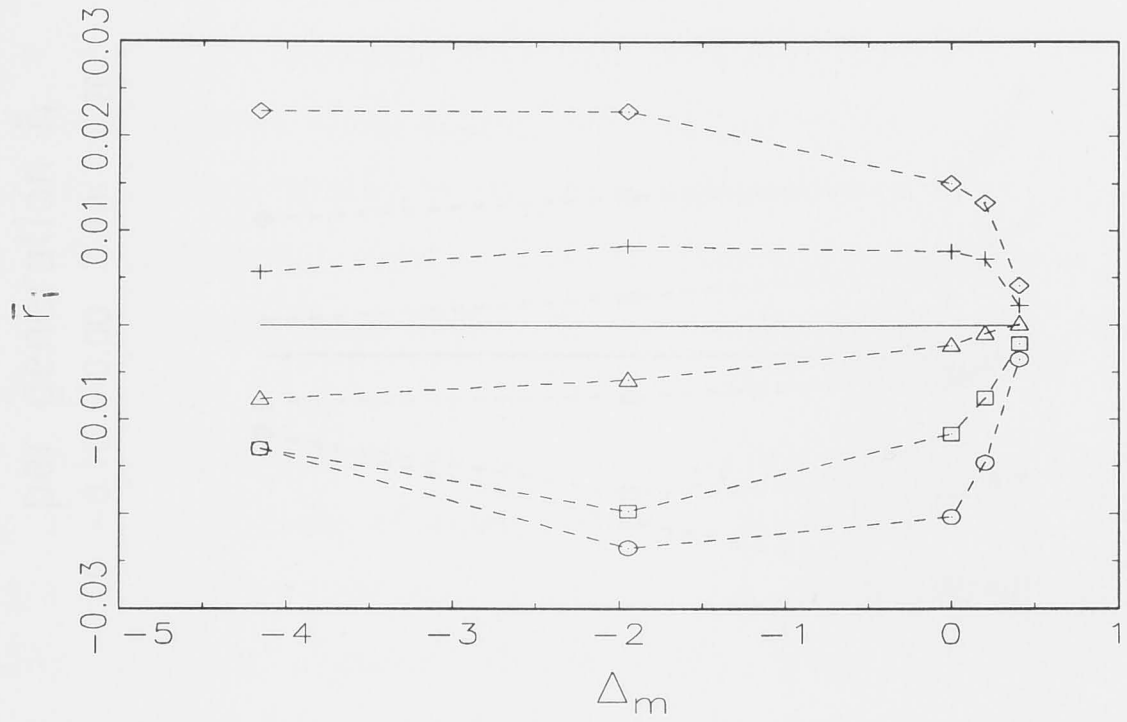

(a)

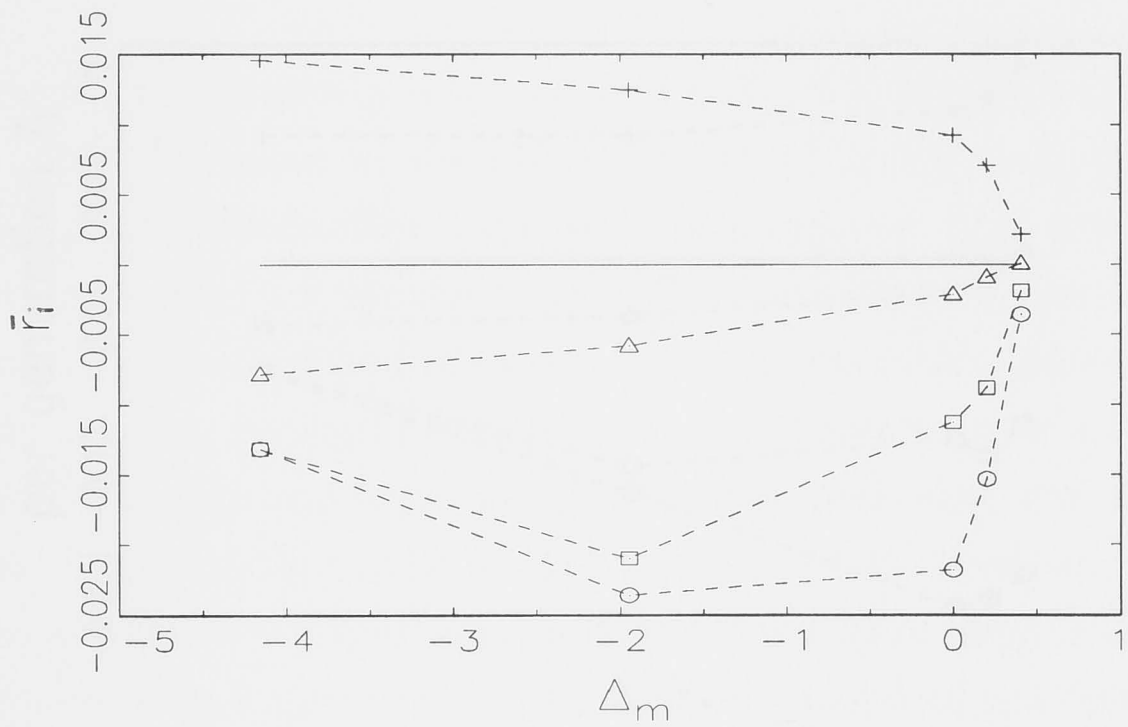

(b)

Figure 6-4: Long-term population growth rate of the invader ($\bar{r}_i$) with different mortality schedules and with σ^2 equals 0 ($\circ$), 0.125 ($\square$), 0.25 ($\triangle$), 0.375 ($+$), and 0.5 ($\diamond$), and $\mu = -0.2$ (a), and with μ equals -0.4 ($\circ$), -0.3 ($\square$), -0.2 ($\triangle$), and -0.1 ($+$), and $\sigma^2 = 0.25$ (b).

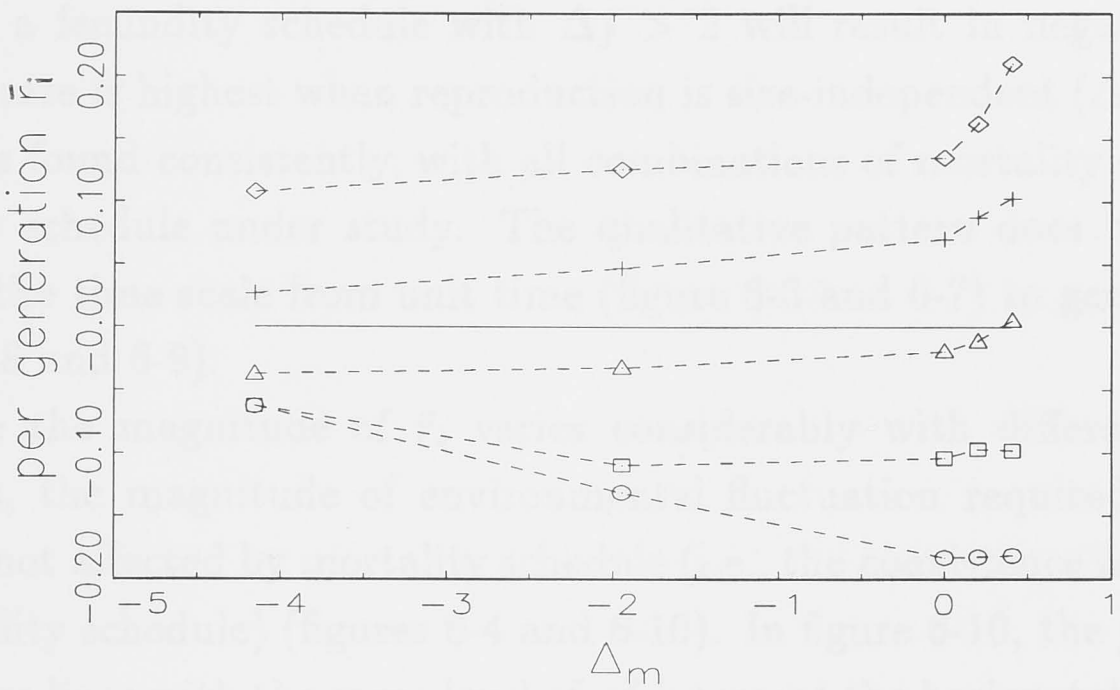

(a)

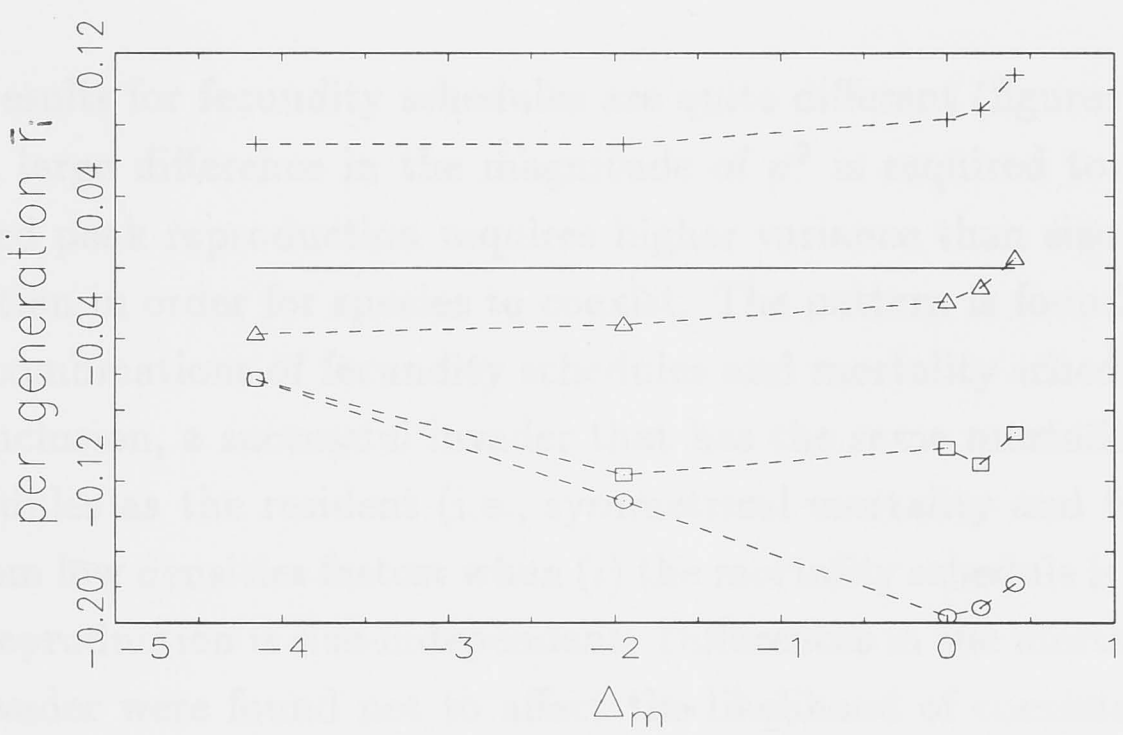

(b)

Figure 6-5: Long-term population growth rate of the invader per generation time ($\bar{r}_i L$) with different mortality schedules with σ^2 equals 0 ($\circ$), 0.125 ($\square$), 0.25 ($\triangle$), 0.375 ($+$), and 0.5 ($\diamond$), and $\mu = -0.2$ (a), and with μ equals -0.4 ($\circ$), -0.3 ($\square$), -0.2 ($\triangle$), and -0.1 ($+$), and $\sigma^2 = 0.25$ (b).

σ^2 (figures 6-6, 6-7, 6-8 and 6-9) is similar to those with structured mortality above, but there are major qualitative differences in the way $\bar{r}_i$ and $\bar{r}_i L$ change in response to Δ_m and Δ_f. For example, figure 6-6(a) shows that, with $\mu = -0.2$ and $\sigma^2 = 0.375$, a fecundity schedule with $\Delta_f < 2$ will result in positive $\bar{r}_i$, while a fecundity schedule with $\Delta_f > 2$ will result in negative $\bar{r}_i$. The recovery rate is highest when reproduction is size-independent ($\Delta_f = 0$). This pattern is found consistently, with all combinations of mortality schedule and fecundity schedule under study. The qualitative pattern does not change if we alter the time scale from unit time (figure 6-6 and 6-7) to generation time (figure 6-8 and 6-9).

While the magnitude of $\bar{r}_i$ varies considerably with different mortality schedules, the magnitude of environmental fluctuation required to produce $\bar{r}_i = 0$ is not affected by mortality schedule (i.e., the coexistence is not affected by mortality schedule) (figures 6-4 and 6-10). In figure 6-10, the pairs of solid and dashes lines with the same level of σ^2 intercept the horizontal line ($\bar{r}_i = 0$) at almost the same value of μ. There is a weak tendency that, to have $\bar{r}_i = 0$, (i) an invader with a type III mortality schedule requires higher σ^2 than an invader with a type II mortality schedule, and (ii) an invader with a type I mortality schedule requires lower σ^2 than an invader with a type II mortality schedule.

The results for fecundity schedules are quite different (figures 6-6, 6-7 and 6-11). A large difference in the magnitude of σ^2 is required to achieve $\bar{r}_i = 0$. Delayed peak reproduction requires higher variance than size-independent reproduction in order for species to coexist. The pattern is found consistently with all combinations of fecundity schedules and mortality schedules.

In conclusion, a successful invader that has the same mortality and fecundity schedules as the resident (i.e., symmetrical mortality and fecundity) recovers from low densities fastest when (i) the mortality schedule is of a type III, and (ii) reproduction is size-independent. Differences in the mortality schedule of the invader were found not to affect the likelihood of coexistence between the invader and the resident. However, differences in the fecundity schedule did affect the likelihood of coexistence. An invader with size-independent reproduction, i.e., with offspring produced uniformly across size classes, can invade readily compared with an invader with early or delayed peak reproduction. In other words, the coexistence is least stringent (the invader requires lower σ^2 to attain zero long-term population growth rate) when reproduction is size-independent with broader range of inferiority of the invader from the

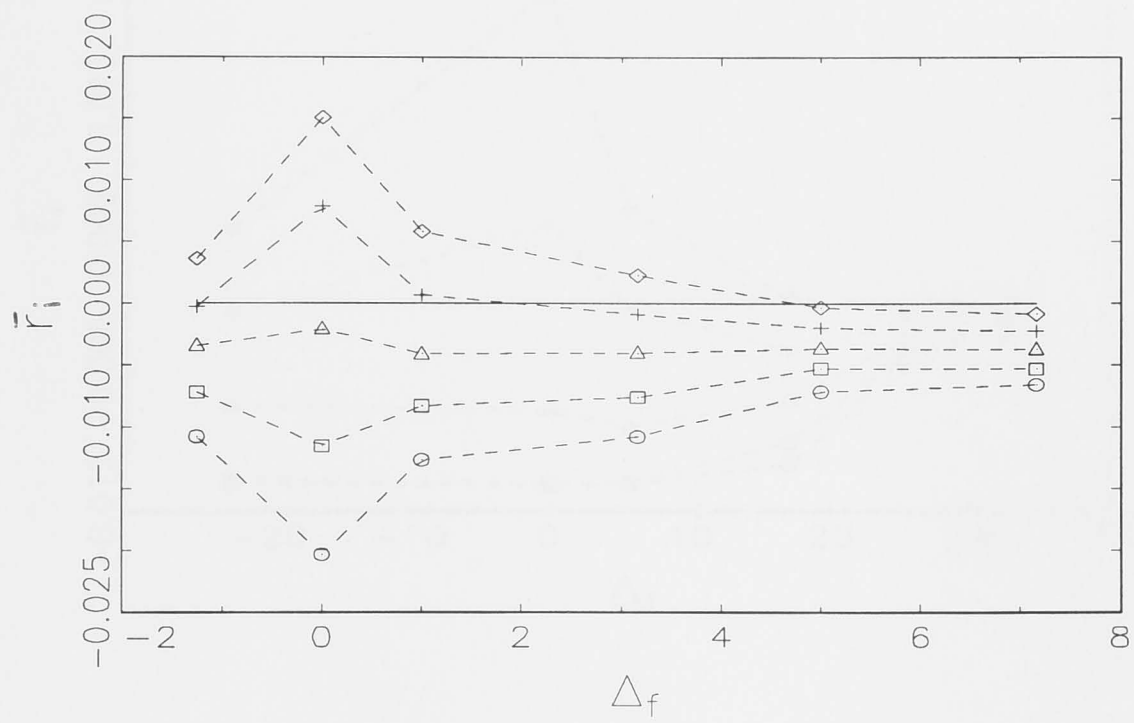

(a)

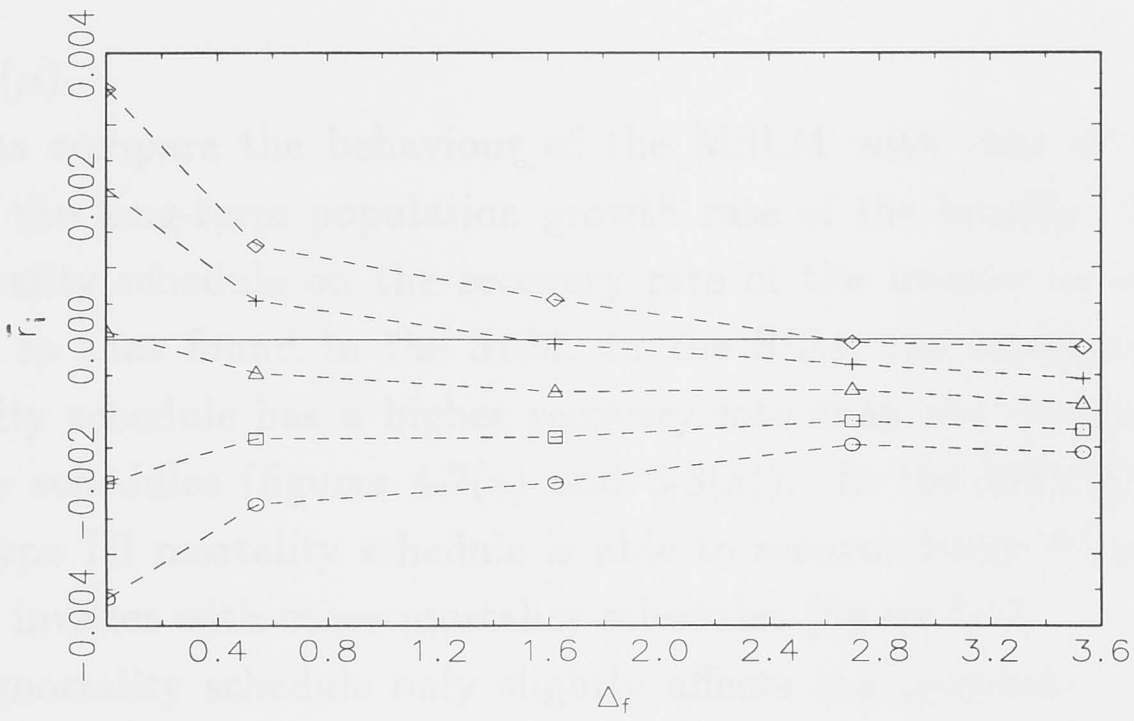

(b)

Figure 6-6: Long-term population growth rate of the invader ($\bar{r}_i$) with different fecundity schedules and size-independent mortality (a), and with different fecundity schedules and a type I mortality schedule with $\Delta_m = 0.2025$ (b). σ^2 equals 0 ($\circ$), 0.125 ($\square$), 0.25 ($\triangle$), 0.375 ($+$), and 0.5 ($\diamond$), and $\mu = -0.2$.

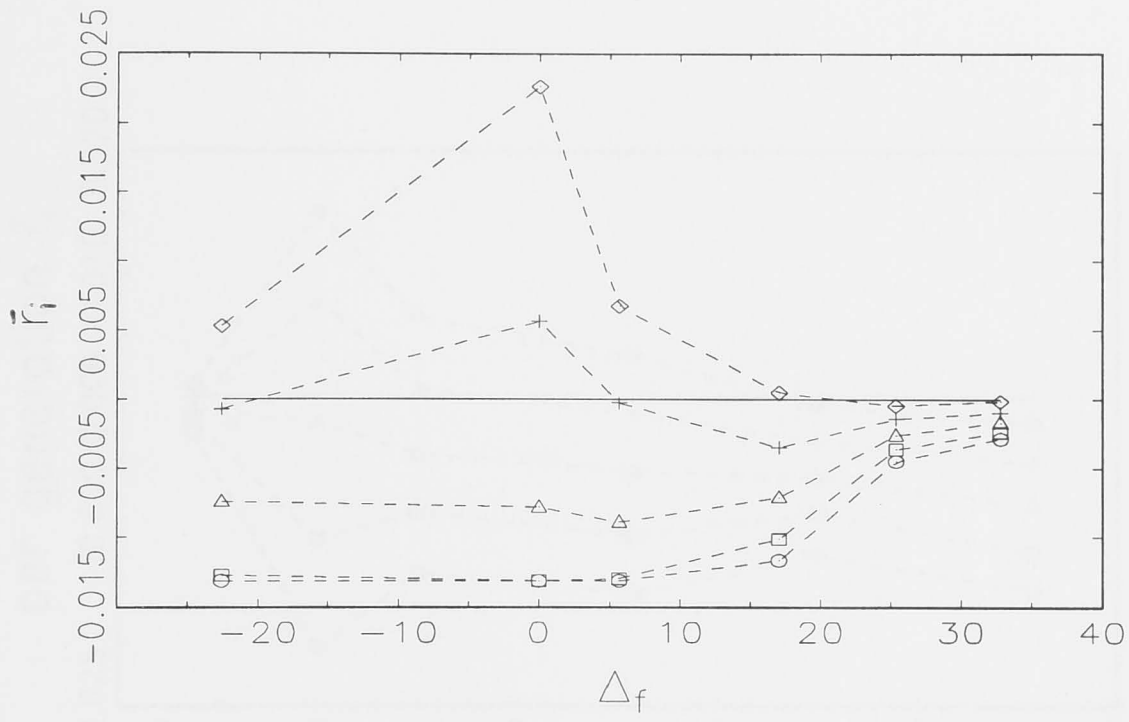

Figure 6-7: Long-term population growth rate of the invader ($\bar{r}_i$) with different fecundity schedules and a type III mortality schedule with $\Delta_m = -4.1589$. σ^2 equals 0 ($\circ$), 0.125 ($\square$), 0.25 ($\triangle$), 0.375 ($+$), and 0.5 ($\diamond$), and $\mu = -0.2$.

resident (μ).

Let us compare the behaviour of the MSLM with that of the SLM, in terms of the long-term population growth rate of the invader. The effect of the mortality schedule on the recovery rate of the invader in the MSLM is opposite to that found in the SLM. In the SLM, the invader with a type I mortality schedule has a higher recovery rate than the invader with other mortality schedules (figures 4-7(a) and 5-3(a)). In the MSLM, the invader with a type III mortality schedule is able to recover faster from low density than the invader with other mortality schedules (figure 6-4).

The mortality schedule only slightly affects the coexistence in the SLM and the MSLM. The direction of these small effects in the SLM is opposite to those in the MSLM. In the SLM, an invader with a type III mortality schedule ($\Delta_m < 0$) requires slightly lower σ^2 than an invader with a type II mortality schedule ($\Delta_m = 0$) or a type I mortality schedule ($\Delta_m > 0$) (figure 4-2). In the MSLM, an invader with a type I mortality schedule requires slightly lower σ^2 than an invader with a type II or a type III mortality schedule (figure 6-10).

The recovery rate of the invader in the SLM is highest when there is early peak reproduction ($\Delta_f < 0$) (figure 4-7(b)), whereas in the MSLM when there

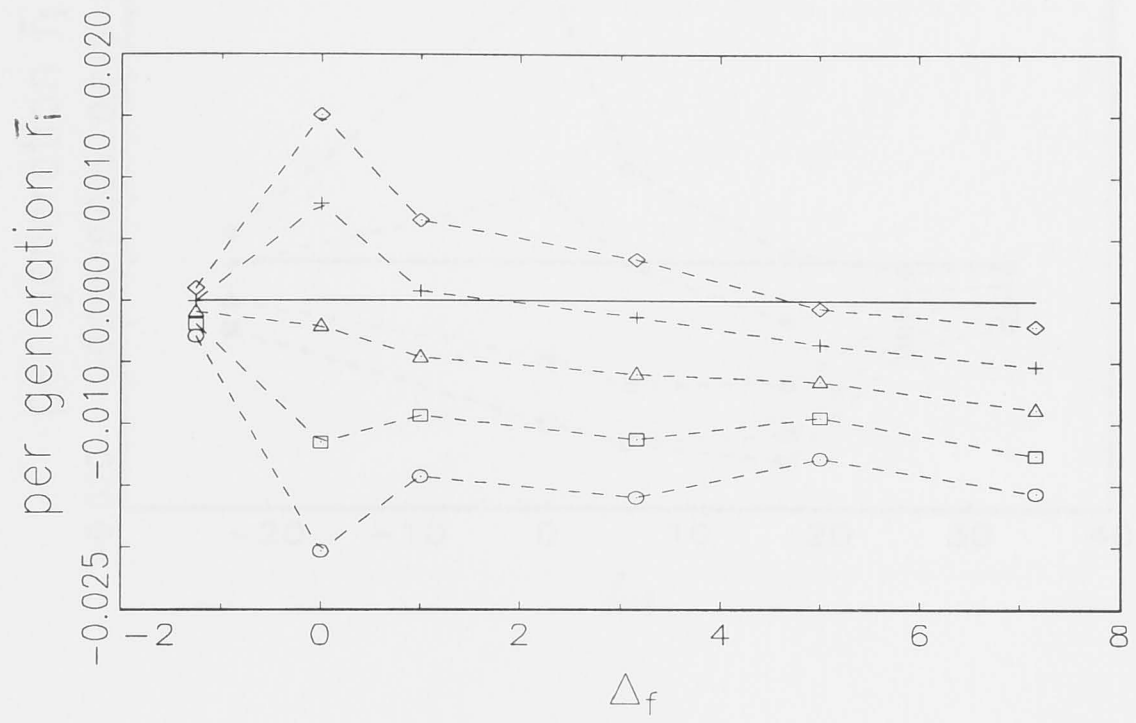

(a)

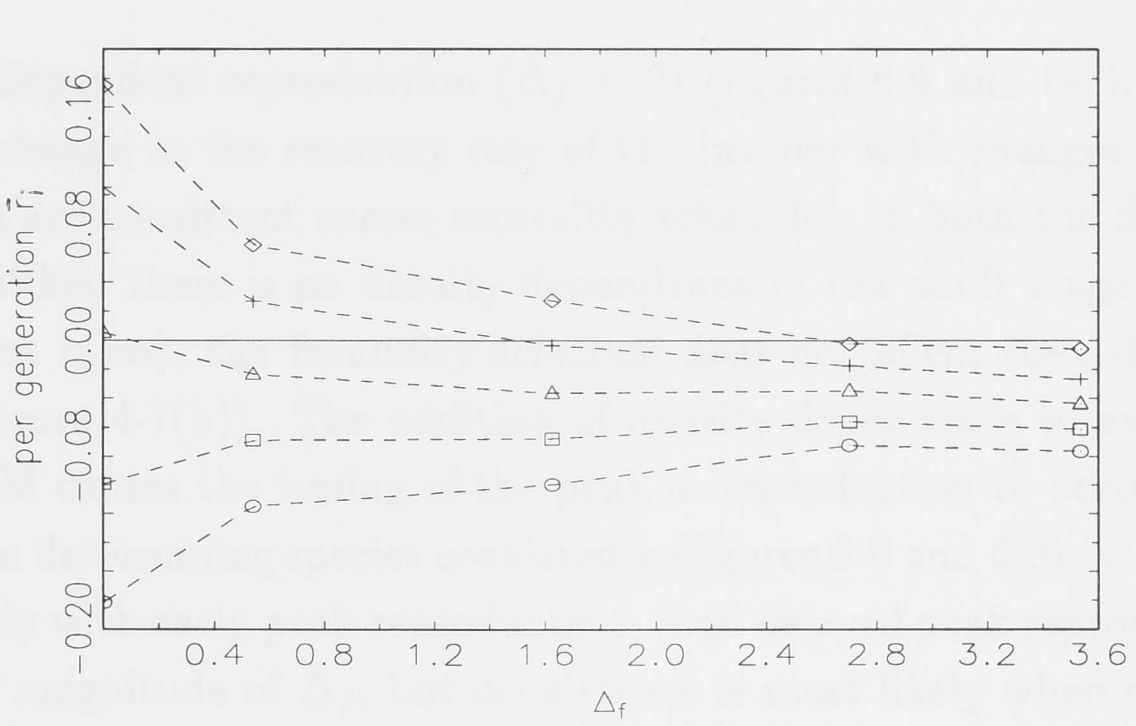

(b)

Figure 6-8: Long-term population growth rate of the invader per generation time ($\bar{r}_i L$) with different fecundity schedules and size-independent mortality (a), and with different fecundity schedules and a type I mortality schedule with $\Delta_m = 0.2025$ (b). σ^2 equals 0 ($\circ$), 0.125 ($\square$), 0.25 ($\triangle$), 0.375 ($+$), and 0.5 ($\diamond$), and $\mu = -0.2$.

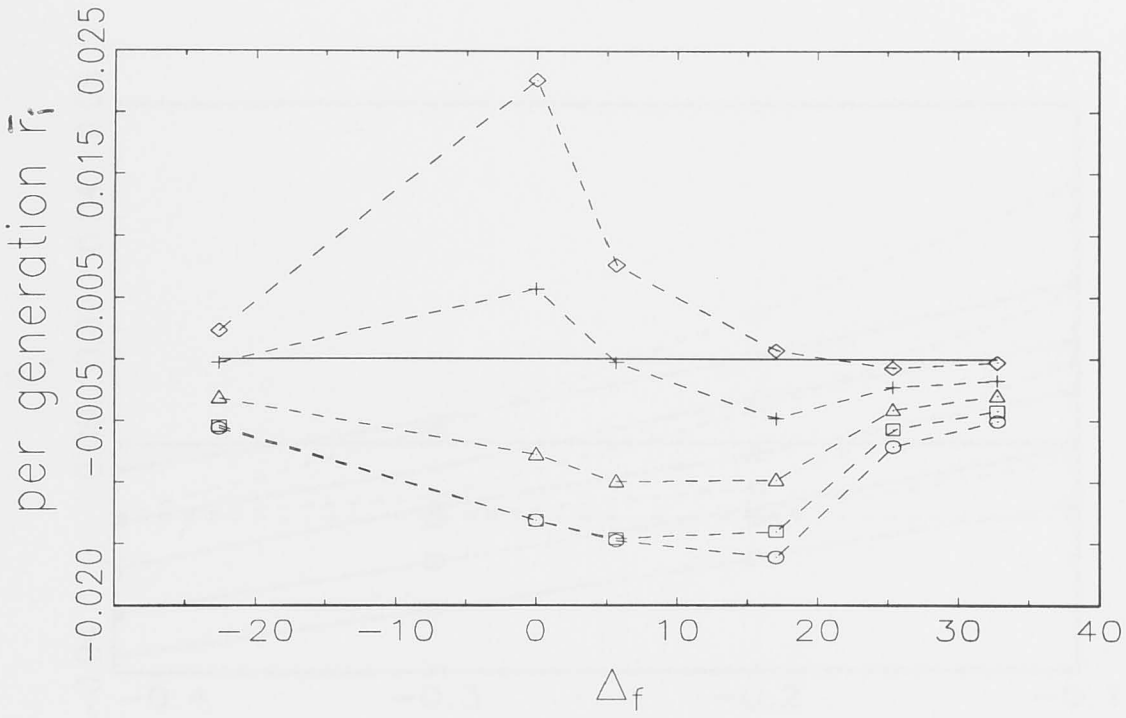

Figure 6-9: Long-term population growth rate of the invader per generation time ($\bar{r}_i L$) with different fecundity schedules and a type III mortality schedule with $\Delta_m = -4.1589$. σ^2 equals 0 ($\circ$), 0.125 ($\square$), 0.25 ($\triangle$), 0.375 ($+$), and 0.5 ($\diamond$), and $\mu = -0.2$.

is size-independent reproduction ($\Delta_f = 0$) (figures 6-6 and 6-7). These patterns of change in the recovery rate of the invader with changes in fecundity schedules are consistent across mortality schedules, in both the SLM and the MSLM. When there is no density dependence in the adult stage (other than in the first class), the fecundity schedule does not affect coexistence significantly (figure 4-7(b)). The addition of density dependence to every stage in the MSLM causes the timing of the peak in reproduction to become very important in determining species coexistence (figures 6-6 and 6-8). Coexistence is more likely with early peak reproduction, than delayed peak reproduction with a similar magnitude of Δ_f, but coexistence is most likely when reproduction is spread uniformly ($\Delta_f = 0$).

6.4.2 Density-dependent expected lifetime, density- dependent net reproductive rate, and density- dependent size distribution

I will now examine three life-history characteristics in the MSLM, namely the density-dependent expected lifetime, density-dependent net reproductive rate,

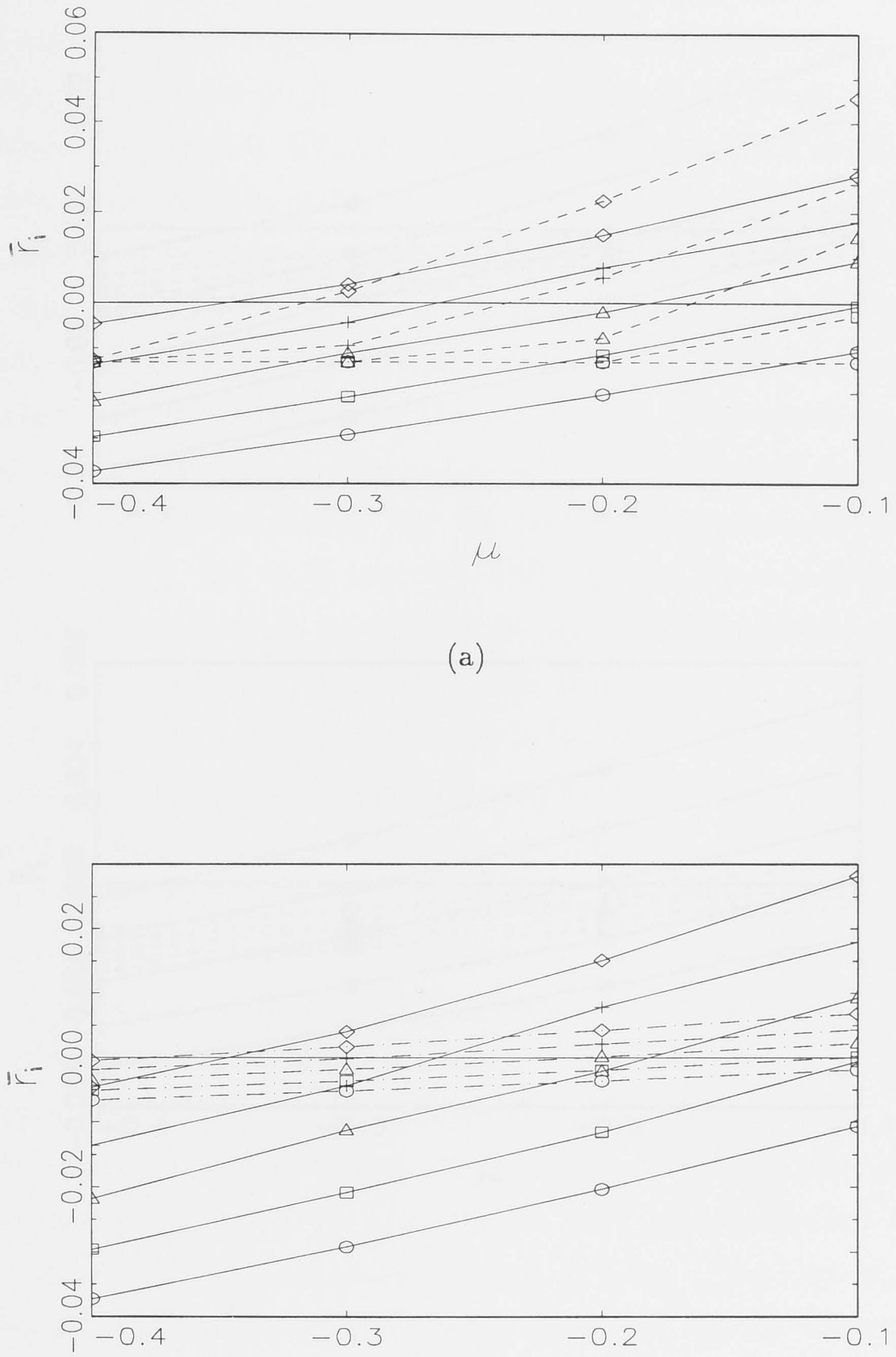

(a)

(b)

Figure 6-10: Long-term population growth rate of the invader ($\bar{r}_i$) with mortality schedule of a type II (solid lines) and a type III mortality schedule with $\Delta_m = -4.1589$ (short dashes) (a). The long-term population growth rate of the invader ($\bar{r}_i$) with mortality schedule of a type II (solid lines) and a type I mortality schedule with $\Delta_m = 0.2025$ (long dashes) (b). σ^2 equals 0 ($\circ$), 0.125 ($\square$), 0.25 ($\triangle$), 0.375 ($+$), and 0.5 ($\diamond$).

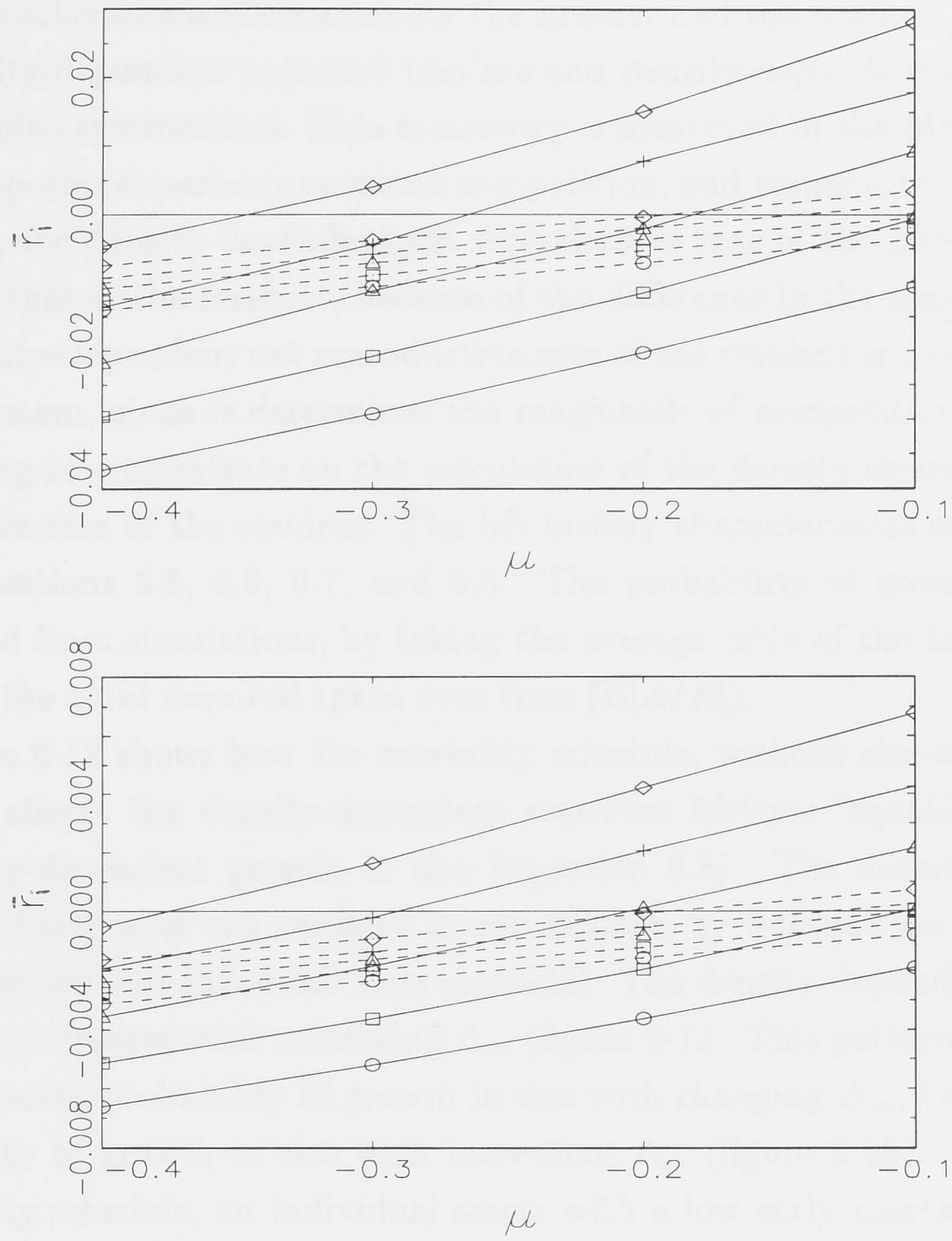

Figure 6-11: Long-term population growth rate of the invader ($\bar{r}_i$) with mortality schedule of a type II with size-independent reproduction (solid lines) and delayed peak reproduction with $\Delta_f = 5$ (short dashes) (a), and a type I with $\Delta_m = 0.4086$ and size-independent reproduction (solid lines) and delayed peak reproduction with $\Delta_f = 2.7015$ (b). σ^2 equals 0 ($\circ$), 0.125 ($\square$), 0.25 ($\triangle$), 0.375 ($+$), and 0.5 ($\diamond$).

and density-dependent size distribution of the resident. It is these characteristics that determine the behaviour of the NLM and the SLM, though they are independent of density in these two models. Because the mortality and fecundity schedules are the same for the invader and the resident in my study, the density-dependent expected lifetime and density-dependent size distribution are also symmetrical. This symmetry is preserved in the MSLM because the two species experience common competition, and respond to it identically. However, the density-dependent net reproductive rate of the invader is different from that of the resident, because of the difference in the mean birth rate. The density-dependent net reproductive rate of the resident is more important to the system, since it determines the magnitude of competition. Therefore, I am going to concentrate on the calculation of the density-dependent net reproductive rate of the resident. The life-history characteristics are calculated using equations 6.5, 6.6, 6.7, and 6.8. The probability of growth in size is calculated from simulations, by taking the average ratio of the total available space to the total required space over time ($\mathrm{E}[A/R]$).

Figure 6-12 shows how the mortality schedule, without size-dependent fecundity, affects the density-dependent expected lifetime (equation 6.5), due to density-dependent growth in size (equation 6.8). The density-dependent expected lifetime of the resident is not affected by fluctuations in the birth rate of the resident (hence all lines coincide). The density-dependent expected lifetime is increased with increasing Δ_m (figure 6-12. This pattern is related to the decreasing probability of growth in size with changing Δ_m, i.e., decreasing probability of growth in size with increasing Δ_m (figure 6-15). With a type I mortality schedule, an individual starts with a low early mortality rate and progresses slowly thorugh later size classes, and so experiences the low early mortality rate for a relatively long period of time. This causes the high expected lifetime with a type I mortality schedule. On the other hand, with a type III mortality schedule, a high probability of growth in size does not increase the density-dependent expected lifetime, presumably because of the high mortality rate to begin with.

Changes in the probability of growth in size also explain the pattern of changes in the density-dependent expected lifetime when both mortality and fecundity are structured. With a type I mortality schedule, the density-dependent expected lifetime decreases with increasing Δ_f (figure 6-13(a)) due to the increase in the probability of growth in size (figure 6-16(a)). The fast growth in size with delayed peak reproduction causes an individual with a

type I mortality schedule to progress quickly through size classes, and much of the population experiences the high late mortality rates. Therefore, the density-dependent expected lifetime is reduced compared with that of a type I mortality schedule and early peak reproduction. With a type II mortality schedule, the density-dependent expected lifetime is not affected by changes in Δ_f (figure 6-13(b)), even though the probability of growth in size increases with increasing $|\Delta_f|$ (figure 6-16(b)). This is because the mortality rate is constant over size classes with a type II mortality schedule. With a type III mortality schedule, the density-dependent expected lifetime is larger with delayed peak fecundity (figure 6-14), because the probability of growth in size is increased with increasing $|\Delta_f|$ (figure 6-17). An individual is most likely to stay in the small size classes, in which mortality rates are high, for a relatively short period of time, and therefore shows a longer expected lifetime.

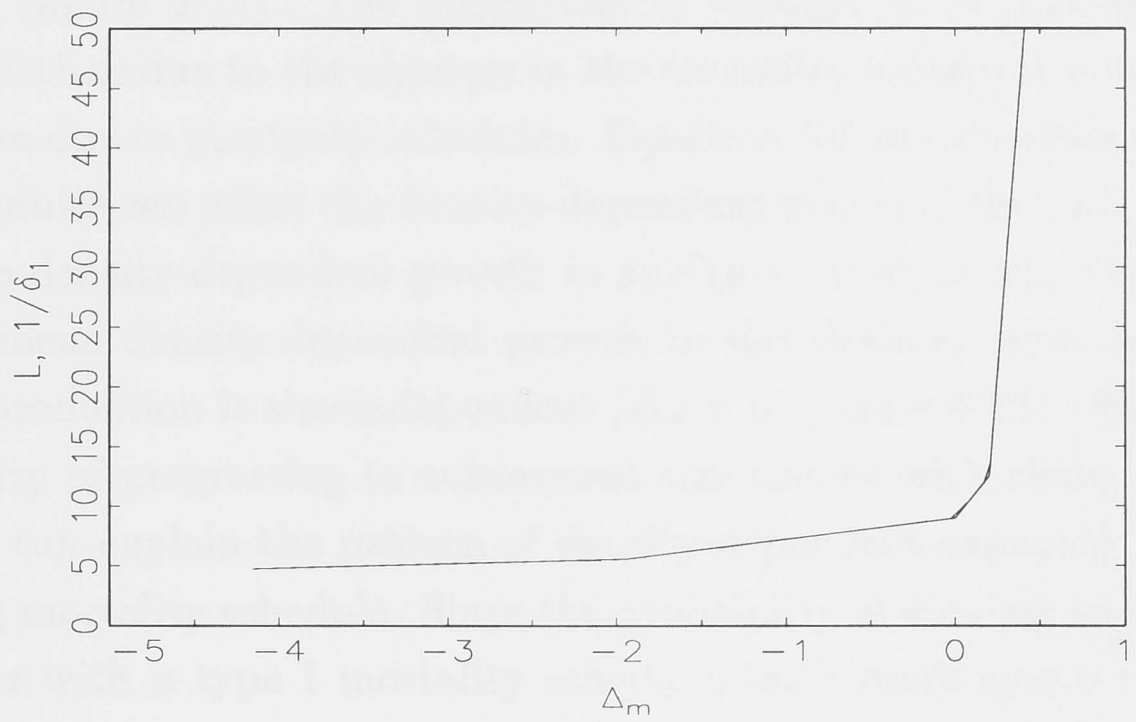

Figure 6-12: The density-dependent expected lifetime (L) (solid line) and the reciprocal of early mortality rate ($1/\delta_1$) (dashes) with different mortality schedules, with all levels of σ^2 coincide.

The density-dependent expected lifetime coincides with $1/\delta_1$ (the reciprocal of early mortality rate) when reproduction is aize independent (figure 6-12, making the early mortality rate the critical feature of the mortality schedule. Figures 6-13 and 6-14 show changes in the density-dependent expected lifetime with fecundity schedules, combined with type I, type II, or type III mortality schedules. Fluctuations in the birth rate of the resident do not affect the

density-dependent expected lifetime when both mortality and fecundity are size-dependent (hence all lines coincide). However, the density-dependent expected lifetime deviates from the reciprocal of the early mortality rate.

Without density-dependent growth in size, as in the SLM, the fecundity schedule will not have any effect on the expected lifetime. Likewise without size-dependent mortality, the density-dependent expected lifetime in the MSLM is the same, regardless of fecundity schedule, i.e., it remains equal to nine, as in the SLM (figure 6-13(b)). However, when combined with size-dependent mortality, fecundity schedules do affect the density-dependent expected lifetime. The density-dependent expected lifetime is lower with increasing Δ_f when the mortality schedule is of type I (figure 6-13(a)). With the combination of a type III mortality schedule and early peak reproduction, the density-dependent expected lifetime hardly changes with changes in Δ_f (figure 6-14). However, when a type III mortality schedule is combined with delayed peak reproduction, the density-dependent expected lifetime increases with Δ_f (figure 6-14). The magnitude of changes in density-dependent expected lifetime due to the changes in the fecundity schedules is less than that of changes due to mortality schedules. Equation 6.5 should explain why fecundity schedules can affect the density-dependent expected lifetime, i.e., through the mean density-dependent growth in size ($p = A/R$) in equation 6.8.

The mean density-dependent growth in size declines with increasing Δ_m when reproduction is size-independent ($\Delta_f = 0$) (figure 6-15). This pattern of probability of progressing to subsequent size classes with changing mortality schedule can explain the pattern of density-dependent expected lifetime with changing mortality schedule. Since the probability of moving up one size class is smaller with a type I mortality schedule, individuals spend more time in smaller size classes, when the early mortality rate is low. Therefore the density-dependent expected lifetime increases (figure 6-12).

Analogously, when reproduction is size-dependent and the mortality schedule is of type I (figure 6-16(a)), the probability of moving up one size class is larger with larger Δ_f, such that individuals stay in the small size classes for shorter periods. Consequently, individuals spend longer in the larger size classes with higher late mortality rate, and therefore the density-dependent expected lifetime is shorter (figure 6-13(a)). With a type II mortality schedule, changes in the probability of moving up one size class (figure 6-16(b)) do not affect the expected lifetime (figure 6-13(b)), because mortality rates are the same in all size classes. With a type III mortality schedule, the probability

of moving up one size class increases when reproduction departs from constant reproduction (figure 6-17). With a delayed peak reproduction, i.e., when the probability of moving up is higher, individuals spend less time in the small size classes where they experience high early mortality, thus increasing the density-dependent expected lifetime (figure 6-14). However, with a type III mortality schedule and early peak reproduction, it seems that the density-dependent expected lifetime remains constant despite changes in the probability of moving up (figure 6-14).

These results differ from those obtained from the SLM. In the SLM, there is no density-dependent growth in size, and a constraint is applied to fix the expected lifetime and net reproductive rate. In the MSLM the density-dependent expected lifetime and the density-dependent net reproductive rate cannot be fixed, since density-dependent growth in size affects both these parameters.

The density-dependent net reproductive rate increases with Δ_m when reproduction is size-independent (figure 6-18), a pattern similar to that of the density-dependent expected lifetime. Size-dependent reproduction (both early peak reproduction and delayed peak reproduction) decreases the density- dependent net reproductive rate, when combined with any mortality schedule (figure 6-19, 6-20), such that the density-dependent net reproductive rate is at its maximum when $\Delta_f = 0$.

Density-dependent size distributions for three different mortality schedules are shown in figure 6-21. The type I, II and III mortality schedules do not result in significantly different density-dependent size distributions, even though their age distributions might be different. However, each type of mortality schedule, when combined with size-dependent fecundity schedule, affects the density-dependent size distribution (figure 6-22, 6-23). With early peak reproduction, the population is more heavily concentrated in the small size classes, compared with delayed peak reproduction.

It seems that the density-dependent expected lifetime and the sendity-dependent net reproductive rate cannot explain completely and consistently the patterns of response of the recovery rate of the invader and species coexistence to changes in mortality and/or fecundity schedules. With size-independent reproduction, a type I mortality schedule produces a high density-dependent expected lifetime and a high density-dependent net reproductive rate, yet the recovery rate of the invader ($\bar{r}_i$) is much lower than it is with a type III mortality schedule which produces lower density-dependent expected lifetime and lower density-dependent net reproductive rate. However, an in-

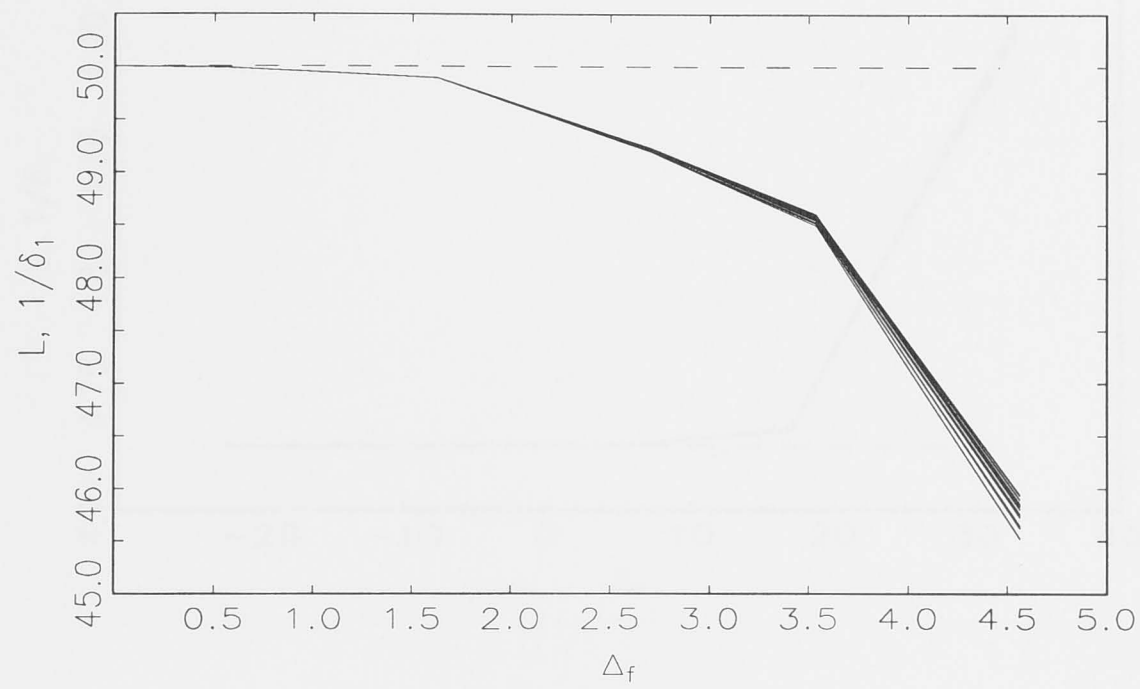

(a)

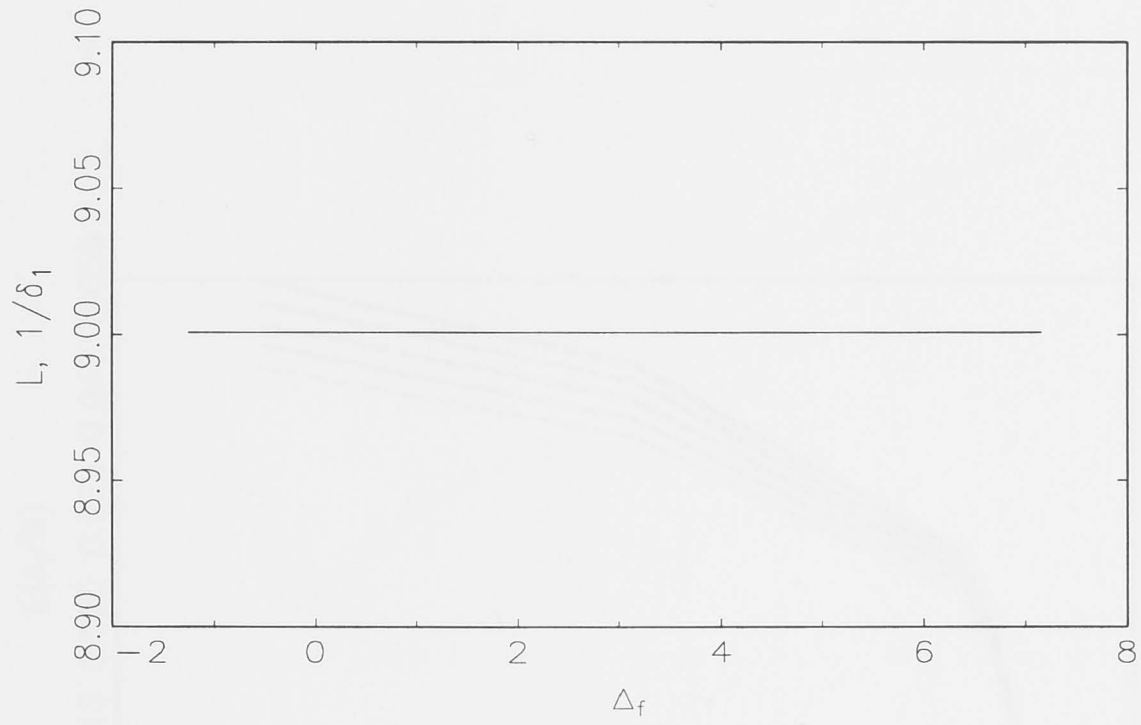

(b)

Figure 6-13: The density-dependent expected lifetime (L) (solid line) and the reciprocal of early mortality rate ($1/\delta_1$) (dashes) with different fecundity schedules and a type I mortality schedule with $\Delta_m = 0.4086$ (a), a type II mortality schedule (b), with all levels of σ^2 coincide.

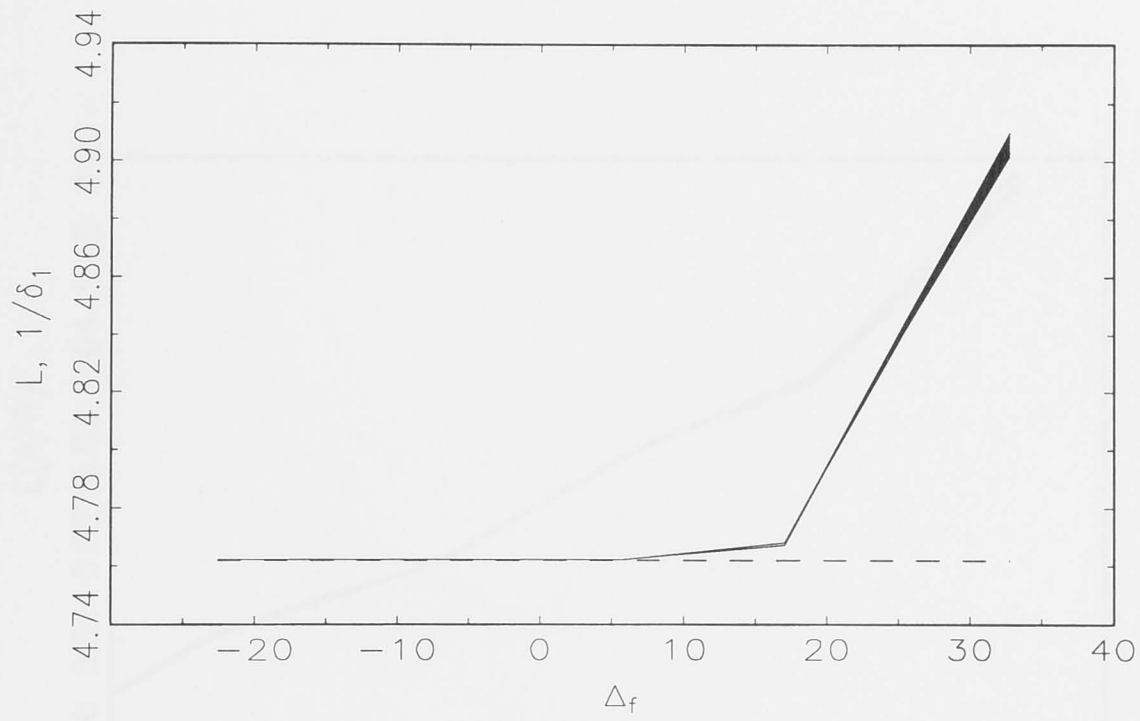

Figure 6-14: The density-dependent expected lifetime (L) (solid line) and the reciprocal of early mortality rate ($1/\delta_1$) (dashes) with different fecundity schedules and a type III mortality schedule with $\Delta_m = -4.1589$, with all levels of σ^2 coincide.

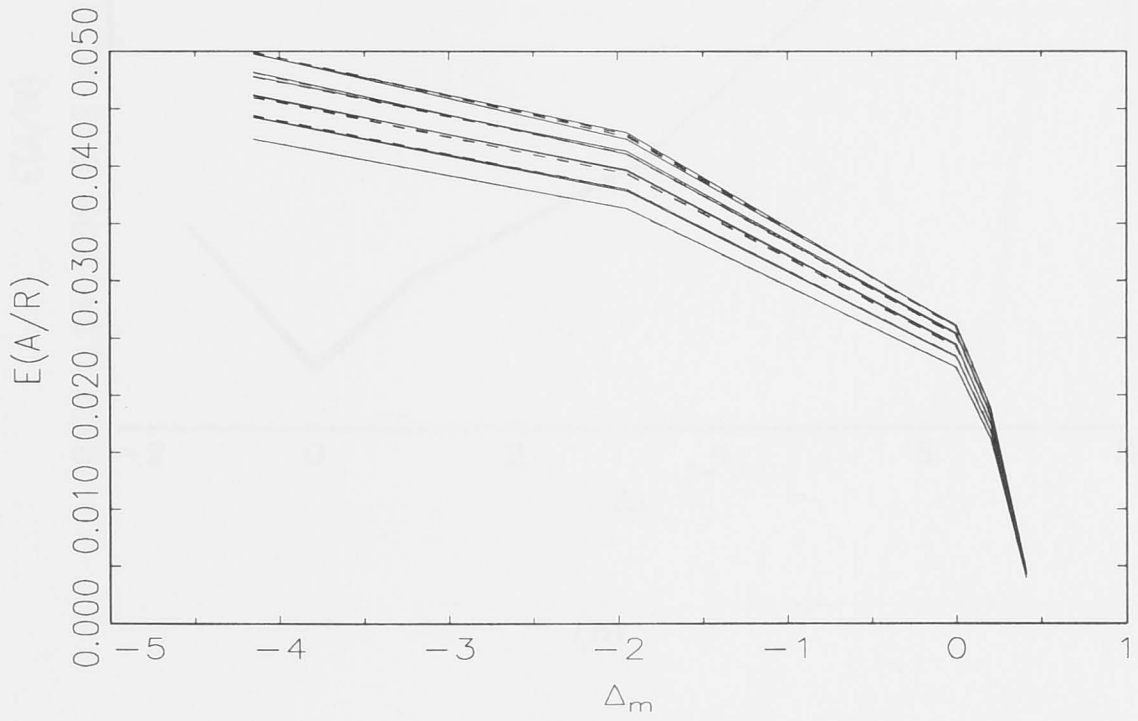

Figure 6-15: The mean of (A/R) with different mortality schedules with all levels of σ^2 coincide.

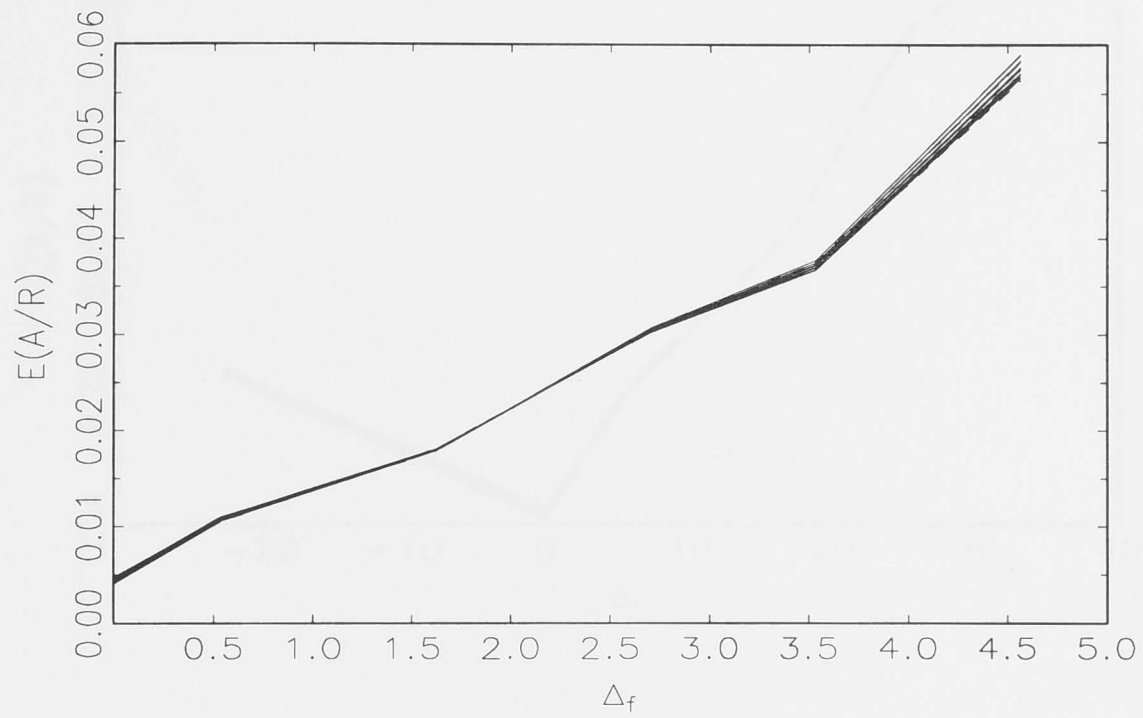

(a)

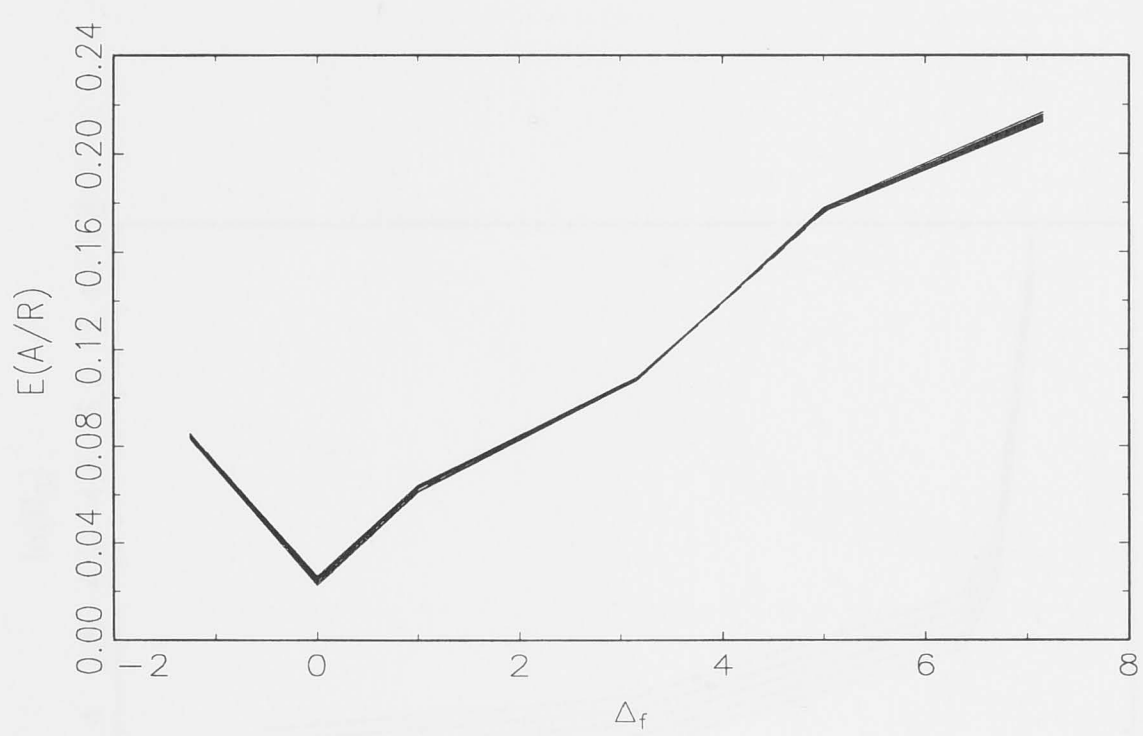

(b)

Figure 6-16: The mean of (A/R) with different fecundity schedules and a type I mortality schedule with $\Delta_m = 0.4086$ (a), a type II mortality schedule (b), with all levels of σ^2 coincide.

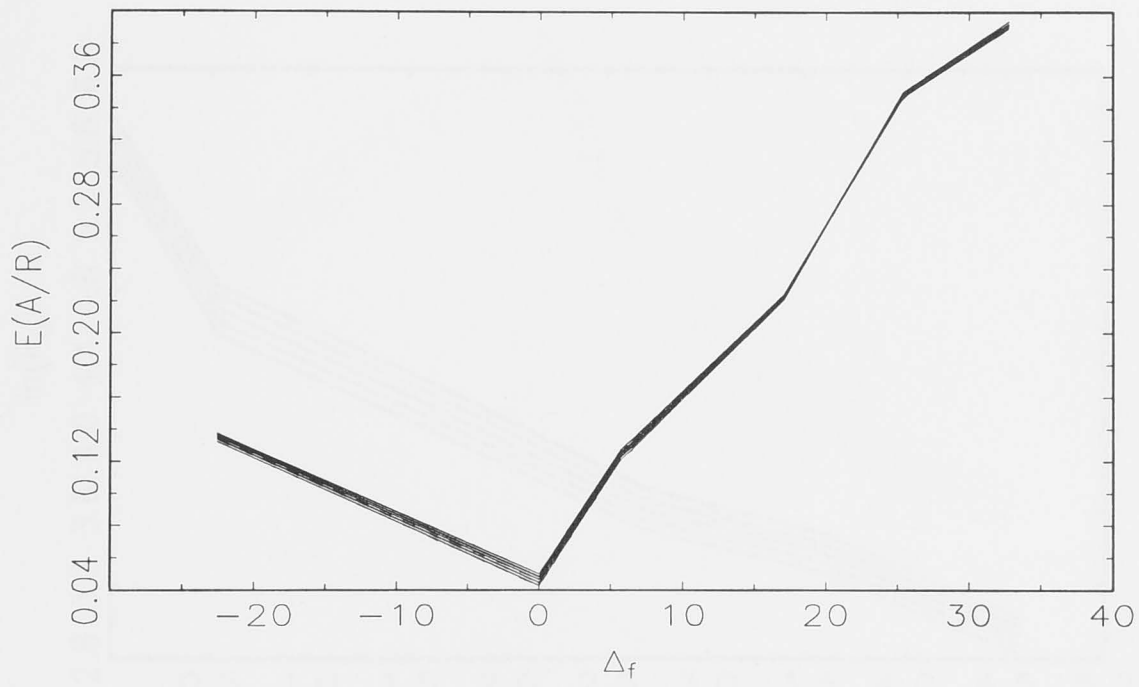

Figure 6-17: The mean of (A/R) with different fecundity schedules and with a type III mortality schedule with $\Delta_m = -4.1589$, with all levels of σ^2 coincide.

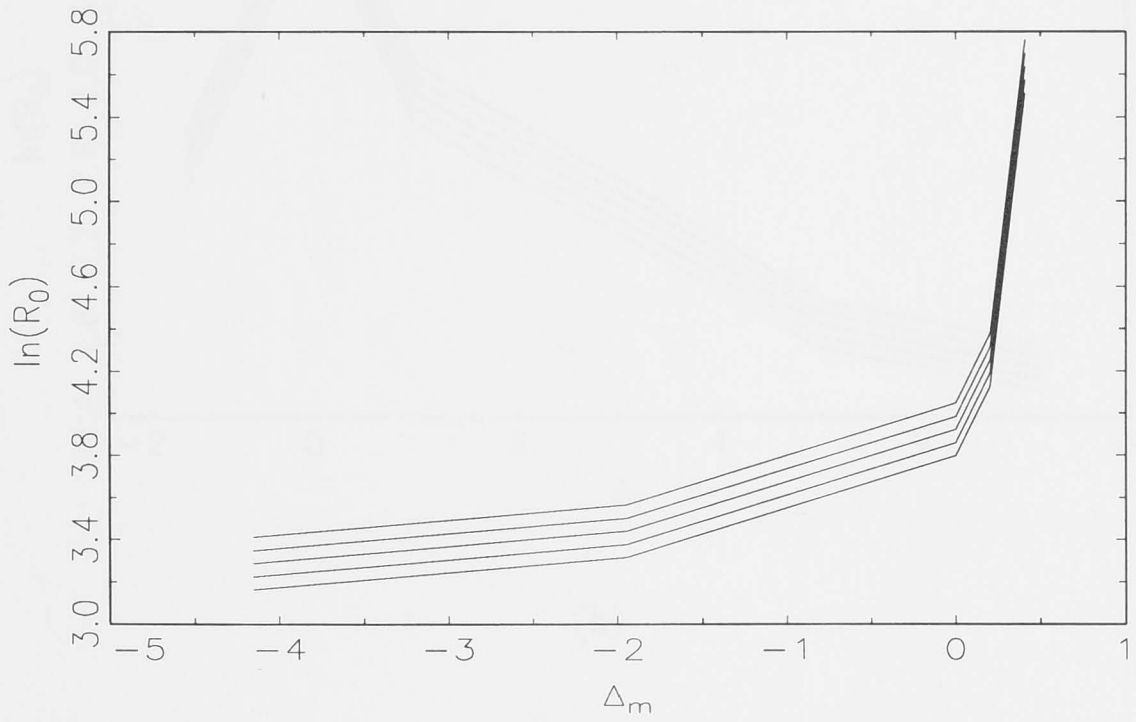

Figure 6-18: The density-dependent net reproductive rate with different mortality schedules. The lines are for $\sigma^2 = 0$ to 0.5 from top to bottom.

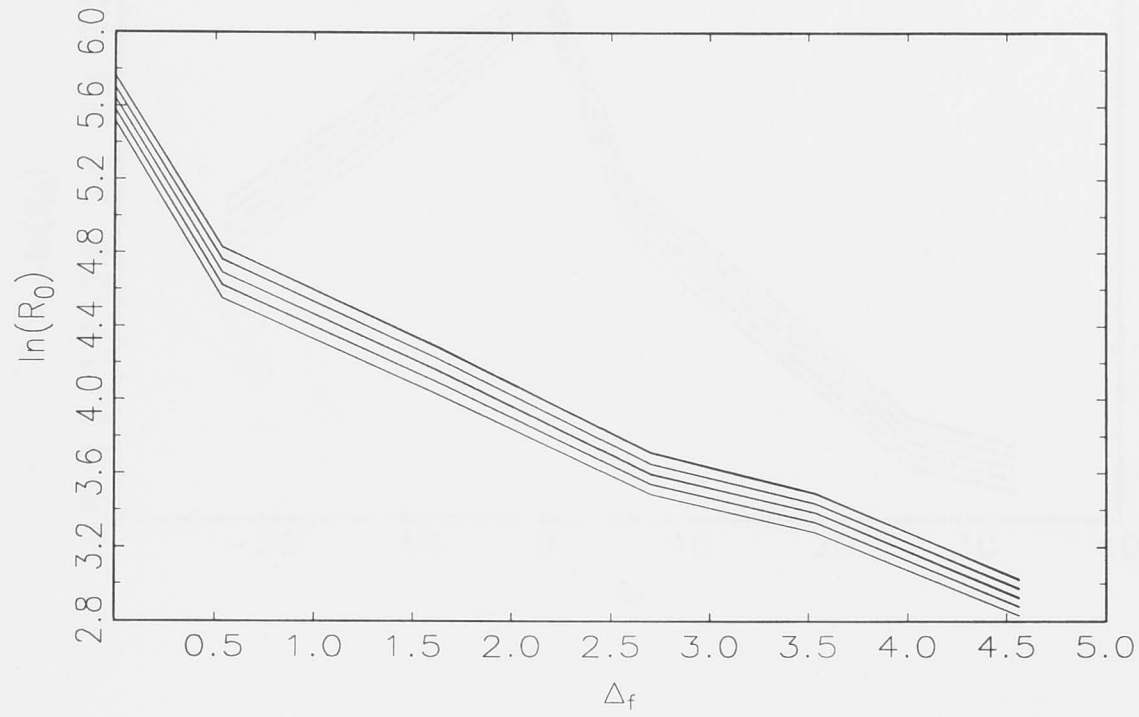

(a)

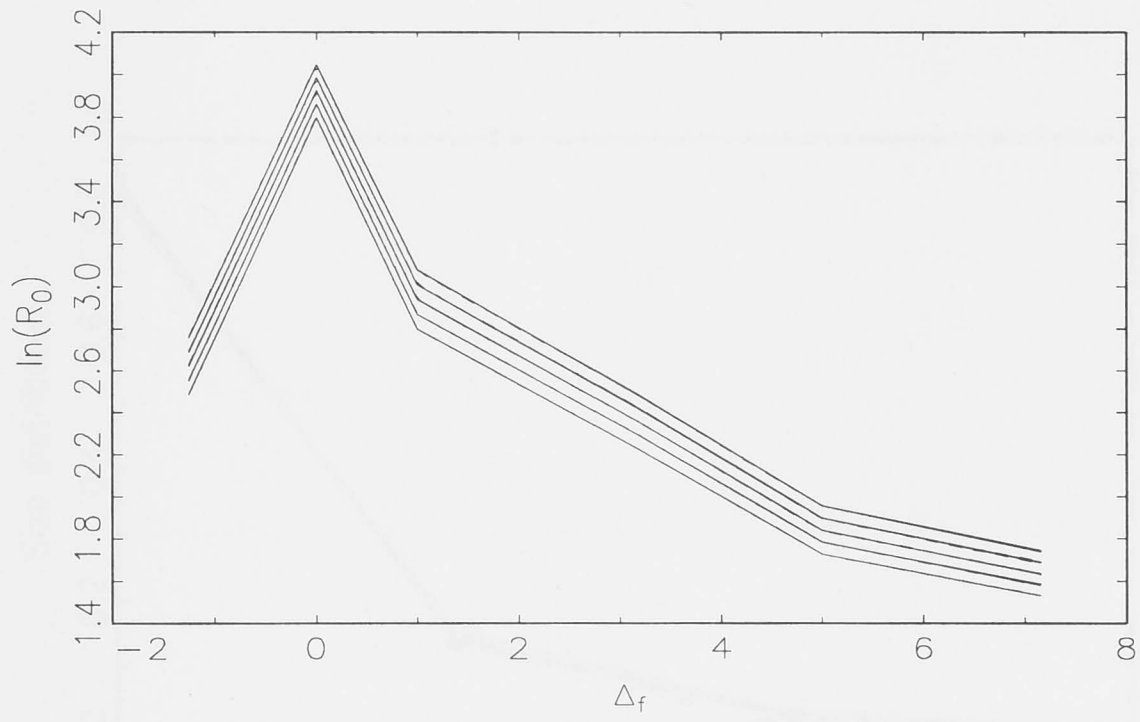

(b)

Figure 6-19: The density-dependent net reproductive rate with different fecundity schedules and a type I mortality schedule with $\Delta_m = 0.4086$ (a) and a type II mortality schedule (b). The lines are for $\sigma^2 = 0$ to 0.5 from top to bottom.

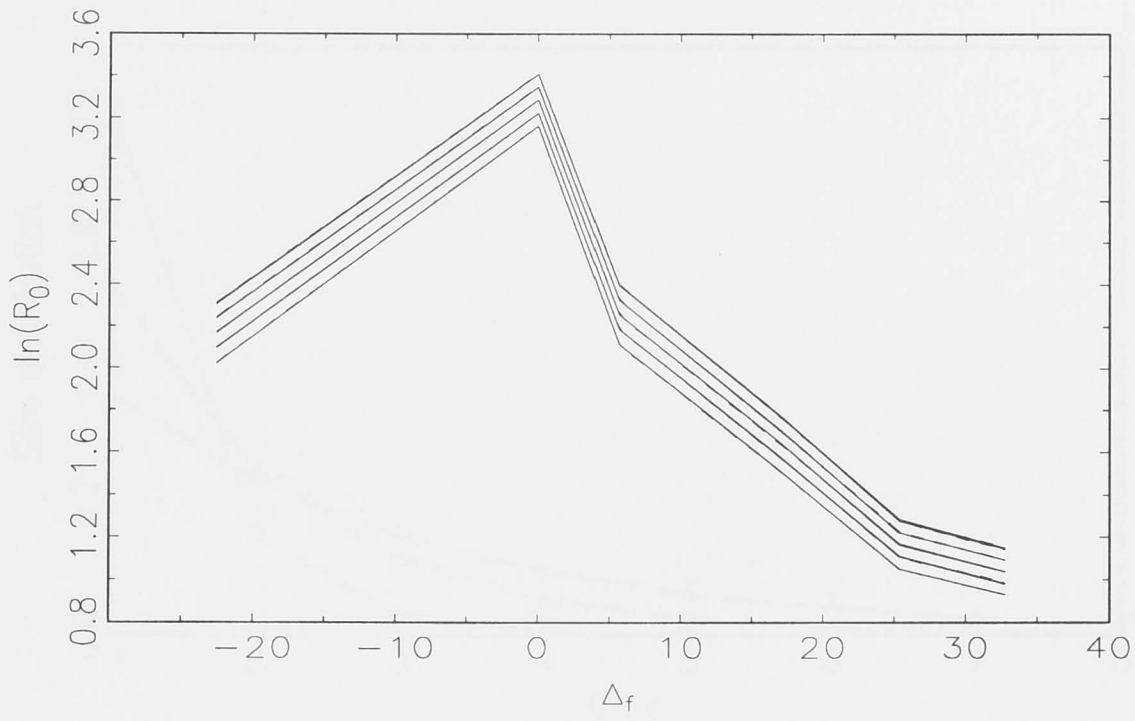

Figure 6-20: The density-dependent net reproductive rate with different fecundity schedules and a type III mortality schedule with $\Delta_m = -1.9485$. The lines are for $\sigma^2 = 0$ to 0.5 from top to bottom.

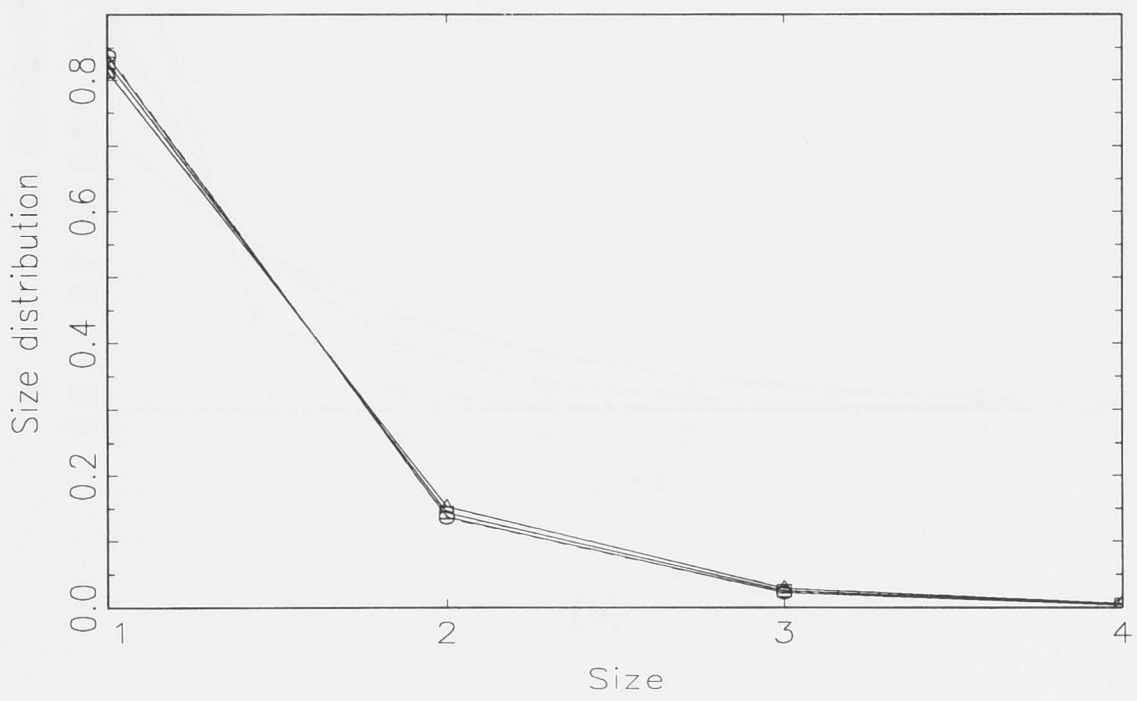

Figure 6-21: The mean density-dependent size distribution and a type I mortality schedule with $\Delta_m = 0.4086$ (short dashes), a type II mortality schedule (solid line) and a type III mortality schedule with $\Delta_m = -1.9485$ (long dashes), with all levels of σ^2 coincide.

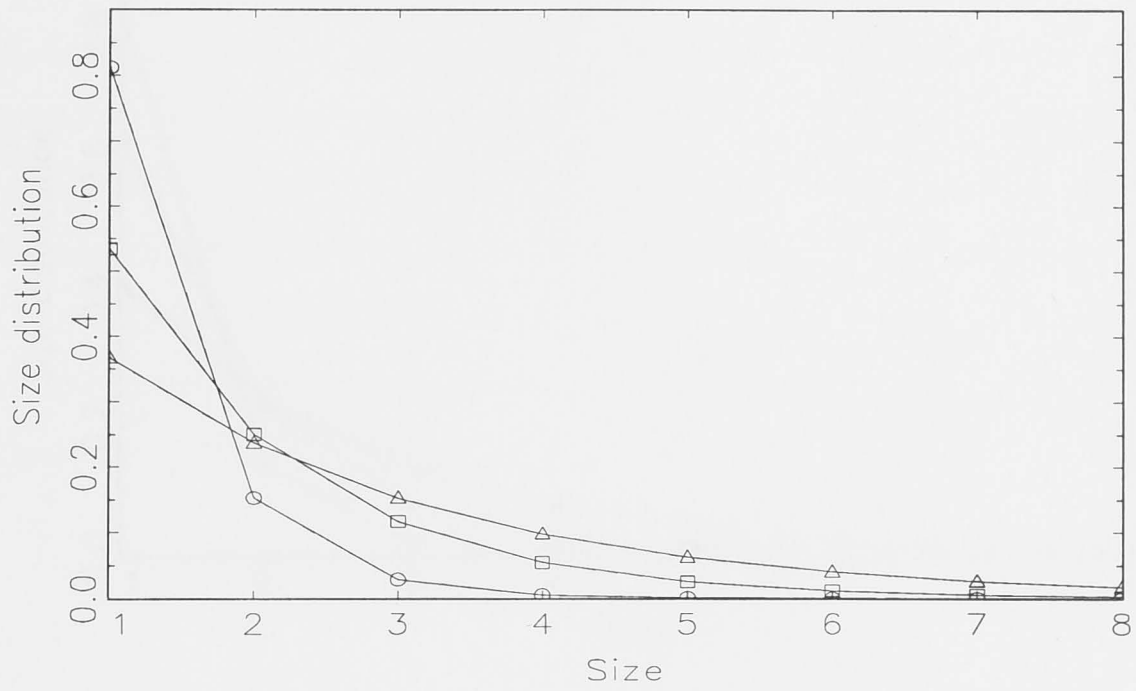

(a)

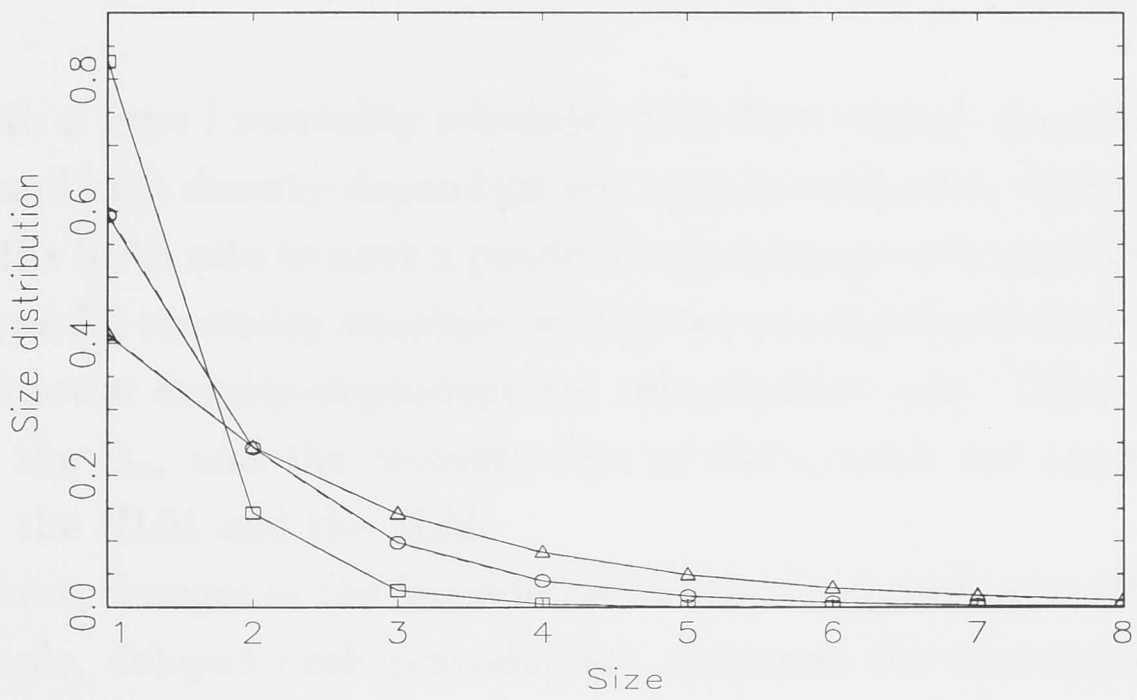

(b)

Figure 6-22: The mean density- dependent size distribution with a type I mortality schedule with $\Delta_m = 0.4086$ and size-independent reproduction (solid line), delayed peak reproduction ($\Delta_f = 1.6264$, long dashes), and delayed peak ($\Delta_f = 3.5373$, short dashes) and (a) and a type II mortality, with early peak reproduction ($\Delta_f = -1.2545$, solid line), size- independent fecundity (long dashes) and a delayed peak reproduction ($\Delta_f = 5$, short dashes) (b).

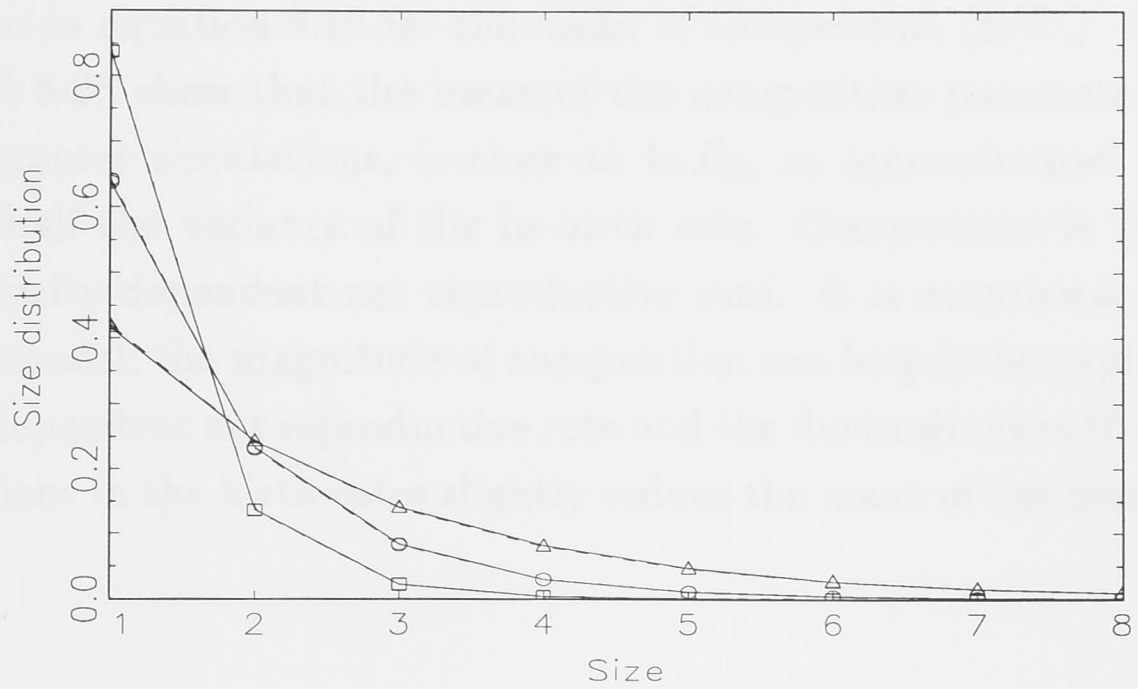

Figure 6-23: The mean density-dependent size distribution with a type III mortality schedule with $\Delta_m = -1.9485$ and an early peak reproduction with $\Delta_f = -12.2130$ (solid line), size-independent reproduction (long dashes), and a delayed peak reproduction with $\Delta_f = 9.9659$ (short dashes).

vader with a type I mortality schedule, with high density-dependent expected lifetime and high density-dependent net reproductive rate, requires less fluctuation in the birth rate to have a positive long-term growth rate than an invader with a type III mortality schedule, with lower density-dependent expected lifetime and lower density-dependent net reproductive rate. These relationships between the Δ_m and the recovery rate of the invader are opposite to those found in the NLM and the SLM.

However, changes in the fecundity schedule may give rise to different trends for example, delayed peak reproduction decreases the density-dependent expected lifetime and density-dependent net reproductive rate, while at the same time decreases the long-term population growth rate.

6.4.3 Competition

We have examined competition in the previous sections in terms of the mean of A/R, the probability of capturing a unit of space. For a better relationship with previous chapters, and for understanding the storage effect discussions below, I shall briefly present results for the competition parameter as defined

for the discussions of the storage effect, viz as $C = \ln(R/A)$.

The density-dependent net reproductive rate $\ln R_0$ seems to be the dominant term in equation 6.10 for the mean of competition (E[C]). Figures 6-24, 6-25, and 6-26 show that the mean of the competition parameter, calculated from computer simulations, is close to $\ln R_0$, as approximated by equation 6.6, less half the variance of the ln birth rate. Competition is stronger with larger density-dependent net reproductive rate. It is surprising, that in this complex model, the magnitude of competition can largely be explained by the density-dependent net reproductive rate and the fluctuations in the birth rates. Fluctuations in the birth rates slightly reduce the mean of the competition parameter.

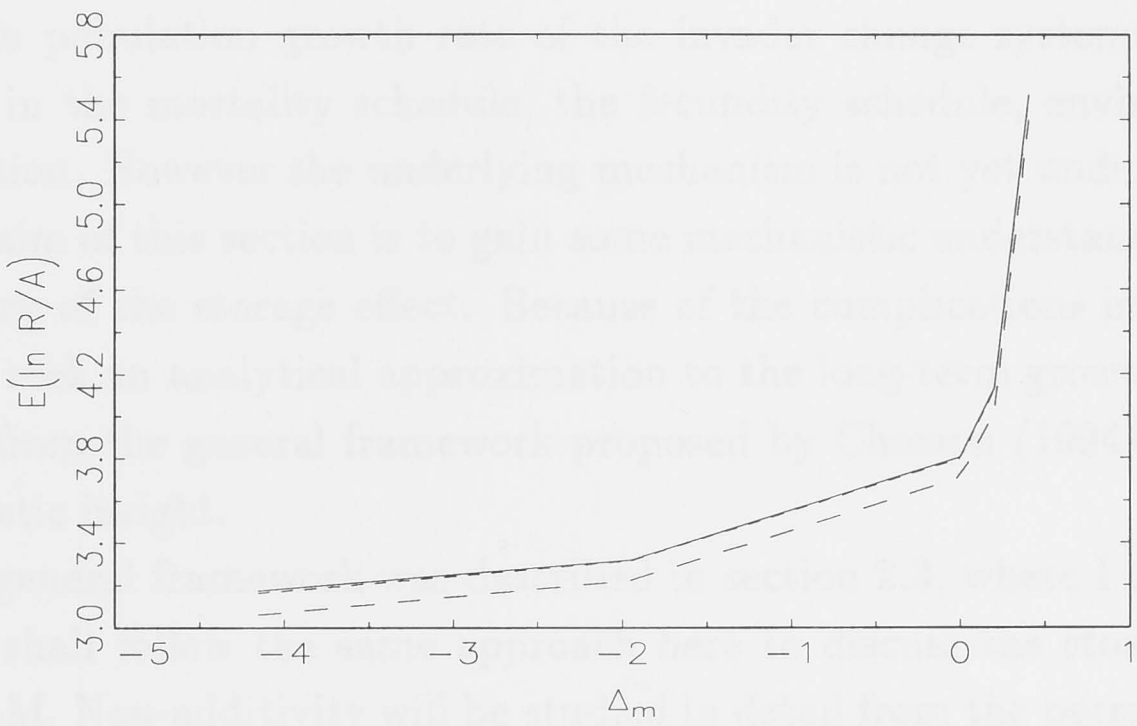

Figure 6-24: The mean of competition of different mortality schedules when reproduction is size-independent from simulation (solid lines), equation 6.10 (long dashes) and $\ln R_0$ from equation 6.6 less $0.5\sigma^2$ (short dashes).

It will be necessary to assess the importance of the competition parameter, and determine the extent to which other parameters can be ignored, in order to reduce the number of dimensions and the complexity of the model, given that the density-dependent net reproductive rate is known. This is not a simple task. First, let us see if there is any consistent relationship between the long-term population growth rate of the invader and the mean of the competition parameter, or similarly with the density-dependent reproductive rate. A type III mortality schedule causes weak competition on average, and

yields a higher long-term population growth rate of the invader, given that there is enough environmental fluctuation to allow coexistence. Early peak reproduction produces stronger competition than delayed peak reproduction, yet it results in a much higher long-term population growth rate of the invader if coexistence occurs. This shows that the relationship between competition, coexistence, and recovery rate is subtle. I will attempt to tackle this problem by investigating the storage effect in the following section. Moreover I will investigate why E[C] alone cannot entirely explain the long-term population growth rate of the invader.

6.5 The storage effect in the MSLM

In the previous section, I showed how some life-history characteristics and the long-term population growth rate of the invader change systematically with changes in the mortality schedule, the fecundity schedule, environment and competition. However the underlying mechanism is not yet understood.

The aim of this section is to gain some mechanistic understanding through the theory of the storage effect. Because of the complications in the MSLM, I do not seek an analytical approximation to the long-term growth rate of the invader from the general framework proposed by Chesson (1994), but simply mechanistic insight.

The general framework was described in section 2.3, where I discussed the NLM. I shall follow the same approach here to discuss the storage effect in the MSLM. Non-additivity will be studied in detail from the perspective of life history, as proposed by Chesson (Chesson 1990).

In the case of the MSLM, sub-additivities of the invader and the resident (γ_i and γ_j, respectively) fluctuate over time, and a modification to equation 2.2 is necessary. This fluctuation is due to fluctuations in (i) the size distribution, and (ii) the contribution of each size class to the whole population growth rate. These factors are absent in the NLM and the SLM. The long-term population growth rate of the resident is zero. The long-term population growth rate of the invader can be approximated using a quadratic equation, as defined is section 2.2.2. The original environment parameter (E), the original competition parameter (C), the standard environment parameter ($\mathcal{E}$), and the standard competition parameter ($\mathcal{C}$) are defined as in section 2.2.2. In the MSLM, E is the ln of temporal birth rate modulation, $b_j(t)$, and C as defined above, is $\ln(R/A)$. From section 2.2.2, the growth rate of the population is

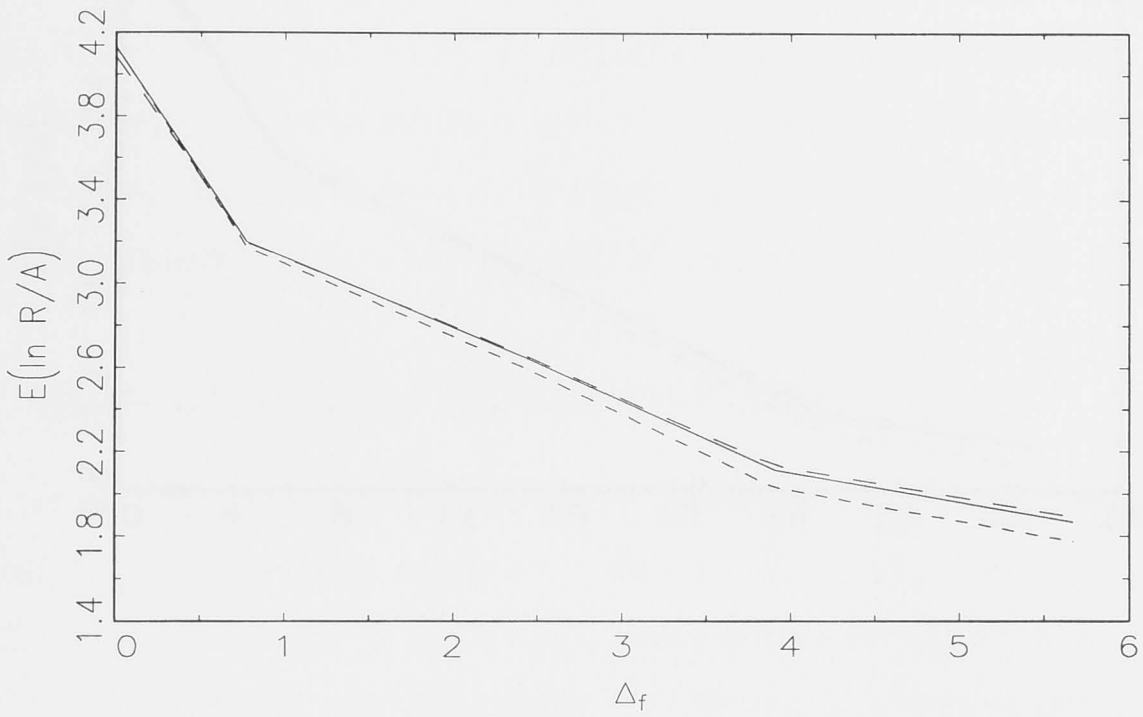

(a)

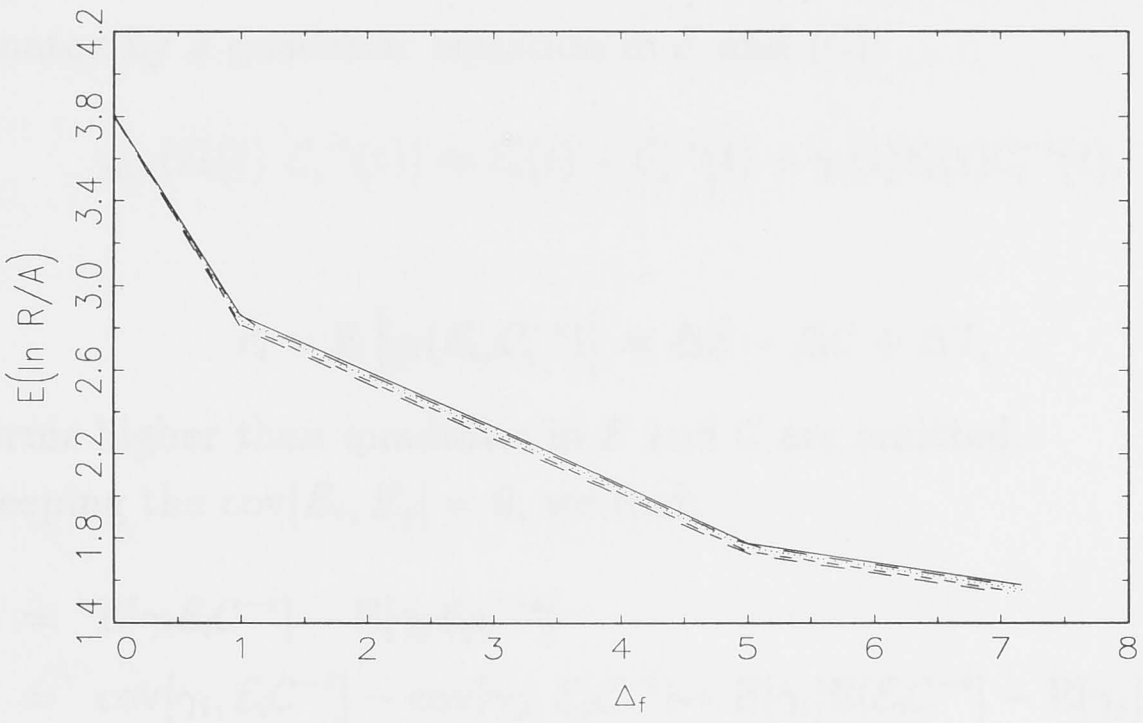

(b)

Figure 6-25: The mean of competition for different fecundity schedules and a type I mortality schedule with $\Delta_m = 0.4086$ (a) and a type II mortality schedule (b). Solid lines: simulation; long dashes: equation 6.10; short dashes: $\ln R_0$ from equation 6.6 less $0.5\sigma^2$.

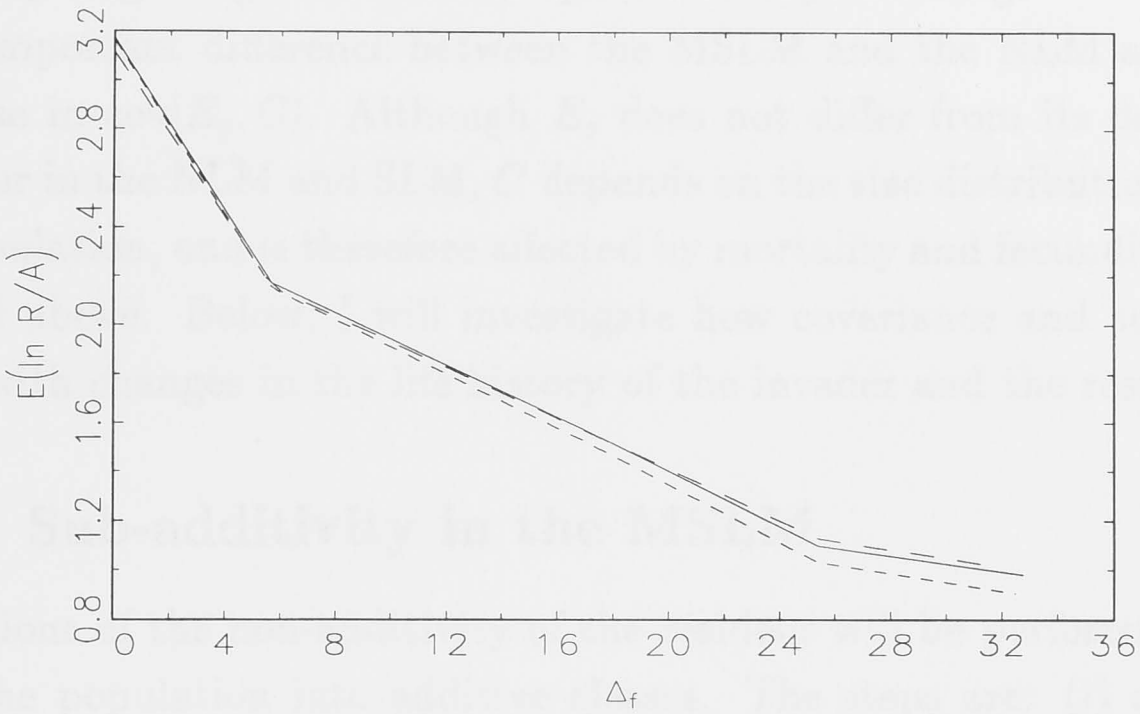

Figure 6-26: The mean of competition with different fecundity schedules and a type III mortality schedule with $\Delta_m = -1.9485$ from simulation(solid line), equation 6.10 (long dashes), and $\ln R_0$ from equation 6.6 less $0.5\sigma^2$ (short dashes).

approximated by a quadratic equation in $\mathcal{E}$ and $(\mathcal{C})$:

$$g_{i,t}(\mathcal{E}_i(t), \mathcal{C}_i^{-i}(t)) \approx \mathcal{E}_i(t) - \mathcal{C}_i^{-i}(t) + \gamma_i(t)\mathcal{E}_i(t)\mathcal{C}_i^{-i}(t),$$

and

$$\bar{r}_i = \mathrm{E}\left[g_i(\mathcal{E}_i, \mathcal{C}_i^{-i})\right] \approx \Delta\mathcal{E} - \Delta\mathcal{C} + \Delta I, \tag{6.11}$$

where terms higher than quadratic in $\mathcal{E}$ and $\mathcal{C}$ are omitted.

By keeping the $\mathrm{cov}[E_i, E_j] = 0$, we find:

$$\begin{aligned} \Delta I &= \mathrm{E}[\gamma_i\mathcal{E}_i\mathcal{C}^{-i}] - \mathrm{E}[\gamma_j\mathcal{E}_j\mathcal{C}^{-i}] \\ &= \mathrm{cov}[\gamma_i, \mathcal{E}_i\mathcal{C}^{-i}] - \mathrm{cov}[\gamma j, \mathcal{E}_j\mathcal{C}^{-i}] + \mathrm{E}[\gamma_i]\mathrm{E}[\mathcal{E}_i\mathcal{C}^{-i}] - \mathrm{E}[\gamma_j]\mathrm{E}[\mathcal{E}_j\mathcal{C}^{-i}] \\ &\approx -\mathrm{E}[\gamma_j]\chi_{jj}^{-i}, \end{aligned} \tag{6.12}$$

where:

$$\chi_{jj}^{-i} \approx (\mathrm{E}[\alpha_j])\mathrm{E}[\beta_j]\ \mathrm{Cov}[E_j, C].$$

One assumption of particular importance is that fluctuations in E_i, E_j, and C are small, except that I do not make any assumption about the small order of $\mathrm{E}[E_i]$ and $\mathrm{E}[E_j]$. Only the μ, i.e., the difference between the two expected

natural logs of birth rates, is kept small. $\mathrm{E}[E_i]$ and $\mathrm{E}[E_j]$ are required to be sufficiently large to guarantee that space is always limiting.

An important difference between the MSLM and the NLM and the SLM may arise in $\mathrm{cov}[E_j, C]$. Although E_j does not differ from its definition and behaviour in the NLM and SLM, C depends on the size distribution of the resident population, and is therefore affected by mortality and fecundity schedules, as found above. Below, I will investigate how covariance and sub-additivity change with changes in the life history of the invader and the resident.

6.5.1 Sub-additivity in the MSLM

Calculations of the non-additivity of the resident will be performed by subdividing the population into additive classes. The steps are: (i) calculate the contribution of each class to new total population at time $t+1$, (ii) determine the sensitivities of these contributions to changes in environment, competition, and the interaction between environment and competition, and (iii) calculate means and covariances of these sensitivities over the different classes weighted by the contributions of the classes to the new total population. This method provides insight into how the life history of a species produces non-additivity.

Below, I will describe in mathematics the technique outlined above used to calculate non-additivity in a structured population, such as the MSLM. The technique was proposed by Chesson (1990) for models which have non-dynamic structure, i.e., non-fluctuating size distributions.

Let us suppose the following general model:

$$P_{j\cdot}(t+1) = G(E, C)(t) P_{j\cdot}(t), \tag{6.13}$$

where
$P_{j\cdot}(t)$ is the population density of species j at time t,
$G(E, C)(t)$ is the finite rate of increase of species j from t to $t+1$, and
E and C are the environment and competition, respectively. For simplicity, the subscript j on E and C is omitted in this subsection.

I will measure non-additivity by exploring within-population heterogeneity of response to environment and competition. The non-additivity is expressed as:

$$\gamma = \frac{\partial^2 g}{\partial E \partial C}$$

where $g = \ln G$.

Suppose m virtual subpopulations can be formed from the population, and the contribution of each subpopulation to the population growth rate is known.

Thus, the growth rate of the entire population can be written as:

$$G(E,C) = \sum_{l=1}^{m} G_l(E,C), \tag{6.14}$$

where $G_l(E,C)$ is the contribution of subpopulation l to the population growth rate.

By "virtual subdivision" I mean that the population is not explicitly subdivided into subpopulations while bookkeeping of the density of each subpopulation for each time step is done as in the structured model. Depending on the model, we may or may not be able to make such a subdivision, depending on our knowledge of the contribution of each subpopulation to the population growth rate. One example of a model in which subdivision is possible is the NLM. The population can be subdivided into two subpopulations, juvenile and adult, whose contribution to the population growth rate is known explicitly from the model. Clearly, this model is structured, in the sense that the population can be divided into subpopulations. However, if contributions $G_l(E,C)$ vary with time only through variation in E and C, as implied by the notation, the model has non-dynamic structure according to my definition. The NLM has non-dynamic structure, but as we shall see below, the MSLM is more complex, and has a dynamic structure.

The sensitivity of each subpopulation to the environment (α_l), competition (β_l), and the interaction (γ_l), are, respectively, defined as:

$$\begin{aligned} \alpha_l &= \frac{\partial g_l}{\partial E} \\ \beta_l &= -\frac{\partial g_l}{\partial C} \\ \gamma_l &= \frac{\partial^2 g_l}{\partial E \partial C}. \end{aligned}$$

From (Chesson 1990), the non-additivity (γ) is expressed as:

$$\gamma = \bar{\gamma} - \sum_{l=1}^{m} (\alpha_l - \bar{\alpha}) \left(\beta_l - \bar{\beta}\right) \frac{G_l}{\sum_{l=1}^{m} G_l(t)}, \tag{6.15}$$

where $G_l = e^{g_l}$, and
the weighted average of α is expressed as:

$$\bar{\alpha} = \sum_{l=1}^{m} \alpha_l(t) \frac{G_l(t)}{\sum_{l=1}^{k} G_l(t)}.$$

The terms $\bar{\beta}$ and $\bar{\gamma}$ can be expressed similarly.

The sum in equation 6.15 is a weighted covariance of sensitivity to the environment and sensitivity to competition, as these quantities vary across the different virtual subpopulations in the population. The weights are the relative contributions of these different virtual subpopulations to the population at time $t+1$. This covariance is referred to as the covariance of sensitivity to environment and competition.

The population can be subdivided arbitrarily into subpopulations, without affecting the value of γ, but it is useful to consider a case where $\gamma_l = 0$ for all l, and hence $\bar{\gamma} = 0$. This means that, within each subpopulation, every individual responds to the environment and competition uniformly. Then the non-additivity can be found as simply the negative of the covariance between sensitivity to the environment of each subpopulation and sensitivity to competition of each subpopulation, weighted according to the contribution of that subpopulation to the whole population growth rate.

Positive covariance between α and β gives a negative γ, i.e., sub-additivity. Negative covariance between α and β gives super-additivity, and zero covariance gives additivity. An example of a model with sub-additivity is the the NLM, where we consider two subpopulations: juveniles and adults. The covariance between sensitivity to the environment and sensitivity to competition is positive, because juveniles are sensitive to both the environment and competition and adults are not sensitive to either the environment or competition. Such a difference between juveniles and adults results in sub-additivity.

The storage effect, through sub-additivity, is a consequence of within-population heterogeneity of individual responses to the environment and competition. This heterogeneity may be due to different life-history stages, physiological stages, etc.

The technique just described can be modified to cater to models with dynamic structure, though there are some complications. I will deal directly with the MSLM as a dynamic structured model, and describe the technique used to calculate non-additivity. In the MSLM, the population is genuinely divided into size classes, and the dynamics of each size class are recorded over the time periods.

By rewriting the life cycle graph of the MSLM in figure 6-1, we get:

$$\begin{aligned} P_{j\cdot}(t+1) &= b_j(t)p(t)\sum_{x=1}^{n+1} k_x P_{jx}(t) + s_1 P_{j1}(t)\,(1-p(t)) + \\ &\quad s_1 P_{j1}(t)p(t) + s_2 P_{j2}(t)\,(1-p(t)) + \\ &\quad \ldots + \end{aligned}$$

$$s_{n-1}P_{j,n-1}(t)p(t) + s_nP_{jn}(t)\,(1-p(t)) +$$
$$s_nP_{jn}(t)p(t) + s_{n+1}P_{j,n+1}(t),$$

where $p(t) = (A/R)(t) = e^{-C(t)}$, the ratio of available space to required space, is the probability of progressing from one size class to the next at time t. Note that $p(t)$ is a parameter common to the invader and the resident, and so I have dropped the subscript j.

Denoting the size distribution of class x at time t as $u_x(t)$, the above equation can be rewritten as:

$$\begin{aligned} P_{j\cdot}(t+1) \;=\; & P_{j\cdot}(t)\Big[b_j(t)p(t)\sum_{x=1}^{n+1}k_xu_{jx}(t) + s_1u_{j1}(t)\,(1-p(t)) + \\ & s_1u_{j1}(t)p(t) + s_2u_{j2}(t)\,(1-p(t)) + \\ & \ldots + \\ & s_{n-1}u_{j,n-1}(t)p(t) + s_nu_{jn}(t)\,(1-p(t)) + \\ & s_nu_{jn}(t)p(t) + s_{n+1}u_{j,n+1}(t)\,\Big]. \end{aligned}$$

It is important to note that $u_{jx}(t)$ is dependent on $b_j(t-1)$ and $p(t-1)$ at earlier times, but independent of $b_j(t)$ and $p(t)$, reflecting the dynamic structure of the MSLM. With the introduction of the size distribution u_x, the contribution of each size class to population growth rate can be calculated.

It has been mentioned that subdivision of the population will give insight into the role of life history in determining sub-additivity, when response to the environment and competition is uniform within each subpopulation. Here, each size class is subdivided into three virtual subpopulations, based on contributions to the whole population growth rate: a reproduction contribution, a remain-in-the-same-size-class contribution, and a move-up contribution, with the exception that the last size class does not have a move-up-contribution. Recall that $\ln b_j(t)$ and $\ln(R/A)(t) = \ln 1/p(t)$ are the $E_j(t)$ and $C(t)$, respectively. Then a reproduction contribution ($G_{jx}^{(r)}$), a remain-in-the-same-class contribution ($G_j^{(s)}$), and a move-up contribution ($G_{jx}^{(m)}$) for each size class are:

$$\begin{aligned} G_j^{(r)} &= k_je^{E(t)-C(t)}u_{jx}(t) \text{ for } x = 1,\cdots,n+1, \\ G_{jx}^{(s)} &= s_x\left(1-e^{-C(t)}\right)u_{jx}(t) \text{ for } x = 1,\cdots,n, \\ G_{j,n+1}^{(s)} &= s_{n+1}u_{j,n+1}(t), \text{and} \\ G_{jx}^{(m)} &= s_xe^{-C(t)}u_{jx}(t) \text{ for } x = 1,\cdots,n. \end{aligned}$$

Before proceeding further, we recall from Chapter 2 that Chesson's quadratic approximations require choice of a values E_i^* of E_i and E_j^* of E_j about which the quadratic approximation is made. In the lottery models of this thesis sensible values for both of these would be the average of $E[E_i]$ and $E[E_j]$. Corresponding to these, chosen to give zero growth of the population are C_i^* and C_j^* for the competition parameters of the invader and resident. In the MSLM there will also be equilibrial size structures, u_{jx}^*, and u_{ix}^*.

Differentiating the above, and treating u_{jx} as a constant, we get:

$$\begin{aligned}
\alpha_x^{(r)} &= 1, \\
\alpha_x^{(s)} &= \alpha_x^{(m)} = 0, \\
\beta_x^{(r)} &= 1, \\
\beta_x^{(s)} &= -\frac{e^{-C^*}}{1-e^{-C^*}}|_{C=C^*}, \text{and} \\
\beta_x^{(m)} &= 1.
\end{aligned}$$

In all cases:

$$\gamma_x^{(y)} = 0.$$

For the averages:

$$\bar{\alpha} = \sum_x k_{jx} e^{E^*-C^*} u_{jx}^*. \tag{6.16}$$

Equation 6.16 is the sum over $\alpha_x^{(r)}$ only, and note that $\sum_{x,y}\left(G_{jx}^{(y)}\right)^* = 1$. Therefore:

$$\bar{\alpha} = e^{E^*-C^*} \sum_x k_{jx} u_{jx}^*.$$

Similarly:

$$\bar{\beta} = e^{E^*-C^*} \sum_x k_{jx} u_{jx}^* + e^{-C^*} \sum_x s_x u_{jx}^* - e^{-C^*} \sum_x s_x u_{jx}^*,$$

and hence:

$$\bar{\beta} = e^{E^*-C^*} \sum_x k_{jx} u_{jx}^* = \bar{\alpha}, \tag{6.17}$$

$$\begin{aligned}
\sum_{x,y} \alpha_{jx}^{(y)} \beta_{jx}^{(y)} G_{jx}^{(y)} &= e^{E^*-C^*} \sum_x k_{jx} u_{jx}^* \\
&= \bar{\alpha}.
\end{aligned}$$

Thus the covariance is simply:

$$\bar{\alpha} - (\bar{\alpha})^2 = \bar{\alpha}(1-\bar{\alpha}),$$

and therefore:

$$\gamma_{jo} = -\bar{\alpha}(1-\bar{\alpha}),$$

and:

$$\gamma_j = -\left(\frac{1}{\bar{\alpha}} - 1\right). \tag{6.18}$$

The relationships between $\bar{\alpha}$, $\bar{\beta}$, γ_{jo}, and γ_j are exactly the same as those found in the NLM and the SLM. However, unlike in the NLM and the SLM, where $\bar{\alpha}$ is known to be equal to $\tilde{\delta}$, here we only know $\bar{\alpha}$ from equation 6.16.

6.5.2 Covariance between the environment and competition

The environmentally dependent parameter $(E_j(t))$ and competition parameter $(C(t))$ of the resident were defined in the previous section as:

$$E_j(t) = \ln b_j(t),$$

$$\begin{aligned} C(t) &= \ln\left\{\frac{\left(b_j \sum_{x=1}^{n+1} k_x P_{jx}(t) + \sum_{x=1}^{n}(1-\delta_x)P_{jx}(t)\right)}{\sum_{x=1}^{n+1} x\delta_x P_{jx}(t)}\right\} \\ &= \ln\left\{\frac{b_j Y + Z}{X}\right\}, \end{aligned}$$

X, Y, and Z are statistically independent of b_j. Therefore:

$$\begin{aligned} \mathrm{cov}[E_j, C] &= \mathrm{cov}[E_j, \ln\{(b_j Y + Z)\}] \\ &= \mathrm{cov}[E_j, \ln\{e^{E_j} Y + Z\}]. \end{aligned}$$

Let us find an approximation of the above. For a good approximation, I must first subtract the mean from E_j. Thus, by defining $\hat{E}_j = E_j - \mu_j$, we can write:

$$\begin{aligned} \ln\{e^{E_j} Y + Z\} &= \ln\left\{e^{\hat{E}_j} e^{\mu_j} Y + Z\right\} \\ &= \ln\left\{(e^{\hat{E}_j} - 1)e^{\mu_j} Y + e^{\mu_j} Y + Z\right\} \\ &= \mathrm{const} + \ln\left\{1 + \frac{e^{\mu_j} Y}{e^{\mu_j} Y + Z}(e^{\hat{E}_j} - 1)\right\} \\ &= \mathrm{const} + \frac{e^{\mu_j} Y}{e^{\mu_j} Y + Z}\hat{E}_j, \end{aligned}$$

to first order, where $\mu_j = \mathrm{E}[\ln b_j]$. Therefore:

$$\mathrm{cov}[E_j, C] = \mathrm{E}[\frac{e^{\mu_j} Y}{e^{\mu_j} Y + Z}]\sigma^2 + o(\sigma^2). \tag{6.19}$$

Now, the expected value on the right hand side of equation 6.19 will be approximated by setting the variables Y and Z at their equilibrial values, as follows:

$$Y = \sum_{x=1}^{n+1} k_x u^*_{jx} = \frac{\bar{\alpha}}{(e^{E^*_j - C^*})}, \tag{6.20}$$

$$Z = \sum_{x=1}^{n} s_x u^*_{jx}. \tag{6.21}$$

We need to know how μ_j compares with $E^*_j - C^*$ in equation 6.20. Since $\mu_j - E^*_j$ is $O(\sigma^2)$, then:

$$e^{\mu_j} Y = e^{C^*} \bar{\alpha} + O(\sigma^2). \tag{6.22}$$

We will use equation 6.22 to approximate 6.19.

Now, let us simplify expression 6.21. We know from the non-additivity that, by definition:

$$\sum_{x,y} (G^{(y)}_{jx})^* = 1,$$

and therefore:

$$e^{E^* - C^*} \sum_{x=1}^{n+1} k_x u^*_{jx} + \sum_{x=1}^{n+1} s_x u^*_{jx} = 1.$$

Thus expression 6.21 can be written as:

$$Z = \sum_{x=1}^{n} s_x u^*_{jx} = 1 - \bar{\alpha} - s_{n+1} u^*_{j,n+1}. \tag{6.23}$$

The last term is a result of the fact that c (competitiveness) for the last class is 0, and the simple result is due to the simple c function (i.e., $c_x = 1$ for $x = 1, 2, ..., n$).

Substituting equations 6.22 and 6.23 into equation 6.19, we obtain:

$$\mathrm{cov}[E_j, C] \approx \frac{e^{C^*} \bar{\alpha} \sigma^2}{e^{C^*} \bar{\alpha} + 1 - \bar{\alpha} - s_{n+1} u^*_{j,n+1}} + o(\sigma^2). \tag{6.24}$$

Since e^{C^*} is going to be about the same size as R_0, and it is not unreasonable to expect R_0, and thus $R_0 \bar{\alpha}$, to be large, $\mathrm{cov}[E_j, C] \approx \sigma^2$, as in the NLM and the SLM.

6.5.3 Results and discussion

To calculate the storage effect, as in equation 6.12, I only need to calculate the expected non-additivity in terms of standard parameters ($\mathrm{E}[\gamma_j] =$

$\mathrm{E}[\gamma_{j0}]/\bar{\alpha}_j\bar{\beta}_j$), and the covariance between the standard environment parameter and the standard competition parameter ($\chi_{jj}^{-i} = \mathrm{cov}[E_j, C]\bar{\alpha}_j\bar{\beta}_j$), since the way $\mathrm{E}[C]$ changes with mortality and fecundity schedules is known, and the remaining parameters, $\mathrm{E}[E_j]$ and $\mathrm{E}[E_i]$, are given. I will attempt to sort out which terms in the equation are affected most by mortality and fecundity schedules, by looking at the density-dependent expected lifetime, the density-dependent net reproductive rate, and the density-dependent size distribution. The qualitative pattern of relationships between the mortality schedule, the fecundity schedule, and other parameters, such as $\mathrm{E}[E_i]$, $\mathrm{E}[E_j]$, and the amount of fluctuation in both E_i and E_j, can be obtained.

Figures 6-27(a), 6-28(a), 6-29(a), and 6-29(a) show that the sensitivity of growth rate to the environment ($\bar{\alpha}_j$) is equal to the sensitivity of growth rate to competition ($\bar{\beta}_j$). These sensitivities are calculated numerically from simulations, assuming that every $E_j(t)$ and $C(t)$ are E^* and C^*. This means that I assume that the population growth rate of resident is zero. During the simulations, I keep the records of the growth rate of each subpopulation, in order to calculate the contribution of each subpopulation to the population growth rate over time.

The sensitivity of population growth rate to the environment and to competition declines with the Δ_m. With a type III mortality schedule, population growth rate is more sensitive to the environment and competition than it is with a type II or a type I mortality schedule (figure 6-27(a)). The magnitudes of $\bar{\alpha}_j$ and $\bar{\beta}_j$ are very similar to that of the reciprocal of the density-dependent expected lifetime ($1/L$).

Changes in Δ_f with fixed Δ_m only affect $\bar{\alpha}_j$ and $\bar{\beta}_j$ slightly (figures 6-28(a), 6-29(a), and 6-30(a)). With a type II mortality schedule and equal ($\tilde{\delta}$), $\bar{\alpha}_j$ and $\bar{\beta}_j$ are the same in the NLM, the SLM and the MSLM. Figures 6-28(a), 6-29(a) and 6-30(a) also show that the sensitivity of the population growth rate to the interaction between the original parameters, γ_{jo}, is negative in this MSLM. γ_{jo} declines with larger Δ_m, but is only slightly affected by changes in Δ_f, provided Δ_m is fixed. With a type II mortality schedule, the magnitude of γ_{jo} is also exactly the same as it is in the NLM and the SLM, i.e., it is equal to 0.0987.

The relationship between the magnitude of sub-additivity and Δ_m and Δ_f changes from that of the original parameters (figures 6-27(b), 6-28(b), 6-29(b) and 6-30(b)). $|\gamma_j|$ increases sharply with increases in Δ_m when reproduction is size-independent (figure 6-27(b)), and coincides with $-(L-1)$. With a type I

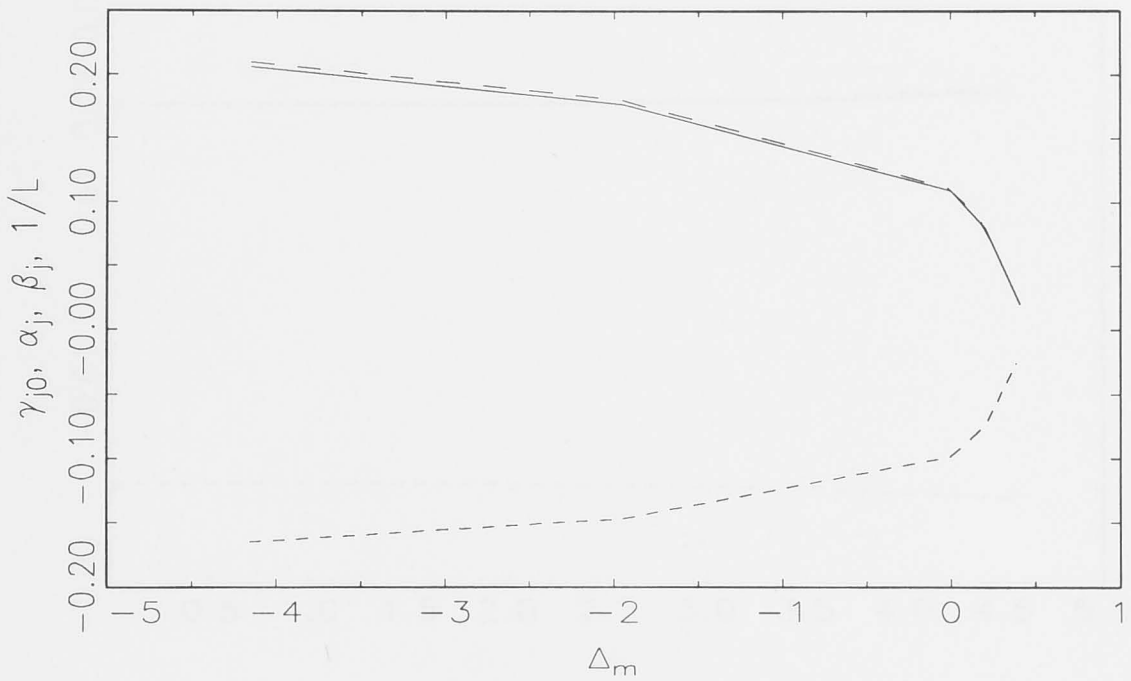

(a)

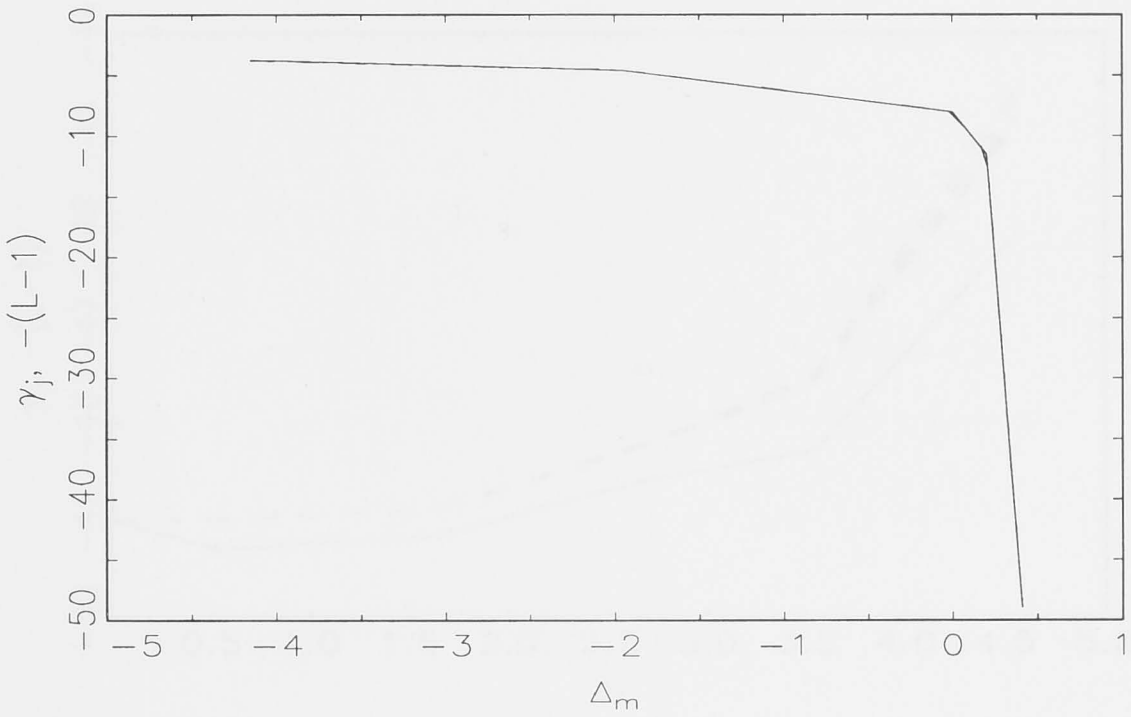

(b)

Figure 6-27: The mean of sub-additivity in terms of original parameters (γ_{jo}) (dashes), the sensitivity of growth rate to E_j ($\bar{\alpha}_j$) and C ($\bar{\beta}_j$) (solid lines) and the reciprocal of the density-dependent expected lifetime ($1/L$) (long dashes), with different mortality schedules and size-independent reproduction (a). The mean of sub-additivity in terms of standard parameters (γ_j) (solid line) and $-(L-1)$ (long dashes) with different mortality schedules and size-independent reproduction (b). All levels of σ^2 coincide.

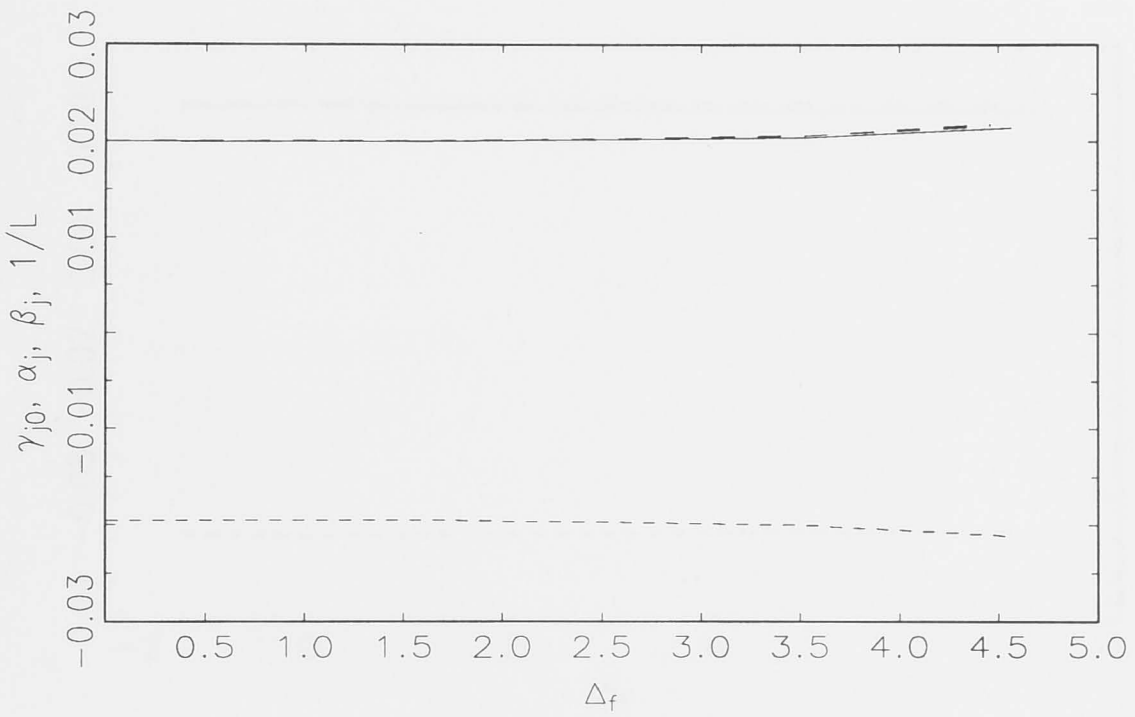

(a)

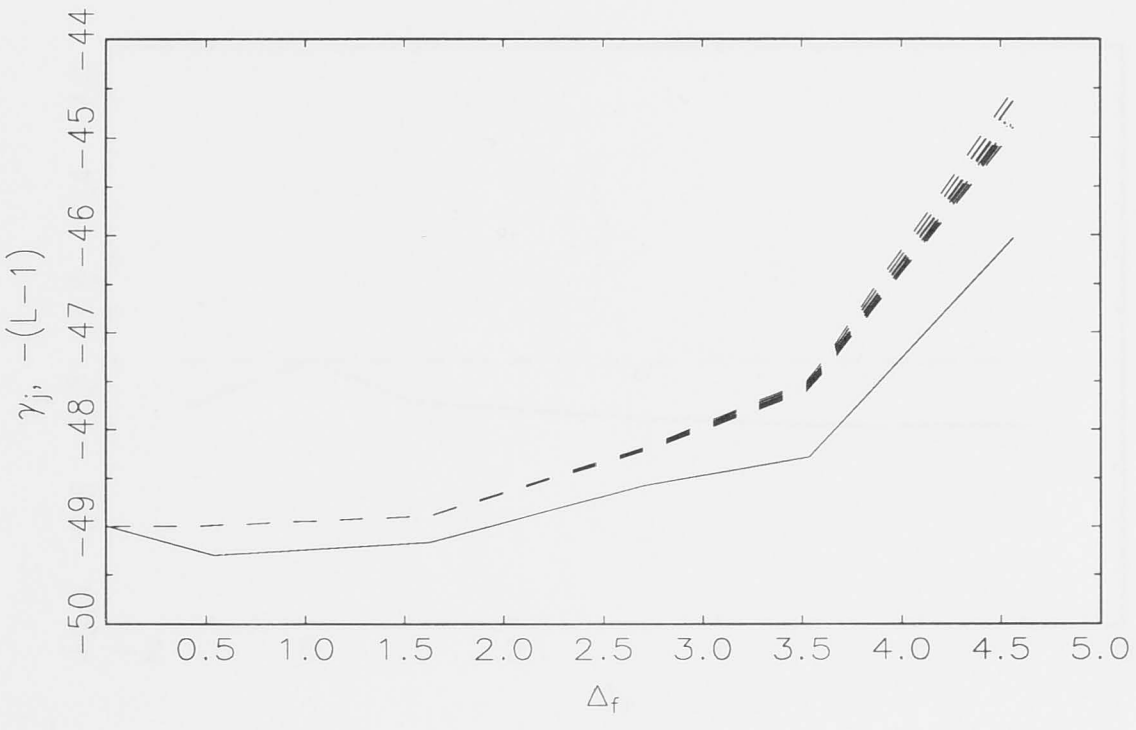

(b)

Figure 6-28: The mean of sub-additivity in terms of original parameters (γ_{jo}) (dashes), the sensitivity of growth rate to E_j $\bar{\alpha}_j$ and C ($\bar{\beta}_j$) (solid lines) and the reciprocal of the density-dependent expected lifetime ($1/L$) (long dashes), with a type I mortality schedule and size-dependent fecundity (a). The mean of sub-additivity in terms of standard parameters (γ_j) (solid line) and $-(L-1)$ (long dashes) with a type I mortality schedule and size-dependent fecundity (b). All levels of σ^2 coincide.

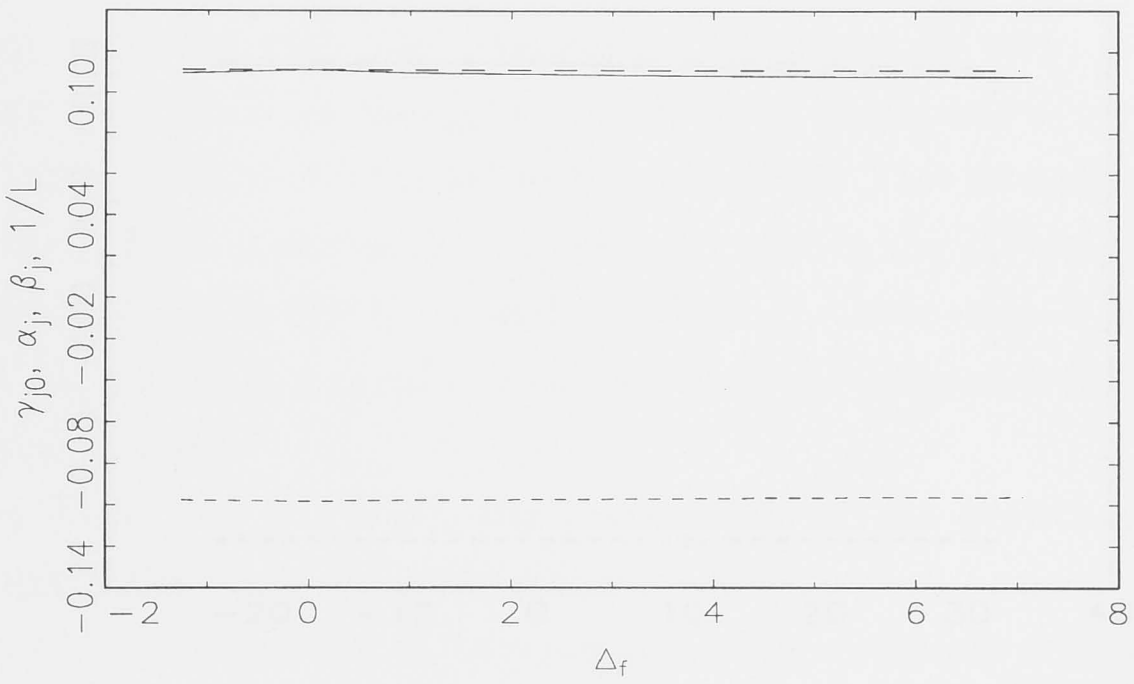

(a)

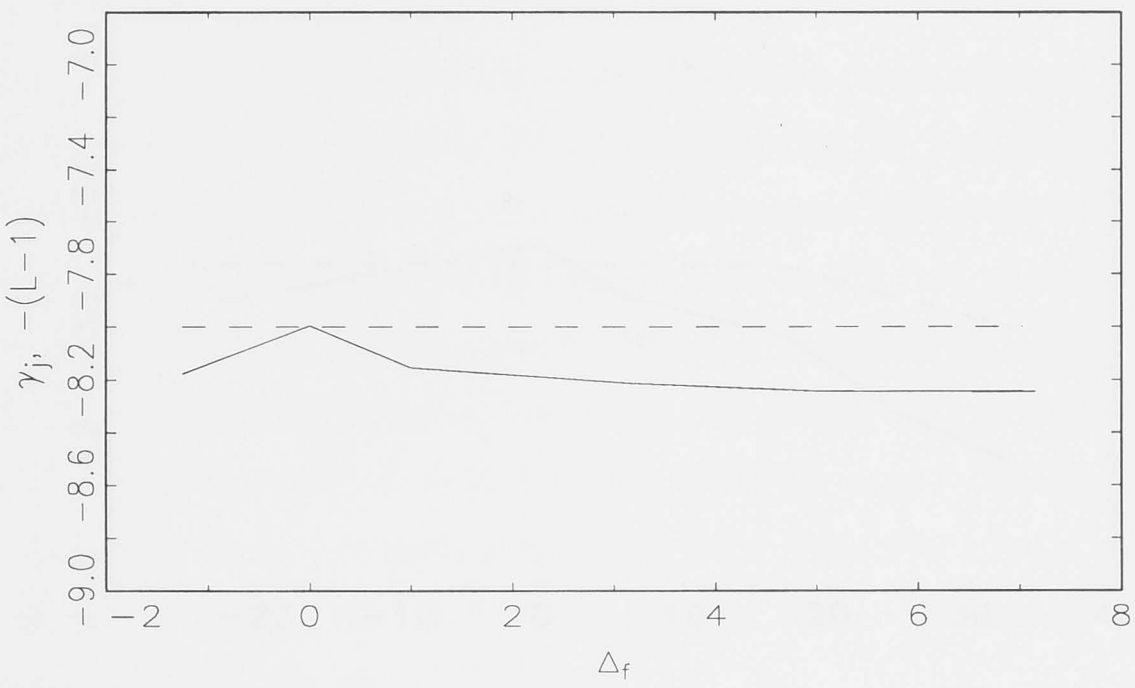

(b)

Figure 6-29: The mean of sub-additivity in terms of original parameters γ_{jo} (dashes), the sensitivity of growth rate to E_j ($\bar{\alpha}_j$) and C ($\bar{\beta}_j$) (solid lines) and the reciprocal of the density-dependent expected lifetime ($1/L$) (long dashes), with a type II mortality schedule and size-dependent fecundity (a). The mean of sub-additivity in terms of standard parameters γ_j (solid line) and $-(L-1)$ (long dashes) with a type II mortality schedule and size-dependent fecundity (b). All levels of σ^2 coincide.

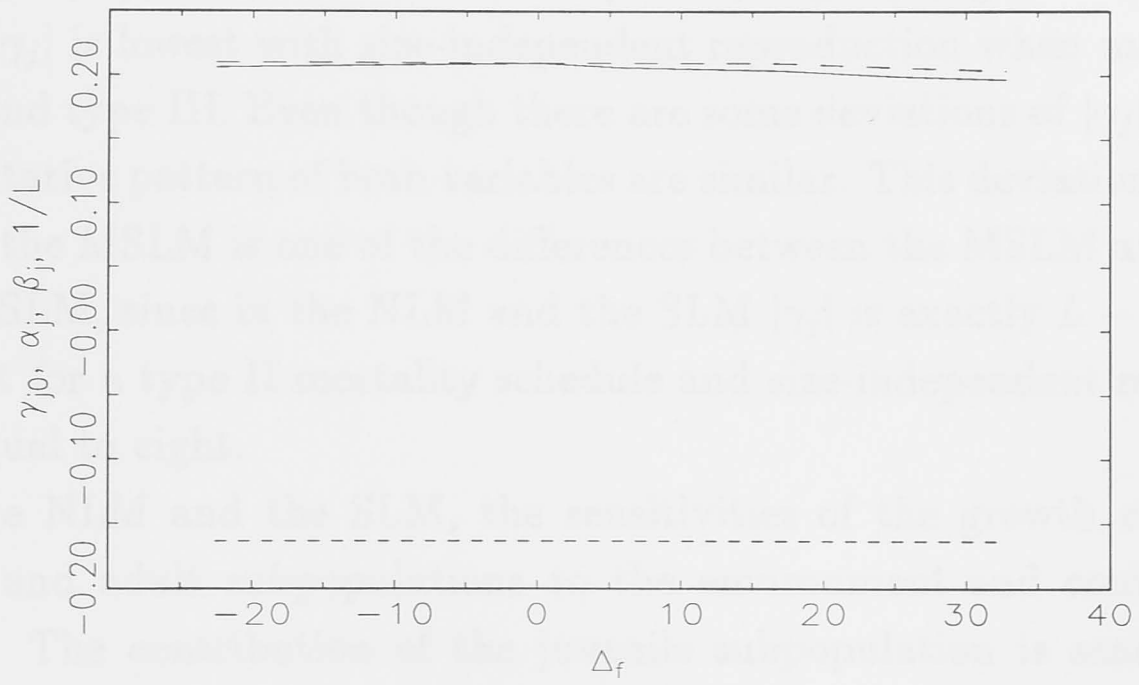

(a)

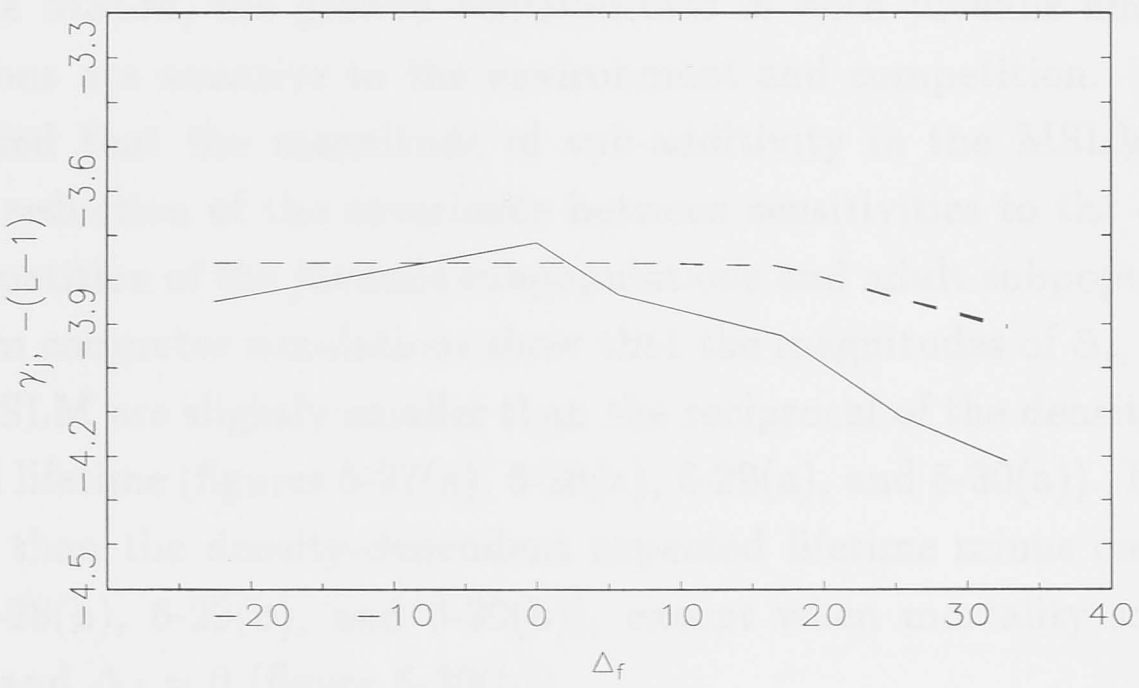

(b)

Figure 6-30: The mean of sub-additivity in terms of original parameters γ_{jo} (dashes), the sensitivity of growth rate to E_j ($\bar{\alpha}_j$) and C ($\bar{\beta}_j$) (solid lines) and the reciprocal of the density-dependent expected lifetime $(1/L)$ (long dashes), with a type III mortality schedule and size-dependent fecundity (a). The mean of sub-additivity in terms of standard parameters γ_j (solid line) and $-(L-1)$ (long dashes) with a type III mortality schedule and size-dependent fecundity (b). All levels of σ^2 coincide.

mortality schedule, $|\gamma_j|$ decreases with larger Δ_f, and deviates from $-(L-1)$ (figure 6-28(b)). With type II and type III mortality schedules, $|\gamma_j|$ increases with larger $|\Delta_f|$, and deviates from $-(L-1)$ slightly (figures 6-29(b) and 6-30(b)). $|\gamma_j|$ is lowest with size-independent reproduction when mortality is of type II and type III. Even though there are some deviations of $|\gamma_j|$ from $L-1$, the qualitative pattern of both variables are similar. This deviation of $|\gamma_j|$ from $L-1$ in the MSLM is one of the differences between the MSLM and the NLM and the SLM, since in the NLM and the SLM $|\gamma_j|$ is exactly $L-1$. However, note that for a type II mortality schedule and size-independent reproduction, $|\gamma_j|$ is equal to eight.

In the NLM and the SLM, the sensitivities of the growth contributions juvenile and adult subpopulations to the environment and competition are distinct. The contribution of the juvenile subpopulation is sensitive to the environment but not sensitive to competition, while the contribution of the adult subpopulation is sensitive to competition but not sensitive to the environment. The magnitudes of $\bar{\alpha}_j$ and $\bar{\beta}_j$ in the NLM and the SLM are equal to the reciprocal of the expected lifetime, and the magnitude of γ_{jo} is equal to $-\bar{\alpha}_j(1-\bar{\alpha}_j)$. The magnitude of $|\gamma_j|$ is equal to $L-1$.

In the MSLM, the growth contributions of both juvenile and adult subpopulations are sensitive to the environment and competition. Therefore, it is expected that the magnitude of sub-additivity in the MSLM is reduced through reduction of the covariance between sensitivities to the environment and competition of the juvenile subpopulations and adult subpopulations. Results from computer simulations show that the magnitudes of $\bar{\alpha}_j$, $\bar{\beta}_j$, and $|\gamma_{jo}|$ in the MSLM are slightly smaller than the reciprocal of the density-dependent expected lifetime (figures 6-27(a), 6-28(a), 6-29(a), and 6-30(a)). However, $|\gamma_j|$ is larger than the density-dependent expected lifetime minus one (figures 6-27(b), 6-28(b), 6-29(b), and 6-30(b)), except when mortality schedule is of type III and $\Delta_f = 0$ (figure 6-30(b)).

The covariance between the original environment parameter and original competition parameter, calculated from simulations, increases with increasing $|\Delta_m|$ (figure 6-31(a)), and decreases consistently with increasing Δ_f (figures 6-32(a), 6-33(a), and 6-34(a)). Compared with the NLM, $\mathrm{cov}[E_j, C_j]$ in the MSLM is lower; for a type II mortality schedule in the MSLM, the covariance is equal to 0.4195, while in the NLM it is equal to the fluctuation in the birth rate (σ^2), i.e., equal to 0.5. This is expected from equation 6.24, where $\mathrm{cov}[E, C]$ decreases with smaller R_0. With increasing Δ_f, $\ln R_0$ decreases (figures 6-19

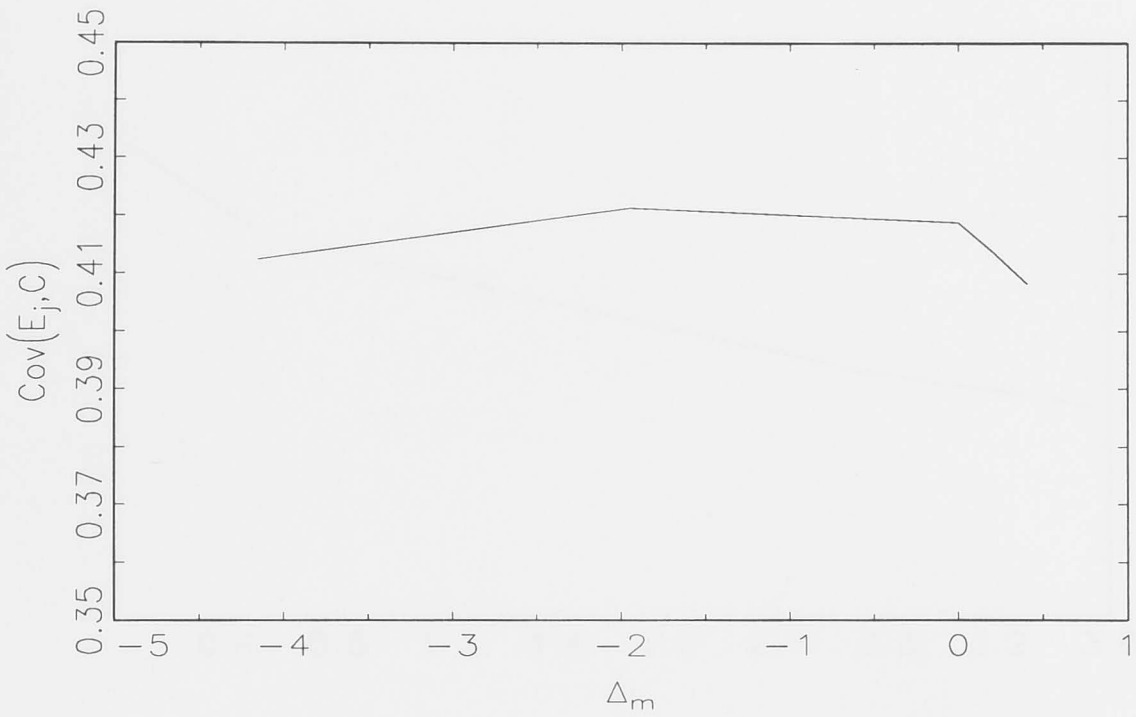

(a)

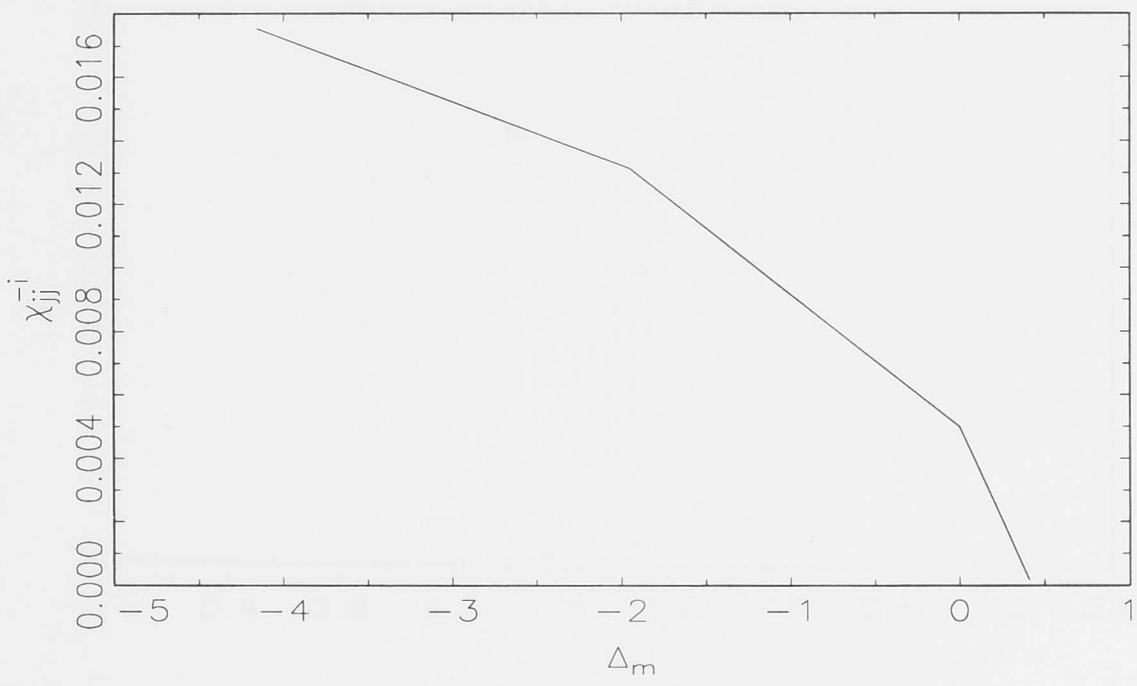

(b)

Figure 6-31: The covariance between the original parameters E_j and C with different mortality schedules and size-independent reproduction with $\sigma^2 = 0.5$ (a). The covariance between the standard parameters $\mathcal{E}_j$ and $\mathcal{C}$ (χ_{jj}^{-i}) with different mortality schedules and size-independent reproduction with $\sigma^2 = 0.5$ (b).

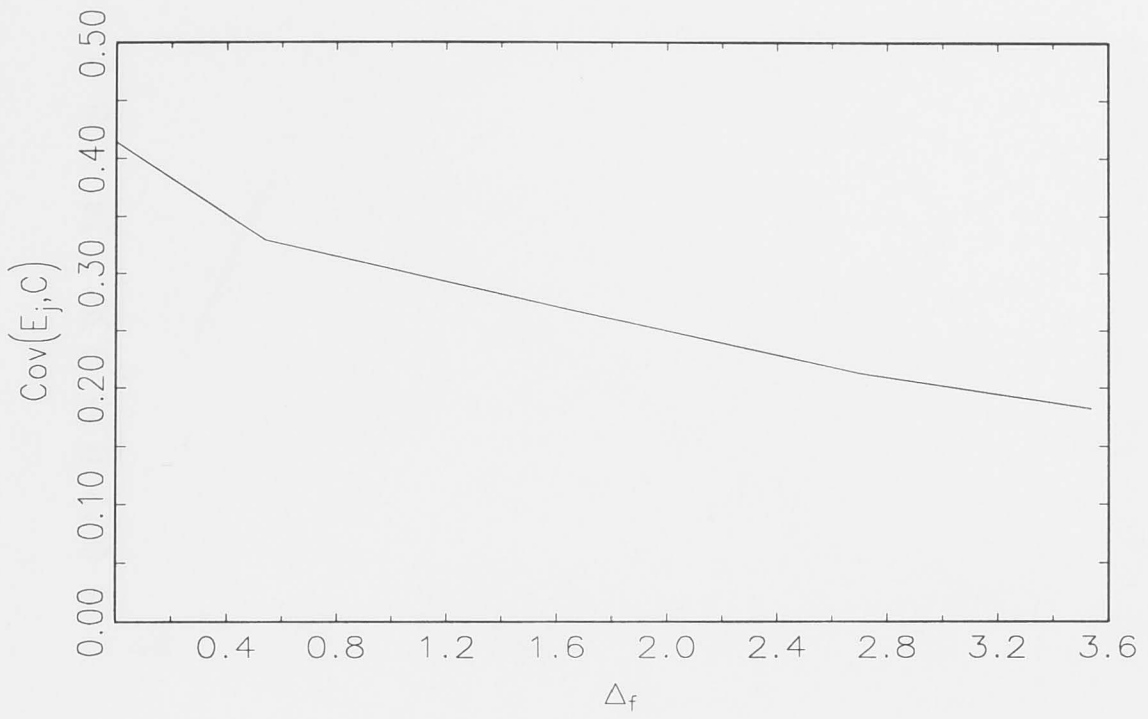

(a)

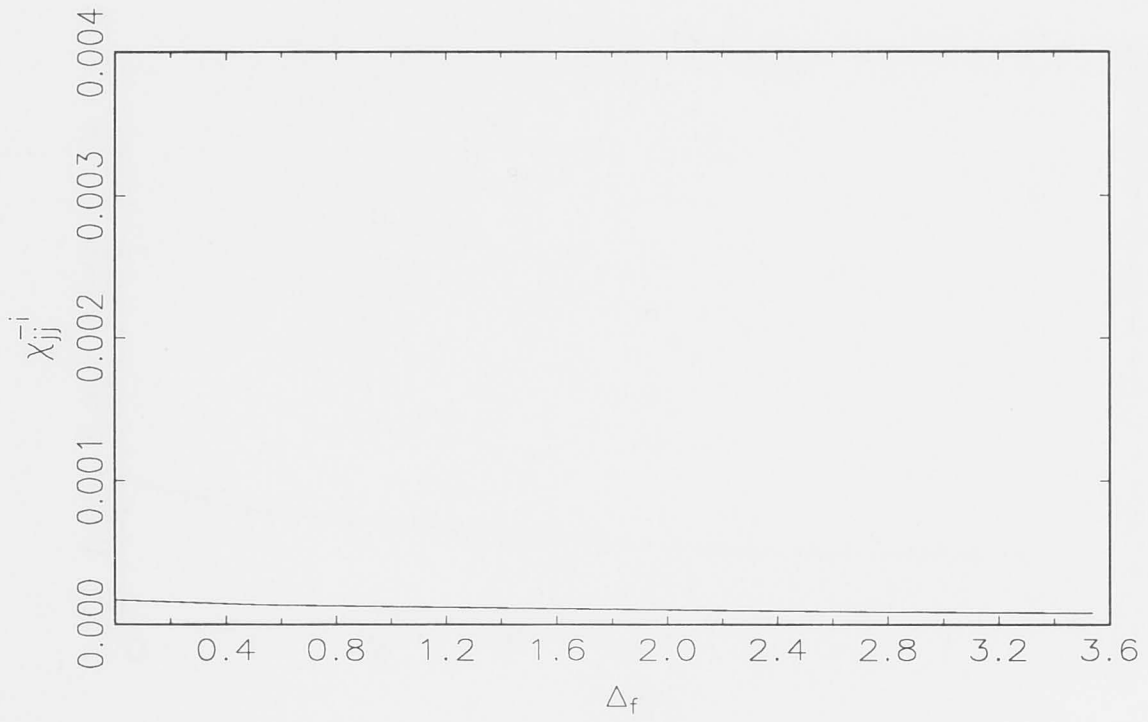

(b)

Figure 6-32: The covariance between the original parameters E_j and C with a type I mortality schedule and size-dependent reproduction with $\sigma^2 = 0.5$ (a). The covariance between the standard parameters $\mathcal{E}_j$ and $\mathcal{C}$ (χ_{jj}^{-i}) with a type I mortality schedule and size-dependent reproduction with $\sigma^2 = 0.5$ (b).

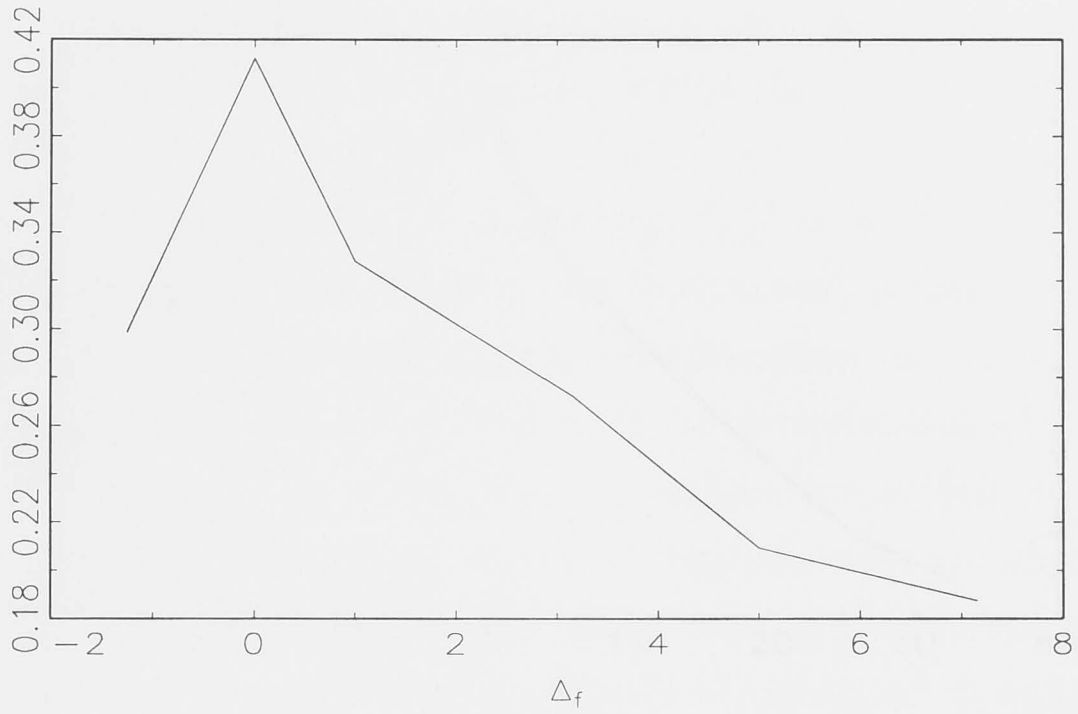

(a)

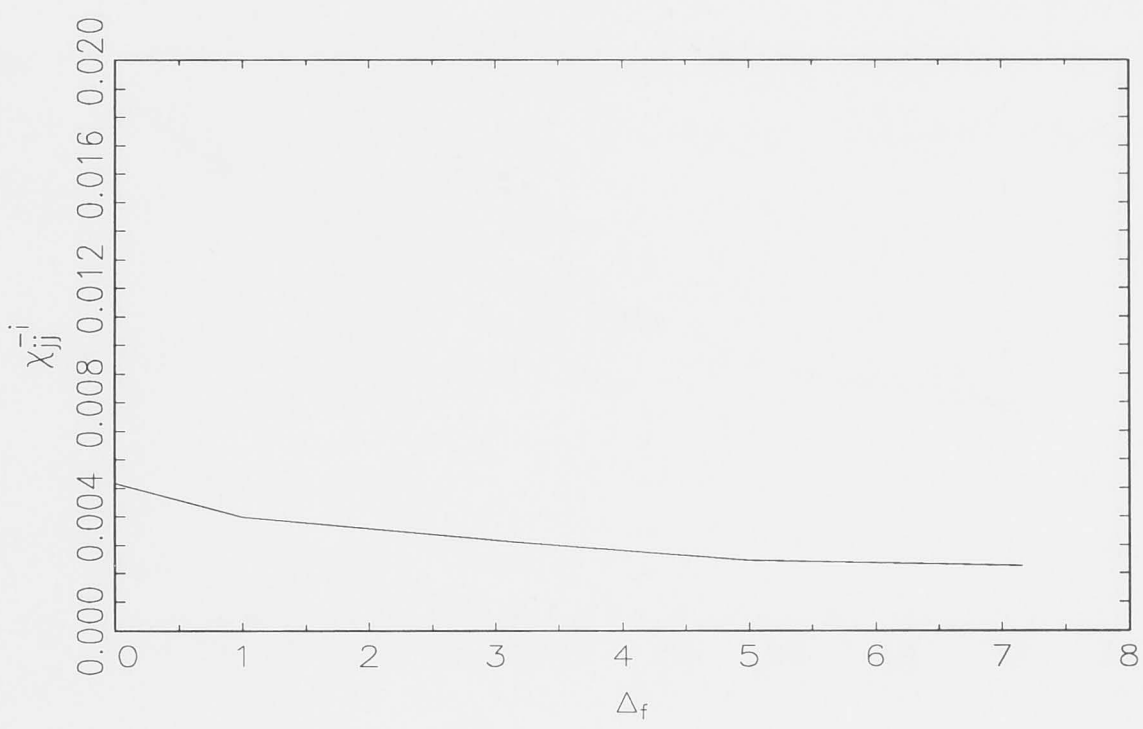

(b)

Figure 6-33: The covariance between the original parameters E_j and C with a type II mortality schedule and size-dependent reproduction with $\sigma^2 = 0.5$ (a). The covariance between the standard parameters $\mathcal{E}_j$ and $\mathcal{C}$ (χ_{jj}^{-i}) with a type II mortality schedule and size-dependent reproduction with $\sigma^2 = 0.5$ (b).

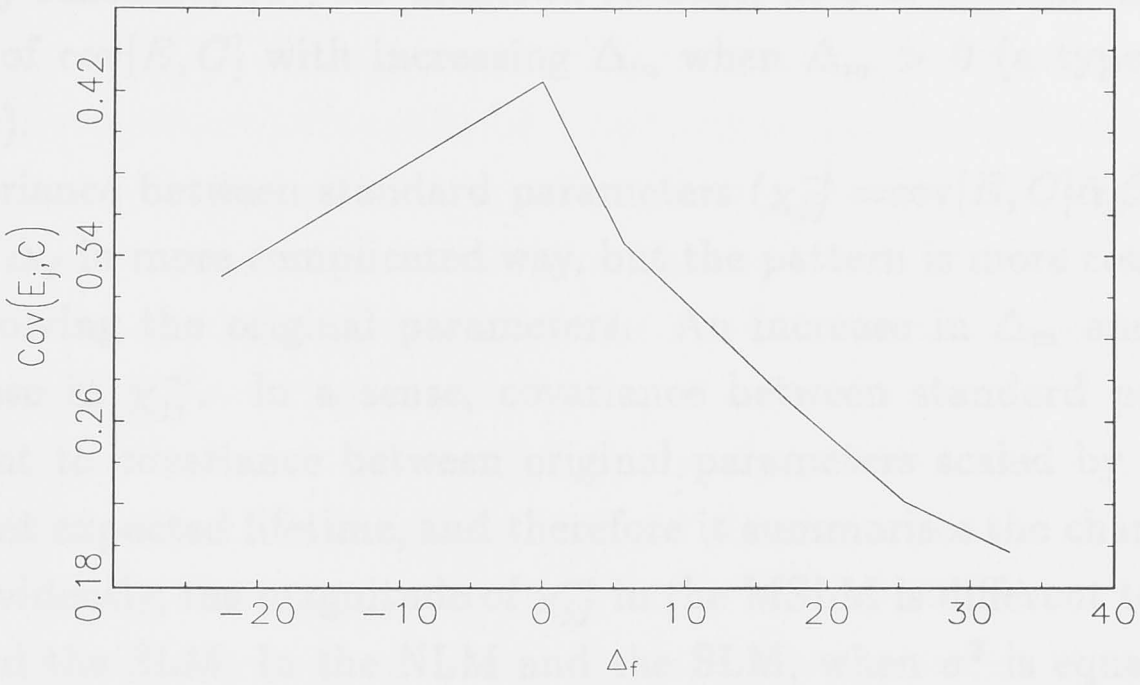

(a)

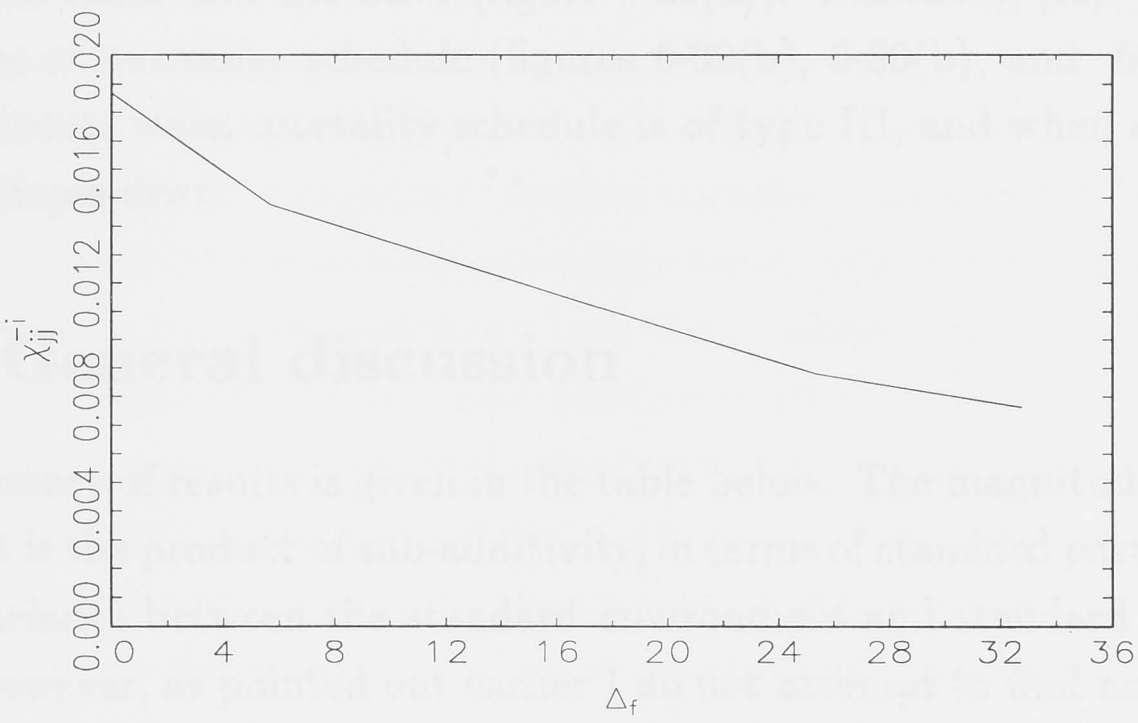

(b)

Figure 6-34: The covariance between the original parameters E_j and C with a type III mortality schedule and size-dependent reproduction with $\sigma^2 = 0.5$ (a). The covariance between the standard parameters $\mathcal{E}_j$ and $\mathcal{C}$ ($\bar{\chi}^i_{jj}$) with a type III mortality schedule and size-dependent reproduction with $\sigma^2 = 0.5$ (b).

and 6-20), which might explain the decrease in the cov$[E, C]$ (figures 6-32(a), 6-33(a), and 6-34(a)). This relationship between R_0 and the cov$[E, C]$ can also explain the pattern of increasing cov$[E, C]$ with increasing Δ_m for a type III mortality schedule, but, for unknown reasons, fails to explain the decreasing pattern of cov$[E, C]$ with increasing Δ_m when $\Delta_m > 0$ (a type I mortality schedule).

Covariance between standard parameters (χ_{jj}^{-i} =cov$[E, C]\bar{\alpha}_j\bar{\beta}_j$) relates to Δ_m and Δ_f in more complicated way, but the pattern is more consistent than that involving the original parameters. An increase in Δ_m and Δ_f causes a decrease in χ_{jj}^{-i}. In a sense, covariance between standard parameters is equivalent to covariance between original parameters scaled by the density-dependent expected lifetime, and therefore it summarises the change in L and ln R_0. Evidently, the magnitude of χ_{jj}^{-i} in the MSLM is different to that in the NLM and the SLM. In the NLM and the SLM, when σ^2 is equal to 0.5 and the expected lifetime is equal to 9, χ_{jj}^{-i} is equal to 0.0062. In the MSLM, with size-independent mortality and size-independent reproduction, χ_{jj}^{-i} is equal to 0.005. With a type III mortality schedule, χ_{jj}^{-i} is larger than it is in the NLM and the SLM, but with other mortality schedules, χ_{jj}^{-i} is smaller than it is in the NLM and the SLM (figure 6-31(a)). Increasing $|\Delta_f|$ reduces χ_{jj}^{-i}, regardless of mortality schedule (figures 6-32(b), 6-33(b), and 6-34(b)). χ_{jj}^{-i} is a maximum when mortality schedule is of type III, and when reproduction is size-independent.

6.6 General discussion

The summary of results is given in the table below. The magnitude of the storage effect is the product of sub-additivity, in terms of standard parameters (γ_j), and covariance between the standard environment and standard competition (χ_{jj}^{-i}). However, as pointed out earlier I do not attempt to find an approximation to the long-term population growth rate of the invader by calculating the storage effect, because of the complexity that arises in the MSLM. However, qualitatively we can expect that the pattern of response of the long-term population growth rate of the invader in the MSLM with changing mortality and fecundity schedules reflects the pattern of response of the storage effect with changing mortality and fecundity schedules. Looking at table 6.6, we see that of the above two variables determining the magnitude of storage effect, it is covariance between the standard environment and standard competition (χ_{jj}^{-i})

that has the same pattern with the long-term population growth rate per unit time $\bar{r}_i$ with changing in mortality and/or fecundity schedules.

Covariance between the standard environment and standard competition is a product of covariance between the original environment and original competition ($\mathrm{cov}[E, C]$), and the sensitivity of the population growth rate to the original environment parameter ($\bar{\alpha}_j$) and the original competition parameter ($\bar{\beta}_j$). Changes in Δ_m and/or Δ_f affect the magnitude of $\mathrm{cov}[E, C]$ through changes in the mean of the competition parameter, or approximately, through changes in the ln of the density-dependent net reproductive rate. With larger R_0, the $\mathrm{cov}[E, C]$ becomes closer to the variance in the birth rates (σ^2). The effects of Δ_m and Δ_f on χ_{jj}^{-i} through $\bar{\alpha}_j$ and $\bar{\beta}_j$ are most likely due to changes in the density-dependent lifetime. $\bar{\alpha}_j$ and $\bar{\beta}_j$ are found to be similar to the reciprocal of the density-dependent expected lifetime ($1/L$).

Changes in the average probability of capturing a unit of space and moving up one size class (p) in the MSLM, due to changes in the mortality and fecundity schedules and the nature of competition, may be used to explain changes in the density-dependent expected lifetime and the density-dependent net reproductive rate. This average probability of growth in size is the mean over time of the ratio of total available spaces to total required spaces. When reproduction is size-independent and mortality is of type I (low early mortality rate and high late mortality rate), growing faster in size (larger p) reduces the density-dependent expected lifetime, because individuals do not spend as long in the smaller size classes where mortality rate is low. Therefore, they experience the high late mortality rate for a longer period. Similarly with a type III mortality schedule and smaller p, individuals tend to remain in smaller size classes (i.e., where the mortality rate is high), and therefore, the density-dependent expected lifetime is reduced. The density-dependent net reproductive rate is largest with the smallest p, which is reached when reproduction is size-independent, or when mortality is of type III. When p is large and individual growth in size is fast an individual does not remain in any size class for long. Therefore, in cases of structured fecundity, an individual passes quickly through the classes with maximum fecundity, leading to a reduced net reproductive rate.

Now let us compare the MSLM with the SLM. I use the same ranges of parameters of the difference between the mean of birth rates of the invader and the resident (μ), variance in the birth rate of the invader and the resident (σ^2) and age/size-independent mortality rate ($\tilde{\delta}$), in studying both models. The

magnitude of the long-term population growth rate of the invader in the two models are similar (mostly ranging from -0.04 to 0.04). However, the patterns of the changes in $\bar{r}_i$ with Δ_m and Δ_f are different. In the SLM, $|\bar{r}_i|$ increases with Δ_m and decreases with Δ_f, such that a type I mortality schedule and an early peak reproduction consistently show a larger $|\bar{r}_i|$. This is caused by: (i) the smaller average death rate over age classes of the invader ($\hat{\delta}_i$) than $\tilde{\delta}$ (the average death rate experienced by as stationary population, e.g., the resident) with a type I mortality schedule, and (ii) the larger average modulation of reproduction over age classes of the invader ($\hat{k}_i$) than $\tilde{k} = 1$ (i.e., the larger net reproductive rate of the invader than $\mathrm{E}[b]/\tilde{\delta}$) with an early peak reproduction, when $\bar{r}_i > 0$.

The deviation in the magnitude of $\bar{r}_i$ in the SLM from the NLM results entirely from the above phenomena, i.e., deviation in the population average death rate and the net reproductive rate from the values found in a stationary population, due to nonzero $\bar{r}_i$, and to a lesser extent, fluctuations in age structure of the invader. Covariance between the original environment parameter and the original competition parameter is not affected by Δ_m and Δ_f. Therefore, the SLM can be looked at as a case of asymmetrical age-independent death rate between the invader and the resident in the NLM, with the complication that the invader's death rate is a function of its long-term growth rate.

In the MSLM, $|\bar{r}_i|$ decreases with Δ_m and $|\Delta_f|$, not because of the nonzero population growth rate, as in the SLM, but mainly due to the existence of the density-dependent probability of growth in size. The expected lifetime and the net reproductive rate also become density-dependent. In addition, covariance between the original environment parameter and the original competition parameter decreases in the MSLM, because of the density-dependent growth in size, and decreases further with increasing Δ_m and Δ_f.

The coexistence, in terms of the magnitude of σ^2 required for the invader to have non-negative $\bar{r}_i$, in the SLM changes little with Δ_m and does not change with Δ_f. This is not surprising, because when $\bar{r}_i$ is equal to zero, it is expected that the average death rate over age classes and the average modulation of reproduction over age classes of the invader are equal to $\tilde{\delta}$ and 1, respectively. However, the fluctuation in the age distribution of the invader over time, presumably, causes a slight change in coexistence criterion in the SLM with changing mortality schedules.

In the MSLM, the expected lifetime and net reproductive rate are not

fixed independent of density as they are in the SLM. The changes seen in the long-term invader growth rate and the coexistence region with fecundity and mortality schedules arise predominantly from their interaction with the probability of growth in size.

This study improves our understanding of how modifying a life history characteristic changes the outcome in a community ecology model. More commonly, people study life history characteristics from the point of view of fitness in a single-species population. To understand underlying mechanisms is an important step towards studying more complex models. The general framework of Chesson (Chesson 1994) is shown to be a useful tool to gain insights about the MSLM, even in the absence of a quantitative approximation to $\bar{r}_i$.

For the next step, it will be important to generalize the study of the MSLM into an arbitrary number of species. Suggestions for further study of the MSLM are investigating the model with: (i) asymmetric mortality and fecundity schedules between the invader and the resident, (ii) different competition functions such as one-sided competition, convex and concave function, and (iii) age/size structured competition functions In combining points (ii) and (iii), in particular, a study of the MSLM with size-dependent competitiveness, such that c_x is proportional to age or size (x), while fecundity is also proportional to age or size (x), will be a more realistic model for plants.

	Notation	$\Delta_m \uparrow$ $\Delta_f = 0$	$\Delta_m < 0$ $\lvert\Delta_f\rvert \uparrow$	$\Delta_m = 0$ $\lvert\Delta_f\rvert \uparrow$	$\Delta_m > 0$ $\Delta_f \uparrow$
Density-dependent expected lifetime	L	$\uparrow$	$\uparrow$	$-$	$\downarrow$
Density-dependent growth in size	p	$\downarrow$	$\uparrow$	$\uparrow$	$\uparrow$
Density-dependent net reproductive rate	R_0	$\uparrow$	$\downarrow$	$\downarrow$	$\downarrow$
Mean of competition	$\mathrm{E}[C]$	$\uparrow$	$\downarrow$	$\downarrow$	$\downarrow$
Sensitivity to environment (E), competition (C)	$\bar{\alpha}_j$,$\bar{\beta}_j$	$\downarrow$	$\downarrow$	$\downarrow$	$\uparrow$
Sub-additivity (original)	$\lvert\gamma_{jo}\rvert$	$\downarrow$	$-$	$-$	$\uparrow$
Sub-additivity (standardised)	$\lvert\gamma_j\rvert$	$\uparrow$	$\uparrow$	$\uparrow$	$\downarrow$
Covariance between environment and competition (original)	$\mathrm{cov}[E_j,C]$	$\uparrow$	$\downarrow$	$\downarrow$	$\downarrow$
Covariance between environment and competition (standardised)	χ_{jj}^{-i}	$\downarrow$	$\downarrow$	$\downarrow$	$\downarrow$
Population growth rate of the invader per unit time	$\lvert\bar{r}_i\rvert$	$\downarrow$	$\downarrow$	$\downarrow$	$\downarrow$
Population growth rate of the invader per generation time	$\lvert\bar{r}_i\rvert L$	$\uparrow$	$\downarrow$	$\downarrow$	$\downarrow$
Coexistence criterion	σ^2 for $\bar{r}_i = 0$	$-$	$\uparrow$	$\uparrow$	$\uparrow$

Table 6.1: Summary of pattern of some parameters of the MSLM with increasing Δ_m and Δ_f ($\downarrow$= decrease, $\uparrow$= increase, and $-$ = no effect).

Chapter 7

Conclusion

The lottery model without age or size structure (the NLM) has been known for more than a decade (Chesson and Warner 1981). The NLM is a multispecies competition model in which environmental fluctuations generate new temporal niche axes resulting in species coexistence. Competition occurs during the recruitment process (i.e., in the juvenile stage) and environmental fluctuations are manifested in terms of temporal fluctuations in birth rates. Although I often speak as if fluctuations arise from the birth rate alone, the parameter $b(t)$ really takes account of early juvenile mortality (before juveniles start competing) and any differences in the competitive abilities of individuals of different species. Early juvenile mortality and competitive ability could fluctuate over time and lead to effects identical to fluctuations in birth rates. Fluctuations in early juvenile mortality are in fact very important in nature and may be important in the way the storage effect operates in natural systems.

We can look at populations in the NLM as consisting of two classes: juvenile and adults, although the state variable in the model is the adult population at the end of each period of recruitment. Each class responds differently to environment and competition. Juveniles are sensitive to competition, while adults are not. Whether adults or juveniles or both are sensitive to the environment in the model depends on the interpretation of $b(t)$ as discussed above. For example, if $b(t)$ is strictly the birth rate, then it means adult sensitivity to the environment, but if the fluctuations in $b(t)$ are entirely due to fluctuations in early juvenile mortality then juveniles are alone sensitive to the environment. This ambiguity is resolved when we think of dividing the growth rate of the population into different components. The two important components in the lottery model are recruitment and adult survival. No matter how $b(t)$ is interpreted, adult survival is insensitive to competition, and insensitive to the

environment, while recruitment, which involves birth into the juvenile phase, survival of juveniles and competition among juveniles, is sensitive to both environment and competition. This heterogeneity in responses to environment and competition results in sub-additivity.

The storage effect occurs when subadditivity is combined with asynchronous responses of species to the environment, and covariance between environment and competition. Covariance between environment and competition occurs very simply in the lottery model. The favourability of the environmental conditions determines how many juveniles there are competiting with each other, or the competitiveness of these juveniles, and hence it determines how strong competition is. In the NLM, even when a species has a lower mean birth rate than other species, this species can coexist with other species in the community if the magnitude of the storage effect is large enough to cancel out its disadvantage.

The importance of the storage effect as a mechanism of species coexistence, particularly in the lottery model, motivates this study of structured versions of the lottery model. Since different levels of synchrony of species response to the environment affects the storage effect equivalently to that of different levels of environmental variance, I do not focus on the effects of synchrony. With independent responses to the environment, the storage effect can be expressed as a product of sub-additivity and the covariance between the environment and competition.

My study is restricted to two-species models. According to the invasibility criterion for coexistence, the two species coexist when they are both able to increase from low density in the presence of the other species. In this study, one species was always superior to the other, and clearly able to invade a system consisting of the other species. Thus, I was able to focus on invasion by an inferior species, which had a lower mean birth rate than the other species, and was called the invader, while the other species was called the resident. In this situation, I was able to conclude that the two species could coexist when the long-term population growth rate of the invader was positive. To understand the effects of the three ingredients of the storage effect and changes in these ingredients in different models, quadratic approximation to the per capita population growth rate is useful. This technique yields approximations to the long-term per capita population growth rate of the invader, and allows quantification of the storage effect in terms of its ingredients (Chesson 1994). In Chapter 2, simulations verified the accuracy of this approximation

for the two-species NLM. An important aspect of the storage effect in the NLM, for comparison with the more complex models, is that the magnitude of sub-additivity depends on the expected lifetime. The longer the expected lifetime, the larger the storage effect is. The covariance between environment and competition in the NLM is simply the variance in the birth rate, which was assumed the same for both invader and resident. Therefore, the longer the expected lifetime, and the greater the birth rate fluctuations, the easier it is for species to coexist.

With the need to consider the effects of structured vital rates on the lottery model, I set out to investigate ways of summarising the effects of age-structured vital rates on the population growth rate in a density-independent setting. This led to the development of the Δ-measures. Although the Δ-measures work best for predicting the effects of demography at low rates of population growth, I do not consider that as a restriction in the present study because the lottery model is of most interest for long-lived species, which normally have low long-term population growth rates. Also, for the study of species coexistence, the region of zero growth rate of the invader is of particular importance.

Chapter 3 described the development of the Δ-measures in summarising and quantifying the mortality and fecundity schedules in demographic models with constant vital rates and with fluctuating vital rates. The Δ-measures were shown to be useful for: (i) summarising the simulation results for the population growth rate with changing mortality and fecundity schedules and (ii) providing a means to approximate the population growth rate in general demographic models with constant and variable vital rates. The results of my study of the population growth rates in general demographic models were consistent with widely-known results, i.e., early low mortality rates (a type I mortality schedule) and early high birth rates (early peak reproduction) show a higher population growth rate than early high mortality rates (type III mortality schedules) and early low birth rates (delayed peak reproduction) when populations are increasing. The formula approximating the population growth rate shows that the effect of mortality and fecundity schedules on the population growth rate is weakened when the expected lifetime is longer.

I modified the NLM to have age structure by introducing age-dependent mortality and fecundity. In the two-species age-structured lottery model (the SLM), a resident competes just with itself, and it is negligibly affected by a low-density invader. Therefore, the resident converges on the stationary age distribution determined by its mortality rate. The population dynamics of the

invader could then be represented in terms of a linear stochastic model. Hence work on stochastic projection matrices (Tuljapurkar 1982) applies directly as presented in Chapter 5. The long-term population growth rate of the invader in the two-species SLM is approximated well by Tuljapurkar's formula. The pattern of changes in the population growth rates with changing mortality and fecundity schedules in this two-species competition model agrees with that in single-species general demographic models.

The mortality and fecundity schedules in the SLM are generated such that both the expected lifetime and net reproductive rate are fixed. This constraint is natural, since biologists most commonly deal with those two characteristics when age structures are ignored. The long-term population growth rate of the invader in the SLM is compared with that in the NLM (Chapter 4). Differences in the storage effect are measured through the quadratic approximation technique. The covariance between the environment and competition in the SLM remains equal to the variance in birth rate as it is in the NLM. The magnitude of sub-additivity of the resident is also the same as that in the NLM since the resident is always at its stationary distribution where the dynamics of the competition parameter, and its relationship to the environmental parameter, are independent of age-structure in the adult population. However, the long-term population growth rate of the invader deviates from that in the NLM. This deviation results from the interaction of nonstationarity of the invader population and structured mortality and fecundity. A consequence of this interaction is a deviation of the the average mortality rate and birth rate in the population from the values applying in a stationary population. Therefore, the SLM can be looked upon as similar to an asymmetrical case of the NLM in terms of the mortality rates between the two species. However, unlike the NLM, in the SLM the behaviour of the population- level mortality rates is frequency dependent. Whichever species is the invader receives a perturbation of its population-level mortality rate away from the stationary value in a direction predicted by its mortality schedule and long-term growth rate.

As in general demographic models, the Δ-measure was found to be useful in both summarising the results and approximating the long-term population growth rate of the invader. The approximation technique using the Δ-measure in the SLM also showed that with longer expected lifetimes, the mortality and fecundity schedules have smaller effects on the long-term population growth rate of the invader.

In Chapter 6, I studied the lottery model with competition occurring in

adults as well as in juveniles. Structure in the populations is introduced as size-dependent mortality and fecundity. In this structured lottery model with multiple competitive classes (the MSLM), an individual can move up to another size class with a probability that depends on population density. This extension of the structured lottery model leads us one step closer to a realism. I generated mortality and fecundity schedules constrained using the same techniques as in the previous chapters, except that variation in rates refers to size not age. With these techniques, the expected lifetime and net reproductive rate are only fixed when the probability of advancing to the next size class in one unit of time is one. However, in the MSLM, the probability of growth in size is generally less than one and is density dependent. As a consequence, the expected lifetime and net reproductive rate are density dependent, and structured mortality and fecundity bring major changes in the density-dependent expected lifetime and the density-dependent net reproductive rate of both the resident and the invader.

The magnitude of sub-additivity in the MSLM is similar to that of the NLM and the SLM, if we take account of the density-dependent expected lifetime. However, the strength of the storage effect changes from that of the NLM and the SLM. These changes are mainly due to a reduction in the covariance between environment and competition with the changes in the density-dependent expected lifetime and the density-dependent net reproductive rate. The pattern of changes of the long-term population growth rate of the invader with changing mortality schedules in the MLSM is opposite to that in the NLM and SLM. In the MSLM, a type I mortality schedule leads to a lower long-term invader population growth rate. The long-term population growth rate of the invader is reduced by deviations from unstructured fecundity. Although in the MSLM I did not attempt to approximate the long-term population growth rate of the invader using the Δ-measures, the Δ-measures remained useful tools for understanding the pattern of the changes in the density-dependent expected lifetime, the density-dependent net reproductive rate, the covariance between the environment and competition, and the magnitude of sub-additivity.

The results from these various analyses demonstrate the robustness of the storage effect as a coexistence mechanism under the extension of the NLM to age structured models (the SLM) and the spreading of density dependence in size structured models (the MSLM). The two special ingredients of the storage effect, positive covariance between environment and competition and sub-additivity only change quantitatively in the MSLM from those in the NLM

and the SLM.

I conclude that the changes in the storage effect, and consequently in species coexistence, in the different models studied here depend on the changes in the life history characteristics (i.e., the expected lifetime and the net reproductive rate) with model modification. In my study, the expected lifetime and the net reproductive rate are affected significantly under the introduction of the density-dependent probability of growth in size. Therefore, whether or not a prediction or behaviour of a model changes substantially, with the addition of age or size structure and with the modification of the stages in which competition takes place, depends on whether or not the important life-history characteristics are affected substantially. Different model formulations that lead to major changes in the density-dependent probability of growth in size would be fruitful for further study.

I believe that in general the changes in the life-history characteristics, such as the expected lifetime and the net reproductive rate, are the first factors to look at when one modifies a model. However, in a model where competition is not defined at the population level but instead is defined at the subpopulation level (e.g., Kohyama 1993), the calculation of the expected lifetime and the net reproductive rate can be more complicated. Nevertheless, in my opinion, it is worthwhile putting in the effort to make these calculations, since they might provide critical clues to model behaviour.

The study of different versions of lottery model has been enlightened by the introduction of the Δ-measures. The scope of the application of the Δ-measures might be broadened to the study of life-history evolution, demography and other age- or size-structured ecological models, if the region of interest is confined to small rates of population growth.

Bibliography

Abrams, P. (1984). Variability in resource consumption rates and the coexistence of competing species. *Theoretical Population Biology 25*, 106–124.

Aptech Systems, I. (1992). *GAUSS volume I and II*. Aptech Systems, Inc.

Armstrong, R. A. and R. McGehee (1980). Competitive exclusion. *American Naturalist 115*(2), 151–170.

Bengtsson, J., T. Fagerstrom, and H. Rydin (1994). Competition and coexistence in plant communities. *TREE 9*(7), 246–250.

Benton, T. G. and A. Grant (1996). How to keep fit in the real world: elasticity analyses and selection pressures on life histories in a variable environment. *American Naturalist 147*(1), 115–139.

Bernadelli, H. (1941). Population waves. *Journal of the Burma Research Society 31*, 1–18.

Botsford, L. (1997). Dynamics of populations with density-dependent recruitment and age structure. In S. Tuljapurkar and H. Caswell (Eds.), *Structured-population Models in Marine, Terrestrial, and Freshwater Systems*, pp. 371–408. Chapman and Hall.

Bulmer, M. G. (1985). Selection for iteroparity in a variable environment. *American Naturalist 126*(1), 63–71.

Caswell, H. (1978). A general formula for the sensitivity of population growth rate to changes in life history parameters. *Theoretical Population Biology 14*, 215–230.

Caswell, H. (1982). Life history theory and the equilibrium status of populations. *American Naturalist 120*(3), 317–339.

Caswell, H. (1989). *Matrix Population Models: Construction, Analysis, and Interpretation*. Sunderland, Massachusetts: Sinauer Associates, Inc. Publishers.

Caswell, H. (1997). Matrix methods for population analysis. In S. Tuljapurkar and H. Caswell (Eds.), *Structured-population Models in Marine, Terrestrial, and Freshwater Systems*, pp. 19–58. Chapman and Hall.

Caswell, H., R. Nisbet, A. de Roos, and S. Tuljapurkar (1997). Structured-population models: many methods, a few basic concepts. In S. Tuljapurkar and H. Caswell (Eds.), *Structured-population Models in Marine, Terrestrial, and Freshwater Systems*, pp. 3–18. Chapman and Hall.

Charlesworth, B. (1994). *Evolution in age-structured populations* (2 ed.). Cambridge University Press.

Charnov, E. (1993). *Life History Invariants: Some Explorations of Symmetry in Evolutionary Ecology*. New York: Oxford Unifersity Press Inc.

Chesson, P. (1986). Environmental variation and the coexistence of species. In J. Diamond and T. Case (Eds.), *Community Ecology*, pp. 240–256. Harper and Row.

Chesson, P. (1994). Multispecies competition in variable environments. *Theoretical Population Biology 45*(3), 227–276.

Chesson, P. and N. Huntly (1988). Community consequences of life-history traits in avariable environments. *Ann. Zool. Fennici 25*, 5–16.

Chesson, P. and N. Huntly (1989). Short-term instabilities and long-term community dynamics. *TREE 4*(10), 293–298.

Chesson, P. and N. Huntly (1997). The roles of harsh and fluctuations conditions in the dynamics of ecological communities. *American Naturalist 150*, 519–553.

Chesson, P. L. (1982). The stabilizing effect of a random environment. *Journal of Mathematical Biology 15*, 1–36.

Chesson, P. L. (1989). A general model of the role of environmental variability in communities of competing species. *Lectures on Mathematics in the Life Sciences 20*, 97–123.

Chesson, P. L. (1990). Geometry, heterogeneity and competition in variable environments. *Phil. Trans. R. Soc. Lond. B 330*, 165–173.

Chesson, P. L. and S. Ellner (1989). Invasibility and stochastic boundedness in monotonic competition models. *J. Math. Biol. 27*, 117–138.

Chesson, P. L. and R. R. Warner (1981). Environmental variability promotes coexistence in lottery competitive systems. *American Naturalist 117*(6),

923–943.

Cohen, J. E. (1976). Contractive inhomogeneous products of non-negative matrices. *Math. Proc. Camb. Phil. Soc 86*, 351–365.

Cohen, J. E. (1977). Ergodicity of age-structure in populations with markovian vital rates. ii. general states. *Adv. Appl. Prob. 9*, 18–37.

Cohen, J. E. (1979). Long-run growth rates of discrete multiplicative processes in markovian environments. *Journal of Mathematical Analysis and Applications 69*, 243–251.

Cole, L. (1954). The population consequences of life history phenomena. *Quarterly Review of Biology 29*(2), 103–137.

Comins, H. and I. Noble (1985). Dispersal, variability, and transient niches: species coexistence in a uniformly variable environment. *American Naturalist 126*(5), 706–723.

de Jong, G. (1994). The fitness of fitness concepts and the description of natural selection. *The Quarterly Review of Biology 69*(1), 3–29.

DeAngelis, D. L., L. J. Svoboda, S. W. Christensen, and D. S. Vaughan (1980). Stability and return times of leslie matrices with density-dependent survival: application to fish populations. *Ecological Modelling 8*, 149–163.

Ellner, S. (1984). Asymptotic behavior of some stochastic difference equation population models. *J. Math. Biology 19*, 169–200.

Ellner, S. (1989). Convergence to stationary distributions in two-species stochastic competition models. *J. Math. Biol. 27*, 451–462.

Ellner, S. and N. G. Hairston (1994). Role of overlapping generations in maintaining genetic variation in a fluctuating environment. *American Naturalist 143*(3), 403–417.

Fisher, R. (1930). *The Genetical Theory of Natural Selection.* Oxford: Clarendon Press.

Goldberg, D. (1996). Competitive ability: definitions, contigency and correlated traits. *Phil. Trans. R. Soc. Lond. B 351*, 1377–1385.

Gradshtein, I. S. and I. M. Ryzhik (1980). *Table of Integrals, Series, and Products.* London: Academic Prrss, Inc.

Hatfield, J. and P. Chesson (1997). Multispecies lottery competition: a diffusion analysis. In S. Tuljapurkar and H. Caswell (Eds.), *Structured-*

population Models in Marine, Terrestrial, and Freshwater Systems, pp. 615–622. Chapman and Hall.

Hatfield, J. S. and P. L. Chesson (1989). Diffusion analysis and stationary distribution of the two-species lottery competition models. *Theoretical Population Biology 36*, 251–266.

Hatfield, J. S., W. A. Link, and D. K. Dawson (1996). Coexistence and community structure of tropical trees in a hawaiian montane rain forest. *Biotropica 28(4b)*, 746–758.

Henri, L. and R. M. Cowling (1994). Lottery coexistence models extended to plants with disjoint generations. *Journal of Vegetation Science 5*, 161–168.

Heyde, C. C. (1985). An asymptotic representation for products of random matrices. *Stochastic Processes and their Applications 20*, 307–314.

Huston, M., D. DeAngelis, and W. Post (1988). New computer models unify ecological theory. *BioScience 38*, 682–691.

Hutchinson, G. E. (1961). The paradox of the plankton. *American Naturalist 45*, 137–145.

Iwasa, Y., T. Kubo, and K. Sato (1995). Maintenance of forest species diversity and latitudinal gradient. *Vegetatio 121*, 127–234.

Iwasa, Y., K. Sato, M. Kakita, and T. Kubo (1993). Modelling biodiversity: latitudinal gradient of forest species diversity. In E. D. Schulze and H. A. Mooney (Eds.), *Biodiversity and Ecosystem Function*, Volume 99 of *Ecological Studies*, pp. 433–451. Springer Verlag.

Judson, O. P. (1994). The rise of the individual-based model in ecology. *TREE 9*(1), 9–14.

Kisdi, E. and G. Meszena (1993). Density dependent life history evolution. In J. Yoshimura and C. W. Clark (Eds.), *Adaptations in Stochastic Environments*, Volume 98 of *Lecture Notes in Biomathematics*, pp. 26–60. Heidelberg: Springer-Verlag.

Kohyama (1991). Simulating stationary size distribution of trees in rain forests. *Annals of Botany 68*, 173–180.

Kohyama, T. (1992). Density-size dynamics of trees simulated by a one-sided competition multi-species model of rain forest stands. *Annals of Botany 70*, 451–460.

Kohyama, T. (1993). Size-structured tree populations in gap-dynamics forest - theforest architecture hypothesis for the stable coexistence of species. *Journal of Ecology 81*, 131–143.

Kohyama, T. and T. Hara (1989). Frequency distribution of tree growth rate in natural forest stands. *Annals of Botany 64*, 47–57.

Kohyama, T., T. Hara, and Y. Tadaki (1990). Patterns of trunk diameter, tree height and crown depth in crowded abies stands. *Annals of Botany 65*, 567–574.

Kozlowski, J. (1993). Measuring fitness in life-history studies. *TREE 8*(3), 84–85.

Kubo, T. and Y. Iwasa (1996). Phenological pattern of tree regeneration on a model for forest species diversity. *Theoretical Population Biology 49*, 90–117.

Lamont, B. B. and E. Witkowski (1995). A test for lottery recruitment among four banksia species based on their demography and biological attributes. *Oecologia 101*, 299–308.

Lande, R. (1982). Elements of a quantitative genetic model of life history evolution. In H. Dingle and J. Hegmann (Eds.), *Evolution and Genetics of LIfe Histories*, pp. 21–29. New York: Springer-Verlag.

Leslie, P. H. (1945). On the use of matrices in certain population mathematics. *Biometrika 33*, 183–212.

Leslie, P. H. (1948). Some further notes on the use of matrices in population mathematics. *Biometrika 35*, 213–245.

Levin, S., B. Grenfell, A. Hastings, and A. Perelson (1997). Mathematical and computational challenges in population biology and ecosystems science. *Science 275*, 334–344.

Levin, S. A. and C. P. Goodyear (1980). Analysis of an age-structured fishery model. *J. Math. Biology 9*, 245–274.

Lewontin, R. C. (1965). Selection for colonizing ability. In H. G. Baker and G. L. Stebbins (Eds.), *The Genetics of Colonizing Species*, pp. 77–94. New York: Academic Press.

Lopez, A. (1961). *Problems in Stable Population Theory*. Princeton, N.J.: Princeton University Press.

MacArthur, R. (1969). Species packing, and what interspecies competition minimizes. *Proc. Natl. Acad. Sci. USA 64*, 1369–1371.

MacArthur, R. and R. Levins (1967). The limiting similarity, convergence, and divergence of coexisting species. *American Naturalist 101*, 377–385.

MacArthur, R. H. and E. O. Wilson (1967). *The Theory of Island Biogeography*. New Jersey: Princeton University.

May, R. and R. MacArthur (1972). Niche overlap as a function of environmental variability. *Proc. Nat. Acad. Sci. USA 69*(5), 1109–1113.

Metz, J. A. J., R. M. Nisbet, and S. A. H. Geritz (1992). How should we define 'fitness' for general ecological scenarios? *TREE 7*(6), 198–202.

Orzack, S. (1997). Life-history evolution and extinction. In S. Tuljapurkar and H. Caswell (Eds.), *Structured-population Models in Marine, Terrestrial, and Freshwater Systems*, pp. 273–302. Chapman and Hall.

Orzack, S. H. (1993). Life history evolution and population dynamics in variable environments: some insights from stochastic demography. In *Lecture Notes in Biomathematics*, Volume 98, pp. 63–104. Heidelberg: Springer-Verlag.

Orzack, S. H. and S. Tuljapurkar (1989). Population dynamics in variable environments. vii. the demography and evolution of iteroparity. *American Naturalist 133*(6), 901–923.

Pacala, S. W. and J. A. Silander Jr. (1985). Neighborhood models of plant population dynamics. 1. single-species models of annuals. *American Naturalist 125*(3), 385–411.

Persson, L. and L. Johansson (1992). On competition and temporal variations in temperate freshwater fish populations. *Netherlands Journal of Zoology 42*(2-3), 304–322.

Pinder, J., J. Wiener, and M. Smith (1978). The weibull distribution: a new method of summarizing survivorship data. *Ecology 59*, 175–179.

Roff, D. A. (1992). *The Evolution of Life Histories*. Chapman and Hall.

Roughgarden, J., Y. Iwasa, and C. Baxter (1985). Demographic theory for an open marine population with space-limited recruitment. *Ecology 66*(1), 54–67.

Ruelle, D. (1979). Analytic properties of the characteristic exponents of random matrix products. *Advances in Mathematics 32*, 68–80.

Runkle, J. (1989). Synchrony of regeneration, gaps, and latitudinal differences in tree species diversity. *Ecology 70*(3), 546–547.

Sale, P. F. (1977). Maintenance of high diversity in coral reef fish communities. *American Naturalist 111*(978), 337–359.

Schaffer, W. (1974). Selection for optimal life histories: the effects of age structure. *Ecology 55*, 291–303.

Shmida, A. and S. Ellner (1984). Coexistence of plant species with similar niches. *Vegetatio 58*, 29–55.

Stearns, S. C. (1992). *The Evolution of Life Histories*. New York: Oxford University Press.

Taylor, H. and S. Karlin (1994). *An Introduction to Stochastic Modeling* (2nd ed.). Academic Press, Inc.

Tuljapurkar, S. (1990). *Population Dynamics in Variable Environments*, Volume 85 of *Lecture Notes in Biomathematics*. Berlin Heidelberg: Springer-Verlag.

Tuljapurkar, S. (1997). Stochastic matrix models. In S. Tuljapurkar and H. Caswell (Eds.), *Structured-population Models in Marine, Terrestrial, and Freshwater Systems*, pp. 59–88. Chapman and Hall.

Tuljapurkar, S. D. (1982). Population dynamics in variable environments. iii. evolutionary dynamics of r-selection. *Theoretical Population Biology 21*, 141–165.

Turelli, M. and J. H. Gillespie (1980). Conditions for the existence of stationary densities for some two-dimensional diffusion processes with applications in population biology. *Theoretical Population Biology 17*, 167–189.

Wolfram, S. (1988). *Mathematica: A System for Doing Mathematics by Computer*. Addison-Wesley Publishing Company, Inc.